

ABSTRACT

MENESES EVANS, CONSTANZA STEFANIA. Animal Models of Radiation-induced Oral Mucositis and Pain and their Application to the study of Tumor-Promoting Effects of Pain (Under the direction of Dr. B. Duncan X. Lascelles and Dr. Michael W. Nolan).

Radiation therapy (RT) is an important treatment modality for head and neck cancer (HNC), however, aggressive courses can result in radiation-associated pain (RAP) that arises along with radiation-induced oral mucositis (RIM). RAP is challenging to manage and is the primary cause of unplanned RT breaks in HNC; such breaks are known to limit the efficacy of RT by decreasing local tumor control. This is often attributed to accelerated repopulation, but it is unknown whether pain or pain signaling constituents might alter tumor behavior and hasten metastatic disease progression.

In this body of work, we first provided a literature review about RIM and RAP in human HNC. We focus on identifying the epidemiology, clinical course, risk factors, pathogenesis, diagnosis, and management of both RIM and RAP, as well as to describe their implications on oral function, quality of life, and treatment outcomes. As a way to begin exploring the idea that RAP promotes tumor development, we first assessed the reliability of new behavioral assays to phenotype acute, orofacial RAP (aoRAP) in mice. Results here demonstrated that nesting and grooming behaviors are good proxy indicators of RIM progression and severity, and that our developed scoring systems are reliable methods for measuring the affective/motivational aspects of aoRAP in our model. Then, we assessed the tumor-promoting effects of aoRAP using a tail vein model of pulmonary metastasis. AoRAP both promoted 4T1-tumor growth in BALB/c mice and death in MOC2-bearing C57BL/6 mice, however, it did not affect the growth of B16-F0 tumors in C57BL/6 mice. Remarkably, 4T1-tumor growth was normalized when aoRAP was mitigated using a potent TRPV1 agonist (resiniferatoxin). Therefore, we decided to replicate this experiment in

MOC2-bearing C57BL/6 mice to determine whether aoRAP mitigation via resiniferatoxin improved survival. However, unacceptable resiniferatoxin-associated mortality was encountered. Therefore, we explored in subsequent experiments the tolerability and ablative efficacy of different resiniferatoxin dosing regimens in this strain. According to our results, the response to resiniferatoxin greatly differs between mouse strains (BALB/c vs C57BL/6), as well as between C57BL/6 substrains (B6NCrl vs B6/J). While effective and long-lasting ablation of TRPV1-expressing neurons was well-tolerated in B6/J mice using doses ranging from 10 to 300 $\mu\text{g}/\text{kg}$ RTX, B6NCrl mice developed serious toxicities when using the same doses. Finally, and as a first step to validate pet dogs with naturally-occurring HNC as an adequate animal model to study potential interventions to prevent and treat human RIM and aoRAP, we described the epidemiology and clinical features of RIM in dogs undergoing definitive-intent RT (DRT) for the treatment of oral, nasal and cranial cavity tumors, and assessed aspects of reliability and validity of a novel clinical metrology instrument (CMI) designed to measure aoRAP in this species. Here we provide the first body of evidence suggesting that the clinical features of RIM in pet dogs (i.e., progression, severity, and secondary side effects) as a result of HNC irradiation share similarities with its human counterpart. Moreover, we found that the progression and severity of aoRAP, as in humans, echoes the progression and severity of RIM in this species (as indicated by the applied CMIs).

Results from this dissertation offer valuable insights to understanding the clinical significance of the crosstalk between pain and cancer, and will hopefully contribute to the development of effective strategies for managing aoRAP in HNC patients, and thus, improve cancer treatment outcomes. Future work will be focused on refining and validating our preclinical animal models of aoRAP (i.e., mouse, dog) to further provide a comprehensive knowledge of the

biological pathways driving the potential tumor-promoting effects of this particular pain type in different cancer model systems.

© Copyright 2022 by Constanza Stefania Meneses Evans

All Rights Reserved

Animal Models of Radiation-induced Oral Mucositis and Pain and their Application to the study
of Tumor-Promoting Effects of Pain

by
Constanza Stefania Meneses Evans

A dissertation submitted to the Graduate Faculty of
North Carolina State University
in partial fulfillment of the
requirements for the degree of
Doctor of Philosophy

Comparative Biomedical Sciences

Raleigh, North Carolina
2022

APPROVED BY:

Dr. B. Duncan X. Lascelles
Committee Chair

Dr. Michael W. Nolan

Dr. Margaret E. Gruen

Dr. Matthew Breen

DEDICATION

To my beloved parents, Sarah and Pedro, for giving me love, support, and so many opportunities throughout my life.

BIOGRAPHY

Constanza Meneses is from Viña del Mar, Chile. She attended the College of Veterinary Medicine at the Austral University of Chile (UACH) in Valdivia, Chile, and earned her degree as Doctor of Veterinary Medicine in 2013. After graduation, she completed her Master and Clinical Residency Program in Veterinary Anesthesiology and Pain Management (dual degree) in 2017. Following this dual program, she worked at the UACH Veterinary Teaching Hospital as a veterinary anesthesiologist. In 2018, she began her PhD in Comparative Biomedical Sciences with a concentration in neuroscience at the College of Veterinary Medicine, North Carolina State University (NCSU). Dr. Meneses is a member of the Translational Research in Pain (TRiP) program at NCSU and a board member of the Non-Human Pain Special Interest Group of the International Association for the Study of Pain (IASP). Under the mentorship of Dr. B. Duncan X. Lascelles and Dr. Michael Nolan, she focused her research on radiation-associated pain and head and neck cancer during her PhD program. Upon completion of her PhD studies, she is planning to return to Chile to support and encourage high-quality pain research in her own country.

ACKNOWLEDGMENT

I would like to thank my mentors, Dr. Duncan Lascelles and Dr. Michael Nolan, for their outstanding mentorship. When times were hard, their encouraging and kind words were essential for keeping my spirit high and my mind on the objective. I will be forever grateful for having the opportunity to work with these visionary researchers. I would also like to thank my committee members, Drs. Margaret Gruen and Matthew Breen for their guidance and support during my program; your advice was crucial to developing this work.

I would like to express gratitude to all the members of the Translational Research in Pain Program (past and present) for their collaboration and comradery. To Andrea Thomson for all the love and support, and Morika Williams, Derek Adrian, Beatriz Belda, and Ankita Gupta for your friendship. I also thank all Dr. Nolan's Laboratory members for their assistance in my various projects, especially to Karen Marcus for helping me to conduct practically all my experiments and for being my closet and dearest ally, to Yen Hao Lai for the training in calcium imaging and neuron culture, and to Tammy Hawkes for instructing me how to operate the linear accelerator.

To my dear "minions", Brooke Bollinger, Yarines Gonzalez, Kayla Freeman, Raisa Vélez-Contreras, and Jennifer Piatt for supporting me in the conduct of several experiments, but mostly, to thank for the laughs and long conversations when collecting the nesting and grooming data. I also want to reiterate my gratitude to Brooke and Raisa for collecting the data that allowed to me finish Chapter 4 (immunofluorescence and resiniferatoxin-related studies, respectively).

To Emily Gidcumb for paving the way to develop this research, and to Dr. Santosh Mishra to support our work. To Joshua Wheeler for collecting calcium imaging during my absence.

I'm also grateful to Dr. Debra Tokarz for taking the time to help me interpret our histopathological samples (Chapter 4), and to Dr. Dorothy Brown for her generosity and support during the conduct of one of the most challenging but exciting studies (Chapter 5).

I'm also grateful to Drs. Gregory Palmer and Mark Dewhirst from Duke University, Drs. Michael Wendt from Case Western Reserve University, Dr. Clint Allen from the National Institutes of Health (NIH), and Dr. Alexis Nahama from Sorrento Therapeutics for providing us with some of the important resources that allowed us to conduct this work.

To Dr. Steve Marks for his permanent support and guidance.

I would also like to thank the National Agency for Research and Development (ANID) of Chile for the scholarship that allowed me to get here.

I want to be grateful also to all the research animals that were at the service of this work; I will always value with respect and honor their contribution to science.

Lastly, I'm also grateful to my life partner Nico for his love and support during these last years. Thank you for waiting for me, and for building the amazing life that we are about to live.

TABLE OF CONTENTS

| | |
|-----------------------|----|
| LIST OF TABLES | ix |
| LIST OF FIGURES | xi |

| | |
|--|----------|
| Chapter 1: Introduction – An Overview of Oral Mucositis and Pain associated to Radiotherapy in Head and Neck Cancer | 1 |
| 1.1 Introduction..... | 2 |
| 1.2 Radiation-induced oral mucositis in head and neck cancer..... | 7 |
| 1.2.1 Epidemiology: Incidence, severity, and clinical course..... | 7 |
| 1.2.2 Risk factors | 8 |
| 1.2.3 Pathogenesis..... | 9 |
| 1.2.4 Diagnosis..... | 10 |
| 1.2.5 Management..... | 12 |
| 1.3 Radiation-associated pain in head and neck cancer..... | 16 |
| 1.3.1 Epidemiology: Incidence, severity, and clinical course..... | 16 |
| 1.3.2 Risk factors | 17 |
| 1.3.3 Pathogenesis..... | 17 |
| 1.3.4 Diagnosis..... | 22 |
| 1.3.5 Management..... | 23 |
| 1.4 Clinical implications of RIM/RAP | 25 |
| 1.4.1 Oral function | 25 |
| 1.4.2 Quality of life | 26 |
| 1.4.3 Success of cancer treatment | 27 |
| 1.5 Preclinical models of radiation-induced mucositis and pain | 27 |
| 1.6 Rationale for this work: pain as a driver of cancer progression | 32 |
| 1.7 Overview of work in this dissertation..... | 34 |
| 1.8 References..... | 37 |

| | |
|---|-----------|
| Chapter 2: Development and Evaluation of Behavioral Assays of Acute Orofacial Pain in a Mouse Model of Lingual Irradiation | 78 |
| 2.1 Introduction..... | 79 |
| 2.2 Material and Methods..... | 82 |
| 2.2.1 Experimental overview | 82 |
| 2.2.2 Animals | 83 |
| 2.2.3 Animal Irradiations | 83 |
| 2.2.4 Assessment of RIM and associated body weight loss..... | 85 |
| 2.2.5 Nesting and grooming assays..... | 86 |
| 2.2.6 Reliability and validity assessment of nesting and grooming assays..... | 90 |
| 2.2.7 Burrowing and eye wiping assays..... | 94 |
| 2.2.8 Statistical analysis | 95 |
| 2.3 Results..... | 97 |
| 2.3.1 RIM and associated weight loss in irradiated female BALB/c mice | 97 |
| 2.3.2 Time course of nesting and grooming assays in relation to RIM and body weight loss in irradiate female BALB/c mice | 98 |

| | |
|---|-----|
| 2.3.3 Nesting and grooming assay scores benchmarked against eye wiping and burrowing activities in female BALB/c mice | 98 |
| 2.3.4 Nesting and grooming scores in relation to RIM scores across sex, strain, and IR modalities | 100 |
| 2.3.5 Real-time versus remote scoring (reproducibility assessment)..... | 102 |
| 2.3.6 Reliability assessment | 103 |
| 2.3.7 Validity assessment (responsiveness) | 105 |
| 2.4 Discussion..... | 111 |
| 2.5 References..... | 124 |

| | |
|--|------------|
| Chapter 3: Painful Radiation-induced Oral Mucositis Promotes Metastatic Tumor Development in Murine Models of Breast and Oral Cancer, a Phenomenon that Shows Dependency on TRPV1-Expressing Neurons..... | 134 |
| 3.1 Introduction..... | 135 |
| 3.2 Material and Methods | 137 |
| 3.2.1 Animals | 140 |
| 3.2.2 Cell lines | 140 |
| 3.2.3 Irradiations | 141 |
| 3.2.4 Assessments of radiation-induced mucositis and body weight..... | 142 |
| 3.2.5 Screening for radiation-associated pain | 142 |
| 3.2.6 Tumor cell inoculation | 142 |
| 3.2.7 Tumor burden and growth..... | 143 |
| 3.2.8 Modulation of ambient temperature..... | 144 |
| 3.2.9 Selective chemical ablation of transient receptor potential vanilloid 1 expressing neurons | 145 |
| 3.2.10 Statistical analysis | 146 |
| 3.3 Results..... | 147 |
| 3.3.1 Single fraction (27 Gy) irradiation of the rostral tongue is associated with mucositis and pain in BALB/c and C57BL/6 mice..... | 147 |
| 3.3.2 Lung tumor burden in BALB/c mice is significantly increased when 4T1-Luc2 cells are intravenously injected at the time of severe mucositis and pain..... | 148 |
| 3.3.3 Off-target radiation does not increase the burden of 4T1 lung tumors | 149 |
| 3.3.4 Standard (subthermoneutral) housing conditions do not appear to enhance 4T1 lung tumor burden | 149 |
| 3.3.5 Tongue irradiation does not increase the burden of B16F10-Luc2 lung tumors, but was associated with early (lung tumor attributable) death in MOC2-Luc2 bearing mice | 153 |
| 3.3.6 The growth-promoting effects that tongue irradiation had on 4T1 lung tumors was mitigated by systemic ablation of TRPV1 sensory nerves | 154 |
| 3.4 Discussion..... | 156 |
| 3.5 References..... | 163 |
| 3.6 Supplementary Material..... | 173 |
| 3.7 Afterword..... | 178 |
| Chapter 4: Systemic Administration of Resiniferatoxin in C57BL/6 Mice: Troubleshooting Unexpected Morbidity and Mortality | 180 |

| | |
|--|-----|
| 4.1 Introduction..... | 181 |
| 4.2 Material and Methods | 183 |
| 4.2.1 Overall experimental rationale and scheme | 184 |
| 4.2.2 Animals | 187 |
| 4.2.3 RTX administration..... | 187 |
| 4.2.4 Animal monitoring..... | 187 |
| 4.2.5 Assessment of RTX-mediated ablation of TRPV1-expressing neurons..... | 188 |
| 4.2.6 Post-mortem assessment | 189 |
| 4.2.7 Calcium imaging | 189 |
| 4.2.8 Cellular immunofluorescence staining..... | 190 |
| 4.2.9 Statistical analysis | 191 |
| 4.3 Results..... | 191 |
| 4.3.1 Experiment 1 | 191 |
| 4.3.2 Experiment 2 | 192 |
| 4.3.3 Experiment 3 | 194 |
| 4.3.4 Experiment 4 | 196 |
| 4.3.5 Experiment 5 | 197 |
| 4.4 Discussion..... | 200 |
| 4.5 References..... | 209 |

Chapter 5: Characterization of Radiation-induced Oral Mucositis and Validity Testing of a Subjective Oral Pain Scale in Pet Dogs Undergoing Definitive Radiation Therapy for the Treatment of Oral, Nasal and Cranial Cavity Tumors 217

| | |
|---|-----|
| 5.1 Introduction..... | 218 |
| 5.2 Material and Methods | 220 |
| 5.2.1 Subjects | 220 |
| 5.2.2 Recruitment and patient care..... | 221 |
| 5.2.3 Data collection | 221 |
| 5.2.4 Definitive-intent radiation therapy (DRT) | 221 |
| 5.2.5 Patient’s characteristics..... | 222 |
| 5.2.6 Assessment of oral radiation-induced mucositis..... | 222 |
| 5.2.7 Measures of pain and function interference | 223 |
| 5.2.8 Statistical analysis | 223 |
| 5.3 Results..... | 228 |
| 5.3.1 Patient’s characteristics..... | 228 |
| 5.3.2 Clinical features of oral radiation-induced oral mucositis in pet dogs..... | 232 |
| 5.3.3 Assessment of aspects of reliability and validity of the Oral Pain Scale in dogs with RIM | 248 |
| 5.3.4 Pain assessment using PSS, PIS, OIS, and OPS in pet dogs with RIM | 254 |
| 5.3.5 Exploration of individual question responsiveness and discriminatory ability | 260 |
| 5.4 Discussion..... | 265 |
| 5.5 References..... | 278 |

Chapter 6: Conclusions and Future Directions 290

| | |
|---------------------|-----|
| 6.1 References..... | 299 |
|---------------------|-----|

LIST OF TABLES

Chapter 1

| | | |
|-----------|--|----|
| Table 1.1 | Comparison of commonly used RIM scoring systems..... | 11 |
|-----------|--|----|

Chapter 2

| | | |
|-----------|---|-----|
| Table 2.1 | Experiment's list and sample sizes used for each experiment | 97 |
| Table 2.2 | Inter-rater reliability assessment | 104 |
| Table 2.3 | Test-retest reliability assessment..... | 105 |
| Table 2.4 | Assay's responsiveness assessment (pilot study)..... | 106 |

Chapter 3

| | | |
|-----------|--|-----|
| Table 3.1 | List of experiments and sample sizes used..... | 146 |
|-----------|--|-----|

Chapter 4

| | | |
|-----------|---|-----|
| Table 4.1 | Details about experimental conditions, applied RTX dose, and mortality rate of each experiment and cohort | 186 |
|-----------|---|-----|

Chapter 5

| | | |
|------------|--|-----|
| Table 5.1 | Demographics of dogs at enrollment (n = 58)..... | 229 |
| Table 5.2 | Tumor types diagnosed at enrollment (n = 58) | 230 |
| Table 5.3 | Information about oral mucositis, dental prophylaxis, appetite, diet acceptance, and type of diet documented at enrollment | 231 |
| Table 5.4 | Summary statistics of elapsed days from DRT initiation (enrollment) to the end of this study (i.e., 3 weeks after DRT finalization)..... | 232 |
| Table 5.5 | Total DRT dose administered by each assessment time point (i.e., from DRT initiation to completion) | 232 |
| Table 5.6 | RIM time course and severity (using VRTOGs, scale: 0 - 3) across groups at each assessment time point | 236 |
| Table 5.7 | Body weight change from baseline (%) for each group at each assessment time point | 240 |
| Table 5.8 | Body conditions scores (0-9) in each group, at each assessment time point..... | 241 |
| Table 5.9 | Appetite scores (0-10) for each group, at each assessment time point..... | 242 |
| Table 5.10 | Diet acceptance scores (0-10) for each group, at each assessment time point | 243 |
| Table 5.11 | Nasal mucositis scores (0-10) for each group, at each assessment time point | 244 |
| Table 5.12 | Radiodermatitis scores (0-10) for each group, at each assessment time point..... | 245 |
| Table 5.13 | Oral RIM risk factors (ordinal and logistic regression) | 247 |
| Table 5.14 | Inter-correlation matrix (assessment time point: visit 2)..... | 251 |
| Table 5.15 | Item-total statistics (assessment time point: visit 2)..... | 252 |
| Table 5.16 | Communalities (assessment time point: visit 2)..... | 253 |
| Table 5.17 | Factor loadings extracted from the PCA (assessment time point: visit 2) | 253 |

| | |
|---|-----|
| Table 5.18 Comparison of individual item question scores documented at baseline against those documented at visit 4 (comparison using p-values) | 263 |
|---|-----|

LIST OF FIGURES

Chapter 2

| | | |
|------------|--|-----|
| Figure 2.1 | Fractionated lingual irradiation using XRAD 320 kilovolt X-ray irradiator..... | 85 |
| Figure 2.2 | Nesting assay | 87 |
| Figure 2.3 | Grooming assay | 88 |
| Figure 2.4 | Example of Microsoft PowerPoint presentations used during the reliability assessment | 92 |
| Figure 2.5 | Changes in nesting and grooming assays in relation to RIM, body weight loss, eye wiping, and burrowing activities in female BALB/c mice..... | 99 |
| Figure 2.6 | Ability of nesting and grooming assays to discriminate mice with RIM of 0 to those with RIM > 2 across sex, strain, and IR modalities | 101 |
| Figure 2.7 | Progression of RIM, nesting, and grooming scores across times in female C57BL/6 mice | 103 |
| Figure 2.8 | Changes in RIM, body weight, nesting, and grooming activities in female BALB/c mice treated with systemic IgG or anti-NGF mAb | 108 |
| Figure 2.9 | Changes in RIM, body weight, nesting, and grooming activities in female BALB/c mice treated with systemic RTX or its excipient | 110 |

Chapter 3

| | | |
|------------|--|-----|
| Figure 3.1 | Summary of experiments..... | 138 |
| Figure 3.2 | Tongue irradiation in BALB/c and C57BL/6 mice results in RAP..... | 148 |
| Figure 3.3 | Tumor burden promoting effect of RAP in breast carcinoma tumor-bearing female and male BALB/c mice (4T1-Luc2 model) | 151 |
| Figure 3.4 | Tumor burden promoting effect of RAP in melanoma (B16F10-Luc2) and oral (MOC2-Luc2) tumor-bearing female C57BL/6 mice | 154 |
| Figure 3.5 | Effects of systemic ablation of TRPV1-expressing neurons on tumor burden in breast carcinoma tumor-bearing female BALB/c mice (4T1-Luc2 model) | 156 |

Chapter 4

| | | |
|------------|---|-----|
| Figure 4.1 | Systemic administration of RTX at a dose of 50 µg/kg (given once) in 10-week-old female C57BL/6NCr1 mice (n=10)..... | 192 |
| Figure 4.2 | Systemic administration of RTX at a dose of either 2 µg/kg (n = 4) or 600 µg/kg (n=8) in 14-week-old female C57BL/6J mice..... | 194 |
| Figure 4.3 | Systemic administration of RTX at a dose of either 10 µg/kg (n = 8) or 300 µg/kg (n=4) in 16-week-old female C57BL/6J mice..... | 196 |
| Figure 4.4 | Systemic administration of RTX at a dose of 10 µg/kg in female B6/NCr1 (n = 46) or female and male B6/J mice (n=16)..... | 198 |
| Figure 4.5 | Calcium imaging and immunofluorescences studies in 13-week-old female and male B6/J mice (n=16; 10 µg/kg RTX)..... | 199 |

Chapter 5

| | | |
|------------|--|-----|
| Figure 5.1 | RIM progression over time for oral, nasal, and cranial DRT groups | 237 |
| Figure 5.2 | Change in individual OPS question scores overtime during and following RT | 250 |
| Figure 5.3 | Pain severity scale (PSS)..... | 256 |
| Figure 5.4 | Pain intensity scale (PSS)..... | 257 |
| Figure 5.5 | Overall impression scale (OIS)..... | 258 |
| Figure 5.6 | Oral pain scale (OPS)..... | 260 |
| Figure 5.7 | Individual item question' scores for the PSS (A to D) and PIS (D to I) questionnaires 261 | |
| Figure 5.8 | Individual item question' scores for the OPS (A to G) questionnaires | 262 |
| Figure 5.9 | Adapted OPS (AOPS) | 265 |

Appendices

Chapter 5

| | | |
|--------------|---|-----|
| Appendix 5.1 | Veterinary Radiation Therapy Oncology Group (VRTOG) acute morbidity scoring scheme | 305 |
| Appendix 5.2 | The Canine Brief Pain Inventory (CBPI)..... | 306 |
| Appendix 5.3 | The Oral Pain Scale (OPS)..... | 307 |
| Appendix 5.4 | Body Condition Score (BCS)..... | 308 |
| Appendix 5.5 | Appetite, diet acceptance and current diet form..... | 309 |

**Chapter 1: “Introduction – An Overview of Oral Mucositis and Pain associated to
Radiotherapy in Head and Neck Cancer”**

1.1 Introduction

Head and neck cancer (HNC) is the seventh most common cancer worldwide, accounting for over 900,000 new cases and 450,000 deaths per year globally (Borsetto et al., 2020; Bray et al., 2018). HNC comprises a broad category of diverse malignancies that arise in the oral cavity, pharynx, larynx, paranasal sinuses, salivary glands, cervical esophagus, thyroid glands, and surrounding soft and bone tissues (Argiris et al., 2008; Bose et al., 2013; Davies & Welch, 2006; Muzaffar et al., 2021). However, approximately 90% of all malignancies occurring in the head and neck region are derived from the mucosal epithelium in the oral cavity, pharynx, and larynx, and are collectively categorized as head and neck squamous cell carcinoma (HNSCC) (Aupérin, 2020; Muzaffar et al., 2021). The prognosis of HNSCC patients with locoregionally advanced (i.e., stage III/IV) tumors – which make up approximately 50% of all cases – is generally considered to be poor, as indicated by 5-year overall survival rates ranging from 36 to 65% (percentage of people who are alive five years after diagnosis) (Adrien et al., 2014; Bonner et al., 2010; Elbers et al., 2019; Guizard et al., 2017; Pulte & Brenner, 2010; Van Der Schroeff et al., 2010). Despite continue advances in cancer therapy, patients with locoregionally advanced HNSCC often experience high rates of locoregional recurrence (50-60%) and distant metastasis (20-30%) within the first 2 years of follow-up after primary treatment, jeopardizing the therapeutic success and increasing the risk of cancer-related death (Duprez et al., 2017; Muzaffar et al., 2021; Samra et al., 2018; Seiwert & Cohen, 2005). HNC recurrence and metastasis are major causes of treatment failure in this population, and when it occurs, prognosis is considered dismal (Lee et al., 2013). Indeed, it has been reported that patients diagnosed with recurrent/metastatic HNC have a median overall survival ranging from 5 to 10 months and an estimated proportion of deaths attributable to primary-site recurrence and distant metastasis (commonly spread to lungs, bones, and liver) of 40% to 50%

and 15% to 20%, respectively (Coatesworth et al., 2002; Haddad & Shin, 2008; Kotwall et al., 1987; Merino et al., 1977; Wiegand et al., 2015).

Failure in HNC occurs following the three main cancer therapy modalities, which are surgery with or without adjuvant postoperative radiation therapy to sterilize microscopic tumor spread beyond the surgical margins, or radiation therapy with or without chemotherapy to manage locoregionally advanced unresectable disease (Rosenthal et al., 2002; Syrigos et al., 2009). According to most clinical studies, poor treatment outcomes in the general HNC population can be attributable to late diagnosis. Indeed, a major problem that patients face is that their disease is often diagnosed at an advanced stage where treatment options may not be curative (Adrien et al., 2014; McGurk et al., 2005; Stordeur et al., 2020). Moreover, extensive investigations have indicated that other factors (either cancer or non-cancer related factors), such as site of the primary tumor (e.g., oral cavity tumors), human papilloma virus-negative HNSCC tumors, presence of multiple comorbidities, genetics (e.g., old age, male sex, black race), low socioeconomic status and/or poorer access to health care, pretreatment weight lost and/or low body muscle mass, poor dental health, anemia, or heavy tobacco and alcohol use, can also be important causes of treatment failure and may affect prognosis (Dilling et al., 2011; Dixon et al., 2017; Gillison et al., 2015; Khlifi & Hamza-Chaffai, 2010; Stingone et al., 2013; Wells et al., 2016; Zakeri et al., 2014). Failure can also be attributable to the side effects that arise as a direct result of cancer treatment, and it has been widely recognized that the success of these therapies can be directly impacted by complications that arise from aggressive treatment regimens (Lazarev et al., 2018; Mazul et al., 2020; Saedi et al., 2019; Sroussi et al., 2017). Radiation therapy (RT), for example, has become the standard of care for locally advanced HNSCC, and it can either be used for curative-intent purposes (often in combination with surgery and chemotherapy) or for palliative-intent purposes

to mitigate disease-related symptoms (Alzahrani et al., 2020). However, aggressive courses of curative-intent RT– which are often required for locoregional disease control – can adversely affect exposed tissues and lead to the development of painful lesions that might limit the efficacy of RT (Sonis, 2004a).

Pain as a side-effect of RT, also known as radiation-associated pain (RAP), is extremely frequent among HNC patients receiving curative-intent RT, with an incidence ranging from 58% to 75% (Epstein et al., 2009). Patients typically report the onset of RAP shortly after having started a course of RT (i.e., 1 to 2 weeks after RT initiation), with increasing levels of RAP and RAP-related interference with daily activities 5 weeks following RT initiation, which can last after RT completion despite the use of potent analgesics (Epstein et al., 2007; Epstein et al., 2001). RAP usually arises along with other toxicities that develop shortly after the start of RT, such as mucositis within the oral cavity (Epstein et al., 2009; Fall-Dickson et al., 2007; Wong et al., 2006). Oral mucositis as a result of RT, commonly termed as radiation-induced oral mucositis (hereinafter referred to as “RIM”), is the most recognized and studied source of RAP in this population and it has been extensively accepted that the presence of RIM combined with RAP can greatly impact the patient’s quality of life, treatment outcomes, and survival (Brown & Wingard, 2004; Moslemi et al., 2016; Sroussi et al., 2017). RAP from established RIM (hereinafter referred to as “RIM/RAP”) can significantly limit critical activities such as eating, drinking, speaking, and/or sleeping, impacting the patient’s general health and nutritional status (Epstein & Barasch, 2018). These side-effects have an obvious potential for negatively influencing the patient’s quality of life, and can carry important socio-economic consequences (Peterman et al., 2001). In addition, it has been extensively accepted that RIM/RAP can also compromise the continuity of cancer therapy, and its presence has been associated with cancer relapse and high mortality rates (Brown &

Wingard, 2004). One suggested reason for this is that severe grades of RIM/RAP can limit the patient's ability to tolerate additional RT, and therefore, its presence commonly leads to unplanned treatment breaks, delays, or discontinuations (Russo et al., 2008). Such modifications in the prescribed RT course may be given to allow the recovery of normal tissues from sub-lethal radiation damage between treatments, allowing the repopulation of normal tissue cells. However, these pauses can also trigger the repopulation of surviving tumor cells, and therefore, limiting the efficacy of RT by decreasing local tumor control (Bese et al., 2007; Dörr & Kummermehr, 1990; Rosenthal, 2007; Suwinski et al., 2003; Tarnawski et al., 2002).

Although modern RT planning and dose delivery techniques (e.g., intensity-modulated RT, stereotactic body RT, or heavy-ion irradiation) offer precise dose delivery and reduce the damage of surrounding normal tissues without compromising target coverage (Alterio et al., 2019; Thariat et al., 2011), the rate of serious RAP as a consequence of oral mucosa damage in HNC remains high with unsatisfactory treatment results (Cramer et al., 2018). Currently, poorly controlled RAP continues to be commonly reported in most HNC patients during and after RT, and opioid-based therapies represent the only alternative to provide pain relief (Thompson, 2000). This is problematic because opioid use represents a serious public health concern, and patients have a higher risk of developing opioid-related problems (i.e., depression, opioid addiction, tobacco or alcohol abuse, and death) (Muzumder et al., 2018). According to some authors, the absence of effective, non-opioid analgesics for the management of RAP has been partially attributable to the fact that little is known about the neurobiological mechanisms underlying RAP (Epstein et al., 2009). While the current understanding of the biological events responsible for RIM, such as inflammation and tissue injury, has helped to identify some molecular and cellular mechanisms that might be potentially involved in the modulation of RAP (Wong et al., 2006), there is no

information in the current scientific literature regarding the exact signaling pathways engaged in RAP processing or the involvement of such pathways mediating the development and progression of HNC. This is relevant because it has been demonstrated that HNC survivors with intermediate/high levels of post-treatment pain have increased risk of early disease recurrence and shorter survival in comparison to patients who have reported no pain or low levels (Cramer et al., 2018; Scharpf et al., 2009). Hence, there is a growing necessity to understand the direct biological influence of RAP on outcomes among HNC patients.

In the last decades, significant research efforts have been made to understand the pathophysiology of RIM and to explore therapies targeting RIM through the use of preclinical models (Gruber et al., 2015; Lee et al., 2007; Sonis et al., 2000). Several animal models of RIM – either induced by single or multiple fractionated RT doses – are currently available in the literature, which include rats, mice, and hamsters (Ara et al., 2008; Dörr, Spekl, & Martin, 2002; Rezvani & Ross, 2004). However, the pain that accompanies these forms of acute RIM has been poorly modeled. Loss in body weight, for example, has been used in few studies as proxy indicator of RIM-related discomfort (Alvarez et al., 2003; Maria et al., 2017; Nakajima et al., 2015). While body weight loss is usually associated with RIM, not all HNC patients experiencing RIM/RAP report this side effect (Li et al., 2017). Thus, this outcome measure may not be a thoughtful reflection of RAP in preclinical settings, and future investigations should focus in developing suitable outcomes measures in this species to improve the development of effective mechanism-based treatments in the clinical practice.

In the current chapter (Chapter 1), the author will first provide a brief overview of the current understanding of both RIM and RAP in the context of HNC, including evidence about their epidemiology (incidence, severity, and clinical course), risk factors, pathogenesis, diagnosis, and

management. In addition, the author will detail the clinical implications of RIM/RAP in oral function and quality of life of HNC patients, as well as to describe the impact of RIM/RAP on treatment outcomes. Finally, this chapter will focus on describing the currently available preclinical models of RIM in the literature, in addition to discuss the present state-of-research in the field of RAP and the necessity to add animal models of naturally-occurring HNC to bridge the gap between basic research and human clinical trials.

1.2 Radiation-induced oral mucositis in head and neck cancer

1.2.1 Epidemiology: Incidence, severity, and clinical course

One of the most feared consequences of RT among HNC patients is the possibility of developing RIM. However, its incidence, severity, and clinical course may vary across studies. This variability has been associated with many factors, such as location/staging of tumors or applied RT modality (i.e., RIM is most commonly developed in patient with advanced-stage oral cavity tumors that require aggressive RT regimens), as well as the scoring system used to characterize or grade the extent of RIM (Franco et al., 2017; Parulekar et al., 1998). Nevertheless, there is a general consensus that the incidence of oral mucositis in the general HNC population undergoing RT as a single modality treatment is considerably higher compared to that reported in patients treated with chemotherapy or surgery alone (Lalla et al., 2019; Saedi et al., 2019; Vera-Llonch et al., 2006). According to most clinical studies, virtually all HNC patients develop some degree of RIM during the course of RT (Blakaj et al., 2019; Maria et al., 2017). The incidence of the different grades of RIM varies depending on the applied assessment scale (Table 1.1). Yet, clinical research has revealed that more than half of patients (57%) treated with altered fractionated courses of RT (i.e., hyperfractionation or accelerated fractionation) experience maximum grades

of RIM, which is higher than the frequency reported in patients submitted to conventional fractionated RT (34%) (Franco et al., 2017; Trotti et al., 2003; Vera-Llonch et al., 2006).

In general, the onset of RIM usually occurs within or after 2 weeks from the beginning of RT (patients begin to develop mucosal soreness), and progressively increases in severity during treatment reaching maximum grades of RIM (i.e., confluent mucosal ulcer formation) 4 to 6 weeks after RT initiation (Murphy et al., 2009; Trotti et al., 2003). RIM resolution commonly occurs in most patients 2 to 4 weeks following RT completion. However, and while RIM is considered a self-limited type of injury, some patients experience slower healing rates than others, and life-threatening complications (e.g., systemic infection) associated with severe RIM can occur (Murphy et al., 2009; Saedi et al., 2019; Satheesh Kumar et al., 2009; Trotti et al., 2003; Wong et al., 2006).

1.2.2 Risk factors

To date, there is still a lack of consensus pertaining to the risk factors of RIM. However, several studies have proposed that factors associated with tumor location, cancer therapy modality, and patient's characteristics might play a relevant role in the development of RIM. In particular, the risk to develop RIM is significantly higher among patients with oral cavity, oropharynx or nasopharynx primary tumors, and in patients receiving altered fractionated courses of RT or RT combined with the use of chemotherapeutic agents (e.g., alkylating, anthracyclines, and antimetabolites agents) (Maria et al., 2017; Trotti et al., 2003; Vera-Llonch et al., 2006). Although the risk factors related to the patient's characteristics are less clear, it has been suggested that factors such as age and gender might contribute to the onset of RIM. Specifically, it has been described that those patients younger than 45 years old with HNC are more prone to develop RIM in comparison to older patients, which has been associated to an increased mitotic rate of oral

mucosa cells in the young-age group (Morais-Faria et al., 2020). Other studies have proposed that males develop severe RIM more frequently than female, however, the evidence is conflicting, and it remains unclear how gender might affect the incidence RIM (Nishii et al., 2020). Other commonly factors associated to the occurrence of RIM include poor oral hygiene and/or periodontal disease (potentially linked to an exacerbate inflammatory response induced by microbial colonization), impaired salivary function (i.e., inadequate salivary flow), low leukocyte/lymphocyte counts or use of immunosuppression drugs that might ultimately impair the inflammatory response and increase the risk of infectious complications, tobacco and alcohol consumption (agent known to inhibit healing of mucosal injury), and poor nutritional status or low body mass index (uncertain mechanism, likely associated to an interfere with mucosal regeneration) (Elting et al., 2007; Gobbo et al., 2014; McCarthy et al., 1998; Nagatani et al., 2017; Raber-Durlacher, 1999; Saito et al., 2012; Vera-Llonch et al., 2006; Vesty et al., 2020).

1.2.3 Pathogenesis

The biological processes by which RIM develops and resolves have been divided into four phases: an initial inflammatory/vascular phase; an epithelial phase; an ulcerative/bacteriological phase; and a healing phase. The RT-induced cascade of events begins with the initial induction of free radicals and reactive oxygen species (ROS) that can cause cell death (via DNA damage), damaging epithelial and vascular endothelial cells, fibroblasts, and tissue macrophages (Mallick et al., 2016). This will in turn active nuclear transcription factors, such as the nuclear factor kappa B (NF- κ B), that will secondarily promote cell apoptosis and will stimulate the release of pro-inflammatory cytokines (e.g., interleukin 1 β (IL-1 β) and tumor necrosis factor- α (TNF α)), chemotactic molecules (e.g., MIP-1, MCP-1, MCP-5, IL-8), prostaglandins, histamine, matrix metalloproteinases, and pro-fibrotic mediators such as transforming growth factor (TGF)- β

(Brzozowska & Gołębiowski, 2019; Gruber et al., 2017; Khaw et al., 2014; Sonis, 2004a). These events will further increase the damage by increasing vascular permeability, which subsequently promotes the infiltration and recruitment of inflammatory cells (e.g., leukocytes, macrophages, and neutrophils) that will further amplify the inflammatory reaction, apoptosis, and tissue damage within the oral mucosa (Gruber & Dörr, 2016; Redding, 2005). Once proliferation and epithelial replacement have ceased as a result of this inflammatory event cascade, the mucosa becomes erythematous and ulcerated. In particular, the destruction of the basement membrane protective barrier leads to the formation of ulcer pseudomembrane and inflammatory exudate. Subsequently, secondary bacterial and fungal infections can occur, enhancing the installed host inflammatory response and complicating the already existing inflammation (Shih et al., 2003). Finally, and if managed correctly, a healing phase will begin after cessation of RT exposure to allow cell regeneration and establishment of normal microbial flora. However, late manifestations of vascular and soft tissue damage can potentially induce secondary atrophy, increasing the epithelial vulnerability to develop chronic ulcers or osteoradionecrosis in those more severe cases (Maria et al., 2017; Redding, 2005).

1.2.4 Diagnosis

Diagnosis of RIM is clinical, and based on the appearance, timing, and location of the lesions. Several scoring systems have been developed to grade RIM. The most commonly used RIM grading criteria are the World Health Organization's Oral Toxicity Scale (WHO), the National Cancer Institute Common Terminology Criteria for Adverse Events (NCI-CTCAE), and the Toxicity criteria of the Radiation Therapy Oncology Group (RTOG) (Table 1.1). The WHO scoring system include functional outcomes (e.g., tolerance to diet) and objective parameter of RIM (i.e., ulceration and erythema) and is the most extensively used for intervention efficacy

studies, whereas the NCI-CTCAE scoring system is completely dependent on patient-reported outcomes and has been most commonly applied to describe adverse events experienced in oncology trials. The RTOG scoring system combines both modalities, requiring both patient’s and clinician’s input for scoring (Judge et al., 2021; Maria et al., 2017; Parulekar et al., 1998; Scully et al., 2003; Villa et al., 2021).

Table 1.1: Comparison of commonly used RIM scoring systems.

| Source | Grade | | | | | |
|------------------|-------------|---|--|--|--|---------------------------|
| | 0 | 1 | 2 | 3 | 4 | 5 |
| WHO | No findings | Erythema and soreness; no ulcers | Oral erythema, ulcers, solid diet tolerated | Oral ulcers, liquid diet only | Not able to tolerate a solid or liquid diet | NA |
| NCI-CTCAE | No findings | Asymptomatic or mild symptoms; intervention not indicated | Moderate pain or ulcer that does not interfere with oral intake; modified diet indicated | Severe pain; interfering with oral intake | Life-threatening consequences: urgent intervention indicated | Death related to toxicity |
| RTOG | No findings | Painless ulcers, erythema or mild soreness | Painful erythema, edema, or ulcers, can eat | Painful erythema, edema, or ulcers, cannot eat | Requires parenteral or enteral support | NA |

1.2.5 Management

Despite extensive research dedicated to find specific RIM strategies to prevent its onset or reduce its severity, the wide variation of outcomes across clinical studies has limited the generalizability of several interventions in HNC and only few studies have actually provided therapeutic alternatives with strong scientific evidence (Elad et al., 2020). To improve the interpretation of clinical significance in the literature and thus, improve clinical outcomes, the Mucositis Study Group of the Multinational Association of Supportive Care in Cancer/International Society of Oral Oncology (MASCC/ISOO) has developed evidence-based management guidelines (based on systematic reviews of interventional and observational studies) to guide clinicians on which interventions are truly effective for preventing and treating RIM or RIM-related symptoms secondary to cancer therapy (Ariyawardana et al., 2019; Bowen et al., 2013; Lalla et al., 2014). According to the latest clinical practice guidelines update published in 2020 (which covers evidence from 1197 publications), there is no agent or method that is uniformly effective in preventing or treating RIM in HNC, however, most studies have consistently find a positive effect of basic oral care (i.e., prophylaxis/treatment of oral infections) and symptom palliation (e.g., pain, eating difficulties and nutritional compromise) strategies for the management of RIM in HNC patients submitted to RT (Elad et al., 2020).

Regarding RIM prevention, expert opinion supports the idea that the maintenance of good oral hygiene is crucial in reducing the incidence of RIM among HNC patients being considered for curative-intent RT (Elad et al., 2020). While RIM is not an infectious disease and, furthermore, there is a lack of clarity regarding the role of oral microbiota in the pathogenesis of RIM, many authors have hypothesized that microbial colonization (before RT initiation) may potentially stimulate host inflammatory responses that might contribute to the onset of RIM (Khaw et al.,

2014; Nishii et al., 2020; Vanhoecke et al., 2015; Vesty et al., 2020). The guidelines recommend that basic oral care (BOC) strategies should include: 1) mechanical cleaning (nontraumatic tooth brushing and flossing procedures) and frequent mouth rinses with bland solutions (saline and/or sodium bicarbonate) to reduce bacterial build-up; 2) application of mouthwash solutions with anti-inflammatory agents (benzylamine hydrochloride as the most recommended) to inhibit the production of pro-inflammatory cytokines (i.e., TNF α and IL-1 β); 3) avoidance of dry oral environment (i.e., application of moisturizing agents and cessation of tobacco smoking and alcohol drinking); and 4) professional oral care assistance and educational interventions to improve oral practices in patients during cancer therapy (Elad et al., 2020; McGuire et al., 2006; Saadeh, 2005).

When RIM is established, treatment is challenging and there are no universally accepted protocols. According to the MASCC/ISOO guidelines, standard of care for established RIM should primarily focus on supportive care and symptom palliation, which includes BOC strategies (as mentioned above) to avoid secondary microbial colonization of oral lesions that could cause clinically relevant local and/or systemic infections, nutritional support and pain management. Colonization of the oral ulcerations by opportunistic pathogens (e.g., *Candida* spp. *Tannerella*, *Sneathia*, *Mycoplasma*, *Capnocytophaga*, *Bacteroidales* G2, *Porphyromonas* and *Eikenella*) is a common concern among clinicians when RIM is developed (Vesty et al., 2020). While a number of topical antimicrobial agents have been studied for managing secondary infections, including antibacterial, antiviral, and antifungal agents, studies have either yield negative or conflicting results. In consequence, researchers are currently suggesting that achieving oral flora symbiosis (by decontaminating the oral cavity with appropriate BOC protocols) might represent a better strategy than sterilizing the oral cavity with antimicrobial therapies (Ingrosso et al., 2021; Stringer & Logan, 2015). The current MASCC/ISOO guidelines recommend against the routine use of

antimicrobial lozenges (polymyxin-tobramycin-amphotericin B lozenges/paste and bacitracin-clotrimazole-gentamicin lozenges), chlorhexidine mouth rinse, and iseganan mouth rinse for RIM management due to lack of consistent evidence of efficacy. Regarding nutritional support, experts in the field recommend that the patient's diet should be modified if needed to increase the likelihood that the diet will be tolerable. This includes soft diets and elimination of potential sources of irritation such as acidic, spicy, hot and crispy/rough foods. If food intake is limited, a nutrition specialist should be consulted and the use of intravenous fluids and/or parenteral or enteral feeding should be implemented in severe cases (Barasch et al., 2006; Kuten-Shorrer et al., 2021; Sonis, 2011). The third important foundation of care in RIM consists of pain management. Although sustained research effort has been devoted to developing interventional agents for managing RAP associated to RIM, only few agents have demonstrated robust scientific evidence for efficacy in HNC (Elad et al., 2020). The MASCC/ISOO has examined the different analgesics, topical preparations, and other approaches currently available in the literature, and have developed pain management guidelines that will be later addressed in this chapter (section 1.3.5).

Finally, other complementary therapeutic strategies that aim to reduce oral mucosal injury and downregulate the inflammatory pathways related to cancer therapy have been suggested and widely studied. Palifermin, for example, is a recombinant human keratinocyte growth factor-1 that stimulates the proliferation and the differentiation of epithelial cells, and has shown promising antiapoptotic, antioxidant and anti-pro-inflammatory effects in clinical settings (Blijlevens & Sonis, 2007; Panjwani, 2013; Villa & Sonis, 2016). Palifermin became the first agent approved by the U.S. Food and Drug Administration (FDA) to decrease the incidence and duration of severe oral mucositis in patients undergoing total body irradiation and high-dose chemotherapy for autologous stem-cell transplantation (Spielberger et al., 2004; Vadhan-Raj et al., 2013). Regarding

the use of palifermin in HNC, two clinical trials have studied the beneficial effect of palifermin in the management of RIM in patients with locally advanced HNC that have either received definitive chemoradiotherapy (Le et al., 2011) or conventionally-fractionated RT after a complete or incomplete resection with or without concurrent chemotherapy (Henke et al., 2011). Results from these trials showed that palifermin was effective in reducing the incidence of severe RIM (grade 3/4, WHO scoring system), however, it did not decrease the use opioid analgesic neither reduced mouth nor throat soreness. Therefore, additional investigation is needed before palifermin can gain FDA approval for managing RIM in HNC patients undergoing curative-intent RT as cancer therapy (Bossi et al., 2012). Other therapeutic strategies that have been studied and have shown promising results in clinical settings to reduce RIM in HNC include the use of amifostine (a free-radical scavenger used as a mucoprotective agent) (Karacetin et al., 2004; Vacha et al., 2003; Veerasarn et al., 2006), sucralfate (a mucosal coating protective agent) (Etiz et al., 2000; Makkonen et al., 1994; Saunders et al., 2013), cryotherapy (which induce vasoconstriction of the superficial blood vessels, limiting the delivery of cytotoxic drugs to the oral tissue and reducing damage to the oral mucosa) (Katrancı et al., 2012; Peterson et al., 2013), and photobiomodulation (i.e., use of low-level energy (laser and other light therapy) to stimulate anti-inflammatory and pro-healing effects) (Migliorati et al., 2013; Schubert et al., 2007). However, the application of these therapeutic approaches has generated inconsistent results, and the MASCC/ISOO does not recommend its use in this particular treatment setting (i.e., RT).

1.3 Radiation-associated pain in head and neck cancer

1.3.1 Epidemiology: Incidence, severity, and clinical course

HNC patients have the highest prevalence of RAP among cancer patients (van den Beuken-van Everdingen et al., 2007), and this form of pain is often one of the major reasons for seeking care during and after cancer therapy (Astrup et al., 2015). Similar to RIM, its incidence can vary across studies depending on the location and/or staging of the tumor, the applied RT regimen and/or modality, and the assessment tools used to grade its severity (Franco et al., 2017; Parulekar et al., 1998; Wong et al., 2006). However, most reports unambiguously indicate that orofacial RAP tends to increase in severity through the course of RT (especially in those cases with established RIM), and episodes of ongoing and untreatable RAP following RT completion have been described in numerous patients (Kallurkar et al., 2019; Karri et al., 2021). Evidence from rigorous systematic reviews and observational (non-interventional) studies have revealed that the pain that arises along with RIM (RIM/RAP) is reported in approximately 80% of patients during RT, and 70% at the completion of treatment (Epstein et al., 2007; Epstein et al., 2010; Epstein et al., 2009). While most HNC patients report baseline levels of discomfort or pain before RT initiation, it appears that the onset of RAP generally mirrors the onset of RIM. In particular, patients usually experience mouth/throat soreness and tenderness within the first week of RT, and escalation of pain intensity generally starts at week 3, peaking at week 5 with episodes of serious pain that can potentially interfere with daily activity and/or lead to treatment alterations (e.g., RT delay, interruption or reduction). After RT completion, RAP can persist for 2 to 4 weeks with a gradual reduction in its severity in most cases (Epstein et al., 2001; Franco et al., 2017; Muzumder et al., 2018). Yet, some studies have indicated that up to 40% of the patients still report varying degrees

of pain 6 months after RT completion and RIM resolution, and 30% can experience spontaneous pain episodes beyond 6 months (Cleeland et al., 2000; Epstein et al., 2010).

1.3.2 Risk factors

Despite the concerning incidence of RAP among HNC patients, only a few studies have identified the potential predictors of RAP in this population. Similar to RIM, it appears that the occurrence and severity of RAP are associated with tumor location (most severe in oral cavity, pharynx and larynx HNC), higher-dose RT courses combined with chemotherapy agents, young age, consumption of food or liquids categorized as spicy, hot, or acidic, and active cigarette smoking. Moreover, patients that have reported pain before RT, use pain medications, feeding tube placement, as well as patients experiencing xerostomia, difficulty swallowing, poor physical and mental health, low levels of activity, sleeping problems, and depressive symptoms seem to have greater risk to develop increasing levels of RAP (Astrup et al., 2015; Chen et al., 2011; Epstein et al., 2009; Huang et al., 2003; Lewis et al., 2013; Logan et al., 2010; Rogers et al., 2012; Scharpf et al., 2009). Unfortunately, the considerable methodological heterogeneity and the inconsistency in results across studies, in addition to the lack of assessment standards for RAP in this particular clinical setting (i.e., RT as single modality for managing HNC), has decreased the certainty of evidence.

1.3.3 Pathogenesis

RAP pathogenesis is multifactorial. As mentioned before, the onset of RAP has been mostly linked to the occurrence of RIM. However, long-lasting episodes of spontaneous RAP can occur in some HNC patients despite RIM resolution, suggesting that RAP might be a phenomenon driven by other molecular/cellular signaling mechanisms that are independent to RIM. In addition,

the author of this work believes that previous episodes of pain in cancer patients – such as those related with the cancer itself, diagnosis methods or preceding cancer therapies (e.g., surgery, chemotherapy) – could potentially boost the onset and severity of RAP by enhancing the magnitude, frequency and duration of synapses in pain-sensing neurons at the peripheral and central nervous system level, phenomenon referred to as peripheral and central sensitization, respectively (Ji et al., 2003; Latremoliere & Woolf, 2009).

1.3.3.1 Acute RAP as a result of acute RIM: Although there is a lack of clarity regarding the nociceptive pathways and mediators of RIM/RAP, it has been hypothesized that RAP as a result of acute RIM appears to have both inflammatory and neuropathic components (Epstein et al., 2009). At the peripheral nervous system, injury and inflammation of the oral mucosa as a result of RT triggers the release of pro-nociceptive mediators from the injured site that will in turn activate and sensitize a subset of specialized sensory neurons that mediate pain (called nociceptors) within the trigeminal system. Specifically, these mediators will modify the intracellular homeostasis of trigeminal nociceptors (predominantly $A\delta$ and C fibers) through the activation of voltage-gated ion channels and/or ligand-gated receptors, increasing the sensitivity (i.e., response to stimuli) and reducing the threshold of excitation of these neurons (Benoliel et al., 2007; Smith & Epstein, 2010). While there is no current evidence regarding the pathogenesis of RIM/RAP at the central nervous system level, it has been theorized that nociceptive information associated to RIM should be propagated proximally toward central nerve terminals of the trigeminal branches. These terminals will then synapse with central neurons of the spinal trigeminal nucleus and will project nociceptive signals to the thalamus and the somatosensory cortical regions, which are the areas of awareness of painful sensation and location (Benoliel et al., 2007; Chung et al., 2021).

Though there is currently no evidence regarding the exact pro-nociceptive mediators involved in RAP processing, pronociceptive actions have been associated with the peptide hormone endothelin-1 (ET-1). In preclinical settings, researchers have demonstrated that ET-1 mediates nociception in all trigeminal branches (Chichorro et al., 2010). Moreover, others have shown that ET-1 is highly secreted in oral squamous cell carcinoma cells, and that the algesic effects of this nociceptive mediator in the tumor microenvironment can be blocked using specific ET-1 antagonists or opioids (Pickering et al., 2008; Quang & Schmidt, 2010). In addition to its neurotrophic features, nerve growth factor (NGF) has also shown to be an important driver of oral pain. NGF is actively secreted by inflammatory cells, and overexpression of NGF in trigeminal ganglia neurons appears to induce pain in animals and humans (Ye et al., 2011). While there is no current information about the role of NGF in RAP pathogenesis, it has been shown in *in vitro* studies that NGF expression is upregulated following irradiation (IR) of both human salivary and submandibular glands (Li et al., 2021). This is particularly interesting because there is evidence showing that NGF is highly expressed by oral cancer cells, and that it plays a key role in mediating oral pain in these models (Dudás et al., 2018; Kolokythas et al., 2010; Ye et al., 2011). Indeed, NGF blockade with anti-NGF monoclonal antibodies seems to reduce IR-induced cell apoptosis and to produce significant mechanical pain relief, normalizing oral function in a mouse model of oral cancer (Ye et al., 2011). Other authors have revealed that TNF- α – a cytokine produced by activated macrophages – is increased in HNC patients undergoing chemoradiation (Akmansu et al., 2005; Watanabe et al., 2010). In patients with active oral mucositis, it has been demonstrated that serum TNF α mRNA is highly overexpressed in buccal samples, and its presence was significantly associated with oral mucositis pain (Fall-Dickson et al., 2007). Within the transient receptor potential (TRP) family of sensory ion-channel proteins, preclinical studies have

demonstrated DNA damage and associated oxidative stress induced by IR activates the transient receptor potential vanilloid-1 (TRPV1) and 4 (TRPV4) channels following oral mucosal trauma (Ito et al., 2017; Masumoto et al., 2013; Ohsaki et al., 2018; Priya et al., 2020). TRPV1 and TRPV4 receptors are abundantly expressed in sensory myelinated A δ and C fibers, and a marked calcium ion influx-mediated depolarization occurs following their activation, which will in turn convey heat/acid and cold/mechanical-sensitive information to the trigeminal system, respectively (Binshtok, 2011; Kobayashi et al., 2005; Shibasaki, 2020; Urata et al., 2015). In a mouse model of RIM, severe glossitis was associated with the upregulation of TRPV1 and 4 channels in trigeminal ganglion neurons, which was accompanied by spontaneous pain-like behaviors. In this study, the genetic deletion of TRPV1 appeared to effectively mitigate these painful responses (Lai et al., 2021).

1.3.3.2 Chronic RAP as a result of delayed complications: In addition to RIM, RT may produce chronic pain syndromes that are difficult to manage within a few months after the end of RT, or even up to several years later, and its course is often progressive and irreversible (Bennett et al., 2019). It has been reported that up to 54% of HNC cases report chronic RAP 6 to 24 months after the end of RT (Srivastava et al., 2015), however, prevalence estimates vary widely across prevalence studies, and no research has sought to determine whether the prevalence of chronic pain in this treatment settings (i.e., RT) is associated to previous RIM/RAP. While it has been hard to identify the causes that ultimately lead to transition from acute to chronic RAP, some studies have theorized that chronic RAP might be a result of delayed response to trauma to adjacent nerves, bones, or soft tissues (Bennett et al., 2019; Edwards et al., 2019), or secondary to vasculature damage within the irradiated field resulting in increased vascular permeability and succeeding fibrin deposition, collagen formation, and fibrosis (Cooper et al., 1995; Delanian et al., 2012). Still,

the recognition of chronic RAP remains a challenge in the clinical practice, and very limited data can be found respecting its pathogenesis among HNC patients treated with RT.

1.3.3.3 Other causes of pain in HNC patients

1.3.3.3.a) Cancer-related sources: Pain due to tumor progression is commonly reported in HNC patients, and is usually what drives patients to pursue consultation with medical oncologists (Epstein et al., 2009). It has been recognized that cancer cells can release, as well as to promote the release of, pronociceptive mediators (e.g., cytokines, interleukins, chemokines, prostanoids, endothelins, growth factors, etc.) that can modify the intracellular homeostasis of surrounding sensory neurons, leading to increased sensitivity to painful stimuli in HNC (as mentioned above) (Amit et al., 2016; Grivennikov et al., 2010; Schmidt, 2015). Clinical interventions also represent an important and often underappreciated source of discomfort in patients. Invasive diagnostic interventions, such as bone marrow biopsy, may cause short-lived and mild discomfort that could promote painful signaling pathways (Hjortholm et al., 2013; Kato et al., 2014; Vanhelleputte et al., 2003).

1.3.3.3.b) Sources related to other cancer-therapies: Treatment in HNC patients is usually multimodal, with surgery, RT, and chemotherapy being the main means for curative management of locally advanced HNC (Nigro et al., 2017). Despite the use of modern surgical techniques, surgery still is a common cause of treatment-related pain in HNC patients (List & Bilir, 2004). Post-operative pain most commonly results from tissue damage, triggering the release of nociceptive (inflammatory and neuropathic) factors that sensitize peripheral and central A δ and C fibers that elicit non-evoked pain, heat and mechanical hyperalgesia (Loeser & Melzack, 1999; Pogatzki-Zahn et al., 2017). Chemotherapy is also a common source of pain in HNC. Commonly used chemotherapy agents include paclitaxel, docetaxel, vincristine, cisplatin, oxaliplatin,

thalidomide, and bortezomib (Burgess et al., 2021). These substances have distinct neurotoxic and neuroinflammatory properties, and similar to RT, they can trigger a series of biological events in response to oxidative stress leading to cell arrest and cell death (Ricci & Zong, 2006). Chemotherapy-induced peripheral neuropathy (CIPN) represents the degeneration and damage of axons triggered by chemotherapeutic agents, and is the best-recognized potential source of pain among cancer patients. CIPN is a major dose-limiting side effect of several chemotherapeutic agents, and it can elicit shock-like pain, as well as mechanical or cold-related allodynia or hyperalgesia (Bernhardson et al., 2007; Starobova & Vetter, 2017).

1.3.4 Diagnosis

RAP has been typically graded by patients using the Visual Analogue Scale (VAS), which rates pain from a score of 0 (no pain) to 10 (maximal experienced pain) (Velez et al., 2014). However, the use of patient-reported outcome questionnaires that rate the severity and interference of pain using functional and quality of life outcomes measures have been shown to be a better approach in cancer patients (Fitzsimmons et al., 2009; Kemmler et al., 1999; Meyer et al., 2009). Indeed, there is strong evidence showing that these health-related quality-of-life instruments can enhance patient-provider communication, improving the assessment of pain and guiding treatment interventions throughout the courses of RT. Several questionnaires are currently available in the literature to either measure in HNC patients' quality of life and/or functional outcomes (e.g., University of Washington Questionnaire (UW-QOL), Head and Neck Performance Status Scale (PSS-HN), Head and Neck Radiotherapy Questionnaire (HNRQ)), or oral pain directly (e.g., University of California San Francisco (UCSF) Oral Cancer Pain Questionnaire) (Heutte et al., 2014). However, the Oral Mucositis Weekly Questionnaire-Head and Neck Cancer (OMWQ-HN) appears to have superior sensitivity in comparison to other questionnaires to detect early changes

in pain related to RIM. This scale is composed of 12 items designed to assess pain using global health and quality of life measures, and captures data on the impact of mouth and throat soreness on sleeping, swallowing, drinking, eating, talking, brushing teeth (Epstein et al., 2007; Franco et al., 2017).

1.3.5 Management

Because RAP is usually associated with oral mucositis, current strategies for pain management rely on general treatment for acute RIM (i.e., BOC practices and symptomatic relief). In the most recent MASCC/ISOO guidelines for the management of RIM, morphine-based analgesia was listed as the only recommended alternative for RAP palliation (Elad et al., 2020). While patient-controlled analgesia with systemic morphine or transdermal fentanyl is suggested for some patients undergoing RT experiencing great levels of RIM/RAP, the risk to develop opioid-associated side effects (e.g., addiction, intoxication, and death) is high (Zayed et al., 2021). Therefore, methods of topical opioid-based medication delivery that may produce local effects with little risk of systemic effects have been developed, such as mouthwashes. Currently, the use of morphine mouthwash (0.2% solution) has been listed as the most effective topical strategy to reduce pain in HNC patients treated with chemoradiotherapy (Cerchietti, 2007; Elad et al., 2020; Lalla et al., 2014; Vayne-Bossert et al., 2010). Nonsteroidal anti-inflammatory (NSAIDs) drugs have also been formulated in mouthwash solutions. Besides its anti-inflammatory properties, benzydamine hydrochloride also has anesthetic and analgesic properties, and benzydamine-based mouthwashes have been recommended to relieve pain in patients who are receiving moderate doses of RT without concomitant chemotherapy (Elad et al., 2020; Sheibani et al., 2015). Topical formulations containing aspirin and/or corticosteroids have also been suggested to be effective in managing RAP, however data are not considered strong (Brennan et al., 2020; Robertson, 2016).

Certain agents with analgesic properties such as tricyclic antidepressants (e.g., doxepin 0.5% mouthwash) and antiepileptic agents (e.g., gabapentin 5% mouthwash) have been also tested for the management of RAP (S. Ala et al., 2020; Cook et al., 2022; Epstein et al., 2008; Leenstra et al., 2014; Starmer et al., 2014). While the use of these agents has shown promising results enhancing pain management and preventing escalating doses of opioids in HNC patients with RIM/RAP, the current literature provides no robust evidence (insufficient or conflicting evidence) regarding their efficacy and safety to support their use in these clinical settings. Similarly, the use of topical solutions containing local anesthetics (e.g., lidocaine) has been proposed to control mucosal sensitivity (Silva et al., 2017; Yamashita et al., 2002), however, results from studies have consistently failed to demonstrate a benefit that would support in its use for managing RAP (Barasch et al., 2006; Elad et al., 2020).

With respect to complementary alternatives to treat RAP, methods to relieve salivary hypofunction and/or xerostomia (dry mouth) as a result of RT are highly recommended to palliate the discomfort associated to food intake and to the continuous friction between mucosal surfaces and teeth (Ariyawardana et al., 2019; Lalla et al., 2014). The agent Gelclair, for example, is a concentrated bioadherent oral gel (composition: polyvinylpyrrolidone, sodium hyaluronate, and glycyrrhetic acid) approved by the FDA to reduce oral mucositis symptom. Gelclair is applied to the surface of the oral mucosa in the form of a viscous gel that forms a protective adhesive barrier over the surface of the epithelium (Cawley & Benson, 2005; Lindsay et al., 2009). According to several interventional studies, it appears that this gel offers rapid and durable pain relief (five to seven hours post-application) in patients with oral lesions, and experts have recommended that Gelclair should be use at least one hour before meals (Barber et al., 2007; Flook et al., 2005; Innocenti et al., 2002; McKenzie et al., 2006; Short & Fung, 2008). Other relevant

non-pharmaceutical pain-relief strategies focus on relieving the psychological side-effect related to the occurrence of RAP, such as anxiety, depression, mood disturbances, distress, and emotional challenges (Thomas et al., 2010). Indeed, the use of music therapy (O’Callaghan et al., 2007), hypnosis (Stalpers et al., 2005), aromatherapy massages (Wilkinson et al., 2007), meditation (Matchim & Armer, 2007), or acupuncture (Johnstone et al., 2001), just to name a few, have shown to be effective tools for coping the effects of RAP, however, the results may vary across patients.

1.4 Clinical implications of RIM/RAP

In general, the presence of RIM/RAP negatively affects three distinct components in HNC patients: the function of the oral cavity, the patient’s quality of life, and the success of treatment (Epstein et al., 2001; Franco et al., 2017; Shu-Ching, 2019).

1.4.1 Oral function

The presence of RIM/RAP has been highly associated with nutritional deficits. HNC patients often experience a combination of events that compromise the oral function as a result of severe mucosal ulceration, including anorexia, dysphagia, xerostomia, and taste alterations (Shih et al., 2003). Using health-related quality-of-life instruments, such as the OMWQ-HN, studies have reported that more than half of HNC patients complain of mouth and throat soreness over the course of treatment and after, accompanied by dry mouth and difficulty to chew and swallow solid food or liquids (Franco et al., 2017; Murphy et al., 2009). Moreover, RT can also damage taste buds, causing temporary or permanent taste alternations or loss. Indeed, some patients have reported decreased taste sensations or even difficulty tolerating bitter, sour, or sweet foods, while others have a reported metallic taste in their mouths after eating (Madeya, 1996; McLaughlin & Mahon, 2014). Additionally, RIM/RAP is often associated with a decreased production of saliva

in the oral cavity (related to salivary gland damage induced by RT), making eating and drinking much more difficult (Jensen et al., 2003). Ultimately, these oral complications can lead to a decrease in oral intake, as well as to increase the need for enteral/parental nutrition, resulting in a noticeable weight loss and dehydration (Ackerman et al., 2018; Bressan et al., 2016).

1.4.2 Quality of life

Alterations in nutrition and oral intake deficits have a profound effect on the patient's psychological status and quality of life (Brown & Wingard, 2004). Cross-sectional comparison studies have determined that the oral complications mentioned above, in addition to speech difficulties that arise from these complications, are strongly correlated to low quality-of-life scores (OMWQ-HN scale) (Epstein et al., 2007). Certainly, high levels of depression, fatigue, anxiety, emotional distress and even suicidal ideation can result from these comorbidities, especially when patients are in pain (Chang et al., 2019; Franco et al., 2017). Additionally, these symptoms can have a great impact on the activities of daily living, such as enjoyment of food and social interactions (Borbasi et al., 2002). It has been reported that the patients' social life can be dramatically reduced when RIM/RAP and associated comorbidities coexist. People tend to avoid social gatherings, especially when these meetings involve eating or drinking (Epstein et al., 2007; Morgan et al., 2011). Furthermore, the incremental cost of cancer therapy when RIM/RAP is established in HNC patients is high (i.e., \$1700-\$6000, depending on the grade), heavily impacting the patient's quality of life (Elting et al., 2007). When symptoms are severe, RIM/RAP can lead to increased work absence or decreased active employment rates (Carlotto et al., 2013), as well as to increase the cost of care. These costs include the need for prescription medications (e.g., opioids), additional diagnostic tests and procedures, transportation and health care supplies, admission and prolonged periods in the hospital, ICU admissions, interventional procedures and

intensive supportive care (e.g., intravenous fluids, feeding tubes), and/or psychosocial interventions (Murphy et al., 2009; Peterman et al., 2001).

1.4.3 Success of cancer treatment

As mentioned before, severe and uncontrolled RIM/RAP can lead to the need to interrupt or delay RT to alleviate symptoms, thus compromising local control and overall survival. Clinical research indicates that RIM/RAP is the primary cause of unplanned treatment modifications in HNC patients (Russo et al., 2008). As matter of fact, unplanned RT breaks/delays are significantly more common among patients with pain associated with ulcerative RIM (3.8-fold increase), with incidences ranging from 11% to 46,8% (Bese et al., 2007; Trotti et al., 2003; Vera-Llonch et al., 2006). RT breaks/delays related to RIM/RAP most commonly occur after the 5th week of RT initiation (Mallick et al., 2016), when the doubling time of tumor stem cell repopulation (i.e., length of time required to double a value given a consistent growth rate) is significantly accelerated (about 4 days) in comparison to the second week of RT (about 60 days) (Withers et al., 1988). In the field of radiation biology, the phenomenon of repopulation during a course of RT has been found to be one the cause of early recurrence and lower overall survival in HNC, and it has been reported that every additional day of delay in RT is associated with a 1%-2% lower 5-year relapse-free survival rate (Suwinski et al., 2003). Consequently, patients with inadequate control of pain are particularly prone to treatment failure (Brown & Farquhar-Smith, 2017; Massa et al., 2017; Russo et al., 2008; Vera-Llonch et al., 2006).

1.5 Preclinical models of radiation-induced mucositis and pain

Although clinical studies have undoubtedly contributed to yield information about the efficacy and safety of differing strategies to manage RIM/RAP, preclinical research remains the

cornerstone to advance our understanding about the mechanisms related to its pathophysiology. To date, several animal models of irradiation-induced mucositis have been designed to elucidate the mechanism of mucosal injury and to create new and effective potential antimucotoxic agents.

In 1990, the first model of mucositis secondary to cancer therapy was developed in mice (i.e., tongue and snout mucositis) to study the effects of single or fractionated doses of IR in epithelial repopulation. Using a Seifert Isovolt 320 X-ray machine, Dörr and colleagues were able to design a successful model of severe but reversible RIM in 10- to 12-week-old female mice (Dörr & Kummermehr, 1990). This model has evolved over the years to include chemotherapy and, therefore, replicating the damage triggered by chemoradiation (CRT) in cancer patients (Dörr, 2000; Dörr, Hamilton, et al., 2002). The discovery of the protective role of growth factors, such as the keratinocyte growth factor, in the oral mucosa possibly represent one of the most important contributions of this model. Palifermin has been extensively tested by Dörr's research group to determine whether this drug can successfully regenerate mucosa in their mouse model (Dörr, Bässler, et al., 2005; Dörr, Heider, et al., 2005; Dörr et al., 2001; Dörr, Spekl, & Farrell, 2002; Dörr, Spekl, et al., 2002). In these studies, palifermin consistently reduced the incidence of confluent oral mucositis induced by either IR (single or daily fractionated IR) or CRT, which resulted in a long-lasting inhibition of irradiation-induced inflammatory and immune changes in the mouse tongue. These findings later promoted the conduct of randomized, placebo-controlled clinical trials in HNC patients, where it was proven that weekly palifermin (120 µg/kg per week) was able to decrease the severity and time of onset of oral mucositis in patients undergoing postoperative CRT (Henke et al., 2011; Le et al., 2011; Vadhan-Raj et al., 2010; Vadhan-Raj et al., 2013). However, the safety of palifermin has not been established in HNC patients with nonhematologic malignancies, and moreover, its use has not consistently demonstrated better

patient-reported quality of life outcomes (Bossi et al., 2012; Fromme et al., 2004) (Bossi et al., 2012; Fromme et al., 2004).

The hamster model has also been used to model oral mucositis as a result of cancer therapy. Also in 1990, the first model of chemotherapy-induced mucositis (buccal cheek pouch mucositis) was developed (Sonis et al., 1990), allowing to extend the current understanding about the underlying four phases of mucositis development (i.e., inflammatory/vascular, epithelial, ulcerative/bacteriological, and healing phases) (Sonis, 2004a, 2004b). Later, this hamster model was adapted and designed to study oral mucositis as a consequence of IR (single or fractionated IR) and CRT (Alvarez et al., 2003; Watkins et al., 2010), and it has been used to test many agents, such as keratinocyte, fibroblast and epidermal growth factors, transforming growth factor β , interleukin-11, among others (Alvarez et al., 2003; Ara et al., 2008; Sonis et al., 1997; Sonis et al., 1992).

The rat model has mostly been used to study oral and gastrointestinal mucositis as a consequence of chemotherapy (Howarth et al., 2006; Takeuchi et al., 2020; Vanhoecke et al., 2015), however, some models of oral mucositis induced by IR (single dose) alone or in combination to chemotherapy has also been utilized to study the protective benefit of some agents in RIM, such as propolis, sumatriptan, alpha lipoic acid, epidermal growth factors inhibitors, and N-acetylcysteine (M. Ala et al., 2020; Deniz, 2011; Kim et al., 2020; Kim et al., 2017; Lee et al., 2007; Rezvani & Ross, 2004). However, and comparing to the mouse and hamster models, achieving mucosal damage can be challenging due to the highly keratinized nature of the rat epithelium. Therefore, the relatively resistant feature of this animal model to develop RIM has limited its use in basic research (Gibson et al., 2010).

Despite the vast amount of work dedicated to study RIM, there is no current investigation in the literature addressing the research of RAP in preclinical settings. Indeed, all the aforementioned studies have only assumed the presence of RAP using RIM severity and body weight loss as proxy indicators. Moreover, and while some investigators have dedicated great effort to develop standardized outcomes measures of orofacial pain in small laboratory animals (Anderson et al., 2013; Dolan et al., 2010; Neubert et al., 2008; Neubert et al., 2005; Rossi et al., 2006), none of these assays have been used to measure acute, orofacial RAP in this species. There has been some speculation on the mechanisms underlying RAP based on the current understanding of RIM and the pain descriptors reported by HNC patients undergoing RT (Epstein et al., 2009). Based on this evidence, one can assume that RAP pathophysiology may involve inflammatory and neuropathic pain mechanisms. Yet, this is not sufficient evidence to determine the exact mechanism by which RAP is generated. Certainly, the unavailability of valid animal models of RAP, as well as the lack of assessment tools to monitor the onset and progression RAP, can be major impediments in the discovery of the signalling pathways driving RAP and potentially explain why the management of RAP continues to be suboptimal in HNC.

In the last years, our laboratory has dedicated a lot of research effort to fill some of these gaps in knowledge by developing our own mouse model of RIM (Lai et al., 2021; Nolan et al., 2017). According to this work, experimentally-induced RIM (glossitis) can be modeled using a single high-dose fraction (27 Gy) of lingual IR. In our model, mice usually develop clinical signs of oral mucositis (e.g., slight redness of the oral mucosa to severe inflammation and ulceration) 10 to 12 days after IR, which is accompanied by severe body weight loss. The severity of RIM quickly decreases after this, and 19-21 days after IR we tend to see signs of complete RIM resolution and weight gain. In addition, we have developed outcome measures to evaluate the pain associated

with RIM using two different strategies: 1) the eye wiping assay: a withdrawal reflex-based assay designed to indirectly measure the activation of afferent neurons in the ophthalmic branch of the trigeminal nerve and potential cross-sensitization of other branches, and 2) the burrowing assay: a non-reflexive voluntary pain-related behavior assay commonly used in pain research to measure well-being and/or the impact of pain in normal rodent activities (Lai et al., 2021; Nolan et al., 2017; Price et al., 2021). Both of these assessment tools have helped to refine the characterization of RAP in our model of RIM, in addition to improve our understanding (at least preliminarily) about the complex multidimensional state of RAP. Indeed, these findings represent an important first step to theorize that RAP processing potentially have both sensory and affective dimensions, and therefore, we could use these tools in future investigations to determine what neural circuits contribute to the integration of the different dimensions of RAP and, ultimately, identify and develop better and safer mechanism-based therapies for RAP that will improve the treatment outcomes in HNC.

Although undeveloped models represent an important source of lack of success in translating findings from animal models to clinical studies, the inherent differences between species can also contribute in this “clinical trial-lost in translation” (De Jong & Maina, 2010; Mak et al., 2014; Mankoff et al., 2004). To overcome this gap, several authors have proposed that the study of naturally-occurring diseases in companion animals (e.g., veterinary patients) might help to bridge basic and clinical research (Christopher, 2015; Kol et al., 2015; Lascelles et al., 2018; Paoloni & Khanna, 2008). Over the last 2 decades, translational research investigations in dogs with spontaneous diseases have gain great visibility in the biomedical research community. Indeed, the integration of pet dogs in the preclinical proof-of-concept stages of certain diseases, such as canine osteosarcoma and osteoarthritis, has demonstrated to be a valuable approach to answer

questions that would have been difficult or impossible to answer in rodents alone (Black et al., 2007; Brown et al., 2015; Iadarola et al., 2018; LaRue et al., 1989; Minnema et al., 2020; Ranieri et al., 2013; Regan et al., 2018). In the field of oncology research, there is a growing interest in exploiting naturally-occurring cancers in dogs to investigate innovative therapeutic approaches. Certainly, the low translation success rate of preclinical cancer studies emphasizes the idea that laboratory small animals, such as mice and rats, might not be the best models to define the safety and activity of new anticancer agents. In contrast, tumor-bearing dogs appear to be better in capturing the “essence” of the complex nature and evolution of human malignancies, as well as to recapitulate the clinical responses to conventional cancer treatments as those observed in human patients (Alvarez, 2014; Gordon et al., 2009; Hahn et al., 1994; Hay et al., 2014; Rowell et al., 2011; Tarone et al., 2019). Under this auspice, the author of this literature review believes that preclinical models of canine HNC might enhance and accelerate the development of new and effective therapies for the management of RT-induced toxicities that would both benefit humans and pets. Unfortunately, and while it has been reported in few veterinary studies that dogs can also experience dose-limiting toxicities – such as RIM – during the treatment of HNC (Gieger et al., 2008; Hunley et al., 2010; LaDue-Miller et al., 1996; Mosca et al., 2021; Riggs et al., 2018), currently there is insufficient evidence to determine whether pet dogs are the most appropriate animal model for testing novel therapeutics for the management of RIM/RAP.

1.6 Rationale for this work: pain as a driver of cancer progression

In 1993, Page and colleagues proposed the idea that pain might be an important promoter of cancer (Page et al., 1993). In this study, they first showed in a rat model of breast carcinoma that surgery (i.e., laparotomy) significantly increased lung tumor burden and enhanced metastasis.

Because they were not able to measure pain in this study (lack of appropriate assessment tools), they initially theorized that this effect could possibly be attributable to the suppressive effects of surgery on the immune response. However, and as a first step to validate the theory that pain can enhance tumor progression, in subsequent experiments they gave a single pre- or postoperative dose of morphine (as a pain reliever) or vehicle solution in animals that either received surgery or anesthesia only and that were inoculated with tumor cells 5 hours post-surgery or sham-surgery. Remarkably, they show in these experiments that analgesic treatment blocked enhanced metastatic colonization in operated animals not receiving analgesics, an effect that was not observed in non-operated animals who were not experiencing pain. The concept of pain promoting cancer was then supported in later *in vivo* studies that demonstrated that preoperative systemic opioids (i.e., fentanyl) or intrathecal administration of bupivacaine plus morphine reduced surgery-induced tumor progression in rats (Page & Ben-Eliyahu, 2002; Page et al., 2001), and in *in vitro* studies where it was evidenced that inhibitors of voltage-activated sodium channels, such as local anesthetics (e.g., lidocaine and ropivacaine), can per se inhibit cancer cell growth and tumor cell signaling pathways (Baptista-Hon et al., 2014; Martinsson, 1999). Supporting these research findings in rodent models, retrospective clinical data have also indicated a potential role of pain in cancer progression. Patients with painful episodes (either arising from treatment or from the tumor and/or adjacent tissues) are more at risk to experience recurrence or metastasis during follow-up (Exadaktylos et al., 2006; Groome et al., 2006; Russo et al., 2008).

Currently, the mechanisms that underlie pain-associated tumor progression are unknown, but it has been theorized that the ability of neuronal and non-neuronal cells to produce neurotrophic factors after nerve injury is likely exploited by cancer cells to create a microenvironment that may promote angiogenesis, tumor cell invasion and propagation along neuronal structures (Ceyhan et

al., 2009; Ceyhan et al., 2008; Demir et al., 2010; Demir et al., 2015). The perineural invasion (PNI) phenomenon in pancreatic cancers (i.e., pancreatic ductal adenocarcinoma [PDAC]) is an excellent example of this effect. PNI has its highest prevalence in PDAC (70-98%), and it represents the ability of cancer cells to invade the neuronal sheath of innervating nerves to promote neoplastic proliferation and spread (Demir et al., 2012; Gasparini et al., 2019). Interestingly, PNI and some of the molecules that contribute to PNI and pain onset have also been associated with the progression and/or prognosis of oral tongue squamous cell carcinoma (Hirose et al., 2016; Liang et al., 2016; Shen et al., 2014; Yu et al., 2014). Relevant to RAP, it has been demonstrated that neurotrophic factors such as NGF can be released by cancer cells and promote PNI, which in turn upregulates TRPV1 (Jiang et al., 2020; Zhang et al., 2005; Zhu et al., 2011), promoting the production of ‘pain signals’. As mentioned before, RIM has been associated with upregulation of TRPV1 channels, and several lines of evidence support the idea that blocking the cascade of signals triggered by TRPV1 represents one promising approach to treat RIM and associated pain (Ito et al., 2017; Lai et al., 2021; Nolan et al., 2017; Price et al., 2021). Interestingly, TRPV1 is overexpressed in several cancer types, such as oral squamous cell carcinoma, prostate, colon, and pancreatic cancers (Dömötör et al., 2005; Gonzales et al., 2014; Hartel et al., 2006; Sánchez et al., 2005), pointing out to the idea that TRPV1 might play a relevant role mediating RAP and promoting its tumor-promoting effect.

1.7 Overview of work in this dissertation

Despite the above cited work indicating that pain, and indeed RAP, may be associated with tumor progression, the association is far from proven. The primary aim of this body of work was to determine if RAP promotes tumor progression as a prerequisite to investigations of the signaling

mechanisms that may be involved, and thence onto therapeutic development. To do that, we had to further refine our murine model of RIM, and the outcome measures of RAP. As mentioned before, our laboratory has dedicated a lot of research effort to develop a mouse model of RIM (Lai et al., 2021; Nolan et al., 2017). However, additional characterization is required to maximize the translational utility of our mouse model. In Chapter 2, we tested the reliability of a new behavioral test battery (based on nesting and grooming behaviors) that was designed to measure the impact of RIM/RAP on animal welfare. After developing and validating the use of these behavioral measures to assess RAP in our mouse model of RIM, we assessed the influence of RAP on tumor progression in Chapter 3. The tumor-promoting effect of RAP was studied using a tail vein model of pulmonary metastasis. At the time of maximal RAP, three cell lines were injected (4T1, B16F10, MOC2; each paired to their syngeneic host: BALB/c or C57BL/6), and we assessed tumor progression using *in vivo* transthoracic bioluminescence imaging, *ex vivo* pulmonary nodule quantification, and/or survival analysis. Because we confirmed in Chapter 2 that the severity of RIM and RAP can be significantly reduced using resiniferatoxin (a highly selective TRPV1 agonist that causes ablation of TRPV1-expressing neurons) in BALB/c mice, we assessed changes in the progression of tumors when RAP was mitigated using ablation of TRPV1-expressing neurons. This ‘analgesic strategy’ was associated with high mortality in certain strains of mice; therefore, we explored the tolerability and ablative efficacy of different doses of resiniferatoxin under different experimental conditions (Chapter 4). Because companion dogs, like people, suffer from the spontaneous development of HNC and experience similar comorbidities (such as oral mucositis pain following RT), we were interested in investigating whether companion dogs with naturally-occurring HNC represent a suitable model to study potential interventions to prevent and treat human RIM/RAP. However, there is little information in the literature about the clinical features

of RIM in this species, and moreover, there are no assessment tools designed to measure orofacial RAP. Therefore, and as a first step towards developing this model, in Chapter 5 we characterized the clinical course, severity and potentially related side-effects of RIM in pet dogs undergoing definitive-intent RT for the treatment of oral, nasal, and cranial cavity tumors, and we assessed aspects of reliability and validity of a novel client metrology instrument designed to measure orofacial pain in this species.

1.8 References

- Ackerman, D., Laszlo, M., Provisor, A., & Yu, A. (2018). Nutrition Management for the Head and Neck Cancer Patient. In E. Maghami & A. S. Ho (Eds.), *Multidisciplinary Care of the Head and Neck Cancer Patient* (pp. 187-208). Springer International Publishing.
- Adrien, J., Bertolus, C., Gambotti, L., Mallet, A., & Baujat, B. (2014). Why are head and neck squamous cell carcinoma diagnosed so late? Influence of health care disparities and socio-economic factors. *Oral oncology*, 50(2), 90-97.
- Akmansu, M., Unsal, D., Bora, H., & Elbeg, S. (2005). Influence of locoregional radiation treatment on tumor necrosis factor- α and interleukin-6 in the serum of patients with head and neck cancer. *Cytokine*, 31(1), 41-45.
- Ala, M., Jafari, R. M., Ala, M., Agbele, A. T., Hejazi, S. M., Tavangar, S. M., Mahdavi, S. R. M., & Dehpour, A. R. (2020). Sumatriptan alleviates radiation-induced oral mucositis in rats by inhibition of NF-kB and ERK activation, prevention of TNF- α and ROS release. *Archives of oral biology*, 119, 104919.
- Ala, S., Zamani, N., Akbari, J., Salehifar, E., Janbabai, G., & Koulaeinejad, N. (2020). Efficacy of gabapentin mouthwash in managing oral mucositis pain in patients undergoing chemotherapy: a prospective, randomised, double-blind, controlled clinical trial. *Scottish Medical Journal*, 65(1), 12-18.
- Alterio, D., Marvaso, G., Ferrari, A., Volpe, S., Orecchia, R., & Jereczek-Fossa, B. A. (2019). Modern radiotherapy for head and neck cancer. *Seminars in oncology* (Vol. 46, No. 3, pp. 233-245). WB Saunders.
- Alvarez, C. E. (2014). Naturally occurring cancers in dogs: insights for translational genetics and medicine. *ILAR journal*, 55(1), 16-45.

- Alvarez, E., Fey, E. G., Valax, P., Yim, Z., Peterson, J. D., Mesri, M., Jeffers, M., Dindinger, M., Twomlow, N., & Ghatpande, A. (2003). Preclinical characterization of CG53135 (FGF-20) in radiation and concomitant chemotherapy/radiation-induced oral mucositis. *Clinical Cancer Research*, 9(9), 3454-3461.
- Alzahrani, R., Obaid, A., Al-Hakami, H., Alshehri, A., Al-Assaf, H., Adas, R., Alduhaibi, E., Alsafadi, N., Alghamdi, S., & Alghamdi, M. (2020). Locally advanced oral cavity cancers: what is the optimal care? *Cancer Control*, 27(1), 1073274820920727.
- Amit, M., Na'Ara, S., & Gil, Z. (2016). Mechanisms of cancer dissemination along nerves. *Nature reviews Cancer*, 16(6), 399-408.
- Anderson, E. M., Mills, R., Nolan, T. A., Jenkins, A. C., Mustafa, G., Lloyd, C., Caudle, R. M., & Neubert, J. K. (2013). Use of the Operant Orofacial Pain Assessment Device (OPAD) to measure changes in nociceptive behavior. *JoVE (Journal of Visualized Experiments)* (76), e50336.
- Ara, G., Watkins, B. A., Zhong, H., Hawthorne, T. R., Karkaria, C. E., Sonis, S. T., & Larochele, W. J. (2008). Velafermin (rhFGF-20) reduces the severity and duration of hamster cheek pouch mucositis induced by fractionated radiation. *International journal of radiation biology*, 84(5), 401-412.
- Argiris, A., Karamouzis, M. V., Raben, D., & Ferris, R. L. (2008). Head and neck cancer. *The Lancet*, 371(9625), 1695-1709.
- Ariyawardana, A., Cheng, K. K. F., Kandwal, A., Tilly, V., Al-Azri, A. R., Galiti, D., Chiang, K., Vaddi, A., Ranna, V., Nicolatou-Galitis, O., Lalla, R. V., Bossi, P., Elad, S., & On behalf of the Mucositis Study Group of the Multinational Association of Supportive Care in Cancer/International Society for Oral, O. (2019). Systematic review of anti-inflammatory

- agents for the management of oral mucositis in cancer patients and clinical practice guidelines. *Supportive Care in Cancer*, 27(10), 3985-3995.
- Astrup, G. L., Rustøen, T., Miaskowski, C., Paul, S. M., & Bjordal, K. (2015). Changes in and predictors of pain characteristics in patients with head and neck cancer undergoing radiotherapy. *Pain*, 156(5), 967-979.
- Aupérin, A. (2020). Epidemiology of head and neck cancers: an update. *Current opinion in oncology*, 32(3), 178-186.
- Baptista-Hon, D. T., Robertson, F. M., Robertson, G. B., Owen, S. J., Rogers, G. W., Lydon, E. L., Lee, N. H., Hales, T. G., & Buggy, D. J. (2014). Potent inhibition by ropivacaine of metastatic colon cancer SW620 cell invasion and NaV1.5 channel function. *BJA: British Journal of Anaesthesia*, 113(suppl_1), i39-i48.
- Barasch, A., Elad, S., Altman, A., Damato, K., & Epstein, J. (2006). Antimicrobials, mucosal coating agents, anesthetics, analgesics, and nutritional supplements for alimentary tract mucositis. *Supportive Care in Cancer*, 14(6), 528-532.
- Barber, C., Powell, R., Ellis, A., & Hewett, J. (2007). Comparing pain control and ability to eat and drink with standard therapy vs Gelclair: a preliminary, double centre, randomised controlled trial on patients with radiotherapy-induced oral mucositis. *Supportive Care in Cancer*, 15(4), 427-440.
- Bennett, M. I., Kaasa, S., Barke, A., Korwisi, B., Rief, W., & Treede, R.-D. (2019). The IASP classification of chronic pain for ICD-11: chronic cancer-related pain. *Pain*, 160(1), 38-44.
- Benoliel, R., Epstein, J., Eliav, E., Jurevic, R., & Elad, S. (2007). Orofacial pain in cancer: part I—mechanisms. *Journal of dental research*, 86(6), 491-505.

- Bernhardson, B.-M., Tishelman, C., & Rutqvist, L. E. (2007). Chemosensory changes experienced by patients undergoing cancer chemotherapy: a qualitative interview study. *Journal of pain and symptom management*, 34(4), 403-412.
- Bese, N. S., Hendry, J., & Jeremic, B. (2007). Effects of prolongation of overall treatment time due to unplanned interruptions during radiotherapy of different tumor sites and practical methods for compensation. *International Journal of Radiation Oncology* Biology* Physics*, 68(3), 654-661.
- Binshtok, A. M. (2011). Mechanisms of nociceptive transduction and transmission: a machinery for pain sensation and tools for selective analgesia. *International review of neurobiology*, 97, 143-177.
- Black, L. L., Gaynor, J., Gahring, D., Adams, C., Aron, D., Harman, S., Gingerich, D. A., & Harman, R. (2007). Effect of adipose-derived mesenchymal stem and regenerative cells on lameness in dogs with chronic osteoarthritis of the coxofemoral joints: a randomized, double-blinded, multicenter controlled trial. *Veterinary Therapeutics*, 8(4), 272.
- Blakaj, A., Bonomi, M., Gamez, M. E., & Blakaj, D. M. (2019). Oral mucositis in head and neck cancer: Evidence-based management and review of clinical trial data. *Oral Oncology*, 95, 29-34.
- Blijlevens, N., & Sonis, S. (2007). Palifermin (recombinant keratinocyte growth factor-1): a pleiotropic growth factor with multiple biological activities in preventing chemotherapy- and radiotherapy-induced mucositis. *Annals of Oncology*, 18(5), 817-826.
- Bonner, J. A., Harari, P. M., Giralt, J., Cohen, R. B., Jones, C. U., Sur, R. K., Raben, D., Baselga, J., Spencer, S. A., Zhu, J., Youssoufian, H., Rowinsky, E. K., & Ang, K. K. (2010). Radiotherapy plus cetuximab for locoregionally advanced head and neck cancer: 5-year

- survival data from a phase 3 randomised trial, and relation between cetuximab-induced rash and survival. *The Lancet Oncology*, 11(1), 21-28.
- Borbasi, S., Cameron, K., Quedsted, B., Olver, I., To, B., & Evans, D. (2002). More Than a Sore Mouth: Patients' Experience of Oral Mucositis [Article]. *Oncology nursing forum*, 29(7), 1051.
- Borsetto, D., Fussey, J., Fabris, L., Bandolin, L., Gaudio, P., Phillips, V., Polesel, J., & Boscolo-Rizzo, P. (2020). HCV infection and the risk of head and neck cancer: A meta-analysis. *Oral oncology*, 109, 104869.
- Bose, P., Brockton, N. T., & Dort, J. C. (2013). Head and neck cancer: from anatomy to biology. *International journal of cancer*, 133(9), 2013-2023.
- Bossi, P., Locati, L. D., & Licitra, L. (2012). Palifermin in prevention of head and neck cancer radiation-induced mucositis: not yet a definitive word on safety and efficacy profile. *Journal of clinical oncology: official journal of the American Society of Clinical Oncology*, 30(5), 564-565; 565.
- Bowen, J., Elad, S., Hutchins, R., & Lalla, R. (2013). Methodology for the MASCC/ISOO mucositis clinical practice guidelines update. *Supportive Care in Cancer*, 21(1), 303-308.
- Bray, F., Ferlay, J., Soerjomataram, I., Siegel, R. L., Torre, L. A., & Jemal, A. (2018). Global cancer statistics 2018: GLOBOCAN estimates of incidence and mortality worldwide for 36 cancers in 185 countries. *CA: a cancer journal for clinicians*, 68(6), 394-424.
- Brennan, P. A., Lewthwaite, R., Sakthithasan, P., McGuigan, S., Donnelly, O., Alam, P., Gomez, R. S., & Fedele, S. (2020). Diclofenac Mouthwash as a potential therapy for reducing pain and discomfort in chemo-radiotherapy-induced oral mucositis. *Journal of Oral Pathology & Medicine*, 49(9), 956-959.

- Bressan, V., Stevanin, S., Bianchi, M., Aleo, G., Bagnasco, A., & Sasso, L. (2016). The effects of swallowing disorders, dysgeusia, oral mucositis and xerostomia on nutritional status, oral intake and weight loss in head and neck cancer patients: A systematic review. *Cancer Treatment Reviews*, 45, 105-119.
- Brown, C. G., & Wingard, J. (2004). Clinical consequences of oral mucositis¹ ¹The opinions or assertions contained herein are the private views of the author and are not to be construed as official or as reflecting the views of the Department of the Army or the Department of Defense. *Seminars in Oncology Nursing*, 20(1), 16-21.
- Brown, D. C., Agnello, K., & Iadarola, M. J. (2015). Intrathecal resiniferatoxin in a dog model: efficacy in bone cancer pain. *Pain*, 156(6), 1018-1024.
- Brown, M., & Farquhar-Smith, P. (2017). Pain in cancer survivors; filling in the gaps. *BJA: British Journal of Anaesthesia*, 119(4), 723-736.
- Brzozowska, A., & Gołębiowski, P. (2019). Acute radiation-induced oral mucositis in patients subjected to radiotherapy due to head and neck cancer. *Polish Journal of Public Health*, 129(1).
- Burgess, J., Ferdousi, M., Gosal, D., Boon, C., Matsumoto, K., Marshall, A., Mak, T., Marshall, A., Frank, B., & Malik, R. A. (2021). Chemotherapy-Induced Peripheral Neuropathy: Epidemiology, Pathomechanisms and Treatment. *Oncology and therapy*, 9(2), 385-450.
- Carlotto, A., Hogsett, V. L., Maiorini, E. M., Razulis, J. G., & Sonis, S. T. (2013). The Economic Burden of Toxicities Associated with Cancer Treatment: Review of the Literature and Analysis of Nausea and Vomiting, Diarrhoea, Oral Mucositis and Fatigue. *Pharmacoeconomics*, 31(9), 753-766.

- Cawley, M. M., & Benson, L. M. (2005). Current trends in managing oral mucositis. *Clinical journal of oncology nursing*, 9(5).
- Cerchietti, L. (2007). Morphine mouthwashes for painful mucositis. *Supportive care in cancer*, 15(1), 115-116.
- Ceyhan, G. O., Bergmann, F., Kadihasanoglu, M., Altintas, B., Demir, I. E., Hinz, U., Müller, M. W., Giese, T., Büchler, M. W., & Giese, N. A. (2009). Pancreatic neuropathy and neuropathic pain—a comprehensive pathomorphological study of 546 cases. *Gastroenterology*, 136(1), 177-186. e171.
- Ceyhan, G. O., Demir, I. E., Altintas, B., Rauch, U., Thiel, G., Müller, M. W., Giese, N. A., Friess, H., & Schäfer, K.-H. (2008). Neural invasion in pancreatic cancer: a mutual tropism between neurons and cancer cells. *Biochemical and biophysical research communications*, 374(3), 442-447.
- Chang, D. C., Chen, A. W. G., Lo, Y. S., Chuang, Y. C., & Chen, M. K. (2019). Factors associated with suicidal ideation risk in head and neck cancer: A longitudinal study. *The Laryngoscope*, 129(11), 2491-2495.
- Chen, S.-C., Liao, C.-T., & Chang, J. T.-C. (2011). Orofacial pain and predictors in oral squamous cell carcinoma patients receiving treatment. *Oral Oncology*, 47(2), 131-135.
- Chichorro, J. G., Fiuza, C. R., Bressan, E., Claudino, R. F., Leite, D. F., & Rae, G. A. (2010). Endothelins as pronociceptive mediators of the rat trigeminal system: role of ETA and ETB receptors. *Brain research*, 1345, 73-83.
- Christopher, M. M. (2015). One health, one literature: Weaving together veterinary and medical research. *Science Translational Medicine*, 7(303), 303fs336-303fs336.

- Chung, M.-K., Wang, S., Oh, S.-L., & Kim, Y. S. (2021). Acute and Chronic Pain from Facial Skin and Oral Mucosa: Unique Neurobiology and Challenging Treatment. *International journal of molecular sciences*, 22(11), 5810.
- Cleeland, C. S., Janjan, N. A., Scott, C. B., Seiferheld, W. F., & Curran, W. J. (2000). Cancer pain management by radiotherapists: a survey of radiation therapy oncology group physicians. *International Journal of Radiation Oncology* Biology* Physics*, 47(1), 203-208.
- Coatesworth, A., Tsikoudas, A., & MacLennan, K. (2002). The cause of death in patients with head and neck squamous cell carcinoma. *The Journal of Laryngology & Otology*, 116(4), 269-271.
- Cook, A., Modh, A., Ali, H., Sheqwara, J., Chang, S., Ghanem, T., Momin, S., Wu, V., Tam, S., & Money, S. (2022). Randomized Phase 3, Double-Blind, Placebo-Controlled Study of Prophylactic Gabapentin for the Reduction of Oral Mucositis Pain During the Treatment of Oropharyngeal Squamous Cell Carcinoma. *International Journal of Radiation Oncology* Biology* Physics*, 112(4), 926-937.
- Cooper, J. S., Fu, K., Marks, J., & Silverman, S. (1995). Late effects of radiation therapy in the head and neck region. *International Journal of Radiation Oncology* Biology* Physics*, 31(5), 1141-1164.
- Cramer, J. D., Johnson, J. T., & Nilsen, M. L. (2018). Pain in head and neck cancer survivors: prevalence, predictors, and quality-of-life impact. *Otolaryngology–Head and Neck Surgery*, 159(5), 853-858.
- Davies, L., & Welch, H. G. (2006). Epidemiology of head and neck cancer in the United States. *Otolaryngology-Head and Neck Surgery*, 135(3), 451-457. e453.

- De Jong, M., & Maina, T. (2010). Of mice and humans: are they the same?—Implications in cancer translational research. *Journal of Nuclear Medicine*, 51(4), 501-504.
- Delanian, S., Lefaix, J.-L., & Pradat, P.-F. (2012). Radiation-induced neuropathy in cancer survivors. *Radiotherapy and oncology*, 105(3), 273-282.
- Demir, I. E., Ceyhan, G. O., Liebl, F., D'haese, J. G., Maak, M., & Friess, H. (2010). Neural invasion in pancreatic cancer: the past, present and future. *Cancers*, 2(3), 1513-1527.
- Demir, I. E., Friess, H., & Ceyhan, G. O. (2012). Nerve-cancer interactions in the stromal biology of pancreatic cancer. *Frontiers in physiology*, 3, 97.
- Demir, I. E., Friess, H., & Ceyhan, G. O. (2015). Neural plasticity in pancreatitis and pancreatic cancer. *Nature reviews Gastroenterology & hepatology*, 12(11), 649-659.
- Deniz, K. (2011). Effect of propolis against radiation-induced oral mucositis in rats. *Kulak burun bogaz ihtisas dergisi: KBB= Journal of ear, nose, and throat*, 21(1), 32-41.
- Dilling, T. J., Bae, K., Paulus, R., Watkins-Bruner, D., Garden, A. S., Forastiere, A., Ang, K. K., & Movsas, B. (2011). Impact of gender, partner status, and race on locoregional failure and overall survival in head and neck cancer patients in three radiation therapy oncology group trials. *International Journal of Radiation Oncology* Biology* Physics*, 81(3), e101-e109.
- Dixon, L., Garcez, K., Lee, L. W., Sykes, A., Slevin, N., & Thomson, D. (2017). Ninety-day mortality after radical radiotherapy for head and neck cancer. *Clinical Oncology*, 29(12), 835-840.
- Dolan, J. C., Lam, D. K., Achdjian, S. H., & Schmidt, B. L. (2010). The dolognawmeter: a novel instrument and assay to quantify nociception in rodent models of orofacial pain. *Journal of neuroscience methods*, 187(2), 207-215.

- Dömötör, A., Peidl, Z., Vincze, Á., Hunyady, B., Szolcsányi, J., Kereskay, L., Szekeres, G., & Mózsik, G. (2005). Immunohistochemical distribution of vanilloid receptor, calcitonin-gene related peptide and substance P in gastrointestinal mucosa of patients with different gastrointestinal disorders. *Inflammopharmacology*, 13(1), 161-177.
- Dorr, K. B., B. Hartmann, W. (2000). Repopulation in mouse oral mucosa: changes in the effect of dose fractionation. *International journal of radiation biology*, 76(3), 383-390.
- Dörr, W., Bäessler, S., Reichel, S., & Spekl, K. (2005). Reduction of radiochemotherapy-induced early oral mucositis by recombinant human keratinocyte growth factor (palifermin): experimental studies in mice. *International Journal of Radiation Oncology* Biology* Physics*, 62(3), 881-887.
- Dörr, W., Hamilton, C. S., Boyd, T., Reed, B., & Denham, J. W. (2002). Radiation-induced changes in cellularity and proliferation in human oral mucosa. *International Journal of Radiation Oncology* Biology* Physics*, 52(4), 911-917.
- Dörr, W., Heider, K., & Spekl, K. (2005). Reduction of oral mucositis by palifermin (rHuKGF): dose-effect of rHuKGF. *International journal of radiation biology*, 81(8), 557-565.
- Dörr, W., & Kummermehr, J. (1990). Accelerated repopulation of mouse tongue epithelium during fractionated irradiations or following single doses. *Radiotherapy and oncology*, 17(3), 249-259.
- Dörr, W., Noack, R., Spekl, K., & Farrell, C. (2001). Modification of oral mucositis by keratinocyte growth factor: single radiation exposure. *International journal of radiation biology*, 77(3), 341-347.
- Dörr, W., Spekl, K., & Farrell, C. (2002). The effect of keratinocyte growth factor on healing of manifest radiation ulcers in mouse tongue epithelium. *Cell proliferation*, 35, 86-92.

- Dörr, W., Spekl, K., & Farrell, C. L. (2002). Amelioration of acute oral mucositis by keratinocyte growth factor: fractionated irradiation. *International Journal of Radiation Oncology* Biology* Physics*, 54(1), 245-251.
- Dörr, W., Spekl, K., & Martin, M. (2002). Radiation-induced oral mucositis in mice: strain differences. *Cell proliferation*, 35, 60-67.
- Dudás, J., Dietl, W., Romani, A., Reinold, S., Glueckert, R., Schrott-Fischer, A., Dejaco, D., Johnson Chacko, L., Tuertscher, R., & Schartinger, V. H. (2018). Nerve Growth Factor (NGF)—Receptor Survival Axis in Head and Neck Squamous Cell Carcinoma. *International journal of molecular sciences*, 19(6), 1771.
- Duprez, F., Berwouts, D., De Neve, W., Bonte, K., Boterberg, T., Deron, P., Huvenne, W., Rottey, S., & Mareel, M. (2017). Distant metastases in head and neck cancer. *Head & Neck*, 39(9), 1733-1743.
- Edwards, H. L., Mulvey, M. R., & Bennett, M. I. (2019). Cancer-related neuropathic pain. *Cancers*, 11(3), 373.
- Elad, S., Cheng, K. K. F., Lalla, R. V., Yarom, N., Hong, C., Logan, R. M., Bowen, J., Gibson, R., Saunders, D. P., & Zadik, Y. (2020). MASCC/ISOO clinical practice guidelines for the management of mucositis secondary to cancer therapy. *Cancer*, 126(19), 4423-4431.
- Elbers, J. B. W., Veldhuis, L. I., Bhairosing, P. A., Smeele, L. E., Józwiak, K., van den Brekel, M. W. M., Verheij, M., Al-Mamgani, A., & Zuur, C. L. (2019). Salvage surgery for advanced stage head and neck squamous cell carcinoma following radiotherapy or chemoradiation. *European Archives of Oto-Rhino-Laryngology*, 276(3), 647-655.

- Elting, L. S., Cooksley, C. D., Chambers, M. S., & Garden, A. S. (2007). Risk, outcomes, and costs of radiation-induced oral mucositis among patients with head-and-neck malignancies. *International Journal of Radiation Oncology* Biology* Physics*, 68(4), 1110-1120.
- Epstein, J. B., & Barasch, A. (2018). Oral and dental health in head and neck cancer patients. In *Multidisciplinary Care of the Head and Neck Cancer Patient* (pp. 43-57). Springer.
- Epstein, J. B., Beaumont, J. L., Gwede, C. K., Murphy, B., Garden, A. S., Meredith, R., Le, Q. T., Brizel, D., Isitt, J., & Cella, D. (2007). Longitudinal evaluation of the oral mucositis weekly questionnaire-head and neck cancer, a patient-reported outcomes questionnaire. *Cancer*, 109(9), 1914-1922.
- Epstein, J. B., Epstein, J. D., Epstein, M. S., Oien, H., & Truelove, E. L. (2008). Doxepin rinse for management of mucositis pain in patients with cancer: one week follow-up of topical therapy. *Special Care in Dentistry*, 28(2), 73-77.
- Epstein, J. B., Hong, C., Logan, R. M., Barasch, A., Gordon, S. M., Oberlee-Edwards, L., McGuire, D., Napenas, J. J., Elting, L. S., & Spijkervet, F. K. (2010). A systematic review of orofacial pain in patients receiving cancer therapy. *Supportive care in cancer*, 18(8), 1023-1031.
- Epstein, J. B., Robertson, M., Emerton, S., Phillips, N., & Stevenson-Moore, P. (2001). Quality of life and oral function in patients treated with radiation therapy for head and neck cancer. *Head & Neck*, 23(5), 389-398.
- Epstein, J. B., Wilkie, D. J., Fischer, D. J., Kim, Y.-O., & Villines, D. (2009). Neuropathic and nociceptive pain in head and neck cancer patients receiving radiation therapy. *Head & neck oncology*, 1(1), 1-12.

- Etiz, D., Erkal, H., Serin, M., Küçük, B., Heparı, A., Elhan, A., Tulunay, Ö., & Cakmak, A. (2000). Clinical and histopathological evaluation of sucralfate in prevention of oral mucositis induced by radiation therapy in patients with head and neck malignancies. *Oral oncology*, 36(1), 116-120.
- Exadaktylos, A. K., Buggy, D. J., Moriarty, D. C., Mascha, E., & Sessler, D. I. (2006). Can anesthetic technique for primary breast cancer surgery affect recurrence or metastasis? *The Journal of the American Society of Anesthesiologists*, 105(4), 660-664.
- Fall-Dickson, J. M., Ramsay, E. S., Castro, K., Woltz, P., & Sportés, C. (2007). Oral mucositis-related oropharyngeal pain and correlative tumor necrosis factor- α expression in adult oncology patients undergoing hematopoietic stem cell transplantation. *Clinical therapeutics*, 29(11), 2547-2561.
- Fitzsimmons, D., Gilbert, J., Howse, F., Young, T., Arrarras, J.-I., Brédart, A., Hawker, S., George, S., Aapro, M., & Johnson, C. D. (2009). A systematic review of the use and validation of health-related quality of life instruments in older cancer patients. *European Journal of Cancer*, 45(1), 19-32.
- Flook, C., Calman, F., Mant, M., Subramanian, R., & O'Connell, M. (2005). Gelclair vs Benzydamine in a randomised controlled study in patients with oral mucositis due to radical radiotherapy. *Support Care Cancer*, 13, 443-444.
- Franco, P., Martini, S., Di Muzio, J., Cavallin, C., Arcadipane, F., Rampino, M., Ostellino, O., Pecorari, G., Demo, P. G., & Fasolis, M. (2017). Prospective assessment of oral mucositis and its impact on quality of life and patient-reported outcomes during radiotherapy for head and neck cancer. *Medical Oncology*, 34(5), 81.

- Fromme, E. K., Eilers, K. M., Mori, M., Hsieh, Y.-C., & Beer, T. M. (2004). How accurate is clinician reporting of chemotherapy adverse effects? A comparison with patient-reported symptoms from the Quality-of-Life Questionnaire C30. *Journal of Clinical Oncology*, 22(17), 3485-3490.
- Gasparini, G., Pellegatta, M., Crippa, S., Schiavo Lena, M., Belfiori, G., Doglioni, C., Taveggia, C., & Falconi, M. (2019). Nerves and pancreatic cancer: new insights into a dangerous relationship. *Cancers*, 11(7), 893.
- Gibson, R., Bowen, J., & Keefe, D. (2010). Relationship between Animal Models and Clinical Research: Using Mucositis As A Practical Example. *Preclinical Development Handbook: Toxicology*, 2008, p. 81-108.
- Gieger, T., Rassnick, K., Siegel, S., Proulx, D., Bergman, P., Anderson, C., LaDue, T., Smith, A., Northrup, N., & Roberts, R. (2008). Palliation of clinical signs in 48 dogs with nasal carcinomas treated with coarse-fraction radiation therapy. *Journal of the American Animal Hospital Association*, 44(3), 116-123.
- Gillison, M. L., Chaturvedi, A. K., Anderson, W. F., & Fakhry, C. (2015). Epidemiology of human papillomavirus–positive head and neck squamous cell carcinoma. *Journal of Clinical Oncology*, 33(29), 3235.
- Gobbo, M., Ottaviani, G., Perinetti, G., Ciriello, F., Beorchia, A., Giacca, M., Di Lenarda, R., Rupel, K., Tirelli, G., & Zacchigna, S. (2014). Evaluation of nutritional status in head and neck radio-treated patients affected by oral mucositis: efficacy of class IV laser therapy. *Supportive care in cancer*, 22(7), 1851-1856.

- Gonzales, C. B., Kirma, N. B., Jorge, J., Chen, R., Henry, M. A., Luo, S., & Hargreaves, K. M. (2014). Vanilloids induce oral cancer apoptosis independent of TRPV1. *Oral Oncology*, 50(5), 437-447.
- Gordon, I., Paoloni, M., Mazcko, C., & Khanna, C. (2009). The Comparative Oncology Trials Consortium: using spontaneously occurring cancers in dogs to inform the cancer drug development pathway. *PLoS medicine*, 6(10), e1000161.
- Grivennikov, S. I., Greten, F. R., & Karin, M. (2010). Immunity, inflammation, and cancer. *Cell*, 140(6), 883-899.
- Groome, P. A., O'Sullivan, B., Mackillop, W. J., Jackson, L. D., Schulze, K., Irish, J. C., Warde, P. R., Schneider, K. M., Mackenzie, R. G., & Hodson, D. I. (2006). Compromised local control due to treatment interruptions and late treatment breaks in early glottic cancer: Population-based outcomes study supporting need for intensified treatment schedules. *International Journal of Radiation Oncology* Biology* Physics*, 64(4), 1002-1012.
- Gruber, S., Bozsaky, E., Roitinger, E., Schwarz, K., Schmidt, M., & Dörr, W. (2017). Early inflammatory changes in radiation-induced oral mucositis. *Strahlentherapie und Onkologie*, 193(6), 499-507.
- Gruber, S., & Dörr, W. (2016). Tissue reactions to ionizing radiation—oral mucosa. *Mutation Research/Reviews in Mutation Research*, 770, 292-298.
- Gruber, S., Schmidt, M., Bozsaky, E., Wolfram, K., Haagen, J., Habelt, B., Puttrich, M., & Dörr, W. (2015). Modulation of radiation-induced oral mucositis by pentoxifylline: preclinical studies. *Strahlentherapie und Onkologie*, 191(3), 242-247.

- Guizard, A.-V. N., Dejardin, O. J., Launay, L. C., Bara, S., Lapôtre-Ledoux, B. M., Babin, E. B., Launoy, G. D., & Ligier, K. A. (2017). Diagnosis and management of head and neck cancers in a high-incidence area in France: A population-based study. *Medicine*, 96(26).
- Haddad, R. I., & Shin, D. M. (2008). Recent advances in head and neck cancer. *New England Journal of Medicine*, 359(11), 1143-1154.
- Hahn, K., Bravo, L., Adams, H., & Frazier, D. L. (1994). Naturally occurring tumors in dogs as comparative models for cancer therapy research. *In Vivo*, 8(1), 133-144.
- Hartel, M., Di Mola, F. F., Selvaggi, F., Mascetta, G., Wentz, M. N., Felix, K., Giese, N. A., Hinz, U., Di Sebastiano, P., & Büchler, M. W. (2006). Vanilloids in pancreatic cancer: potential for chemotherapy and pain management. *Gut*, 55(4), 519-528.
- Hay, M., Thomas, D. W., Craighead, J. L., Economides, C., & Rosenthal, J. (2014). Clinical development success rates for investigational drugs. *Nature biotechnology*, 32(1), 40-51.
- Henke, M., Alfonsi, M., Foa, P., Giralt, J., Bardet, E., Cerezo, L., Salzwimmer, M., Lizambri, R., Emmerson, L., & Chen, M.-G. (2011). Palifermin decreases severe oral mucositis of patients undergoing postoperative radiochemotherapy for head and neck cancer: a randomized, placebo-controlled trial. *Journal of Clinical Oncology*, 29(20), 2815-2820.
- Heutte, N., Plisson, L., Lange, M., Prevost, V., & Babin, E. (2014). Quality of life tools in head and neck oncology. *European Annals of Otorhinolaryngology, Head and Neck Diseases*, 131(1), 33-47.
- Hirose, M., Kuroda, Y., & Murata, E. (2016). NGF/TrkA signaling as a therapeutic target for pain. *Pain Practice*, 16(2), 175-182.
- Hjortholm, N., Jaddini, E., Hałaburda, K., & Snarski, E. (2013). Strategies of pain reduction during the bone marrow biopsy. *Annals of hematology*, 92(2), 145-149.

- Howarth, G. S., Tooley, K. L., Davidson, G. P., & Butler, R. N. (2006). A non-invasive method for detection of intestinal mucositis induced by different classes of chemotherapy drugs in the rat. *Cancer biology & therapy*, 5(9), 1189-1195.
- Huang, H.-Y., Wilkie, D. J., Chapman, C. R., & Ting, L.-L. (2003). Pain Trajectory of Taiwanese with Nasopharyngeal Carcinoma Over the Course of Radiation Therapy. *Journal of pain and symptom management*, 25(3), 247-255.
- Hunley, D. W., Mauldin, G. N., Shiomitsu, K., & Mauldin, G. E. (2010). Clinical outcome in dogs with nasal tumors treated with intensity-modulated radiation therapy. *The Canadian veterinary journal = La revue veterinaire canadienne*, 51(3), 293-300.
- Iadarola, M. J., Sapio, M. R., Raithel, S. J., Mannes, A. J., & Brown, D. C. (2018). Long-term pain relief in canine osteoarthritis by a single intra-articular injection of resiniferatoxin, a potent TRPV1 agonist. *Pain*, 159(10), 2105.
- Ingrosso, G., Saldi, S., Marani, S., Wong, A. Y. W., Bertelli, M., Aristei, C., & Zelante, T. (2021). Breakdown of Symbiosis in Radiation-Induced Oral Mucositis. *J Fungi (Basel)*, 7(4).
- Innocenti, M., Moscatelli, G., & Lopez, S. (2002). Efficacy of gelclair in reducing pain in palliative care patients with oral lesions: preliminary findings from an open pilot study. *Journal of pain and symptom management*, 24(5), 456-457.
- Ito, M., Ono, K., Hitomi, S., Nodai, T., Sago, T., Yamaguchi, K., Harano, N., Gunjigake, K., Hosokawa, R., & Kawamoto, T. (2017). Prostanoid-dependent spontaneous pain and PAR2-dependent mechanical allodynia following oral mucosal trauma: Involvement of TRPV1, TRPA1, and TRPV4. *Molecular pain*, 13, 1744806917704138.
- Jensen, S., Pedersen, A., Reibel, J., & Nauntofte, B. (2003). Xerostomia and hypofunction of the salivary glands in cancer therapy. *Supportive care in cancer*, 11(4), 207-225.

- Ji, R.-R., Kohno, T., Moore, K. A., & Woolf, C. J. (2003). Central sensitization and LTP: do pain and memory share similar mechanisms? *Trends in neurosciences*, 26(12), 696-705.
- Jiang, J., Bai, J., Qin, T., Wang, Z., & Han, L. (2020). NGF from pancreatic stellate cells induces pancreatic cancer proliferation and invasion by PI3K/AKT/GSK signal pathway. *Journal of cellular and molecular medicine*, 24(10), 5901-5910.
- Johnstone, P. A., Peng, Y. P., May, B. C., Inouye, W. S., & Niemtzw, R. C. (2001). Acupuncture for pilocarpine-resistant xerostomia following radiotherapy for head and neck malignancies. *International Journal of Radiation Oncology* Biology* Physics*, 50(2), 353-357.
- Judge, L. F., Farrugia, M. K., & Singh, A. K. (2021). Narrative review of the management of oral mucositis during chemoradiation for head and neck cancer. *Annals of Translational Medicine*, 9(10).
- Kallurkar, A., Kulkarni, S., Delfino, K., Ferraro, D., & Rao, K. (2019). Characteristics of chronic pain among head and neck cancer patients treated with radiation therapy: A retrospective study. *Pain Research and Management*, 2019.
- Karacetin, D., Yücel, B., Leblebicioğlu, B., Aksakal, O., Maral, O., & Incekara, O. (2004). A randomized trial of amifostine as radioprotector in the radiotherapy of head and neck cancer. *Journal of BU ON.: official journal of the Balkan Union of Oncology*, 9(1), 23-26.
- Karri, J., Lachman, L., Hanania, A., Marathe, A., Singh, M., Zacharias, N., Orhurhu, V., Gulati, A., & Abd-Elsayed, A. (2021). Radiotherapy-Specific Chronic Pain Syndromes in the Cancer Population: An Evidence-Based Narrative Review. *Advances in Therapy*, 1-22.

- Kato, Y., Maeda, M., Aoki, Y., Ishii, E., Ishida, Y., Kiyotani, C., Goto, S., Sakaguchi, S., Sugita, K., & Tokuyama, M. (2014). Pain management during bone marrow aspiration and biopsy in pediatric cancer patients. *Pediatrics International*, 56(3), 354-359.
- Katrancı, N., Ovayolu, N., Ovayolu, O., & Sevinc, A. (2012). Evaluation of the effect of cryotherapy in preventing oral mucositis associated with chemotherapy—a randomized controlled trial. *European Journal of Oncology Nursing*, 16(4), 339-344.
- Kemmler, G., Holzner, B., Kopp, M., Dünser, M., Margreiter, R., Greil, R., & Sperner-Unterweger, B. (1999). Comparison of Two Quality-of-Life Instruments for Cancer Patients: The Functional Assessment of Cancer Therapy-General and the European Organization for Research and Treatment of Cancer Quality of Life Questionnaire-C30. *Journal of Clinical Oncology*, 17(9), 2932-2932.
- Khaw, A., Logan, R., Keefe, D., & Bartold, M. (2014). Radiation-induced oral mucositis and periodontitis—proposal for an inter-relationship. *Oral diseases*, 20(3), e7-e18.
- Khelifi, R., & Hamza-Chaffai, A. (2010). Head and neck cancer due to heavy metal exposure via tobacco smoking and professional exposure: A review. *Toxicology and Applied Pharmacology*, 248(2), 71-88.
- Kim, H. J., Kang, S. U., Lee, Y. S., Jang, J. Y., Kang, H., & Kim, C.-H. (2020). Protective effects of N-acetylcysteine against radiation-induced oral mucositis in vitro and in vivo. *Cancer research and treatment: official journal of Korean Cancer Association*, 52(4), 1019.
- Kim, J. H., Jung, M. H., Kim, J. P., Kim, H.-J., Jung, J. H., Hahm, J. R., Kang, K. M., Jeong, B.-K., & Woo, S. H. (2017). Alpha lipoic acid attenuates radiation-induced oral mucositis in rats. *Oncotarget*, 8(42), 72739.

- Kobayashi, K., Fukuoka, T., Obata, K., Yamanaka, H., Dai, Y., Tokunaga, A., & Noguchi, K. (2005). Distinct expression of TRPM8, TRPA1, and TRPV1 mRNAs in rat primary afferent neurons with a δ /c-fibers and colocalization with trk receptors. *Journal of Comparative Neurology*, 493(4), 596-606.
- Kol, A., Arzi, B., Athanasiou, K. A., Farmer, D. L., Nolta, J. A., Rebhun, R. B., Chen, X., Griffiths, L. G., Verstraete, F. J. M., Murphy, C. J., & Borjesson, D. L. (2015). Companion animals: Translational scientist's new best friends. *Science translational medicine*, 7(308), 308ps21-308ps21.
- Kolokythas, A., Cox, D. P., Dekker, N., & Schmidt, B. L. (2010). Nerve growth factor and tyrosine kinase A receptor in oral squamous cell carcinoma: is there an association with perineural invasion? *Journal of oral and maxillofacial surgery*, 68(6), 1290-1295.
- Kotwall, C., Sako, K., Razack, M. S., Rao, U., Bakamjian, V., & Shedd, D. P. (1987). Metastatic patterns in squamous cell cancer of the head and neck. *The American Journal of Surgery*, 154(4), 439-442.
- Kuten-Shorrer, M., Zadik, Y., & Elad, S. (2021). Oral Mucositis Following Cancer Therapy. In E. Schmidt (Ed.), *Diseases of the Oral Mucosa: Study Guide and Review* (pp. 389-399). Springer International Publishing.
- LaDue-Miller, T., Price, G. S., Page, R. L., & Thrall, D. E. (1996). Radiotherapy of canine non-tonsillar squamous cell carcinoma. *Veterinary Radiology & Ultrasound*, 37(1), 74-77.
- Lai, Y., Bäumer, W., Meneses, C., Roback, D. M., Robertson, J. B., Mishra, S. K., Lascelles, B. D. X., & Nolan, M. W. (2021). Irradiation of the Normal Murine Tongue Causes Upregulation and Activation of Transient Receptor Potential (TRP) Ion Channels. *Radiation Research*, 196(4), 331-344.

- Lalla, R. V., Bowen, J., Barasch, A., Elting, L., Epstein, J., Keefe, D. M., McGuire, D. B., Migliorati, C., Nicolatou-Galitis, O., Peterson, D. E., Raber-Durlacher, J. E., Sonis, S. T., & Elad, S. (2014). MASCC/ISOO clinical practice guidelines for the management of mucositis secondary to cancer therapy. *Cancer*, 120(10), 1453-1461.
- Lalla, R. V., Brennan, M. T., Gordon, S. M., Sonis, S. T., Rosenthal, D. I., & Keefe, D. M. (2019). Oral mucositis due to high-dose chemotherapy and/or head and neck radiation therapy. *JNCI Monographs*, 2019(53), Igz011.
- LaRue, S., Withrow, S., Powers, B., Wrigley, R., Gillette, E., Schwarz, P., Straw, R., & Richter, S. (1989). Limb-sparing treatment for osteosarcoma in dogs. *Journal of the American Veterinary Medical Association*, 195(12), 1734-1744.
- Lascelles, B., Brown, D., Maixner, W., & Mogil, J. (2018). Spontaneous painful disease in companion animals can facilitate the development of chronic pain therapies for humans. *Osteoarthritis and cartilage*, 26(2), 175-183.
- Latremoliere, A., & Woolf, C. J. (2009). Central sensitization: a generator of pain hypersensitivity by central neural plasticity. *The journal of pain*, 10(9), 895-926.
- Lazarev, S., Gupta, V., Ghiassi-Nejad, Z., Miles, B., Scarborough, B., Misiukiewicz, K. J., Reckson, B., Sheu, R.-D., & Bakst, R. L. (2018). Premature discontinuation of curative radiation therapy: insights from head and neck irradiation. *Advances in Radiation Oncology*, 3(1), 62-69.
- Le, Q.-T., Kim, H. E., Schneider, C. J., Muraközy, G., Skladowski, K., Reinisch, S., Chen, Y., Hickey, M., Mo, M., & Chen, M.-G. (2011). Palifermin reduces severe mucositis in definitive chemoradiotherapy of locally advanced head and neck cancer: a randomized, placebo-controlled study. *J Clin Oncol*, 29(20), 2808-2814.

- Lee, J. H., Song, J. H., Lee, S. N., Kang, J. H., Kim, M. S., Sun, D. I., & Kim, Y.-S. (2013). Adjuvant postoperative radiotherapy with or without chemotherapy for locally advanced squamous cell carcinoma of the head and neck: the importance of patient selection for the postoperative chemoradiotherapy. *Cancer research and treatment: official journal of Korean Cancer Association*, 45(1), 31-39.
- Lee, S.-w., Jung, K. I., Kim, Y. W., Jung, H. D., Kim, H. S., & Hong, J. P. (2007). Effect of epidermal growth factor against radiotherapy-induced oral mucositis in rats. *International Journal of Radiation Oncology* Biology* Physics*, 67(4), 1172-1178.
- Leenstra, J. L., Miller, R. C., Qin, R., Martenson, J. A., Dornfeld, K. J., Bearden, J. D., Puri, D. R., Stella, P. J., Mazurczak, M. A., & Klish, M. D. (2014). Doxepin rinse versus placebo in the treatment of acute oral mucositis pain in patients receiving head and neck radiotherapy with or without chemotherapy: a phase III, randomized, double-blind trial (NCCTG-N09C6 [Alliance]). *Journal of Clinical Oncology*, 32(15), 1571.
- Lewis, S., Salins, N., Kadam, A., & Rao, R. (2013). Distress screening using distress thermometer in head and neck cancer patients undergoing radiotherapy and evaluation of causal factors predicting occurrence of distress. *Indian journal of palliative care*, 19(2), 88-92.
- Li, Wu, C.-z., Zhang, B.-w., Qiu, L., Chen, W., Yuan, Y.-H., Liu, X.-c., Li, C.-j., & Li, L.-j. (2021). Nerve growth factor protects salivary glands from irradiation-induced damage. *Life Sciences*, 265, 118748.
- Li, K., Yang, L., Xin, P., Chen, Y., Hu, Q.-y., Chen, X.-z., & Chen, M. (2017). Impact of dose volume parameters and clinical factors on acute radiation oral mucositis for locally advanced nasopharyngeal carcinoma patients treated with concurrent intensity-modulated radiation therapy and chemoradiotherapy. *Oral Oncology*, 72, 32-37.

- Liang, D., Shi, S., Xu, J., Zhang, B., Qin, Y., Ji, S., Xu, W., Liu, J., Liu, L., & Liu, C. (2016). New insights into perineural invasion of pancreatic cancer: More than pain. *Biochimica et Biophysica Acta (BBA)-Reviews on Cancer*, 1865(2), 111-122.
- Lindsay, G., Rushton, R., & Harris, T. (2009). The clinical effectiveness of Gelclair in the management of oral mucositis. *Austral Nurs J*, 16, 30-33.
- List, M. A., & Bilir, S. P. (2004). Functional outcomes in head and neck cancer. *Seminars in radiation oncology* (Vol. 14, No. 2, pp. 178-189). WB Saunders.
- Loeser, J. D., & Melzack, R. (1999). Pain: an overview. *The Lancet*, 353(9164), 1607-1609.
- Logan, H. L., Fillingim, R. B., Bartoshuk, L. M., Sandow, P., Tomar, S. L., Werning, J. W., & Mendenhall, W. M. (2010). Smoking Status and Pain Level Among Head and Neck Cancer Patients. *The Journal of Pain*, 11(6), 528-534.
- Madeya, M. L. (1996). Oral complications from cancer therapy: Part 2--Nursing implications for assessment and treatment. *Oncology nursing forum*, 23(5), 808-819.
- Mak, I. W., Evaniew, N., & Ghert, M. (2014). Lost in translation: animal models and clinical trials in cancer treatment. *American journal of translational research*, 6(2), 114-118.
- Makkonen, T. A., Boström, P., Vilja, P., & Joensuu, H. (1994). Sucralfate mouth washing in the prevention of radiation-induced mucositis: a placebo-controlled double-blind randomized study. *International Journal of Radiation Oncology* Biology* Physics*, 30(1), 177-182.
- Mallick, S., Benson, R., & Rath, G. (2016). Radiation induced oral mucositis: a review of current literature on prevention and management. *European Archives of Oto-Rhino-Laryngology*, 273(9), 2285-2293.
- Mankoff, S. P., Brander, C., Ferrone, S., & Marincola, F. M. (2004). Lost in Translation: Obstacles to Translational Medicine. *Journal of Translational Medicine*, 2(1), 14.

- Maria, O. M., Eliopoulos, N., & Muanza, T. (2017). Radiation-induced oral mucositis. *Frontiers in Oncology*, 7, 89.
- Martinsson, T. (1999). Ropivacaine Inhibits Serum-Induced Proliferation of Colon Adenocarcinoma Cells In Vitro. *Journal of Pharmacology and Experimental Therapeutics*, 288(2), 660-664.
- Massa, S. T., Osazuwa-Peters, N., Christopher, K. M., Arnold, L. D., Schootman, M., Walker, R. J., & Varvares, M. A. (2017). Competing causes of death in the head and neck cancer population. *Oral Oncology*, 65, 8-15.
- Masumoto, K., Tsukimoto, M., & Kojima, S. (2013). Role of TRPM2 and TRPV1 cation channels in cellular responses to radiation-induced DNA damage. *Biochimica et Biophysica Acta (BBA)-General Subjects*, 1830(6), 3382-3390.
- Matchim, Y., & Armer, J. M. (2007). Measuring the psychological impact of mindfulness meditation on health among patients with cancer: A literature review. In *Oncology nursing forum* (Vol. 34, No. 5, p. 1059). Oncology Nursing Society.
- Mazul, A. L., Stepan, K. O., Barrett, T. F., Thorstad, W. L., Massa, S., Adkins, D. R., Daly, M. D., Rich, J. T., Paniello, R. C., & Pipkorn, P. (2020). Duration of radiation therapy is associated with worse survival in head and neck cancer. *Oral oncology*, 108, 104819.
- McCarthy, G., Awde, J., Ghandi, H., Vincent, M., & Kocha, W. (1998). Risk factors associated with mucositis in cancer patients receiving 5-fluorouracil. *Oral oncology*, 34(6), 484-490.
- McGuire, D. B., Correa, M. E. P., Johnson, J., & Wienandts, P. (2006). The role of basic oral care and good clinical practice principles in the management of oral mucositis. *Supportive care in cancer*, 14(6), 541-547.

- McGurk, M., Chan, C., Jones, J., O'regan, E., & Sherriff, M. (2005). Delay in diagnosis and its effect on outcome in head and neck cancer. *British Journal of Oral and Maxillofacial Surgery*, 43(4), 281-284.
- McKenzie, M., Papish, S., & Hansen, V. (2006). A randomized open label trial comparing Gelclair with institutional standard magic mouthwash for the treatment of pain associated with radiation or chemotherapy induced mucositis. *Support Cancer Care*, 14, 641.
- McLaughlin, L., & Mahon, S. M. (2014). Taste Dysfunction and Eating Behaviors in Survivors of Head and Neck Cancer Treatment. *Medsurg Nursing*, 23(3), 165-170, 184.
- Merino, O. R., Lindberg, R. D., & Fletcher, G. H. (1977). An analysis of distant metastases from squamous cell carcinoma of the upper respiratory and digestive tracts. *Cancer*, 40(1), 145-151.
- Meyer, F., Fortin, A., Gélinas, M., Nabid, A., Brochet, F., Têtu, B., & Bairati, I. (2009). Health-Related Quality of Life As a Survival Predictor for Patients With Localized Head and Neck Cancer Treated With Radiation Therapy. *Journal of Clinical Oncology*, 27(18), 2970-2976.
- Migliorati, C., Hewson, I., Lalla, R. V., Antunes, H. S., Estilo, C. L., Hodgson, B., Lopes, N. N. F., Schubert, M. M., Bowen, J., & Elad, S. (2013). Systematic review of laser and other light therapy for the management of oral mucositis in cancer patients. *Supportive Care in Cancer*, 21(1), 333-341.
- Minnema, L., Wheeler, J., Enomoto, M., Pitake, S., Mishra, S. K., & Lascelles, B. D. X. (2020). Correlation of artemin and GFR α 3 with osteoarthritis pain: Early evidence from naturally occurring osteoarthritis-associated chronic pain in dogs. *Frontiers in Neuroscience*, 14, 77.
- Morais-Faria, K., Palmier, N. R., de Lima Correia, J., de Castro Júnior, G., Dias, R. B., da Graça Pinto, H., Lopes, M. A., Ribeiro, A. C. P., Brandão, T. B., & Santos-Silva, A. R. (2020).

- Young head and neck cancer patients are at increased risk of developing oral mucositis and trismus. *Supportive care in cancer*, 28(9), 4345-4352.
- Morgan, M. A., Small, B. J., Donovan, K. A., Overcash, J., & McMillan, S. (2011). Cancer patients with pain: the spouse/partner relationship and quality of life. *Cancer nursing*, 34(1), 13-23.
- Mosca, A., Gibson, D., Mason, S. L., Dobson, J., & Giuliano, A. (2021). A possible role of coarse fractionated radiotherapy in the management of gingival squamous cell carcinoma in dogs: A retrospective study of 21 cases from two referral centers in the UK. *The Journal of veterinary medical science*, 83(3), 447-455.
- Moslemi, D., Nokhandani, A. M., Otaghsaraei, M. T., Moghadamnia, Y., Kazemi, S., & Moghadamnia, A. A. (2016). Management of chemo/radiation-induced oral mucositis in patients with head and neck cancer: A review of the current literature. *Radiotherapy and oncology*, 120(1), 13-20.
- Murphy, B. A., Beaumont, J. L., Isitt, J., Garden, A. S., Gwede, C. K., Trotti, A. M., Meredith, R. F., Epstein, J. B., Le, Q.-T., & Brizel, D. M. (2009). Mucositis-related morbidity and resource utilization in head and neck cancer patients receiving radiation therapy with or without chemotherapy. *Journal of pain and symptom management*, 38(4), 522-532.
- Muzaffar, J., Bari, S., Kirtane, K., & Chung, C. H. (2021). Recent Advances and Future Directions in Clinical Management of Head and Neck Squamous Cell Carcinoma. *Cancers*, 13(2), 338.
- Muzumder, S., Nirmala, S., Avinash, H., Sebastian, M. J., & Kainthaje, P. B. (2018). Analgesic and opioid use in pain associated with head-and-neck radiation therapy. *Indian journal of palliative care*, 24(2), 176.

- Nagatani, A., Ogawa, Y., Sunaga, T., Tomura, K., Naito, Y., Fujii, N., Okabe, T., Hashimoto, T., Kogo, M., & Sasaki, T. (2017). Analysis of the Risk Factors for Severe Oral Mucositis in Head and Neck Cancer after Chemoradiotherapy with S-1. *Yakugaku Zasshi: Journal of the Pharmaceutical Society of Japan*, 137(2), 221-225.
- Nakajima, N., Watanabe, S., Kiyoi, T., Tanaka, A., Suemaru, K., & Araki, H. (2015). Evaluation of edaravone against radiation-induced oral mucositis in mice. *Journal of Pharmacological Sciences*, 127(3), 339-343.
- Neubert, J. K., King, C., Malphurs, W., Wong, F., Weaver, J. P., Jenkins, A. C., Rossi, H. L., & Caudle, R. M. (2008). Characterization of mouse orofacial pain and the effects of lesioning TRPV1-expressing neurons on operant behavior. *Molecular pain*, 4, 1744-8069-1744-1743.
- Neubert, J. K., Widmer, C. G., Malphurs, W., Rossi, H. L., Vierck, C. J., & Caudle, R. M. (2005). Use of a novel thermal operant behavioral assay for characterization of orofacial pain sensitivity. *Pain*, 116(3), 386-395.
- Nigro, C. L., Denaro, N., Merlotti, A., & Merlano, M. (2017). Head and neck cancer: improving outcomes with a multidisciplinary approach. *Cancer management and research*, 9, 363.
- Nishii, M., Soutome, S., Kawakita, A., Yutori, H., Iwata, E., Akashi, M., Hasegawa, T., Kojima, Y., Funahara, M., Umeda, M., & Komori, T. (2020). Factors associated with severe oral mucositis and candidiasis in patients undergoing radiotherapy for oral and oropharyngeal carcinomas: a retrospective multicenter study of 326 patients. *Supportive Care in Cancer*, 28(3), 1069-1075.

- Nolan, M. W., Long, C. T., Marcus, K. L., Sarmadi, S., Roback, D. M., Fukuyama, T., Baeumer, W., & Lascelles, B. D. X. (2017). Nocifensive behaviors in mice with radiation-induced oral mucositis. *Radiation research*, 187(3), 397-403.
- O'Callaghan, C., Sexton, M., & Wheeler, G. (2007). Music therapy as a non-pharmacological anxiolytic for paediatric radiotherapy patients. *Australasian radiology*, 51(2), 159-162.
- Ohsaki, A., Tanuma, S.-i., & Tsukimoto, M. (2018). TRPV4 channel-regulated ATP release contributes to γ -irradiation-induced production of IL-6 and IL-8 in epidermal keratinocytes. *Biological and Pharmaceutical Bulletin*, 41(10), 1620-1626.
- Page, G. G., & Ben-Eliyahu, S. (2002). Indomethacin attenuates the immunosuppressive and tumor-promoting effects of surgery. *The Journal of Pain*, 3(4), 301-308.
- Page, G. G., Ben-Eliyahu, S., Yirmiya, R., & Liebeskind, J. C. (1993). Morphine attenuates surgery-induced enhancement of metastatic colonization in rats. *Pain*, 54(1), 21-28.
- Page, G. G., Blakely, W. P., & Ben-Eliyahu, S. (2001). Evidence that postoperative pain is a mediator of the tumor-promoting effects of surgery in rats. *Pain*, 90(1-2), 191-199.
- Panjwani, M. (2013). Efficacy of palifermin in the hematopoietic stem cell transplant setting. *Journal of the advanced practitioner in oncology*, 4(2), 89-100.
- Paoloni, M., & Khanna, C. (2008). Translation of new cancer treatments from pet dogs to humans. *Nature reviews Cancer*, 8(2), 147-156.
- Parulekar, W., Mackenzie, R., Bjarnason, G., & Jordan, R. (1998). Scoring oral mucositis. *Oral Oncology*, 34(1), 63-71.
- Peterman, A., Cella, D., Glandon, G., Dobrez, D., & Yount, S. (2001). Mucositis in Head and Neck Cancer: Economic and Quality-of-Life Outcomes. *JNCI Monographs*, 2001(29), 45-51.

- Peterson, D. E., Öhrn, K., Bowen, J., Fliedner, M., Lees, J., Loprinzi, C., Mori, T., Osaguona, A., Weikel, D. S., & Elad, S. (2013). Systematic review of oral cryotherapy for management of oral mucositis caused by cancer therapy. *Supportive Care in Cancer*, 21(1), 327-332.
- Pickering, V., Jay Gupta, R., Quang, P., Jordan, R. C., & Schmidt, B. L. (2008). Effect of peripheral endothelin-1 concentration on carcinoma-induced pain in mice. *European Journal of Pain*, 12(3), 293-300.
- Pogatzki-Zahn, E. M., Segelcke, D., & Schug, S. A. (2017). Postoperative pain—from mechanisms to treatment. *Pain reports*, 2(2).
- Price, M. L., Lai, Y. H., Marcus, K. L., Robertson, J. B., Lascelles, B. D. X., & Nolan, M. W. (2021). Early radiation-induced oral pain signaling responses are reduced with pentoxifylline treatment. *Veterinary Radiology & Ultrasound*, 62(2), 255-263.
- Priya, A. H. H., Rajmohan, H. P. A. K., Raj, S. A., Archana, S., & Venkatanarasu, B. (2020). Evaluation of alteration in oral microbial flora pre-and postradiation therapy in patients with head and neck cancer. *Journal of Pharmacy & Bioallied Sciences*, 12(Suppl 1), S109.
- Pulte, D., & Brenner, H. (2010). Changes in survival in head and neck cancers in the late 20th and early 21st century: a period analysis. *The oncologist*, 15(9), 994-1001.
- Quang, P. N., & Schmidt, B. L. (2010). Endothelin-A receptor antagonism attenuates carcinoma-induced pain through opioids in mice. *The Journal of Pain*, 11(7), 663-671.
- Raber-Durlacher, J. E. (1999). Current practices for management of oral mucositis in cancer patients. *Supportive Care in Cancer*, 7(2), 71-74.
- Ranieri, G., Gadaleta, C., Patruno, R., Zizzo, N., Daidone, M., Hansson, M. G., Paradiso, A., & Ribatti, D. (2013). A model of study for human cancer: Spontaneous occurring tumors in

- dogs. Biological features and translation for new anticancer therapies. *Critical reviews in oncology/hematology*, 88(1), 187-197.
- Redding, S. W. (2005). Cancer therapy-related oral mucositis. *Journal of dental education*, 69(8), 919-929.
- Regan, D., Garcia, K., & Thamm, D. (2018). Clinical, pathological, and ethical considerations for the conduct of clinical trials in dogs with naturally occurring cancer: a comparative approach to accelerate translational drug development. *ILAR journal*, 59(1), 99-110.
- Rezvani, M., & Ross, G. (2004). Modification of radiation-induced acute oral mucositis in the rat. *International journal of radiation biology*, 80(2), 177-182.
- Ricci, M. S., & Zong, W.-X. (2006). Chemotherapeutic Approaches for Targeting Cell Death Pathways. *The Oncologist*, 11(4), 342-357.
- Riggs, J., Adams, V. J., Hermer, J. V., Dobson, J. M., Murphy, S., & Ladlow, J. F. (2018). Outcomes following surgical excision or surgical excision combined with adjunctive, hypofractionated radiotherapy in dogs with oral squamous cell carcinoma or fibrosarcoma. *Journal of the American Veterinary Medical Association*, 253(1), 73-83.
- Robertson, J. J. (2016). Managing pharyngeal and oral mucosal pain. *Current Emergency and Hospital Medicine Reports*, 4(2), 57-65.
- Rogers, S. N., Cleator, A. J., Lowe, D., & Ghazali, N. (2012). Identifying pain-related concerns in routine follow-up clinics following oral and oropharyngeal cancer. *World journal of clinical oncology*, 3(8), 116-125.
- Rosenthal, D. (2007). Consequences of mucositis-induced treatment breaks and dose reductions on head and neck cancer treatment outcomes. *The journal of supportive oncology*, 5, 23-31.

- Rosenthal, D. I., Liu, L., Lee, J. H., Vapiwala, N., Chalian, A. A., Weinstein, G. S., Chilian, I., Weber, R. S., & Machtay, M. (2002). Importance of the treatment package time in surgery and postoperative radiation therapy for squamous carcinoma of the head and neck. *Head & Neck*, 24(2), 115-126.
- Rossi, H. L., Vierck, C. J., Caudle, R. M., & Neubert, J. K. (2006). Characterization of Cold Sensitivity and Thermal Preference Using an Operant Orofacial Assay. *Molecular pain*, 2, 1744-8069-1742-1737.
- Rowell, J. L., McCarthy, D. O., & Alvarez, C. E. (2011). Dog models of naturally occurring cancer. *Trends in molecular medicine*, 17(7), 380-388.
- Russo, G., Haddad, R., Posner, M., & Machtay, M. (2008). Radiation treatment breaks and ulcerative mucositis in head and neck cancer. *The Oncologist*, 13(8), 886-898.
- Saadeh, C. E. (2005). Chemotherapy-and radiotherapy-induced oral mucositis: Review of preventive strategies and treatment. *Pharmacotherapy: The Journal of Human Pharmacology and Drug Therapy*, 25(4), 540-554.
- Saedi, H. S., Gerami, H., Soltanipour, S., Habibi, A. F., Mirhosseyni, M., Montazeri, S., & Nemati, S. (2019). Frequency of chemoradiotherapy-induced mucositis and related risk factors in patients with the head-and-neck cancers: A survey in the North of Iran. *Dental research journal*, 16(5), 354.
- Saito, N., Imai, Y., Muto, T., & Sairenchi, T. (2012). Low body mass index as a risk factor of moderate to severe oral mucositis in oral cancer patients with radiotherapy. *Supportive care in cancer*, 20(12), 3373-3377.

- Samra, B., Tam, E., Baseri, B., & Shapira, I. (2018). Checkpoint inhibitors in head and neck cancer: current knowledge and perspectives. *Journal of Investigative Medicine*, 66(7), 1023-1030.
- Sánchez, M. G., Sánchez, A. M., Collado, B., Malagarie-Cazenave, S., Olea, N., Carmena, M. J., Prieto, J. C., & Díaz-Laviada, I. (2005). Expression of the transient receptor potential vanilloid 1 (TRPV1) in LNCaP and PC-3 prostate cancer cells and in human prostate tissue. *European journal of pharmacology*, 515(1-3), 20-27.
- Satheesh Kumar, P., Balan, A., Sankar, A., & Bose, T. (2009). Radiation induced oral mucositis. *Indian journal of palliative care*, 15(2), 95.
- Saunders, D. P., Epstein, J. B., Elad, S., Allemanno, J., Bossi, P., Van De Wetering, M. D., Rao, N. G., Potting, C., Cheng, K. K., & Freidank, A. (2013). Systematic review of antimicrobials, mucosal coating agents, anesthetics, and analgesics for the management of oral mucositis in cancer patients. *Supportive care in cancer*, 21(11), 3191-3207.
- Scharpf, J., Karnell, L. H., Christensen, A. J., & Funk, G. F. (2009). The Role of Pain in Head and Neck Cancer Recurrence and Survivorship. *Archives of Otolaryngology–Head & Neck Surgery*, 135(8), 789-794.
- Schmidt, B. L. (2015). The neurobiology of cancer pain. *Journal of oral and maxillofacial surgery*, 73(12), S132-S135.
- Schubert, M. M., Eduardo, F. P., Guthrie, K. A., Franquin, J.-C., Bensadoun, R.-J. J., Migliorati, C. A., Lloid, C. M. E., Eduardo, C. P., Walter Filho, N., & Marques, M. M. (2007). A phase III randomized double-blind placebo-controlled clinical trial to determine the efficacy of low-level laser therapy for the prevention of oral mucositis in patients undergoing hematopoietic cell transplantation. *Supportive Care in Cancer*, 15(10), 1145-1154.

- Scully, C., Epstein, J., & Sonis, S. (2003). Oral mucositis: a challenging complication of radiotherapy, chemotherapy, and radiochemotherapy: part 1, pathogenesis and prophylaxis of mucositis. *Head & Neck: Journal for the Sciences and Specialties of the Head and Neck*, 25(12), 1057-1070.
- Seiwert, T., & Cohen, E. (2005). State-of-the-art management of locally advanced head and neck cancer. *British Journal of Cancer*, 92(8), 1341-1348.
- Sheibani, K. M., Mafi, A. R., Moghaddam, S., Taslimi, F., Amiran, A., & Ameri, A. (2015). Efficacy of benzydamine oral rinse in prevention and management of radiation-induced oral mucositis: a double-blind placebo-controlled randomized clinical trial. *Asia-Pacific Journal of Clinical Oncology*, 11(1), 22-27.
- Shen, W. R., Wang, Y. P., Chang, J. Y. F., Yu, S. Y., Chen, H. M., & Chiang, C. P. (2014). Perineural invasion and expression of nerve growth factor can predict the progression and prognosis of oral tongue squamous cell carcinoma. *Journal of Oral Pathology & Medicine*, 43(4), 258-264.
- Shibasaki, K. (2020). TRPV4 activation by thermal and mechanical stimuli in disease progression. *Laboratory investigation*, 100(2), 218-223.
- Shih, A., Miaskowski, C., Dodd, M. J., Stotts, N. A., & MacPhail, L. (2003). Mechanisms for radiation-induced oral mucositis and the consequences. *Cancer nursing*, 26(3), 222-229.
- Short, L., & Fung, D. (2008). Clinical effectiveness of Gelclair in the treatment of oral mucositis: a patient based questionnaire. *Int J Paediatr Dent*, 18(suppl 1), 14.
- Shu-Ching, C. (2019). Oral dysfunction in patients with head and neck cancer: a systematic review. *Journal of Nursing Research*, 27(6), e58.

- Silva, F. C., Marto, J. M., Salgado, A., Machado, P., Silva, A. N., & Almeida, A. J. (2017). Nystatin and lidocaine pastilles for the local treatment of oral mucositis. *Pharmaceutical Development and Technology*, 22(2), 266-274.
- Smith, P. F., & Epstein, J. (2010). Orofacial pain. *Oral Complications of Cancer and its Management*, 241.
- Sonis, S., Peterson, R., Edwards, L., Lucey, C., Wang, L., Mason, L., Login, G., Ymamkawa, M., Moses, G., & Bouchard, P. (2000). Defining mechanisms of action of interleukin-11 on the progression of radiation-induced oral mucositis in hamsters. *Oral Oncology*, 36(4), 373-381.
- Sonis, S., Van Vugt, A., McDonald, J., Dotoli, E., Schwertschlag, U., Szklut, P., & Keith, J. (1997). Mitigating effects of interleukin 11 on consecutive courses of 5-fluorouracil-induced ulcerative mucositis in hamsters. *Cytokine*, 9(8), 605-612.
- Sonis, S. T. (2004a). A biological approach to mucositis. *J Support Oncol*, 2(1), 21-32.
- Sonis, S. T. (2004b). The pathobiology of mucositis. *Nature reviews Cancer*, 4(4), 277-284.
- Sonis, S. T. (2011). Oral mucositis. *Anticancer Drugs*, 22(7), 607-612.
- Sonis, S. T., Costa Jr, J. W., Evitts, S. M., Lindquist, L. E., & Nicolson, M. (1992). Effect of epidermal growth factor on ulcerative mucositis in hamsters that receive cancer chemotherapy. *Oral surgery, oral medicine, oral pathology*, 74(6), 749-755.
- Sonis, S. T., Tracey, C., Shklar, G., Jenson, J., & Florine, D. (1990). An animal model for mucositis induced by cancer chemotherapy. *Oral surgery, oral medicine, oral pathology*, 69(4), 437-443.
- Spielberger, R., Stiff, P., & Bensinger, W. (2004). A phase 3, randomized, double-blind, placebo-controlled trial of palifermin for reduction of mucositis in patients with hematologic

- malignancies undergoing TBI with high-dose chemotherapy with auto-PBPCT. *N Engl J Med*, 351, 2590-2598.
- Srivastava, P., Kingsley, P. A., Srivastava, H., Sachdeva, J., & Kaur, P. (2015). Persistent post-radiotherapy pain and locoregional recurrence in head and neck cancer-is there a hidden link? *The Korean Journal of Pain*, 28(2), 116.
- Sroussi, H. Y., Epstein, J. B., Bensadoun, R. J., Saunders, D. P., Lalla, R. V., Migliorati, C. A., Heavilin, N., & Zumsteg, Z. S. (2017). Common oral complications of head and neck cancer radiation therapy: mucositis, infections, saliva change, fibrosis, sensory dysfunctions, dental caries, periodontal disease, and osteoradionecrosis. *Cancer medicine*, 6(12), 2918-2931.
- Stalpers, L. J., da Costa, H. C., Merbis, M. A., Fortuin, A. A., Muller, M. J., & van Dam, F. S. (2005). Hypnotherapy in radiotherapy patients: a randomized trial. *International Journal of Radiation Oncology* Biology* Physics*, 61(2), 499-506.
- Starmer, H. M., Yang, W., Raval, R., Gourin, C. G., Richardson, M., Kumar, R., Jones, B., McNutt, T., Cheng, S., & Quon, H. (2014). Effect of gabapentin on swallowing during and after chemoradiation for oropharyngeal squamous cell cancer. *Dysphagia*, 29(3), 396-402.
- Starobova, H., & Vetter, I. (2017). Pathophysiology of chemotherapy-induced peripheral neuropathy. *Frontiers in molecular neuroscience*, 10, 174.
- Stingone, J. A., Funkhouser, W. K., Weissler, M. C., Bell, M. E., & Olshan, A. F. (2013). Racial differences in the relationship between tobacco, alcohol, and squamous cell carcinoma of the head and neck. *Cancer Causes & Control*, 24(4), 649-664.
- Stordeur, S., Schillemans, V., Savoye, I., Vanschoenbeek, K., Leroy, R., Macq, G., Verleye, L., De Gendt, C., Nuyts, S., & Vermorken, J. (2020). Comorbidity in head and neck cancer: Is

- it associated with therapeutic delay, post-treatment mortality and survival in a population-based study? *Oral oncology*, 102, 104561.
- Stringer, A. M., & Logan, R. M. (2015). The role of oral flora in the development of chemotherapy-induced oral mucositis. *Journal of Oral Pathology & Medicine*, 44(2), 81-87.
- Suwinski, R., Sowa, A., Rutkowski, T., Wydmanski, J., Tarnawski, R., & Maciejewski, B. (2003). Time factor in postoperative radiotherapy: a multivariate locoregional control analysis in 868 patients. *International Journal of Radiation Oncology* Biology* Physics*, 56(2), 399-412.
- Syrigos, K. N., Karachalios, D., Karapanagiotou, E. M., Nutting, C. M., Manolopoulos, L., & Harrington, K. J. (2009). Head and neck cancer in the elderly: an overview on the treatment modalities. *Cancer treatment reviews*, 35(3), 237-245.
- Takeuchi, I., Kawamata, R., & Makino, K. (2020). A rat model of oral mucositis induced by cancer chemotherapy for quantitative experiments. *Anticancer Research*, 40(5), 2701-2706.
- Tarnawski, R., Fowler, J., Skladowski, K., Świerniak, A., Suwiński, R., Maciejewski, B., & Wygoda, A. (2002). How fast is repopulation of tumor cells during the treatment gap? *International Journal of Radiation Oncology* Biology* Physics*, 54(1), 229-236.
- Tarone, L., Barutello, G., Iussich, S., Giacobino, D., Quaglino, E., Buracco, P., Cavallo, F., & Riccardo, F. (2019). Naturally occurring cancers in pet dogs as pre-clinical models for cancer immunotherapy. *Cancer Immunology, Immunotherapy*, 68(11), 1839-1853.
- Thariat, J., Bolle, S., Demizu, Y., Marcy, P.-Y., Hu, Y., Santini, J., Bourhis, J., & Pommier, P. (2011). New techniques in radiation therapy for head and neck cancer: IMRT, CyberKnife, protons, and carbon ions. Improved effectiveness and safety? Impact on survival? *Anti-cancer drugs*, 22(7), 596-606.

- Thomas, J., Beinhorn, C., Norton, D., Richardson, M., Sumler, S.-S., & Frenkel, M. (2010). Managing radiation therapy side effects with complementary medicine. *Journal of the Society for Integrative Oncology*, 8(2), 65.
- Thompson, A. R. (2000). Opioids and their proper use as analgesics in the management of head and neck cancer patients. *American journal of otolaryngology*, 21(4), 244-254.
- Trotti, A., Bellm, L. A., Epstein, J. B., Frame, D., Fuchs, H. J., Gwede, C. K., Komaroff, E., Nalysnyk, L., & Zilberberg, M. D. (2003). Mucositis incidence, severity and associated outcomes in patients with head and neck cancer receiving radiotherapy with or without chemotherapy: a systematic literature review. *Radiotherapy and oncology*, 66(3), 253-262.
- Urata, K., Shinoda, M., Honda, K., Lee, J., Maruno, M., Ito, R., Gionhaku, N., & Iwata, K. (2015). Involvement of TRPV1 and TRPA1 in incisional intraoral and extraoral pain. *Journal of dental research*, 94(3), 446-454.
- Vacha, P., Fehlauer, F., Mahlmann, B., Marx, M., Hinke, A., Sommer, K., Richter, E., & Feyerabend, T. (2003). Randomized Phase III Trial of Postoperative Radiochemotherapy±Amifostine in Head and Neck Cancer. *Strahlentherapie und Onkologie*, 179(6), 385-389.
- Vadhan-Raj, S., Trent, J., Patel, S., Zhou, X., Johnson, M. M., Araujo, D., Ludwig, J. A., O'Roark, S., Gillenwater, A. M., & Bueso-Ramos, C. (2010). Single-dose palifermin prevents severe oral mucositis during multicycle chemotherapy in patients with cancer: a randomized trial. *Annals of internal medicine*, 153(6), 358-367.
- Vadhan-Raj, S., Goldberg, J. D., Perales, M. A., Berger, D. P., & van den Brink, M. R. (2013). Clinical applications of palifermin: amelioration of oral mucositis and other potential indications. *Journal of cellular and molecular medicine*, 17(11), 1371-1384.

- van den Beuken-van Everdingen, M. H. J., de Rijke, J. M., Kessels, A. G., Schouten, H. C., van Kleef, M., & Patijn, J. (2007). Prevalence of pain in patients with cancer: a systematic review of the past 40 years. *Annals of Oncology*, 18(9), 1437-1449.
- Van Der Schroeff, M. P., Van De Schans, S. A., Piccirillo, J. F., Langeveld, T. P., Baatenburg de Jong, R. J., & Janssen-Heijnen, M. L. (2010). Conditional relative survival in head and neck squamous cell carcinoma: permanent excess mortality risk for long-term survivors. *Head & Neck*, 32(12), 1613-1618.
- Vanhelleputte, P., Nijs, K., Delforge, M., Evers, G., & Vanderschueren, S. (2003). Pain during bone marrow aspiration: prevalence and prevention. *Journal of pain and symptom management*, 26(3), 860-866.
- Vanhoecke, B., Bateman, E., Mayo, B., Vanlancker, E., Stringer, A., Thorpe, D., & Keefe, D. (2015). Dark Agouti rat model of chemotherapy-induced mucositis: establishment and current state of the art. *Experimental Biology and Medicine*, 240(6), 725-741.
- Vayne-Bossert, P., Escher, M., de Vautibault, C. G., Dulguerov, P., Allal, A., Desmeules, J., Herrmann, F. R., & Pautex, S. (2010). Effect of topical morphine (mouthwash) on oral pain due to chemotherapy-and/or radiotherapy-induced mucositis: a randomized double-blinded study. *Journal of palliative medicine*, 13(2), 125-128.
- Veerasarn, V., Phromratanapongse, P., Suntornpong, N., Lorvidhaya, V., Sukthomya, V., Chitapanarux, I., Tesavibul, C., Swangsilpa, T., Khorprasert, C., & Shotelersuk, K. (2006). Effect of Amifostine to prevent radiotherapy-induced acute and late toxicity in head and neck cancer patients who had normal or mild impaired salivary gland function. *JOURNAL-MEDICAL ASSOCIATION OF THAILAND*, 89(12), 2056.

- Velez, I., Spielholz, N. I., Siegel, M. A., & Gonzalez, T. (2014). MuGard, an oral mucoadhesive hydrogel, reduces the signs and symptoms of oral mucositis in patients with lichen planus: a double-blind, randomized, placebo-controlled pilot study. *Oral Surgery, Oral Medicine, Oral Pathology and Oral Radiology*, 118(6), 657-664.e652.
- Vera-Llonch, M., Oster, G., Hagiwara, M., & Sonis, S. (2006). Oral mucositis in patients undergoing radiation treatment for head and neck carcinoma: risk factors and clinical consequences. *Cancer: Interdisciplinary International Journal of the American Cancer Society*, 106(2), 329-336.
- Vesty, A., Gear, K., Biswas, K., Mackenzie, B. W., Taylor, M. W., & Douglas, R. G. (2020). Oral microbial influences on oral mucositis during radiotherapy treatment of head and neck cancer. *Supportive Care in Cancer*, 28(6), 2683-2691.
- Villa, A., & Sonis, S. T. (2016). Pharmacotherapy for the management of cancer regimen-related oral mucositis. *Expert opinion on pharmacotherapy*, 17(13), 1801-1807.
- Villa, A., Vollemans, M., De Moraes, A., & Sonis, S. (2021). Concordance of the WHO, RTOG, and CTCAE v4.0 grading scales for the evaluation of oral mucositis associated with chemoradiation therapy for the treatment of oral and oropharyngeal cancers. *Supportive care in cancer*, 29(10), 6061-6068.
- Watanabe, T., Ishihara, M., Matsuura, K., Mizuta, K., & Itoh, Y. (2010). Polaprezinc prevents oral mucositis associated with radiochemotherapy in patients with head and neck cancer. *International journal of cancer*, 127(8), 1984-1990.
- Watkins, B., Pouliot, K., Fey, E., Tuthill, C., & Sonis, S. (2010). Attenuation of radiation-and chemoradiation-induced mucositis using gamma-d-glutamyl-l-tryptophan (SCV-07). *Oral diseases*, 16(7), 655-660.

- Wells, M., Swartzman, S., Lang, H., Cunningham, M., Taylor, L., Thomson, J., Philp, J., & McCowan, C. (2016). Predictors of quality of life in head and neck cancer survivors up to 5 years after end of treatment: a cross-sectional survey. *Supportive Care in Cancer*, 24(6), 2463-2472.
- Wiegand, S., Zimmermann, A., Wilhelm, T., & Werner, J. A. (2015). Survival after distant metastasis in head and neck cancer. *Anticancer research*, 35(10), 5499-5502.
- Wilkinson, S. M., Love, S. B., Westcombe, A. M., Gambles, M. A., Burgess, C. C., Cargill, A., Young, T., Maher, E. J., & Ramirez, A. J. (2007). Effectiveness of aromatherapy massage in the management of anxiety and depression in patients with cancer: a multicenter randomized controlled trial. *Journal of Clinical Oncology*, 25(5), 532-539.
- Withers, H., Taylor, J., & Maciejewski, B. (1988). The hazard of accelerated tumor clonogen repopulation during radiotherapy. *Acta oncologica*, 27(2), 131-146.
- Wong, P. C., Dodd, M. J., Miaskowski, C., Paul, S. M., Bank, K. A., Shiba, G. H., & Facione, N. (2006). Mucositis pain induced by radiation therapy: prevalence, severity, and use of self-care behaviors. *Journal of pain and symptom management*, 32(1), 27-37.
- Yamashita, S., Sato, S., Kakiuchi, Y., Miyabe, M., & Yamaguchi, H. (2002). Lidocaine toxicity during frequent viscous lidocaine use for painful tongue ulcer. *Journal of pain and symptom management*, 24(5), 543-545.
- Ye, Y., Dang, D., Zhang, J., Viet, C. T., Lam, D. K., Dolan, J. C., Gibbs, J. L., & Schmidt, B. L. (2011). Nerve growth factor links oral cancer progression, pain, and cachexia. *Molecular cancer therapeutics*, 10(9), 1667-1676.

- Yu, E. H., Lui, M. T., Tu, H. F., Wu, C. H., Lo, W. L., Yang, C. C., Chang, K. W., & Kao, S. Y. (2014). Oral carcinoma with perineural invasion has higher nerve growth factor expression and worse prognosis. *Oral diseases*, 20(3), 268-274.
- Zakeri, K., MacEwan, I., Vazirnia, A., Cohen, E. E., Spiotto, M. T., Haraf, D. J., Vokes, E. E., Weichselbaum, R. R., & Mell, L. K. (2014). Race and competing mortality in advanced head and neck cancer. *Oral oncology*, 50(1), 40-44.
- Zayed, S., Lin, C., Boldt, R. G., Sathya, J., Venkatesan, V., Read, N., Mendez, L. C., Moulin, D. E., & Palma, D. A. (2021). Risk of Chronic Opioid Use After Radiation for Head and Neck Cancer: A Systematic Review and Meta-Analysis. *Advances in Radiation Oncology*, 6(2), 100583.
- Zhang, X., Huang, J., & McNaughton, P. A. (2005). NGF rapidly increases membrane expression of TRPV1 heat-gated ion channels. *The EMBO journal*, 24(24), 4211-4223.
- Zhu, Y., Colak, T., Shenoy, M., Liu, L., Pai, R., Li, C., Mehta, K., & Pasricha, P. J. (2011). Nerve growth factor modulates TRPV1 expression and function and mediates pain in chronic pancreatitis. *Gastroenterology*, 141(1), 370-377.

**Chapter 2: “Development and Evaluation of Behavioral Assays of Acute Orofacial Pain in
a Mouse Model of Lingual Irradiation.”**

2.1 Introduction

Head and neck squamous cell carcinoma (HNSCC) is an aggressive malignancy characterized by high morbidity and low survival rates (Chin et al., 2006; Cohen et al., 2018). Radiation therapy (RT) is an important therapeutic modality in the curative-intent management of locoregional HNSCC, however, intense courses of RT can be very toxic (Sroussi et al., 2017). Radiation-associated pain (RAP) represents one of the most common and challenging-to-treat toxicities observed among HNSCC patients presenting ulcerative oral mucositis as a side effect of RT (Cramer et al., 2018; Moslemi et al., 2016). The presence of acute, orofacial RAP (hereafter referred to as “aoRAP”) is problematic because in addition to impair the patient’s functional status and quality of life, it can sometimes lead to interruptions and even discontinuations of RT with potential adverse impact on outcomes (Epstein & Barasch, 2018; Rosenthal, 2007; Sroussi et al., 2017). Although radiation-induced oral mucositis (hereafter referred to as “RIM”) is an acknowledged leading cause of aoRAP (Epstein et al., 2010), remarkably little is known about the specific mechanisms that generate and maintain this pain in HNSCC patients. This fact might explain the absence of effective, non-opioid analgesic strategies for the management of aoRAP in this population, as well as to underscore the need to understand the biological mechanisms driving this form of pain.

In order to study the pathogenesis of aoRAP, appropriate animal models and pain-outcome measures are required. As previously discussed in Chapter 1, several rodent models of RIM currently exist in the literature, either induced by single-dose or fractionated ionizing irradiation (Alvarez et al., 2003; Dörr & Kummermehr, 1990; Dörr et al., 2002; Gruber et al., 2017; Hwang et al., 2005). Yet to our knowledge, none of these animal models have been used to specifically phenotype oral mucositis pain, nor to identify and characterize the direct mediators and pathways

that regulate aoRAP processing. Because modeling of aoRAP is currently limited by a paucity of validated pain assays, our research group has conducted extensive research in the last years in order to develop a translational mouse model of RIM (glossitis) for the study and measurement of aoRAP (Lai et al., 2021; Nolan et al., 2017; Price et al., 2021). In these studies, we have characterized aoRAP by measuring changes in reflexive (i.e., evoked by stimulation) and non-reflexive (voluntary, un-evoked) responses. The eye wiping assay is a reflex-withdrawal based test commonly used in trigeminal pain studies that involves the count of wipes after applying one drop of 0.9% sodium chloride into the animal eyes, which indirectly measures the activation of primary nociceptive afferents of the ophthalmic division within the sensory trigeminal system (Farazifard et al., 2005; Launay et al., 2016). The burrowing assay, conversely, is a preclinical measure of non-evoked pain that quantifies the amount of material (e.g., food pellets) left in an enclosed tube 30 minutes or more after presentation to the mouse. Burrowing is a highly motivated and spontaneous home-cage rodent behavior; therefore, this assay has emerged as a relevant voluntary behavioral tool in the field of pain research to assess wellbeing and/or the “global impact” of pain in rodents with minimal human intervention (Andrews et al., 2012; Jirkof, 2014; Jirkof et al., 2010). The rationale for using these outcome measures in our studies relied on the fact that we are aiming to assess the different dimensions of the aoRAP experience *in vivo*, such as sensory-discriminative dimensions (via the eye wiping assay) and affective dimensions (via the burrowing assay). Additionally, we have measured changes in feeding behaviors (i.e., reduction in body weight) to assess the impact of RIM in oral function. According to our results, an increase in wiping behaviors and decrease in burrowing activity and body weight are consistently observed in mice with visible RIM lesions. While these outcome measures offer a key step towards the validation of our murine model of aoRAP, additional characterization is still needed in order to

capture some dimensions of pain that might be more relevant in the context of HNSCC. In particular, none of our assays provides a metric of spontaneous pain behaviors (i.e., measurement of affective/motivational pain components) in the orofacial region. This is relevant when studying aoRAP because clinical studies have indicated that pain at oral sites is not only strongly affected by sensory components in HNSCC patients, but also by affective/motivational components (Epstein et al., 2009). Hence, it is important to assess the multidimensional nature of aoRAP in rodents to increase the translation of preclinical findings to the clinic.

During the conduct of previous work in our laboratory, we noticed that nesting and grooming behaviors (two voluntary, spontaneous home-cage activities) were strongly impaired in mice with ulcerative RIM. Indeed, watching mice create nests out of provided materials clearly shows they use their mouths to shred the material. We also observed that grooming, which involves repeated licking of paws after the paws are pulled over the fur, was clearly decreased in mice with ulcerative RIM. These findings were particularly interesting because nest building and grooming behaviors have been extensively used as proxy-indicators of postoperative spontaneous pain and to evaluate analgesic efficacy in mice (Gaskill et al., 2013; Jirkof et al., 2013; Kerr & David, 2007; Matsumiya et al., 2012; Negus et al., 2015; Oliver et al., 2018; Spradley et al., 2012). In comparison to reflex-withdrawal based assays, and similar to the burrowing assay, these assays can measure spontaneous pain-related behaviors in a noninvasive and low-stress manner within the animal's home cage, and such outcome measures have been shown to be highly reproducible, and require minimal training (Jirkof, 2014; Jirkof et al., 2013; Rock et al., 2014). However, nesting and grooming activities have not been used as behavioral metrics to assess orofacial pain in mice. In the current work, we introduce a novel behavioral test battery based on nesting and grooming behaviors, which was designed to reflect the onset, progression, and severity of aoRAP as a result

of RIM in mice. The purpose of this study was to assess the ability of our assays to predict changes in RIM under different experimental conditions, as well as to evaluate the reliability and validity of our methods and measurement strategies.

2.2 Material and Methods

2.2.1 Experimental overview

In the first part of this study, we examined whether our newly developed behavioral assays were able to mirror the progression of RIM and associated weight loss in tongue-irradiated BALB/c mice (female) in a similar degree to other behavioral assays, such as the eye wiping and burrowing assays. We then tested their ability to discriminate mice experiencing high-grade RIM from those that never developed RIM across mouse sexes, different strains (BALB/c versus C57BL/6), and differing irradiation regimens (single-dose versus fractionated modality). Afterwards, we evaluated the change of nesting and grooming behaviors through the full progression and resolution of RIM in tongue-irradiated C57BL/6 mice (female). After evaluating the level of agreement between scores obtained in real-time versus those obtained remotely using digital material, we examined the reliability of our scoring systems in terms of internal consistency, inter-observer reliability, and test-retest reliability using a computer-based (remote) scoring modality. Finally, we assessed the validity of our assays (i.e., responsiveness) by comparing nesting and grooming scores between irradiated mice that did and did not receive analgesic strategies.

2.2.2 Animals

In this study, we used 10- to 14-week-old BALB/c (female and males) and C57BL/6 (female) mice purchased from Charles River Laboratories (NCrl substrains). Mice were quarantined and acclimated for at least 2 weeks before the start of experiments. For all experiments, mice were randomly assigned to the defined experimental groups, and group-housed (2-4 animals per cage) in a controlled environment (22°C; humidity 50%) under specific pathogen-free facilities and maintained on a 12-hours day-night cycle. Mice were given ad libitum access to water and commercial pelleted diet; daily nutritional gel (DietGel 76A, ClearH2O) was provided on the floor of the cage from the start to the end of every experiment. Any additional enrichment objects were removed from all cages throughout our studies. Pre-defined criteria for euthanasia included: increased respiratory effort, anorexia for more than 24 hours (once RIM had resolved), hunched posture, or more than 30% weight loss. Euthanasia was performed via asphyxiation (3.5 L/min CO₂ chamber), followed by cervical dislocation. All experimental procedures were approved by the North Carolina State University Institutional Animal Care and Use Committee (protocol #'s: 18-061-B and 19-810-B).

2.2.3 Animal irradiations

Within each experiment, RIM was induced by delivering high doses of lingual ionizing irradiation (IR). In most experiments, a single dose of IR (27 Gy) restricted to the rostral tongue was used to induce severe but reversible acute RIM. IR was performed using a clinical linear accelerator (LINAC) and 6 megavolt X-ray beam (Novalis TX, Varian Medical Systems). A detailed description of this IR protocol has been previously described (Lai et al., 2021). In some experiments, RIM was induced using a 5-fraction IR scheme (6.5 Gy x 5 daily fractions; XRAD 320 kilovolt X-ray irradiator). In this protocol, 4 mice were simultaneously anesthetized and

individually placed inside an immobilization, shielding device (made of plexiglass with lead plates on top) that allowed us to exclusively expose the mouse tongue while protecting the rest of the body from IR (as shown in Figure 2.1A). Tongues were gently exposed using rubber-tipped forceps and the tip of the tongue was held on top of the device's lead shielding using clear adhesive tape. The 4 immobilization boxes were then placed inside the XRAD 320 irradiator (on top of the table); boxes touched corners at the inside edge, and the back (tail) end of them was aligned with the SSD 60 cm line on the tabletop (Figure 2.1B). Tongues were located at the laser crosshair, and actual mouse irradiation was done using the spinning/rotating table option to ensure homogeneous treatment of all mice (Figure 2.1C). Irradiation doses were set to 600-650 cGy for each fraction/day (program 17, SDD 35 cm), and an electrometer was used every time to measure and register the exact dose received in the area where the tongue was located. In most experiments, a control sham-irradiated group (sham-IR) was added for comparison; these mice received sham-irradiation (i.e., 0 Gy) using the same methods described above. During irradiation and sham-irradiation, general anesthesia was done using an intraperitoneal injection of ketamine (50-150 mg/kg, 100 mg/mL, Henry Schein) and xylazine (10 mg/kg, 20 mg/mL, Anased, Lloyd Laboratories).

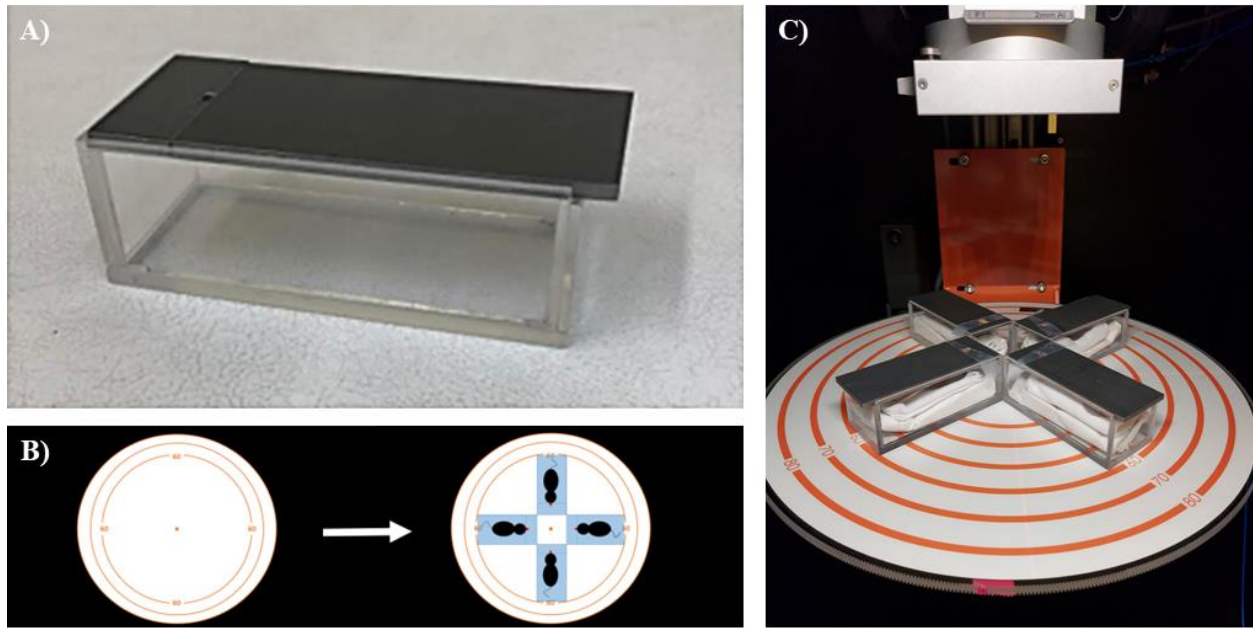


Figure 2.1: Fractionated lingual irradiation using XRAD 320 kilovolt X-ray irradiator. A) Immobilization/shielding device made of plexiglass with lead plates. B) Position of immobilization boxes on top of the spinning/rotating table. C) Image representation of the final settings, and the way that tongues were exposed.

2.2.4 Assessment of RIM and associated body weight loss

RIM progression was monitored daily from day 0 (IR delivery) until the end of every experiment and rated using a 6-point subjective scale. Briefly, a score of zero (0) indicates no change from baseline; (1) erythema, vascular dilation, 1-2 small blister-like lesions, and mild edema; (2) patchy ulceration and/or pseudomembrane formation, 2 or more blister-like lesions, ptyalism, and moderate edema; (3) confluent ulceration or fibrinous membrane formation within the irradiated field; (4) hemorrhage or necrosis; and (5) death. RIM scoring was performed by the author who visually inspected the mucosal lesions by gently extracting the tongue using non-traumatic forceps in mice briefly anesthetized with isoflurane. Measurement of body weight (expressed as percentage change from baseline) acted as a surrogate marker of overall health; for

all experiments, animals were weighed daily with an electronic scale immediately after assessing RIM.

2.2.5 Nesting and grooming assays

2.2.5.1 Assay development: Existing methodologies were used as a basis to develop a strategy to assess aoRAP by means of nesting and grooming activities. We started by critically evaluating previously published protocols and scoring systems (Gaskill et al., 2013; Oliver et al., 2018), and by determining which items would accommodate our testing conditions. By combining published information and observations acquired during the conduct of previous experiments in our laboratory, we developed a methodology to measure nesting and grooming activities during the most active times in their circadian cycle (i.e., dark cycle) with minimal handling (thus avoiding handling-induced stress). Nesting activity was measured using two different criteria: 1) the ability to build a nest, and 2) the ability to shred the nest material; therefore, two independent assays were developed for this outcome measure. Self-grooming behavior was indirectly measured by assessing the changes in physical appearance.

2.2.5.2 Scoring system

2.2.5.2.a Nesting assay: Nesting activity was measured using two assays. The first assay, “Nest Building Assay”, rated the ability of mice to build an adequate nest using a 3-point scale (Figure 2.2A). Briefly, a score of 0 (zero) indicates “normal nest” (i.e., most of the nestlet has been completely torn into small pieces; pieces are arranged together into one area of the cage); (1) “abnormal nest” (i.e., incomplete shredding of the nestlet (large pieces may remain); pieces may remain scattered around the cage (not all arranged together)); and (2) “absent” (i.e., nestlet (white cotton square) was not noticeably touched). The second nesting assay, “Nest Shredding Assay”, rated the ability of mice to shred the nest using a 4-point scale (Figure 2.2B). Briefly, a score of 0

(zero) indicates “fully shredded” (i.e., entire nestlet was torn into small pieces that are essentially the same size); (1) “partially shredded” (i.e., can no longer discern the original square shape of the nestlet; there is a mix of small and mid-sized pieces), (2) “minimally shredded” (i.e., square shape of nestlet is obvious; there are very few smaller pieces); and (3) “not shredded at all” (i.e., nestlet was minimally noticeable touched (retains square shape)). Scores of each subscale were examined separately.

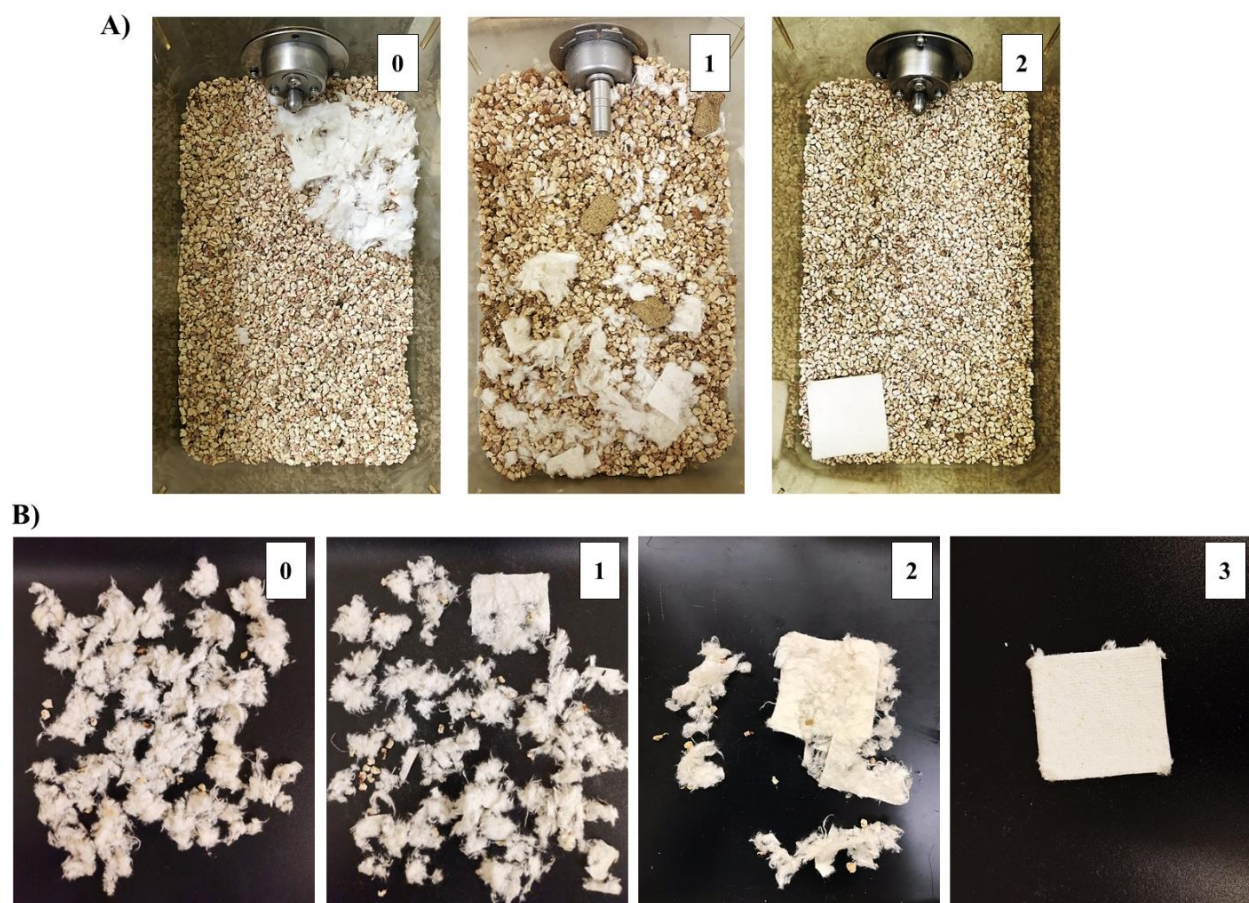


Figure 2.2: Nesting assay. A) Nest building assay (rated using a 3-point scale). B) Nest shredding assay (rated using a 4-point scale).

2.2.5.2.b) *Grooming assay:* Self-grooming behavior (evaluated by means of mouse physical appearance) was rated using a 3-point scale. Briefly, a score of 0 (zero) categorizes grooming

activity as “normal” (i.e., clean, smooth/silky haircoat); (1) “abnormal – moderate” (i.e., face and/or body look messy, with hair “standing on end”; mouse looks dry); and (2) “abnormal – severe” (i.e., disheveled, wet and/or greasy haircoat (especially in the face and neck/chest area); possible discoloration of coat, erythema, and areas of hair loss (alopecia)). The same scoring system was used for white (Figure 2.3A) and black (Figure 2.3B) mice.



Figure 2.3: Grooming assay (rated using a 3-point scale). A) White mice (BALB/c strain). B) Black mice (C57BL/6 strain).

2.2.5.3 Assay methods: For all experiments, mouse cages were tested in a randomized order throughout the study. During acclimation (before IR), mice were habituated to the assay’s materials (e.g., nestlet) for at least 5 days before baseline values were obtained. All behavioral assays were conducted by the author, who was unblinded to the experimental groups and time

points for most assessments. Briefly, mice were sequentially transferred to individual testing cages (i.e., standard mouse cages) containing: 1) standard amount of bedding material (no enrichment added), 2) one commercially available cotton fiber nest material (Nestlet; 5 cm x 5 cm, 5 mm thick, ~2.5 g each; Ancare Corporation) placed in one corner of the cage, 3) food (commercial pellets and DietGel) placed in the opposite corner of the cage (floor), and 4) water (tube placed on the wire-bar lids). Mice were then left alone in their respective testing cages in a quiet room during the dark cycle; all test sessions took place between 5:00 P.M. and 8:00 A.M. The author returned the next day at 8:00 A.M., and scoring was done. Briefly, each cage lid was removed to allow full visualization of the individual nests and animals, allowing to score results from the nest building and grooming assays with minimal interference. Then, each nest was removed from the cage and spread on top of a black surface to visualize individual pieces of the nest material and record scores from the nest shredding assay. During scoring, photographs and/or videos of each nest and mouse were taken for later assessment (reliability evaluation). To keep the uniformity of images, the capture of this content was done using specific techniques. First, all nest photographs obtained for the nest building and shredding assays were taken at a distance of 30-40 centimeters above the mouse cage (as shown in Figure 2.2A) or the black-color tabletop (as shown in Figure 2.2B), respectively, using standard mouse colony lighting (i.e., warm light of low intensity). For the grooming photographs and/or videos, animal were individually placed in a 9.6 x 9.6 x 9.1-inch photo studio box with white backdrop and white LED lighting (Emart International Inc., California); images were taken keeping a 20 centimeters distance between the mouse and the camera lens. All images were captured using a mobile phone (Samsung Galaxy S10, 12-megapixel resolution). After that, each mouse was returned to their respective group cages.

Assays were conducted at different time points following IR depending on the experiment. In all experiments, baseline data was collected the day before irradiation (i.e., absent RIM). Based on our experience with this model of RIM (Nolan et al., 2017), the other selected timepoints of assessment were: 1) the time when no visible signs of RIM are observed (i.e., day 4 post-IR); 2) the time when signs of grade 1 RIM are observed (i.e., day 8 post-IR); 3) the time when signs of grade > 2 RIM are observed (i.e., day 11 post-IR); and 4) the time when signs of RIM resolution are observed (i.e., day 15 or 19 post-IR, depending on the experiment).

2.2.6 Reliability and validity assessment of nesting and grooming assays

2.2.6.1 Score reproducibility assessment: Before testing the reliability of our scoring systems, we first confirmed the ability of a computerized-based (remote) assessment modality to reproduce the results obtained during real-time assessment. The goal here was to determine if results obtained from remote scoring differed from those obtained during the conduction of experiments, potentially paving the way for reliability assessment to be done using a computerized-based assessment modality. For this section, we used the data obtained from an experiment performed in C57BL/6 mice (female).

2.2.6.2 Reliability assessment: The goal here was to assess the reliability of our scoring systems (by means of internal consistency, inter-observer reliability, and test-retest reliability) using a specific set of images and videos collected from some of the experiments conducted in this study. In addition, we used this material to determine the agreement (reproducibility) of scores between expert (i.e., the author of this work, hereafter referred as “Evaluator 1”) and non-expert evaluators (Evaluators 2 to 7). For this assessment, we recruited six students from North Carolina State University with similar education backgrounds (i.e., undergraduate students) to score the selected digital material. All evaluators were blinded to groups, time of assessment, and type of study that

was being conducted. To better understand the applicability of our assays in other mouse-based biomedical research facilities, we divided results from our evaluators into two groups based on their experience working with laboratory mice: 1) evaluators 2 to 4: no experience, and 2) evaluators 5 to 7: basic to high experience.

2.2.6.2.a) Digital material: A total of three Microsoft PowerPoint (MPP) presentations (i.e., one for each nesting assay, and one for the grooming assay) were created and distributed to all evaluators. For each MPP presentation, we included a brief instruction to guide evaluators about the scoring process, and the respective scoring system (scale's description and illustration). After that, a number of slides containing pictures or videos that were considered by the author to be an accurate representation of each item scale were included for scoring. Each slide contained either an image or a video, and the corresponding scoring system that aimed to be used as a guide (see example in Figure 2.4). Each item scale of the nesting assays had 10 representative images (i.e., a total of 30 images for the nesting building assay, and a total of 40 images for the nesting shredding assay), and each item of the grooming assay had 10 representative videos or images (i.e., a total of 40 videos for white mice (BALB/c strain), and a total of 40 images for black mice (C57BL/6 strain)). Slides were distributed in each presentation in a randomized order.

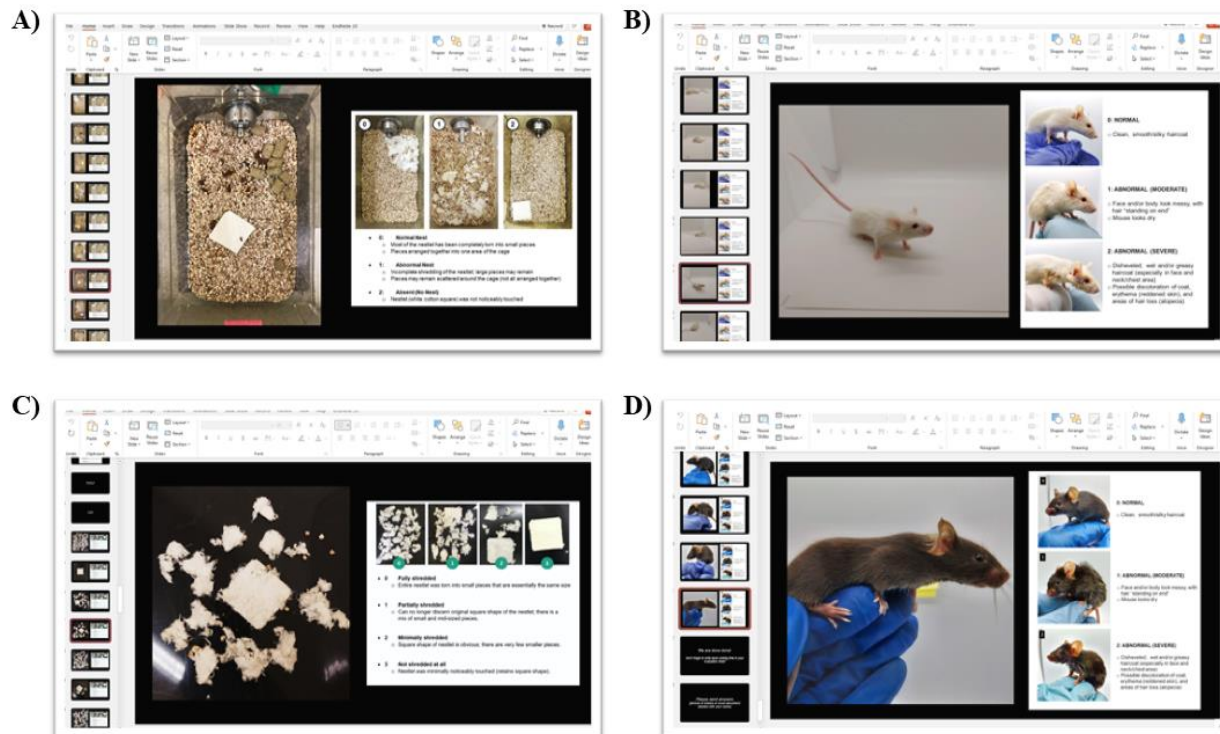


Figure 2.4: Example of Microsoft PowerPoint presentations used for the reliability assessment. A) Nest building assay; B) Nest shredding assay; C) Grooming assay (white mice); D) Grooming assay (black mice).

2.2.6.2.b) *Internal consistency and inter-rater reliability assessment:* Evaluators had 3 days to score all the digital content (i.e., MPP presentations). We asked evaluators to perform all the scoring in one sitting and gave them the option to change their answers at any moment before submitting their final scoring. Results were sent to the author via email (recorded in pre-made Excel sheets). Evaluator 1 was used here as a local (unblinded) observer, and her results were used as a “gold standard” reference.

2.2.6.2.c) *Stability (test-retest) assessment:* In order to measure the test-re-test stability (reliability) of scoring, we asked three of the six recruited evaluators to re-score the digital material 7 days

later using new MPP presentations (same presentations, different slide order). Evaluator 1 also re-scored the digital material using the same MPP presentations.

2.2.6.3 Validity assessment: In this assessment, we determined the responsiveness of the assays to the use of various analgesics to treat aoRAP. We first examined whether our assay's scores changed after administering a single dose of different standard analgesics that are clinically accessible and have demonstrated to be effective in alleviating other types of pain (i.e., carprofen, hydromorphone, and anti-NGF mAb). After determining which strategy was most effective in mitigating aoRAP (i.e., anti-NGF mAb), we conducted a larger study to assess the responsiveness of our assays to the administration of the selected analgesic. We further evaluated responsiveness by effecting pain relief by ablating TRPV1-expressing neurons known to be centrally important in encoding pain.

2.2.6.3.a) Standard analgesics: In a pilot study, 4 groups of 8 female BALB/c mice underwent tongue IR (27 Gy, LINAC) and received a single dose administration of either an NSAID (carprofen 25 mg/kg, subcutaneous), opioid (hydromorphone 22 mg/kg, intraperitoneal), nerve growth factor inhibitor (anti-NGF mAb, 50 μ L/mouse, intraperitoneal), or saline (50 μ L of 0.9% sterile saline solution). Analgesics were given at different times depending on their elimination half-life. The goal here was to conduct our behavioral assays at the time that the maximal analgesic effect was reached. Due to the short duration of some drugs using a single dose, we adapted our assay's time of assessment from a dark-cycle assessment modality (i.e., 5:00 P.M. to 8:00 A.M.) to a 2-hour assessment modality done during the light-cycle (i.e., 8:00 A.M. to 10:00 A.M.). A single injection of carprofen and saline was given at 3:00 A.M. on day 11 post-IR, hydromorphone at 6:00 A.M. on day 11 post-IR, and anti-NGF mAb at 8:00 A.M. on day 9 post-IR. The most effective analgesic was then used to assess responsiveness in a larger, independent experiment.

Here, 84 female BALB/c mice underwent IR or sham-IR (27 versus 0 Gy, LINAC IR), and either received 2 consecutive doses of anti-NGF mAb (8:00 A.M. injections) on day 5 and 9 post-IR (50 μ L/mouse), or an isotype control solution (IgG, 50 μ L/mouse). Mice here were randomly allocated to one of four treatment groups: 1) 0 Gy + IgG; 2) 27 Gy + IgG; 3) 0 Gy + anti-NGF mAb; or 4) 27 Gy + anti-NGF mAb.

2.2.6.3.b) Analgesia via TRPV1-expressing neuron deletion: In this experiment, we selectively deleted TRPV1-expressing neurons using systemic administration of resiniferatoxin (RTX), a potent TRPV1 agonist (Menéndez et al., 2006). Pharmacologic grade RTX (200 μ g/mL) and excipient were kindly provided by Dr. Alexis Nahama (Sorrento Therapeutics). Female BALB/c mice either received a single interscapular subcutaneous dose of 300 μ g/kg of RTX (Al-Mogairen, 2020) or an equivalent volume of the excipient 6 days prior IR or sham-IR (0 versus 27 Gy, LINAC IR). Mice were randomly allocated to one of four treatment groups: 1) 0 Gy + RTX excipient; 2) 27 Gy + RTX excipient; 3) 0 Gy + RTX; or 4) 27 Gy + RTX. Ablation of TRPV1-expressing neurons in the trigeminal pathway was assessed weekly via topical administration of 0.01% capsaicin (diluted in 0.9% sodium chloride; total volume administered: 15 μ L) into the left eye. Responses were video recorded and later reviewed by a blinded observer who counted and recorded the number of facial wipes over 1 minute immediately following topical application of capsaicin. A 50% reduction from baseline in the number of wipes per minute was considered here as a successful ablation.

2.2.7 Burrowing and eye wiping assays

Burrowing and eye wiping assays were performed in selected experiments. Both assays have been extensively used by our laboratory members in the past to track the changes in RIM scores (Lai et al., 2021; Nolan et al., 2017).

2.2.7.1 Burrowing assay: Briefly, mice were single-housed for 30 minutes in standard gerbil-size cages with a small amount of bedding and PVC pipe tubes that contained 150 grams of commercial pelleted rabbit feed (Prolab high-fiber diet, PMI, Brentwood, MO). The contents of the tube were re-weighed after the completion of the assays to determine the residual mass of feed. This assay was conducted on two occasions: once at baseline (prior IR or sham-IR) and once at day 10 post-IR. Before every baseline measure, a total of 3 training sessions were done using the same methodology aforementioned; however, the testing time varied among training sessions. Specifically, training sessions #1 and 2 were done in 1 hour, and training session #3 was done in 30 minutes.

2.2.7.2 Eye wiping assay: Briefly, mice were single-housed in microisolator cages, and the wiping behavior was assessed after the administration of innocuous stimulus (i.e., 15 μ L of 0.9% sodium chloride at 26°C) into the left eye. Responses (i.e., wipes) were video-recorded (Foscam FI9826W camera and Foscam Central Management Software, Shenzhen, PRC), and the number of wipes within the first minute following stimulation were manually counted by a blinded, trained observer with care taken to not score normal grooming behavior as wiping. This assay was conducted on two occasions: once at baseline (prior IR and sham-IR) and once at day 11 post-IR.

2.2.8 Statistical analysis

Results from previous preliminary studies performed in both female BALB/c and C57BL/6 mice were used to calculate sample sizes (JMP 14.1; SAS Institute Inc. Cary, NC, USA), with $\alpha = 0.05$ and 80% power; calculated sample sizes for each experiment are listed in Table 2.1.

2.2.8.1 General data handling: Normal distribution of the numeric data was evaluated by the Shapiro-Wilk normality test analysis, and appropriate parametric or non-parametric statistical tests were applied. Statistical significance was assessed by using Student's t-test (parametric, 2-tailed

unpaired) or Mann-Whitney test (non-parametric, 2-tailed unpaired) for comparisons between two groups. For comparison of two or more groups across time, a 2-way repeated-measures ANOVA analysis was used; p-values were adjusted for multiple comparisons using Tukey's, Dunnett's, or Sidak's post hoc test. Numerical data were plotted as mean + standard deviation (SD). Significant p-values for all analyses were set at < 0.05 . For the pilot study mentioned in section 2.2.6.3.a, we evaluated the effects of pain medications by measuring the total proportion of animals whose scores either 1) improved or not changed from baseline, or 2) worsened from baseline. Due to the small sample size used in this experiment, data were assessed using descriptive statistics (i.e., fraction of total, expressed in percentage). The statistical analysis here was done using commercial software (GraphPad Prism; Prism version 6).

2.2.8.2 Reliability assessment: Internal consistency was evaluated with Cronbach's alpha coefficient by comparing the scores of each assay (i.e., nest building assay scores versus nest shredding assay scores versus grooming assay scores); for this analysis, we used those scores recorded by Evaluator 1. Data were interpreted based on the general rule of thumb that states that α values of 0.70 and above show good internal consistency. Inter-rater and test-retest reliability was assessed using intra-class correlation coefficient (ICC) analysis (2-way mixed design). Based on the rule of thumb, agreement was categorized as follow: "very good" (0.81–1.0), "good" (0.61–0.80), "moderate" (0.41–0.60), "fair" (0.21–0.40), "poor" (<0.20). The statistical analysis here was done using commercial software (IBM SPSS Statistics; version 28.0).

Table 2.1: Sample sizes used for each experiment.

| List of experiment | n per experimental group | Total n/ experiment | Total n used |
|--|--------------------------|---------------------|--------------|
| Lingual irradiation and sham-irradiation in male BALB/c mice (27 vs 0 Gy, LINAC), no pain relief medication | 12 | 24 | 24 |
| Lingual irradiation and sham-irradiation in female C57BL/6 mice (27 vs 0 Gy, LINAC), no pain relief medication | 20 | 40 | 40 |
| Lingual irradiation and sham-irradiation in female C57BL/6 mice (32.5 vs 0 Gy, XRAD), no pain relief medication | 16 | 32 | 30 |
| Lingual irradiation and sham-irradiation in female BALB/c mice (27 vs 0 Gy, LINAC), carprofen vs hydromorphone vs anti-NGF vs saline | 8 | 32 | 32 |
| Lingual irradiation and sham-irradiation in female BALB/c mice (27 vs 0 Gy, LINAC), anti-NGF vs isotype control | 16 | 32 | 32 |
| Lingual irradiation and sham-irradiation in female BALB/c mice (27 vs 0 Gy, LINAC), resiniferatoxin vs excipient | 16 | 64 | 63 |

2.3 Results

2.3.1 RIM and associated weight loss in irradiated female BALB/c mice

As shown in Figure 2.5A, signs of grade 1 RIM started to be evident 8 days after mice received a single fraction of high-dose lingual irradiation (27 Gy). Yet, weight loss at this time point was minimal (i.e., less than 5%; Figure 2.5B). By day 10 post-IR, a rapid increase in RIM scores (overall mean score of 2) and associated decrease in body weight were seen. Maximal RIM scores (overall mean score of 2.3) were observed on the next day (i.e., day 11 post-IR), which was

accompanied by a marked loss in weight (~ 17% loss). Signs of RIM recovery started to be evident by day 12 post-IR (overall mean score of 2.1), and a drastic reduction in its severity was seen by day 13 post-IR (overall mean score of 0.8). RIM scores returned to baseline levels at day 17 post-IR, which was accompanied by a relevant gain in weight. As expected, sham-IR mice did not experience RIM development or weight loss at any time.

2.3.2 Time course of nesting and grooming assays in relation to RIM and body weight loss in irradiate female BALB/c mice

In line with RIM and body weight loss progression, we found at day 11 post-IR that scores from the nest building, shredding, and grooming assays in IR-mice were significantly higher than those scores obtained from baseline measures and from the sham-IR group (Figure 2.5C, D and E, respectively). By day 15 post-IR, nesting scores (from both assays) significantly decreased in IR-mice, yet they did not differ from baseline measures, or from those scores obtained from the sham-IR group. On this day, there was also a significant reduction in grooming scores from day 11 post-IR in IR-mice, however, overall scores at this time remained significantly higher in comparison to baseline measures and to those scores obtained from the sham-IR group. As expected, sham-IR mice did not experience impairment in these behavioral activities at any time.

2.3.3 Nesting and grooming assay scores benchmarked against eye wiping and burrowing activities in female BALB/c mice

Similar to the progression in nesting and grooming scores, and as we have seen in previous studies (Nolan et al., 2017), eye wiping responses (Figure 2.5F) and burrowing activities (Figure 2.5G) also significantly changed from baseline once RIM reached maximal severity. In particular, an exacerbated wiping response in comparison to baseline and sham-IR mice was observed in IR-

mice at day 11 post-IR, as well as a drastic reduction in their ability to burrow at day 12 post-IR; By day 15 post-IR, eye wiping responses were significantly higher in IR-mice in comparison to those scores documented at baseline, yet not different from the scores obtained from the sham-IR group; no data was collected for the burrowing assay at this time point. As expected, we did not see in sham-IR mice exacerbated wiping responses or impairment in burrowing at any time.

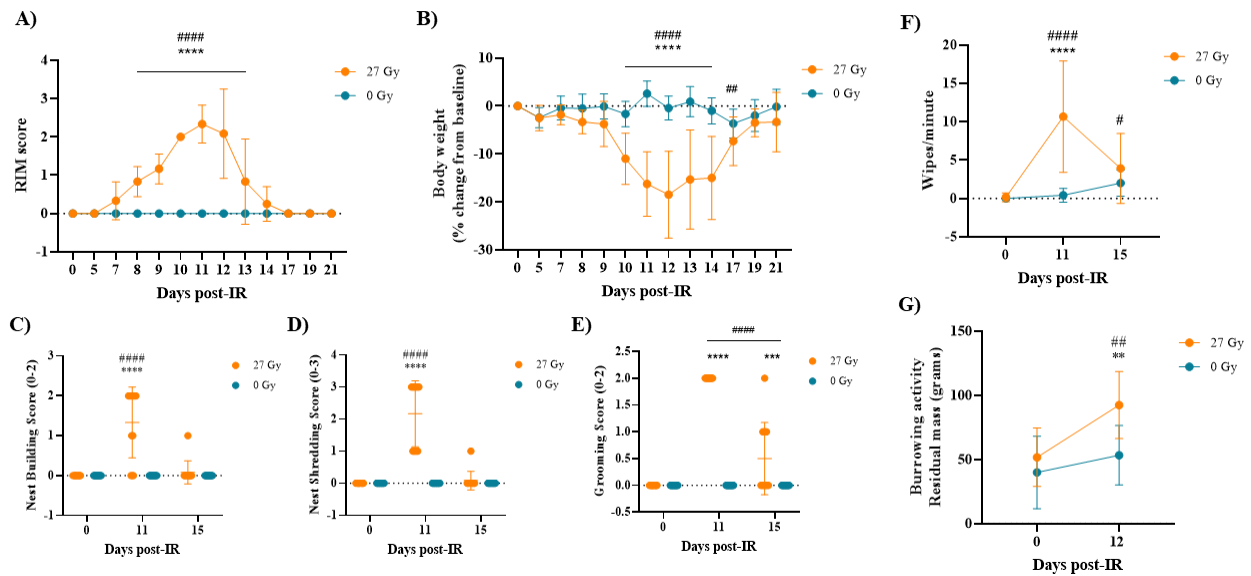


Figure 2.5: Changes in nesting and grooming assays in relation to RIM, body weight loss, eye wiping, and burrowing activities in female BALB/c mice. Plots of overall RIM score (A), body weight loss (B), nest building score (C), nest shredding score (D), grooming score (E), eye wiping (F), and burrowing activity (G) for each group in the time course of the experiments. Comparisons across times and groups were done using 2-way ANOVA analysis (with Sidak’s or Dunnett’s test for pairwise comparisons, respectively); data expressed as mean + SD. Symbol represents difference from baseline measures in the IR group (# $p < 0.05$, ## $p < 0.01$, ### $p < 0.001$, #### $p < 0.001$), and difference between sham-IR and IR groups (* $p < 0.05$, ** $p < 0.01$, *** $p < 0.001$, **** $p < 0.001$).

2.3.4 Nesting and grooming scores in relation to RIM scores across sex, strain, and IR modalities

As shown in Figure 2.6 (panels A to C), and in line with the results obtained in female BALB/c mice, we found that all of our assays successfully discriminated male BALB/c mice with high RIM scores from those mice that never developed RIM at day 11 post-IR. Moreover, these assays were also effective at this time in discriminating these comparative groups when tested in another mouse strain, such as C57BL/6 (Figure 2.6, panels D to F). Finally, we saw that our assays were also capable to differentiate mice with high RIM scores from those that never developed RIM when fractionated IR modalities were used (Figure 2.6, panels G to I).

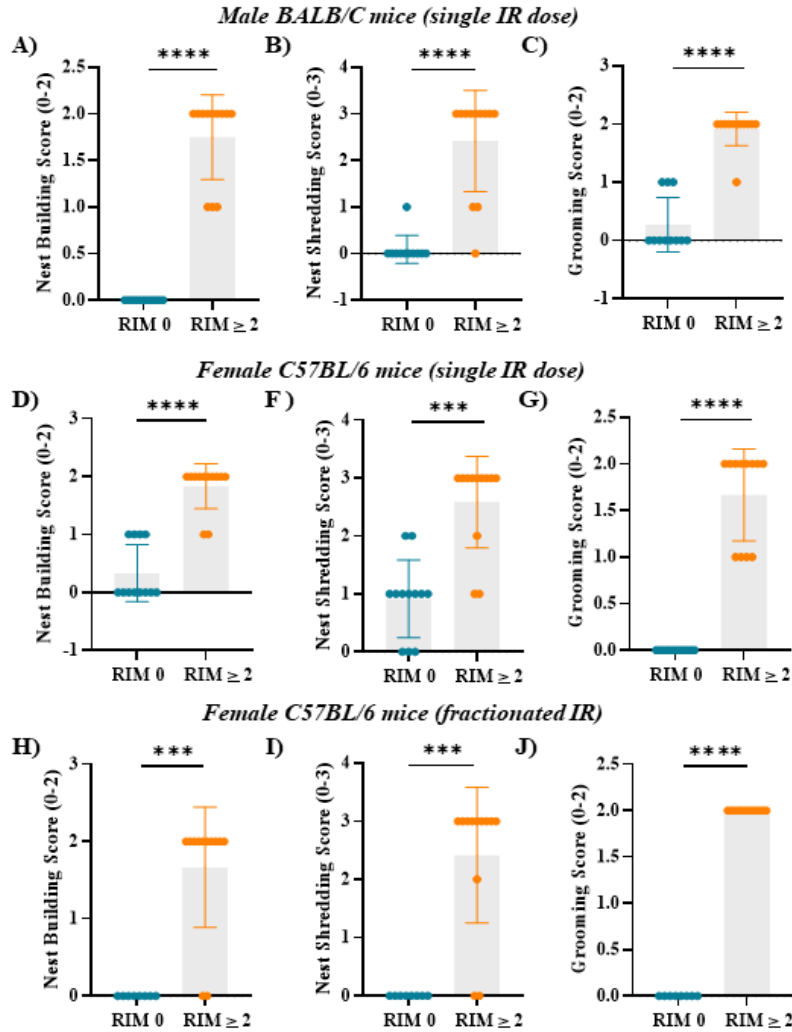


Figure 2.6: Ability of nesting and grooming assays to discriminate mice with RIM of 0 to those with RIM > 2 across sex, strain, and IR modalities. Bar plots of overall scores for the nest building assay (A), nest shredding assay (B), grooming assay (C) in male BALB/c mice (single-dose IR); overall scores for the nest building assay (D), nest shredding assay (E), grooming assay (F) in female C57BL/6 mice (single-dose IR); and overall scores for the nest building assay (G), nest shredding assay (H), grooming assay (I) in female C57BL/6 mice (fractionated IR). Comparisons across comparative groups (RIM 0 versus > 2) were done using unpaired Mann-Whitney test (2-tailed); data expressed as mean + SD. Symbol represents between groups (* $p < 0.05$, ** $p < 0.01$, *** $p < 0.001$, **** $p < 0.0001$).

2.3.5 Real-time versus remote scoring (reproducibility assessment)

For this assessment, we first checked whether RIM progression in female C57BL/6 mice followed the same behavior previously observed in female BALB/c mice (Figure 2.7A). As expected, and in line with previous results found in this strain, signs of grade 1 RIM were first noticed by day 8 post-IR, reaching maximal severity (grade > 2 RIM) at day 11 post-IR, and a complete RIM resolution at day 19 post-IR. Then, we assessed the time course of nesting and grooming scores in relation to the development and resolution of RIM in this specific strain using the data collected in real-time (Figure 2.7, panels B to D). Similar to the progression of RIM, nesting and grooming scores were minimal for all mice (IR and sham-IR) at baseline and 4 days following IR, and signs of score increase for all behavioral assays were first noticed at the time that RIM scores started to increase in severity. At this time (day 8 post-IR), scores from the nest building, nest shredding, and grooming assays were significantly higher than baseline and sham-IR groups measures. Then, by the time of maximal RIM severity (i.e., day 11 post-IR), the highest scores for all assays were observed in IR-mice, indicating maximal aoRAP severity according to our theoretical frame. Yet, and while there was a substantial reduction in scores for all our assays from day 11 to day 19 post-IR, we found differing results across assays at the time of RIM resolution. At this time (day 19 post-IR), scores from the nest building assay in IR-mice were significantly higher than baseline measures, but they were not different from those scores collected from sham-IR mice. However, scores from the nest shredding and grooming assays remained significantly higher than baseline and sham-IR groups measures. As expected, sham-IR mice did not experience RIM development or impairment in these behavioral activities at any time.

Next, we investigated whether scores obtained in real-time differed from those obtained remotely using a computer-based assessment system. Here we saw that scores were practically

identical across all scoring systems at all times using both types of assessment ($p > 0.9999$ for all comparisons).

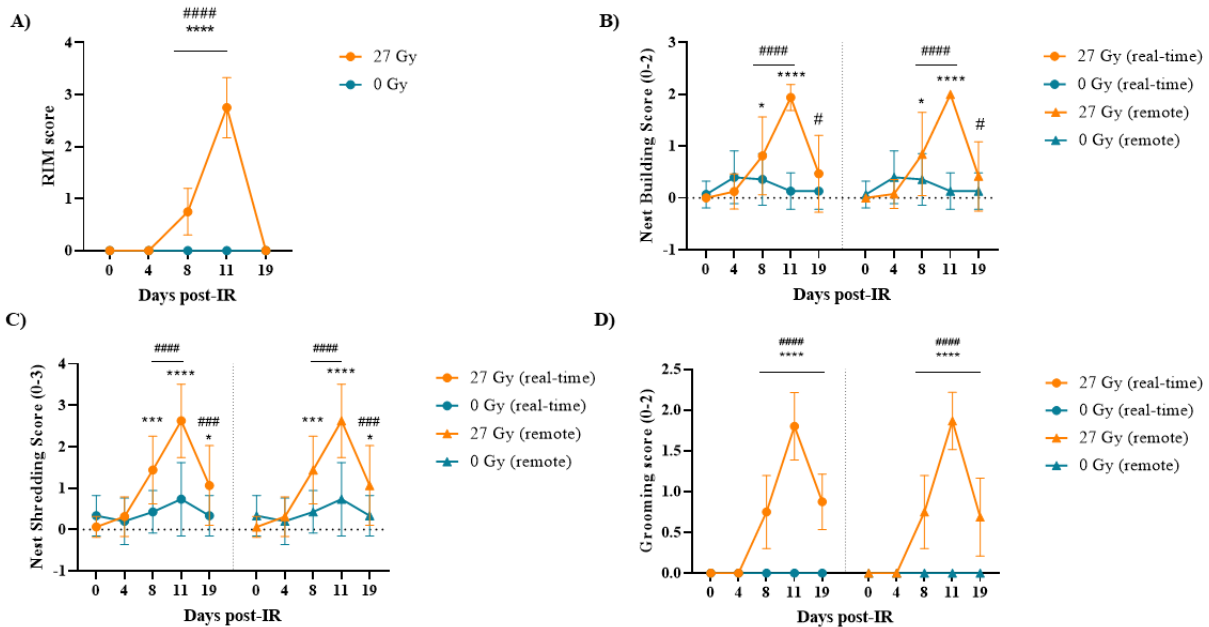


Figure 2.7: Progression of RIM, nesting, and grooming scores across times in female C57BL/6 mice. Plots of overall scores for RIM (A), nest building (B), nest shredding (C), grooming (D) assays in female C57BL/6 mice (single-dose IR). Comparisons across times and groups was done using 2-way ANOVA analysis (with Sidak's or Dunnett's test for pairwise comparisons, respectively); data expressed as mean + SD. Symbol represents difference from baseline measures in the IR group (# $p < 0.05$, ## $p < 0.01$, ### $p < 0.001$, #### $p < 0.001$), and difference between sham-IR and IR groups (* $p < 0.05$, ** $p < 0.01$, *** $p < 0.001$, **** $p < 0.001$).

2.3.6 Reliability assessment

To test the reliability of our behavioral instruments, we first measured the correlation between assays (i.e., nest building versus nest shredding versus grooming scores). Results here showed that there was high consistency between assays (Cronbach' $\alpha = 0.941$). According to our

inter-rater reliability assessment, agreement in scores across all evaluators was very good for all our behavioral assays (i.e., ICC > 0.8 for all assessments). Specifically, our scoring systems were able to produce highly similar scores across all evaluators for the nest building, nest shredding, grooming assays, independent of their familiarity with the assays or expertise with rodent studies (Table 2.2). Moreover, our test-retest reliability assessment (done using a subset of evaluators; i.e., evaluator #1, 2, 3, and 5) showed a strong correlation between the two measures carried out one week apart in all evaluators for all scoring systems (i.e., ICC > 0.9, $p < 0.001$ for all measures; Table 2.3).

Table 2.2: Inter-rater reliability assessment.

| Intraclass Correlation Coefficient | Nest Building Score | Nest Shredding Score | Grooming Score <i>(BALB/c mice)</i> | Grooming score <i>(C57BL/6 mice)</i> |
|---|----------------------------|-----------------------------|---|--|
| Between evaluators with no mouse work experience (evaluator 2 to 4) | 0.98 | 0.992 | 0.983 | 0.968 |
| Between evaluators with mouse work experience (evaluator 5 to 7) | 0.989 | 0.991 | 0.888 | 0.95 |
| Between evaluators with and without mouse work experience (2-7) | 0.991 | 0.996 | 0.976 | 0.981 |
| Between evaluator 1 and 2 to 7 | 0.994 | 0.997 | 0.982 | 0.985 |

Table 2.3: Test-retest reliability assessment.

| Intraclass Correlation Coefficient | Nest Building Score | Nest Shredding Score | Grooming Score (BALB/c mice) | Grooming score (C57BL/6 mice) |
|---|----------------------------|-----------------------------|-------------------------------------|--------------------------------------|
| Single Measures | 0.987 | 0.983 | 0.932 | 0.952 |
| Average Measures | 0.994 | 0.991 | 0.965 | 0.975 |
| Single Measures p-value | <.001 | <.001 | <.001 | <.001 |
| Average Measures p-value | <.001 | <.001 | <.001 | <.001 |

2.3.7 Validity assessment (responsiveness)

2.3.7.1 Standard analgesics (pilot study): As shown in Table 2.4, anti-NGF mAb (at the used dose) appeared to be superior in comparison to the other analgesics in mitigating the impairment of nesting activities associated with RIM at day 11 post-IR. In particular, we saw in the anti-NGF group that a greater proportion of mice were able to maintain or improve their nest building performance from baseline (62.5%) than mice whose performance worsened from baseline (37.5%), as indicated by the change in their scores. This did not occur for the other groups. In the saline and carprofen groups there was an equal proportion of mice whose performance did not change or improve (50%) from baseline and mice whose performance worsened from baseline (50%). Conversely, we saw in the hydromorphone group that a greater proportion of mice whose performance worsened from baseline (87.5%) than mice whose performance either improved or not changed from baseline (12.5%). The nest shredding performance, instead, was not better than baseline in any group by day 11 post-IR. However, the proportion of mice whose performance worsened from baseline (50%) was equal to the proportion of those whose performance improved from baseline (50%) for the anti-NGF group at this time point. Finally, we noticed that grooming performance was completely impaired in all IR mice, independent of the administered analgesic.

Specifically, none of the used analgesics was superior to saline, and the ability to groom had worsened in all animals (100%) at the time of maximal RIM as compared to baseline measures.

Table 2.4: Assay responsiveness assessment (pilot study); total proportion of animals whose performance (i.e., score change) at day 11 post-IR either 1) improved or not changed, or 2) worsened in comparison to baseline.

| Groups | <u>Total proportion of animals (expressed in percentage)</u> | | | | | |
|---------------|---|-----------------|--------------------------------|-----------------|--------------------------------|-----------------|
| | Nest building performance | | Nest shredding performance | | Grooming performance | |
| | <i>Improved or not changed</i> | <i>Worsened</i> | <i>Improved or not changed</i> | <i>Worsened</i> | <i>Improved or not changed</i> | <i>Worsened</i> |
| Carprofen | 50 | 50 | 37.5 | 62.5 | 0 | 100 |
| Hydromorphone | 12.5 | 87.5 | 0 | 100 | 0 | 100 |
| Anti-NGF mAb | 62.5 | 37.5 | 50 | 50 | 0 | 100 |
| Saline | 50 | 50 | 37.5 | 62.5 | 0 | 100 |

2.3.7.2 Standard analgesics (large study): For this part of the study, we first compared the progression of RIM and related weight loss across IR and sham-IR groups. RIM scores in all IR mice (IgG and anti-NGF mAb groups) gradually increased after day 0, reaching its maximal severity at day 11 post-IR (Figure 2.8A). While the progression in RIM was quite similar between both IR groups, anti-NGF mAb significantly reduced the severity of RIM in comparison to IgG from days 10 to 12 post-IR. On these days, anti-NGF mAb also significantly reduced the severity of weight loss associated with RIM (Figure 2.8B). In regard to the ability of mice to build a nest, shred the nest material, and properly self-groom, we saw by day 11 post-IR that the scores from all our assays were significantly higher in all IR groups in comparison to all sham-IR groups (either treated with IgG or anti-NGF mAb) (Figure 2.8, C to D), and moreover, scores at this time were significantly higher in all IR mice in comparison to their own baseline measures (not shown; $p <$

0.0001 for all comparisons). However, anti-NGF mAb was able to partially mitigate these behavioral impairments, and significant differences between both IR groups were seen when the nest building and grooming assays were applied. Conversely, and while the score from the nest shredding assay appeared to be reduced by the effect of anti-NGF mAb, this assay failed to discriminate IR mice that were either treated with IgG or anti-NGF mAb. As expected, none of the sham-IR mice (either treated with IgG or anti-NGF mAb) experienced impairment in these behavioral activities at any time.

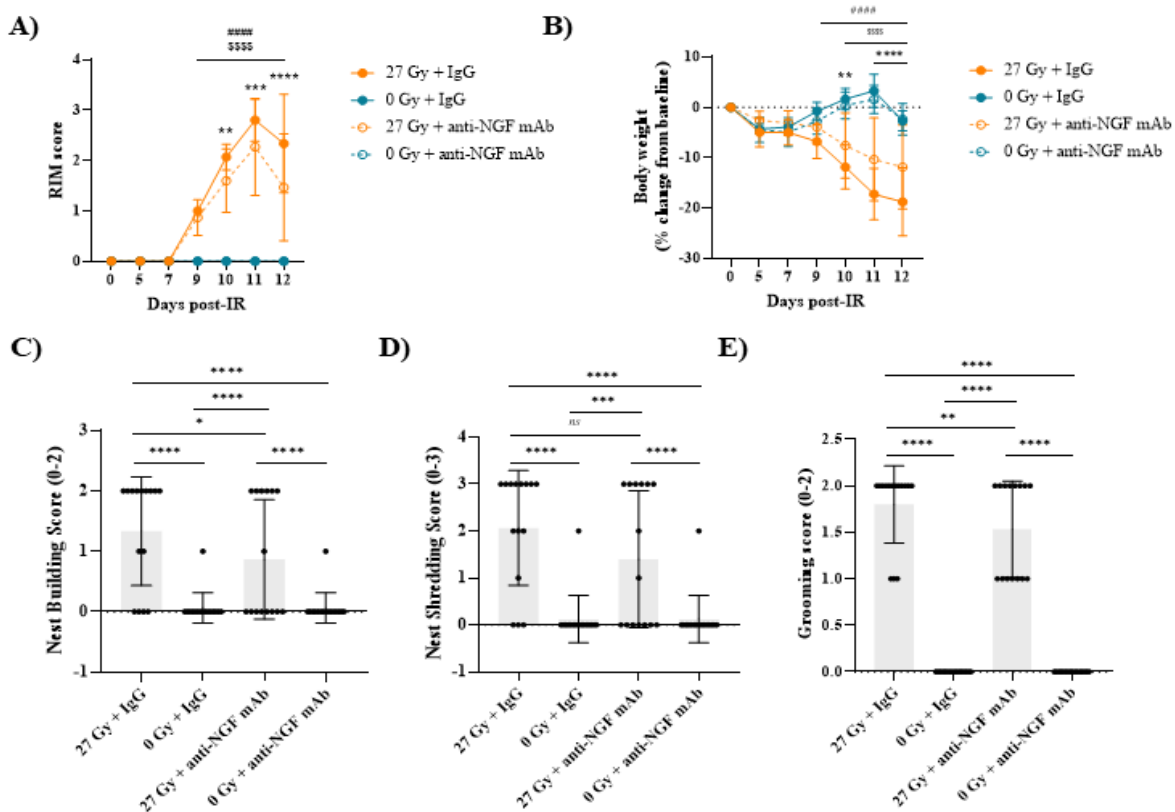


Figure 2.8: Changes in RIM, body weight, nesting, and grooming activities in female BALB/c mice treated with systemic IgG or anti-NGF mAb. Plots of overall RIM score (A) and body weight loss (B) for each group during the time course of experimentations. Comparisons across groups were done using 2-way ANOVA analysis (with Tukey's test for pairwise comparisons); symbol represents the difference between both IR groups (* $p < 0.05$, ** $p < 0.01$, *** $p < 0.001$, **** $p < 0.0001$), difference from baseline measures in both IR-IgG groups (# $p < 0.05$, ## $p < 0.01$, ### $p < 0.001$, #### $p < 0.0001$), and difference from baseline measures in both IR-anti-NGF mAb groups (\$ $p < 0.05$, \$\$ $p < 0.01$, \$\$\$ $p < 0.001$, \$\$\$\$($p < 0.0001$). Bar plot of overall scores for the nest building (C), nest shredding (D), and grooming (E) assays. Comparisons across groups were done using 2-way ANOVA analysis (with Tukey's test for pairwise comparisons); symbol represents the difference between groups (* $p < 0.05$, ** $p < 0.01$, *** $p < 0.001$, **** $p < 0.0001$). Data expressed as mean + SD.

2.3.7.3 TRPV1-expressing neuron deletion: Using RTX to selectively delete TRPV1-expressing ‘pain’ neurons, we confirmed the responsiveness of nesting and grooming assays. According to our eye wiping results (not shown), ablation was successful in all RTX-injected mice (reduction higher than 50% for all mice). As shown in Figure 2.9 (A to B), RIM progression and associated weight loss in IR mice treated with RTX excipient did not differ from what we saw in our previous experiments. However, a significant reduction in RIM scores and weight loss was observed when IR mice were injected with systemic RTX. Indeed, low-grade RIM scores were found in this group from days 8 to 12 post-IR (overall mean score of 1). Presumably as a consequence, body weight loss was minimal (< 5%). Neither RTX nor excipient caused oral lesions (e.g., glossitis) or weight loss in sham-IR mice; in these mice, RIM development and weight loss did not occur at any moment during this study. Matching the development of RIM, we observed here that RTX treatment significantly improved nesting and grooming activities in IR mice by day 11 post-IR (Figure 2.9, C to E). In particular, nesting scores (from both assays) in IR mice receiving RTX were significantly lower than their IR counterpart group (i.e., RTX excipient), and moreover, did not differ from those scores obtained from all sham-IR groups. Regarding the grooming assay, scores were significantly higher than those scores obtained from both sham-IR groups at day 11 post-IR, however, scores here were also significantly lower than their IR counterpart group (i.e., RTX excipient). As expected, none of the sham-IR mice (either treated with RTX or its excipient) experienced impairment in nesting and grooming activities at any time.

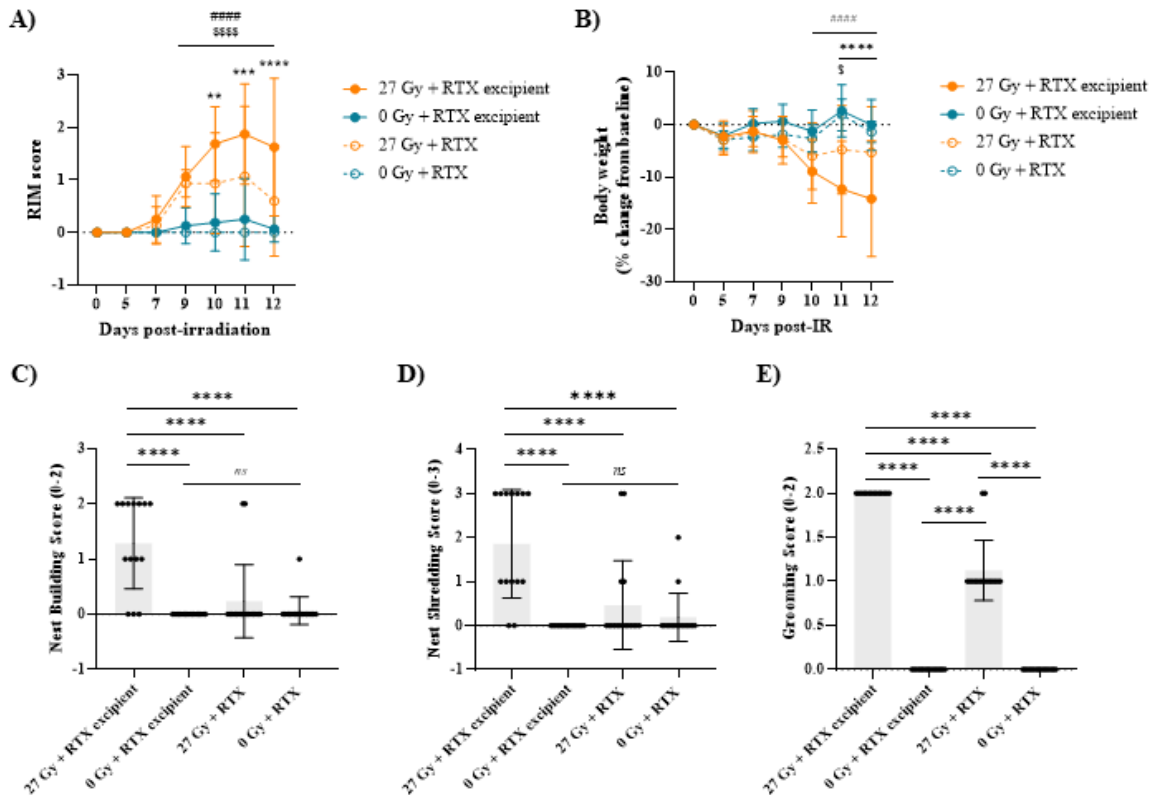


Figure 2.9: Changes in RIM, body weight, nesting, and grooming activities in female BALB/c mice treated with systemic RTX or its excipient. Plots of overall RIM score (A) and body weight loss (B) for each group in the time course of experimentation. Comparisons across groups were done using 2-way ANOVA analysis (with Tukey's test for pairwise comparisons); symbol represents the difference between both IR groups (* $p < 0.05$, ** $p < 0.01$, *** $p < 0.001$, **** $p < 0.001$), difference from baseline measures for both IR-RTX excipient groups (# $p < 0.05$, ## $p < 0.01$, ### $p < 0.001$, #### $p < 0.001$), and difference from baseline measures for both IR-RTX groups (§ $p < 0.05$, §§ $p < 0.01$, §§§ $p < 0.001$, §§§§ $p < 0.001$). Bar plot of overall scores for the nest building (C), nest shredding (D), and grooming (E) assays. Comparisons across groups were done using 2-way ANOVA analysis (with Tukey's test for pairwise comparisons); symbol represents the difference between groups (* $p < 0.05$, ** $p < 0.01$, *** $p < 0.001$, **** $p < 0.001$). Data expressed as mean + SD.

2.4. Discussion

In the present study, we first evaluated the ability of our novel battery of cageside behavioral assays (based on nesting and grooming activities) to predict changes in RIM under different experimental conditions in mice. According to our results, our assays demonstrated to have predictive validity in detecting changes in RIM progression and severity in adult female BALB/c and C57BL/6 mice whose tongues were irradiated using a single-high dose of IR (27 Gy). Moreover, these behavioral assays showed to be equally effective in tracking changes in RIM scores as other parameters have done in the past in this model (i.e., body weight change, eye wiping responses, burrowing activities), as well as to discriminate mice with high-grade RIM (i.e., scores > 2) from those that never develop RIM (i.e., sham-IR mice). Remarkably, their ability to discriminate IR mice from sham-IR mice appeared to hold across sexes, strains and different irradiation modalities. Then, we tested the reliability and validity of our methods and measurement strategies. According to the scores obtained from a computer based post-hoc image assessment, we showed that there was a high internal consistency between the nesting (both building and shredding test modalities) and grooming assays, indicating that all item questions were measuring the same theoretical construct. High levels of inter-observer agreement and test-retest reliability were also found for all assays, and no differences were seen between evaluators that had expertise with the assays and those without expertise, neither between evaluators with experience working with mice and those without experience. Lastly, we showed that our assays were highly responsive (i.e., detection of a relevant change) to pain management strategies, such as anti-NGF mAb or RTX administration, validating the assumption that aoRAP is experienced in mice undergoing experimentally-induced RIM by our methods (single-dose of fractionated IR), and that our assays represent valid behavioral screening tools for the study of aoRAP.

Pain in the orofacial region is a common and debilitating problem in HNSSC patients experiencing RIM. Indeed, clinical studies have shown that episodes of aoRAP are frequently reported in patients undergoing curative-intent RT (either alone or in combination with chemotherapy) from the day of RIM occurrence until the completion of RT (Buchsel & Murphy, 2008; Christoforou et al., 2019; Mirabile et al., 2016; Schaller et al., 2021; Shih et al., 2002). Although there are current available analgesics for managing this pain condition (e.g., morphine, gabapentin, benzydamine), these therapeutic strategies are unsatisfactory due to our poor understanding of aoRAP mechanisms. To overcome this issue, animal models and reliable methods of measuring aoRAP behaviors that translate to the clinic are urgently needed. As mentioned before, we have attempted to fill the gap in this research area by characterizing sensory and affective dimensions of aoRAP in our mouse model of RIM using hypersensitivity (eye wiping assay) and wellbeing (burrowing assay) responses as proxy indicators (Lai et al., 2021; Nolan et al., 2017; Price et al., 2021). Yet, further characterization is required to capture the spontaneous features of mucositis pain in the orofacial region. During the conduct of previous work, we noticed that two voluntary cageside behaviors – nesting and grooming – were markedly reduced when mice were experiencing grade > 2 RIM, around days 10-12 post-IR. This impairment, however, rapidly improved after mice started showing signs of RIM recovery. Based on these observations, we theorized that the impairment seen in these behaviors might be a direct result of pain in the oral cavity associated to RIM. Interestingly, there is no evidence in the current literature indicating that both of these behaviors are mouth-dependent. Moreover, and despite the extensive use of these outcome measures to phenotype other forms of pain (e.g., postoperative pain), there are not standardized methodologies to assess changes in these activities in the context of orofacial pain in mice. Therefore, the author of this work spent substantial time in the mouse colony at NCSU to

gather enough evidence that would support our theory (i.e., nest and grooming activities are impaired as a result of aoRAP in mice experiencing RIM). Two main conclusions were made from this examination: 1) when signs of grade 1-2 RIM start to become evident, nests were commonly left unfinished with several pieces of the nest material left untouched and spread around the cage, and mice displayed a disorganized hair coat; and 2) when signs of grade 3 RIM start to become evident, the nest material was usually left untouched (no indications of nest building or shredding activity), and mice displayed greasy/wet hair along with hair loss or skin erythema within the mouth and neck area. Using these observations, the author developed a method (i.e., scoring system) to quantify the impairment in nest building, nest shredding, and grooming activities in a manner that would require minimal operator interference.

In the first part of our study, we assessed the evolution of RIM scores in adult female BALB/c mice after receiving a single high-dose fraction (27 Gy) of lingual IR. In this experiment, we saw that the progression of RIM scores followed the same behavioral pattern seen before in other mouse strains (Nolan et al., 2017), which was a gradual increase in scores following IR, reaching maximal severity (grade 3) at day 11 post-IR, and a rapid resolution by day 17 post-IR. Moreover, grade > 2 RIM was accompanied by weight loss (> 15%), increased eye wiping responses, and reduced burrowing activity. As expected, our newly developed battery of assays appeared to accurately mirror the progression and severity of RIM in these mice in a similar degree to the eye wiping and burrowing assays. In particular, nesting and grooming scores did not fluctuate from baseline measures at any time point post-IR in the sham-IR group. While all IR mice displayed a great ability to build a nest or shred the nest material before IR (12 of 12), these behaviors were drastically impaired at day 11 post-IR in most IR mice experiencing grade > 2 RIM (9 of 12 for the nest building assay, and 12 of 12 for the nest shredding assay). After RIM was

resolved, nesting behaviors returned to normal in almost all IR mice (11 of 12 mice). Similarly, our grooming assay was also good revealing the absence of impairment in grooming activities at baseline in all IR mice (12 of 12). Conversely, this behavior was drastically reduced in all IR mice (12 of 12) at day 11. However, we noticed that many IR mice (5 of 12) still had difficulties reestablishing their normal haircoat aspect by the time of RIM resolution. While scores were in general much lower than the ones presented at day 11 post-IR, results here suggested that mice might require more time to re-establish grooming behaviors in comparison to the nesting behaviors. This could be attributable to many reasons. First, our previous observations (unpublished) have indicated that grooming activities return to normal by day 19 post-IR, not by 15 post-IR, therefore, results here might be influenced by the selected temporal choice of assessment. Secondly, it has been established that RT can change the properties of saliva (Jensen et al., 2003; Li et al., 2021; Sroussi et al., 2017), therefore, we cannot ignore the fact that results here might be reflecting other comorbidities that arise from IR; in this context, it will be necessary to determine in future experiments whether our IR protocol affects the salivary glands and alter the properties of saliva. Lastly, is it possible that grooming behavior remains abnormal because there is residual aoRAP that is not reflected in RIM scores or by other outcomes measures (body weight or eye wiping responses). This is relevant because persistent states of aoRAP after RT completion has been reported in up to 36% of HNSSC patients despite RIM resolution (Astrup et al., 2015; Kallurkar et al., 2019). One could infer from these results that the grooming assay could be better in indicating long-lasting nociceptive alterations related to RIM than the nesting assays, however, additional assessment timepoints need to be added before making definitive conclusions.

To further understand the applicability of these behavioral assays to measure aoRAP, we tested their ability to discriminate IR and sham-IR groups across mouse sexes, different strains,

and differing IR regimens. According to our results, our three behavioral assays were equally effective (i.e., differences between comparative groups < 0.0001 for all assays) in discriminating male IR mice with grade > 2 RIM against those that never developed RIM. This was not surprising since RIM was equally severe in both sexes (data not shown). However, it was necessary to determine whether our assays can detect differences in pain sensitivity between sexes. Indeed, studies have suggested that gender is an important factor in the modulation of pain and that pain severity is generally greater in female (Mogil, 2012; Wiesenfeld-Hallin, 2005). While here we did not have a sex effect – pointing out that aoRAP can interfere with normal activities in a similar degree in female and male mice experiencing similar RIM grades – we cannot confirm that differences in aoRAP sensitivity do not exist between sexes, especially when considering that sex differences have been hardly investigated in human patients experiencing aoRAP. In a similar line, it was also important to determine whether some mouse strains are less or more sensitive to RIM. Certainly, differences in pain sensitivity have been detected in other models of murine pain (Banik et al., 2006; Mogil, 2019). For example, it has been shown that C57BL/6J strains are more sensitive than A/J strains to inflammatory noxious stimuli such as formalin (Wilson et al., 2002). Therefore, it was important to clarify if this was the case in our model. Similar to BALB/c mice, adult female C57BL/6 mice with grade > 2 RIM (data not shown) had also drastic impairments in nesting and grooming activities by day 11 post-IR in comparison to mice with no signs of RIM. Lastly, we checked whether nesting or grooming behaviors were also affected when mice develop RIM using a different IR modality. Because HNSSC patients are most commonly treated using fractionated IR schemes (Atwell et al., 2020), we used a more clinically relevant IR protocol (i.e., fractionated IR) to irradiate mice. In line with the results obtained from the other experimental conditions, it appears that our assays were also effective in differentiating mice with grade > 2 RIM from mice

that never developed RIM in these settings. Taking all results together, here we confirmed the theory that the establishment of RIM in mice, as in humans, can lead to high-grade aoRAP, and consequently, impact natural rodent behaviors such as nesting and grooming.

We then extended our assessments and evaluated the progression of nesting and grooming scores through the full progression and resolution of RIM in tongue-irradiated C57BL/6 mice (female). The idea here was, on one hand, to gain a more robust picture of the intensity and duration of oral mucositis pain following IR using nesting and grooming activities as proxies of aoRAP, and, on the other hand, to evaluate the level of agreement between scores obtained in real-time versus those obtained remotely using digital material. In this part of the study, we first confirmed that the progression of RIM and associated weight loss in irradiated C57BL/6 mice did not differ from the one displayed by irradiated BALB/c mice. Having that interrogative resolved, we then assessed how our behavioral assay scores changed over the course of the experiment using those scores recorded in real-time. Until day 11 post-IR, we can interpret from our results that: 1) there are no impairments in nesting and grooming activities before IR; and 2) grade 1 RIM correlates with mild interference (i.e., intermediate scores) in nesting and grooming activities; and 3) grade > 2 RIM correlates with an important interference (i.e., maximal scores) in these activities; however, we found discrepancies in results at day 19 post-IR. At this time, we noticed that there was a marked score reduction for all of the assays, however, scores here were still significantly higher than baseline measures, and in some cases, higher than sham-IR groups. Specifically, and opposite to what we have found in BALB/c mice in past studies at day 19 post-IR (unpublished), this particular strain still displayed difficulties building a nest or shredding the nest material when RIM was completely resolved. While scores from these assays were substantially lower than those obtained on day 11 post-IR, some mice were still presenting nesting scores that were higher than

baseline scores. Similar, grooming activities (according to our scoring system) were still reduced after RIM resolution. These findings emphasize the idea that, similar to humans, residual aoRAP after RIM resolution can perpetuate the impairment in normal, voluntary activities, and further on, that RIM might trigger a cascade of intracellular events that promotes the generation and maintenance of peripheral and/or central sensitization states (Kallurkar et al., 2019; Karri et al., 2021; Latremoliere & Woolf, 2009; Vardeh & Naranjo, 2017). However, and while our battery of assays was good mirroring low grades of RIM (i.e., mild nesting and grooming impairment associated to grade 1 RIM), we cannot exclude the possibility that results at this time (day 19 post-IR) were driven by a lack of sensitivity of our assays to detect the changes on aoRAP.

Because we were also interested on creating new guidelines that could be potentially extendable to other research facilities to detect and rate mouse orofacial pain (based on nesting and grooming activities) in a similar way that the Mouse Grimace Scale has offered (Langford et al., 2010), we evaluated the level of agreement between scores obtained in real-time versus those obtained remotely using digital material. Based on our results, we can conclude with confidence that there are no major issues when changing assessment modalities. For the nest assay, in particular, it was highly expected to obtain the same results across modalities. The nest is a static, inanimate material, and the evaluator's perception should not change significantly if scoring is done *in situ* or by looking at a picture. Differences in scores, therefore, could be potentially related to the quality of the picture. Conversely, the author here had some uncertainties about the grooming assay. Specifically, scores from this assay can vary depending on the camera's position and quality of the image or video, and lighting. According to the author, mice sometimes display asymmetric discoloration of coat, erythema, or hair loss, therefore, a grooming score of 2 can be easily confused as a score of 1 if the video or image does not capture the whole mouse body. Moreover,

having a poor picture quality can sometimes lead to inconsistency in results. The author here made a great effort to obtain high-quality digital material, therefore, these difficulties were not encountered. After determining that there was a good association in scores between both assessment modalities, we examined the reliability of our scoring systems. Our reliability assessment revealed that our nesting and grooming assays does not require previous training with mice to get the expected results, therefore, these assays could represent a reliable tool to potentially assess oral pain/interference. This is relevant when considering the possibility to create from these results guidelines that can be easy to implement into other research facilities, and that are highly reproducible.

Finally, and as a first step to validate the use of these assays to assess aoRAP in mice, we examined the responsiveness of our behavioral test battery by comparing nesting and grooming scores between mice that were either received or did not receive analgesic strategies. From the pilot study, we gained some provisional insight regarding the impact of various analgesics (carprofen, hydromorphone, and anti-nerve growth factor) on aoRAP, allowing us to define which analgesic strategy might be better to test the responsiveness of the nesting and grooming assays. As in humans (Ling & Larsson, 2011), the NSAID failed to mitigate RIM-related impairments in normal, voluntary activities such as nesting and grooming, and its analgesic effect was not superior to saline. The opioid appeared to cause a decline in the performance of these activities. However, mice were heavily sedated after hydromorphone was administered and this probably played a large role in the results we saw. These results were rather unexcepted because hydromorphone at doses ranging from 2.2-22 mg/kg are recommended to alleviate pain in mice (Kumar et al., 2008). In mice treated with a single dose of an anti-NGF mAb there appeared to be some mitigation of the impairment of nesting activities associated with RIM. This was not a surprise since anti-NGF mAb

has shown promising pain relief effects in other pain models (Jimenez-Andrade et al., 2011; Miyagi et al., 2017; Sevcik et al., 2005), and moreover, some studies have suggested that NGF might be linked to the pathogenesis of radiation-induced mucositis pain (Ye et al., 2011). Therefore, we decided to use anti-NGF mAb as our ‘analgesic tool’ in a larger study to test the responsiveness of our assays to detect changes in pain severity. As this work was progressing, an opportunity to use RTX was developed. RTX, an ultrapotent analog of capsaicin, has emerged in the last years as the most promising and refined mechanism-based treatment approach to selectively target pain neurons by lesioning TRPV1-expressing nociceptive primary afferent populations. RTX has demonstrated in preclinical studies to be a highly efficacious non-opioid analgesic alternative with no neurological deficits or signs of toxicity, and it is recognized as a promising candidate for the treatment of intractable or chronic pain conditions, such as cancer pain (Brown, 2016; Brown et al., 2015; Iadarola & Gonnella, 2013; Iadarola et al., 2018; Kissin et al., 2005; Menéndez et al., 2006). Interestingly, accumulating preclinical (mouse, rat) evidence has indicated that TRPV1 contribute to trigeminal nerve injury-associated nociception and, therefore, it could potentially play a crucial role encoding orofacial pain (Anderson et al., 2014; Anderson et al., 2013; Neubert et al., 2008; Wu et al., 2018; Yilmaz et al., 2007; Yoo et al., 2020). Therefore, we also used RTX with the assumption that this approach (tool) would allow us to test the ability of our assays to detect aoRAP. According to our results, the provision of presumed analgesia via anti-NFG mAb and RTX resulted in shifts in the nesting and grooming assays. In comparison to IgG, anti-NGF was able to reduce the impairment in nest building (39% reduction), shredding (33% reduction), and grooming (17% reduction) activities that we normally see at day 11 post-IR (time of maximal RIM severity). However, and in contrast to the nest building and grooming assays, the nest shredding assay was not able to differentiate IR groups (i.e., IgG versus anti-NGF

mAb). Based on these results, we theorized that while IR mice can improve their ability to build a nest or self-groom at the time of maximal RIM when anti-NGF mAb is given, the ability to completely shred the nest material can be still compromised. This action requires more mouth-related work as compared to the action of building a nest, however, we cannot conclude from this experiment that the results from this assay were attributable to the lack of analgesic effectivity of anti-NGF mAb or the assay's design. Yet, the interpretation of this result can be improved by looking at the results obtained from the RTX experiment. In this experiment, all of our assays were effective in differentiating IR mice injected with RTX and RTX excipient at day 11 post-IR. On this day, IR mice that received RTX had a remarkable improvement in the performance of nest building (85% reduction), shredding (74% reduction), and grooming (45% reduction) activities, and scores from the nest (building and shredding) and grooming assays did not greatly differ from those obtained from sham-IR controls. Taken together, we can conclude at this stage that measures of spontaneous behavior, such as nesting and grooming, provide a simple framework for quantifying aoRAP in mice with experimentally-induced RIM.

Limitations of this study should be mentioned. While we had in general adequate sample sizes for most experiments according to our sample size calculations, we cannot conclude that carprofen or hydromorphone are ineffective therapies to mitigate aoRAP in our model; small samples sizes were used for that particular experiment, and the design of our assays was modified. Another important limitation of our study was the fact that our scoring systems had a limited number of levels. Indeed, a 3-point system (0-2) provides less room for evaluators to express differentiation than a 5-point scale, for example. This can decrease both the precision and increase the variability of a scale, and thus, increasing the probability of error. Therefore, it will be important to evaluate whether the accuracy of our assays change when additional and more specific

scoring levels are implemented. Another relevant limitation relates to the fact that several of our studies were done independently. While we are very strict about our experimental conditions, and we make great effort to be consistent during the conduct of each experiment, we are aware that our results can be impacted when animals are not being submitted to the exact conditions (e.g., time of the year, different people inside the room, hormonal status, etc.). Therefore, it will be important to confirm the reproductivity of our results. Also, the absence of relevant control groups might limit the accuracy of our instruments. For example, we did not add groups of mice that had pain in areas distant from the head and neck region (e.g., abdominal pain). This is especially relevant because we cannot conclude that our assays are specific for measuring aoRAP without those groups. Moreover, we cannot certify that our assays can measure other forms of orofacial pain (e.g., temporomandibular joint pain, tongue pain induced by formalin or Complete Freund's adjuvant (CFA)). Therefore, further experimentations will be needed to satisfy appropriate data interpretation. In addition, we are uncertain on whether our behavioral tools can detect mild grades of aoRAP. As mentioned before, our assays were capable of differing IR mice with low grades of RIM (grade 1 RIM) against their sham counterparts by day 8 post-IR (C57BL/6 mice experiment). However, we also observed that our assays were unable of differing IR mice that received preemptive RTX and presented grade 1 RIM from sham-IR mice (either treated with RTX or its excipient) by day 11 post-IR (BALB/c mice experiment). Therefore, it may be necessary to reassess the ability of our assays to detect mice experiencing mild levels of RIM in future investigations, and potentially add additional assessment timepoints (e.g., day 13 post-IR, when signs of RIM resolution are first observed) to confirm the predictive accuracy of our assays in detecting mild aoRAP across mouse strains. Lastly, and most important, it is necessary to emphasize that while our assays demonstrated great responsiveness to analgesics and similar

directional shifts, both analgesic tools had a direct effect on RIM severity. Indeed, both anti-NGF mAb and RTX significantly decreased RIM scores from days 10 to 12 post-IR. This was not surprising since it has been revealed in the past that both NGF and TRPV1 have a well-defined pro-inflammatory role in a variety of injury states, in addition to have an important role in pain transduction (Caterina & Julius, 2001; Caterina et al., 2000; Keeble et al., 2005; Minnone et al., 2017). Thus, there is a great chance that changes in nesting and grooming scores might be reflecting the alleviation of RIM rather than a pure analgesic effect. Based on this important piece of evidence, we cannot confirm that anti-NGF mAb or RTX actually provided analgesia, and consequently limiting the predictive validity of our assays to quantify aoRAP. Hence, to overcome this limitation, the use of local pain strategies – such as adding local anesthetic solutions (e.g., lidocaine) directly into the mouse tongue – appears to be the most obvious choice to reduce this confounding factor. Yet, there is vast evidence in the scientific literature suggesting that anesthetic agents have immunomodulatory effects, and therefore, they may exert anti-inflammatory actions that will also reduce the severity of RIM (Cruz et al., 2017; Gray et al., 2016; Kelbel & Weiss, 2001).

In conclusion, the findings of this study suggest that mice (either BALB/c (female and male) or C57BL/6 (female) strains) with grade > 2 RIM induced by single-dose or fractionated IR had significantly higher levels of aoRAP in comparison to their counterparts (sham-IR), as indicated by a relevant impairment in nesting and grooming activities. Remarkably, these side effects can be palliated in irradiated female BALB/c mice when preemptive anti-NGF mAb and RTX are given systematically. Data here, therefore, provided empirical support for our hypothesis that proposes that both activities are highly dependent on the mouth, and that these outcome measures of spontaneous behavior may be relevant parameters for measuring the

affective/motivational aspects of aoRAP in our model. In addition, the results of this study suggest that our proposed standardized scoring systems may potentially provide reliable and valid adjunct tools to screen aoRAP in mice, as well as may help to characterize candidate analgesics and identify compounds with clinical potential in these settings. However, further investigations are needed to confirm the reliability and validity of our instruments. Future work will be focus on understanding the mechanistic underpinnings aoRAP and on determining the nociceptive-specific nature of nesting and grooming behaviors in our model of RIM in order to improve the translation of preclinical findings, and thus, improve outcomes in HNSCC.

2.5 References

- Al-Mogairen, S. M. (2020). Safety of rituximab on testicles, a double-blinded controlled trial in mice. *Journal of Nature and Science of Medicine*, 3(1), 66.
- Alvarez, E., Fey, E. G., Valax, P., Yim, Z., Peterson, J. D., Mesri, M., Jeffers, M., Dindinger, M., Twomlow, N., & Ghatpande, A. (2003). Preclinical characterization of CG53135 (FGF-20) in radiation and concomitant chemotherapy/radiation-induced oral mucositis. *Clinical Cancer Research*, 9(9), 3454-3461.
- Anderson, E. M., Jenkins, A. C., Caudle, R. M., & Neubert, J. K. (2014). The effects of a co-application of menthol and capsaicin on nociceptive behaviors of the rat on the operant orofacial pain assessment device. *PloS one*, 9(2), e89137.
- Anderson, E. M., Mills, R., Nolan, T. A., Jenkins, A. C., Mustafa, G., Lloyd, C., Caudle, R. M., & Neubert, J. K. (2013). Use of the Operant Orofacial Pain Assessment Device (OPAD) to measure changes in nociceptive behavior. *JoVE (Journal of Visualized Experiments)* (76), e50336.
- Andrews, N., Legg, E., Lisak, D., Issop, Y., Richardson, D., Harper, S., Pheby, T., Huang, W., Burgess, G., & Machin, I. (2012). Spontaneous burrowing behaviour in the rat is reduced by peripheral nerve injury or inflammation associated pain. *European Journal of Pain*, 16(4), 485-495.
- Astrup, G. L., Rustøen, T., Miaskowski, C., Paul, S. M., & Bjordal, K. (2015). Changes in and predictors of pain characteristics in patients with head and neck cancer undergoing radiotherapy. *Pain*, 156(5), 967-979.

- Atwell, D., Elks, J., Cahill, K., Hearn, N., Vignarajah, D., Lagopoulos, J., & Min, M. (2020). A review of modern radiation therapy dose escalation in locally advanced head and neck cancer. *Clinical Oncology*, 32(5), 330-341.
- Banik, R. K., Woo, Y. C., Park, S. S., & Brennan, T. J. (2006). Strain and sex influence on pain sensitivity after plantar incision in the mouse. *The Journal of the American Society of Anesthesiologists*, 105(6), 1246-1253.
- Brown, D. C. (2016). Resiniferatoxin: the evolution of the “molecular scalpel” for chronic pain relief. *Pharmaceuticals*, 9(3), 47.
- Brown, D. C., Agnello, K., & Iadarola, M. J. (2015). Intrathecal resiniferatoxin in a dog model: efficacy in bone cancer pain. *Pain*, 156(6), 1018-1024.
- Buchsel, P. C., & Murphy, P. J. (2008). Polyvinylpyrrolidone–sodium hyaluronate gel (Gelclair®): a bioadherent oral gel for the treatment of oral mucositis and other painful oral lesions. *Expert Opinion on Drug Metabolism & Toxicology*, 4(11), 1449-1454.
- Caterina, M. J., & Julius, D. (2001). The vanilloid receptor: a molecular gateway to the pain pathway. *Annual review of neuroscience*, 24(1), 487-517.
- Caterina, M. J., Leffler, A., Malmberg, A. B., Martin, W., Trafton, J., Petersen-Zeitz, K., Koltzenburg, M., Basbaum, A., & Julius, D. (2000). Impaired nociception and pain sensation in mice lacking the capsaicin receptor. *science*, 288(5464), 306-313.
- Chin, D., Boyle, G. M., Porceddu, S., Theile, D. R., Parsons, P. G., & Coman, W. B. (2006). Head and neck cancer: past, present and future. *Expert review of anticancer therapy*, 6(7), 1111-1118.
- Christoforou, J., Karasneh, J., Manfredi, M., Dave, B., Walker, J. S., Dios, P. D., Epstein, J., Kumar, N., Glick, M., & Lockhart, P. B. (2019). World Workshop on Oral Medicine VII:

- Non-opioid pain management of head and neck chemo/radiation-induced mucositis: A systematic review. *Oral diseases*, 25, 182-192.
- Cohen, N., Fedewa, S., & Chen, A. Y. (2018). Epidemiology and demographics of the head and neck cancer population. *Oral and Maxillofacial Surgery Clinics*, 30(4), 381-395.
- Cramer, J. D., Johnson, J. T., & Nilsen, M. L. (2018). Pain in head and neck cancer survivors: prevalence, predictors, and quality-of-life impact. *Otolaryngology–Head and Neck Surgery*, 159(5), 853-858.
- Cruz, F. F., Rocco, P. R. M., & Pelosi, P. (2017). Anti-inflammatory properties of anesthetic agents. *Critical Care*, 21(1), 1-7.
- Dörr, W., & Kummermehr, J. (1990). Accelerated repopulation of mouse tongue epithelium during fractionated irradiations or following single doses. *Radiotherapy and oncology*, 17(3), 249-259.
- Dörr, W., Spekl, K., & Martin, M. (2002). Radiation-induced oral mucositis in mice: strain differences. *Cell proliferation*, 35, 60-67.
- Epstein, J. B., & Barasch, A. (2018). Oral and dental health in head and neck cancer patients. In *Multidisciplinary Care of the Head and Neck Cancer Patient* (pp. 43-57). Springer.
- Epstein, J. B., Hong, C., Logan, R. M., Barasch, A., Gordon, S. M., Oberlee-Edwards, L., McGuire, D., Napenas, J. J., Elting, L. S., & Spijkervet, F. K. (2010). A systematic review of orofacial pain in patients receiving cancer therapy. *Supportive care in cancer*, 18(8), 1023-1031.
- Epstein, J. B., Wilkie, D. J., Fischer, D. J., Kim, Y.-O., & Villines, D. (2009). Neuropathic and nociceptive pain in head and neck cancer patients receiving radiation therapy. *Head & neck oncology*, 1(1), 1-12.

- Farazifard, R., Safarpour, F., Sheibani, V., & Javan, M. (2005). Eye-wiping test: a sensitive animal model for acute trigeminal pain studies. *Brain research protocols*, 16(1-3), 44-49.
- Gaskill, B. N., Karas, A. Z., Garner, J. P., & Pritchett-Corning, K. R. (2013). Nest building as an indicator of health and welfare in laboratory mice. *JoVE (Journal of Visualized Experiments)* (82), e51012.
- Gray, A., Marrero-Berrios, I., Weinberg, J., Manchikalapati, D., SchianodiCola, J., Schloss, R. S., & Yarmush, J. (2016). The effect of local anesthetic on pro-inflammatory macrophage modulation by mesenchymal stromal cells. *International immunopharmacology*, 33, 48-54.
- Gruber, S., Bozsaky, E., Roitinger, E., Schwarz, K., Schmidt, M., & Dörr, W. (2017). Early inflammatory changes in radiation-induced oral mucositis. *Strahlentherapie und Onkologie*, 193(6), 499-507.
- Hwang, D., Popat, R., Bragdon, C., O'Donnell, K. E., & Sonis, S. T. (2005). Effects of ceramide inhibition on experimental radiation-induced oral mucositis. *Oral Surgery, Oral Medicine, Oral Pathology, Oral Radiology, and Endodontology*, 100(3), 321-329.
- Iadarola, M. J., & Gonnella, G. L. (2013). Resiniferatoxin for Pain Treatment: An Interventional Approach to Personalized Pain Medicine. *The open pain journal*, 6, 95-107.
- Iadarola, M. J., Sapio, M. R., Raithel, S. J., Mannes, A. J., & Brown, D. C. (2018). Long-term pain relief in canine osteoarthritis by a single intra-articular injection of resiniferatoxin, a potent TRPV1 agonist. *Pain*, 159(10), 2105-2114.
- Jensen, S., Pedersen, A., Reibel, J., & Nauntofte, B. (2003). Xerostomia and hypofunction of the salivary glands in cancer therapy. *Supportive care in cancer*, 11(4), 207-225.

- Jimenez-Andrade, J. M., Ghilardi, J. R., Castaneda-Corral, G., Kuskowski, M. A., & Mantyh, P. W. (2011). Preventive or late administration of anti-NGF therapy attenuates tumor-induced nerve sprouting, neuroma formation, and cancer pain. *Pain*, 152(11), 2564-2574.
- Jirkof, P. (2014). Burrowing and nest building behavior as indicators of well-being in mice. *Journal of neuroscience methods*, 234, 139-146.
- Jirkof, P., Cesarovic, N., Rettich, A., Nicholls, F., Seifert, B., & Arras, M. (2010). Burrowing behavior as an indicator of post-laparotomy pain in mice. *Frontiers in behavioral neuroscience*, 4, 165.
- Jirkof, P., Fleischmann, T., Cesarovic, N., Rettich, A., Vogel, J., & Arras, M. (2013). Assessment of postsurgical distress and pain in laboratory mice by nest complexity scoring. *Laboratory animals*, 47(3), 153-161.
- Kallurkar, A., Kulkarni, S., Delfino, K., Ferraro, D., & Rao, K. (2019). Characteristics of chronic pain among head and neck cancer patients treated with radiation therapy: A retrospective study. *Pain Research and Management*, 2019.
- Karri, J., Lachman, L., Hanania, A., Marathe, A., Singh, M., Zacharias, N., Orhurhu, V., Gulati, A., & Abd-Elseyed, A. (2021). Radiotherapy-Specific Chronic Pain Syndromes in the Cancer Population: An Evidence-Based Narrative Review. *Advances in Therapy*, 1-22.
- Keeble, J., Russell, F., Curtis, B., Starr, A., Pinter, E., & Brain, S. D. (2005). Involvement of transient receptor potential vanilloid 1 in the vascular and hyperalgesic components of joint inflammation. *Arthritis & Rheumatism: Official Journal of the American College of Rheumatology*, 52(10), 3248-3256.
- Kelbel, I., & Weiss, M. (2001). Anaesthetics and immune function. *Current Opinion in Anesthesiology*, 14(6), 685-691.

- Kerr, B. J., & David, S. (2007). Pain behaviors after spinal cord contusion injury in two commonly used mouse strains. *Experimental neurology*, 206(2), 240-247.
- Kissin, E. Y., Freitas, C. F., & Kissin, I. (2005). Effects of intraarticular resiniferatoxin in experimental knee-joint arthritis. *Anesthesia and analgesia*, 101(5), 1433.
- Kumar, P., Sunkaraneni, S., Sirohi, S., Dighe, S. V., Walker, E. A., & Yoburn, B. C. (2008). Hydromorphone efficacy and treatment protocol impact on tolerance and μ -opioid receptor regulation. *European journal of pharmacology*, 597(1), 39-45.
- Lai, Y., Bäumer, W., Meneses, C., Roback, D. M., Robertson, J. B., Mishra, S. K., Lascelles, B. D. X., & Nolan, M. W. (2021). Irradiation of the Normal Murine Tongue Causes Upregulation and Activation of Transient Receptor Potential (TRP) Ion Channels. *Radiation Research*, 196(4), 331-344.
- Langford, D. J., Bailey, A. L., Chanda, M. L., Clarke, S. E., Drummond, T. E., Echols, S., Glick, S., Ingrao, J., Klassen-Ross, T., & LaCroix-Fralish, M. L. (2010). Coding of facial expressions of pain in the laboratory mouse. *Nature methods*, 7(6), 447-449.
- Latremoliere, A., & Woolf, C. J. (2009). Central sensitization: a generator of pain hypersensitivity by central neural plasticity. *The journal of pain*, 10(9), 895-926.
- Launay, P.-S., Reboussin, E., Liang, H., Kessal, K., Godefroy, D., Rostene, W., Sahel, J.-A., Baudouin, C., Parsadaniantz, S. M., & Le Goazigo, A. R. (2016). Ocular inflammation induces trigeminal pain, peripheral and central neuroinflammatory mechanisms. *Neurobiology of disease*, 88, 16-28.
- Li, Wu, C.-z., Zhang, B.-w., Qiu, L., Chen, W., Yuan, Y.-H., Liu, X.-c., Li, C.-j., & Li, L.-j. (2021). Nerve growth factor protects salivary glands from irradiation-induced damage. *Life Sciences*, 265, 118748.

- Ling, I. S., & Larsson, B. (2011). Individualized pharmacological treatment of oral mucositis pain in patients with head and neck cancer receiving radiotherapy. *Supportive care in cancer*, 19(9), 1343-1350.
- Matsumiya, L. C., Sorge, R. E., Sotocinal, S. G., Tabaka, J. M., Wieskopf, J. S., Zaloum, A., King, O. D., & Mogil, J. S. (2012). Using the Mouse Grimace Scale to reevaluate the efficacy of postoperative analgesics in laboratory mice. *Journal of the American Association for Laboratory Animal Science*, 51(1), 42-49.
- Menéndez, L., Juárez, L., García, E., García-Suárez, O., Hidalgo, A., & Baamonde, A. (2006). Analgesic effects of capsazepine and resiniferatoxin on bone cancer pain in mice. *Neuroscience Letters*, 393(1), 70-73.
- Minnone, G., De Benedetti, F., & Bracci-Laudiero, L. (2017). NGF and Its Receptors in the Regulation of Inflammatory Response. *International journal of molecular sciences*, 18(5), 1028.
- Mirabile, A., Airoidi, M., Ripamonti, C., Bolner, A., Murphy, B., Russi, E., Numico, G., Licitra, L., & Bossi, P. (2016). Pain management in head and neck cancer patients undergoing chemo-radiotherapy: Clinical practical recommendations. *Critical reviews in oncology/hematology*, 99, 100-106.
- Miyagi, M., Ishikawa, T., Kamoda, H., Suzuki, M., Inoue, G., Sakuma, Y., Oikawa, Y., Orita, S., Uchida, K., & Takahashi, K. (2017). Efficacy of nerve growth factor antibody in a knee osteoarthritis pain model in mice. *BMC Musculoskeletal Disorders*, 18(1), 1-8.
- Mogil, J. S. (2012). Sex differences in pain and pain inhibition: multiple explanations of a controversial phenomenon. *Nature Reviews Neuroscience*, 13(12), 859-866.

- Mogil, J. S. (2019). The translatability of pain across species. *Philosophical Transactions of the Royal Society B*, 374(1785), 20190286.
- Moslemi, D., Nokhandani, A. M., Otaghsaraei, M. T., Moghadamnia, Y., Kazemi, S., & Moghadamnia, A. A. (2016). Management of chemo/radiation-induced oral mucositis in patients with head and neck cancer: A review of the current literature. *Radiotherapy and oncology*, 120(1), 13-20.
- Negus, S. S., Neddenriep, B., Altarifi, A. A., Carroll, F. I., Leidl, M. D., & Miller, L. L. (2015). Effects of ketoprofen, morphine, and kappa opioids on pain-related depression of nesting in mice. *Pain*, 156(6), 1153.
- Neubert, J. K., King, C., Malphurs, W., Wong, F., Weaver, J. P., Jenkins, A. C., Rossi, H. L., & Caudle, R. M. (2008). Characterization of mouse orofacial pain and the effects of lesioning TRPV1-expressing neurons on operant behavior. *Molecular pain*, 4, 1744-8069-1744-1743.
- Nolan, M. W., Long, C. T., Marcus, K. L., Sarmadi, S., Roback, D. M., Fukuyama, T., Baeumer, W., & Lascelles, B. D. X. (2017). Nocifensive behaviors in mice with radiation-induced oral mucositis. *Radiation research*, 187(3), 397-403.
- Oliver, V. L., Thurston, S. E., & Lofgren, J. L. (2018). Using cageside measures to evaluate analgesic efficacy in mice (*Mus musculus*) after surgery. *Journal of the American Association for Laboratory Animal Science*, 57(2), 186-201.
- Price, M. L., Lai, Y. H., Marcus, K. L., Robertson, J. B., Lascelles, B. D. X., & Nolan, M. W. (2021). Early radiation-induced oral pain signaling responses are reduced with pentoxifylline treatment. *Veterinary Radiology & Ultrasound*, 62(2), 255-263.

- Rock, M. L., Karas, A. Z., Rodriguez, K. B. G., Gallo, M. S., Pritchett-Corning, K., Karas, R. H., Aronovitz, M., & Gaskill, B. N. (2014). The time-to-integrate-to-nest test as an indicator of wellbeing in laboratory mice. *Journal of the American Association for Laboratory Animal Science*, 53(1), 24-28.
- Rosenthal, D. (2007). Consequences of mucositis-induced treatment breaks and dose reductions on head and neck cancer treatment outcomes. *The journal of supportive oncology*, 5, 23-31.
- Schaller, A. K. S., Peterson, A., & Bäckryd, E. (2021). Pain management in patients undergoing radiation therapy for head and neck cancer—a descriptive study. *Scandinavian Journal of Pain*, 21(2), 256-265.
- Sevcik, M. A., Ghilardi, J. R., Peters, C. M., Lindsay, T. H., Halvorson, K. G., Jonas, B. M., Kubota, K., Kuskowski, M. A., Boustany, L., & Shelton, D. L. (2005). Anti-NGF therapy profoundly reduces bone cancer pain and the accompanying increase in markers of peripheral and central sensitization. *Pain*, 115(1-2), 128-141.
- Shih, A., Miaskowski, C., Dodd, M. J., Stotts, N. A., & MacPhail, L. (2002). A research review of the current treatments for radiation-induced oral mucositis in patients with head and neck cancer. In *Oncology nursing forum* (Vol. 29, No. 7).
- Spradley, J. M., Davoodi, A., Carstens, M. I., & Carstens, E. (2012). Opioid modulation of facial itch-and pain-related responses and grooming behavior in rats. *Acta Derm Venereol*, 92(5), 515-520.
- Sroussi, H. Y., Epstein, J. B., Bensadoun, R. J., Saunders, D. P., Lalla, R. V., Migliorati, C. A., Heavilin, N., & Zumsteg, Z. S. (2017). Common oral complications of head and neck cancer radiation therapy: mucositis, infections, saliva change, fibrosis, sensory

- dysfunctions, dental caries, periodontal disease, and osteoradionecrosis. *Cancer medicine*, 6(12), 2918-2931.
- Vardeh, D., & Naranjo, J. F. (2017). Peripheral and central sensitization. In *Pain medicine* (pp. 15-17). Springer.
- Wiesenfeld-Hallin, Z. (2005). Sex differences in pain perception. *Gender medicine*, 2(3), 137-145.
- Wilson, S. G., Chesler, E. J., Hain, H., Rankin, A. J., Schwarz, J. Z., Call, S. B., Murray, M. R., West, E. E., Teuscher, C., Rodriguez-Zas, S., Belknap, J. K., & Mogil, J. S. (2002). Identification of quantitative trait loci for chemical/inflammatory nociception in mice. *Pain*, 96(3), 385-391.
- Wu, P., Arris, D., Grayson, M., Hung, C.-N., & Ruparel, S. (2018). Characterization of sensory neuronal subtypes innervating mouse tongue. *PLoS One*, 13(11), e0207069.
- Ye, Y., Dang, D., Zhang, J., Viet, C. T., Lam, D. K., Dolan, J. C., Gibbs, J. L., & Schmidt, B. L. (2011). Nerve growth factor links oral cancer progression, pain, and cachexia. *Molecular cancer therapeutics*, 10(9), 1667-1676.
- Yilmaz, Z., Renton, T., Yiangou, Y., Zakrzewska, J., Chessell, I., Bountra, C., & Anand, P. (2007). Burning mouth syndrome as a trigeminal small fibre neuropathy: Increased heat and capsaicin receptor TRPV1 in nerve fibres correlates with pain score. *Journal of clinical neuroscience*, 14(9), 864-871.
- Yoo, M. H., Rhee, Y. H., Jung, J., Lee, S. J., Moon, J. H., Mo, J. H., & Chung, P. S. (2020). TRPV1 regulates inflammatory process in the tongue of surgically induced xerostomia mouse. *Head & neck*, 42(2), 198-209.

**Chapter 3: “Painful Radiation-induced Oral Mucositis Promotes Metastatic Tumor
Development in Murine Models of Breast and Oral Cancer, a Phenomenon that Shows
Dependency on TRPV1-Expressing Neurons.”**

3.1 Introduction

In patients undergoing radiotherapy for squamous cell carcinoma of the head and neck (HNSCC), an unplanned extension of the time over which radiotherapy is administered is associated with diminished locoregional tumor control and reduced progression-free survival rates (Mazul et al., 2020; Russo et al., 2008; Vera-Llonch et al., 2006). That is true when radiotherapy is used for the management of primary HNSCC, and when treatment is delivered postoperatively (Chen et al., 2018; Ho et al., 2018). This increased risk for early relapse, despite definitive irradiation, has been attributed to accelerated repopulation of tumor clonogens, which is a phenomenon whereby sublethal doses of radiation stimulate cellular proliferation via activation of the receptor tyrosine kinase, epidermal growth factor receptor (EGFR) (Schmidt-Ullrich et al., 1997). While EGFR is overexpressed in over 90% of HNSCCs (Grandis & Tweardy, 1993), irradiation may further increase its activity and appears to drive tumor growth. When compared with radiotherapy alone as first-line therapy for locally advanced HNSCC, 5-year survival is improved for patients treated with radiotherapy plus cetuximab (EGFR inhibitor) (Bonner et al., 2006; Bonner et al., 2010).

The impact of treatment course prolongation can be substantial. In one study, a 10-day prolongation of the overall treatment time was associated with a 10% reduction in tumor control probability (Suwinski et al., 2003). Others have estimated a 4.8% higher risk of local relapse per day of interruption (Barton et al., 1992). One reason for treatment course prolongation is Radiation-Associated Pain (RAP). Acute, and sometimes severe, orofacial RAP frequently accompanies radiodermatitis and oral mucositis, which are common complications of head and neck irradiation (Naylor & Mallett, 2001; Trotti et al., 2003; Wong et al., 2006). This pain can be difficult to manage (Scully et al., 2003), and so to improve patient comfort, unplanned treatment

breaks may be recommended by the physician to allow tissue healing before completing the prescribed course of radiotherapy. Thus, pain can prompt treatment course prolongation, which adversely affects patient prognosis, but it is unknown whether this pain (or pain signaling mechanisms) might alter tumor behavior to directly increase the risk for early relapse.

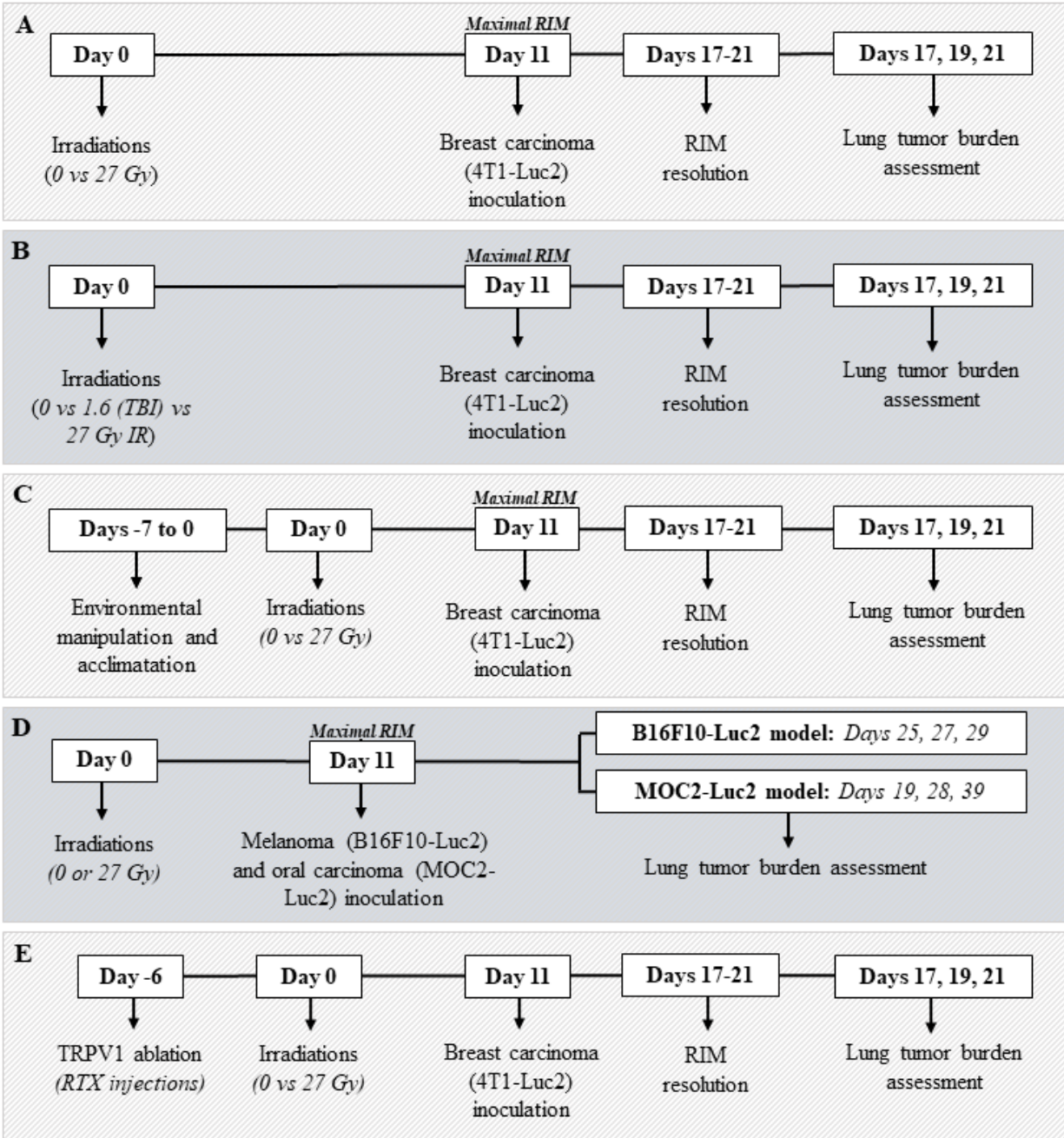
In other realms of cancer research, it has been demonstrated that certain mediators of pain can promote aggressive tumor cell behaviors. For example, nerve growth factor (NGF) is a prototypical neurotrophic factor and well-recognized molecular mediator of pain; receptors for NGF are expressed by both normal breast epithelial cells and breast carcinoma cells, but it is only in the carcinoma cells that NGF binding causes activation of the mitogen-activated protein kinase cascade which is requisite for mitogenic activity (Descamps et al., 1998). This suggests that NGF has the potential to regulate breast tumor growth. Indeed, human breast tumor biopsies display widespread immunoreactivity for NGF, and in xenografted mice, NGF blockade inhibits both tumor growth and metastasis (Adriaenssens et al., 2008). In addition, strategies to reduce pain can also alter cancer progression. It has been shown by Page and colleagues that after tail vein injection of tumor cells into rats, growth of neoplastic lung nodules is hastened by the presence of surgical pain; this effect is mitigated with opioid analgesics (Page et al., 1993; Page et al., 2001). The premise that, for certain cancers, tumor control may be maximized via optimization of intra- and perioperative analgesia and anesthesia is further supported by clinical observations. The use of spinal anesthesia as an alternative to general anesthesia has been associated with lower recurrence rates after transurethral resection of superficial bladder cancers (Choi et al., 2017). Overall survival was longer in a series of patients having undergone open thoracotomy for primary lung tumors with paravertebral blocks instead of intravenous patient-controlled analgesia (E. K. Lee et al., 2017).

These reports provide a rational basis for considering the possibility that pain, or pain signaling mechanisms, may contribute to poor oncologic outcomes in patients undergoing therapeutic irradiation. Here, we adapted the methods of Page and colleagues, to explore (in animal models) if aggressive tumor behavior may be a direct result of severe acute orofacial RAP, or RAP signaling components.

3.2 Materials and Methods

In this work, we began by establishing that in female mice, growth of lung tumors after tail vein injection of an aggressive mammary carcinoma cell line is hastened by the presence of severe acute orofacial RAP. Next, we established that this effect is attributable to local oral irradiation (versus non-target radiation or certain environmental stressors), and is seen in both male and female mice, but is restricted to certain tumor models. Finally, we demonstrated that the effect can be mitigated with the provision of effective analgesia by selectively chemically ablating a subset of sensory neurons that express the transient receptor potential vanilloid type-I receptor (TRPV1). A summary of the experimental design is detailed in Figure 3.1.

Figure 3.1: Summary of experiments. (A) First, we assessed the burden of lung tumors in female and male mice (BALB/c) having undergone tail vein injection of breast carcinoma cells (4T1-Luc2 model) at the time of severe acute RIM and RAP (day 11 post-IR). Tumor burden was assessed via *in vivo* transthoracic BLI at days 17, 19 and 21 post-IR, and confirmed during postmortem evaluation. (B) Using the same tumor model, we assessed the potential effects of off-target radiation dose via low-dose total body irradiation, and (C) environmental stress induced by standard cage temperatures. (D) To assess reproducibility, we repeated the experiments in different tumor models (melanoma, B16F10-Luc2; and oral squamous cell carcinoma, MOC2-Luc2) that utilize a different syngeneic host (C57BL/6 mice). Transthoracic BLI was performed 25, 27, and 29 days post-IR in B16F10-Luc2 bearing mice, and 19, 28 and 39 days post-IR in MOC2-Luc2 bearing mice. (E) Lastly, using our experimental paradigm, we evaluated whether tumor burden was altered by the analgesia provided when a selective sensory afferent neurotoxic agent (resiniferatoxin) is used.



3.2.1 Animals

Wild-type BALB/c (female and males) and C57BL/6 (female) mice, 10-14 weeks old, were purchased from a commercial vendor (Charles River Laboratories). Mice were group-housed (2-4 animals per cage) in specific pathogen-free facilities, and had unrestricted access to water, food pellets, and nutritional gel (DietGel 76A, ClearH2O) in a controlled 12-hr day-night cycle. Studies were performed at room temperature (21-22°C) unless otherwise noted. Pre-defined criteria for euthanasia included: increased respiratory effort, anorexia for more than 24 hours (once glossitis had resolved), hunched posture, or more than 30% weight loss. Euthanasia was performed via asphyxiation (3.5 L/min CO₂ chamber), followed by cervical dislocation. All experimental procedures were approved by the NC State University Institutional Animal Care and Use Committee (protocol #'s: 18-061-B and 19-810-B).

3.2.2 Cell lines

Three different firefly luciferase-expressing mouse cancer cell lines were used: 4T1-Luc2 (mammary carcinoma), B16F10-Luc2 (cutaneous melanoma), and MOC2-Luc2 (oral squamous cell carcinoma). Cell line authentication, preparation, and protocol optimization are detailed in Supplementary Material 3.6.1. Murine 4T1-Luc2 mammary carcinoma cells were provided as a gift from Drs. Gregory Palmer and Mark Dewhirst at Duke University on April 20th, 2018, and they had previously received the cells from Dr. Michael Wendt at Case Western Reserve University. 4T1-Luc2 cells (passage 4) were cultured in Dulbecco's modified eagle medium (DMEM, high in glucose with sodium pyruvate and glutamine, Fisher Scientific) with 10% fetal bovine serum (Genesee Scientific) and 500 µg/mL of zeocin (InvivoGen). Murine B16F10-Luc2 melanoma cells were purchased from ATCC (catalog number: BW124734) and cultured in RPMI 1640 (Gibco) containing 10% fetal bovine serum (Genesee Scientific). The medium was

supplemented with 100 units/mL penicillin and 100 µg/mL streptomycin (Genesee Scientific). Murine MOC2-Luc2 oral cancer cells were provided by Dr. Clint Allen (National Institutes of Health) on March 12th, 2020, with approval (including a Material Transfer Agreement) from Dr. Ravindra Uppaluri at Dana-Farber Cancer Institute. MOC2-Luc2 cells (passage 4) were cultured in HyClone™ Iscove's Modified Dulbecco's Medium (IMDM) and Hams F12 Nutrient Mixture (Fisher Scientific) at a 2:1 mixture with 5% fetal bovine serum, 1% penicillin/streptomycin, 5 ng/mL epidermal growth factor, 400 ng/mL hydrocortisone, and 5 mg/mL insulin (MilliporeSigma). All cell lines were incubated in a humidified incubator at 37 °C in a 5% CO₂ atmosphere, and passaged 1:10 when 75-90% confluent.

3.2.3 Irradiations

Within each experiment, mice were randomly allocated to one of two treatment groups: 1) single-dose irradiation (27 Gy) of the rostral tongue to induce severe but reversible glossitis (hereafter referred to as “IR” mice) or 2) sham irradiation (0 Gy) as the negative control (referred to as “SHAM” mice). In some experiments we also used total body irradiation (1.6 Gy; referred to as “TBI” mice) to simulate the non-target dose the body is exposed to when using the aforementioned 27 Gy protocol (Lai et al., 2021). Irradiations were performed using a clinical linear accelerator and 6 MV X-ray beam (Novalis TX, Varian Medical Systems). A detailed description of these irradiation protocols, including all associated dosimetric verifications, has been described previously (Lai et al., 2021). For irradiation, mice were anesthetized using an intraperitoneal injection of ketamine (50–150 mg/kg, 100 mg/mL, Henry Schein) and xylazine (10 mg/kg, 20 mg/mL, Anased, Lloyd Laboratories).

3.2.4 Assessments of radiation-induced mucositis and body weight

Daily for the first 21 days after irradiation, body weights were recorded and radiotherapy-induced oral mucositis (RIM) severity was assessed on a 5-point scale (Lai et al., 2021), wherein a score of zero (0) reflects a normal tongue, three (3) describes severe edema, hypersalivation, ulceration and pseudomembrane/plaque formation, and five (5) indicates death. RIM severity scoring was performed by a single, unblinded observer who visually inspected the mucosal lesions by gently extracting the tongue using non-traumatic forceps under isoflurane anesthesia.

3.2.5 Screening for radiation-associated pain

Nesting and grooming activities were characterized as indicators of RAP severity (see Supplementary Material 3.6.2 for information related to assay rationale and design). These assessments were made by a single unblinded veterinarian at baseline (before irradiations), at the time of maximal RIM severity (day 11 post-IR), and after RIM resolution (day 19 post-IR).

3.2.6 Tumor cell inoculation

In all experiments, tumor inoculation was performed on day 11 post-irradiation (i.e., at the time of maximal glossitis severity). Mice were manually restrained (Tailveiner Restrainer Tube; TV-150, Braintree scientific, Inc.) without anesthesia, and tumor cells were injected via a lateral tail vein into the syngeneic host using a 30-gauge needle on a low dead space insulin syringe (2×10^5 4T1-Luc2 cells suspended in 0.1 mL of sterile PBS were injected into BALB/c mice; and 2×10^5 B16F10-Luc2 cells in 0.1 mL sterile PBS or 1×10^6 MOC2-Luc2 cells in 0.2 mL sterile PBS were injected into C57BL/6 mice).

3.2.7 Tumor burden and growth

3.2.7.1 *In vivo* assessment: Lung tumor burden was assessed *in vivo* using bioluminescence imaging (BLI) – hereafter referred to as “transthoracic BLI” (IVIS Lumina II *in vivo* imaging system; PerkinElmer Ltd.). To reduce optical scatter and signal loss, the dorsal thoracic skin fur was removed with depilatory cream. Mice then underwent intraperitoneal injection of D-luciferin (150 mg/kg in 0.1 mL sterile PBS; Xenogen Corp.); 10-15 minutes later, mice were isoflurane-anesthetized and positioned in dorsal recumbency for imaging (imaging parameters: 745 nm excitation and >800 nm emission filters, auto exposure time, and a binning factor of 1). For analysis, a 1.5 x 1.5 cm square region of interest (ROI) was manually drawn and placed to cover the thorax. Fluorescence was expressed as the total radiant efficiency (total flux [p/s]).

3.2.7.2 *Ex vivo* assessment: Lung tumor burden was evaluated *ex vivo* at the end of every experiment. Mice were euthanized and the entire thoracic pluck (including tongue, trachea, esophagus, thyroid glands, thymus, heart, and lungs) was removed. To facilitate visualization of nodules in 4T1-Luc2 and MOC2-Luc2 bearing mice, 3 mL of 15% India ink (diluted with PBS, pH 7.4) was instilled into the lungs via the trachea. Lungs were immediately rinsed with unfiltered non-sterile distilled water, and then fixed overnight in 1.5 mL of Fekete's solution (composition: 300 mL of 70% ethanol, 30 mL of 37% formaldehyde, and 5 mL of glacial acetic acid). In B16F10-Luc2 tumor-bearing mice, 3 mL of Fekete's solution was instilled into the lungs, which were then rinsed and fixed, as above. Photographs of each lung lobe's surface were taken using a mobile phone (Galaxy S10, Samsung) and a standard lighting and background setup; tumor burden was quantified by manually counting the total number of pulmonary nodules (data expressed as number of solitary pulmonary nodules per mouse). In experiments with nodules that were too numerous to count, photographs were exported to ImageJ software (version 1.53e, National Institutes of

Health), and converted to 8-bit images. The “freehand selection” tool was used to contour lungs and remove background; a ROI was drawn around each lobe and manual thresholding was used to contour tumor nodules on the images, filling the nodule shape in “red”, and clearing the background in “white” colors. The percent of the surface occupied by tumor nodules was expressed as the total area fraction per mouse.

3.2.8 Modulation of ambient temperature

Standard mouse housing temperatures (22-24°C) induce environmental stress that can alter tumor growth (Hunter et al., 2014; Hylander & Repasky, 2016; Kathleen M. Kokolus et al., 2013). To help establish the translational relevance of our work, and ensure observations were not dependent upon this form of environmental stress, we investigated the effect of standard (STDt; 22-24°C) versus thermoneutral (TNt; 30-31°C) housing temperature on the growth of 4T1-Luc2 tumors in female BALB/c mice, after either lingual or sham irradiation. Mice in the STDt group were housed in a standard research environment (i.e., room temperature of 21-22°C, cages placed on standard steel shelving). For the TNt group, cage warming was achieved by placing a 10" x 20.5" heat mat (iPower Seed Starter Heat Mat) underneath a standard mouse cage. Based on pilot work (see Supplementary Material 3.6.3), the heating pad thermostat was set to 25.6°C, which produced an average cage floor (bedding) temperature of approximately 31°C. Cage floor temperature was monitored daily using a digital thermostat controller (iPower Digital Heat Mat Controller). Mice were acclimatized to this temperature for 7 days before starting the experiment.

3.2.9 Selective chemical ablation of transient receptor potential vanilloid 1 expressing neurons

TRPV1-expressing sensory neurons are the predominant noci-receptive sensory fiber in mice, and activation of these fibers leads to pain (Usoskin et al., 2015; Wu et al., 2018). In pilot work (unpublished), we found that ablation of TRPV1-expressing neurons both reduced pain behaviors associated with RAP, and reduced the severity of glossitis. Ablation was achieved using systemic administration of resiniferatoxin (RTX), a potent TRPV1 agonist (Menéndez et al., 2006). Here, we investigated whether RAP-enhanced tumor progression could be prevented by ablation of TRPV1-expressing sensory neurons using RTX treatment. Pharmacologic grade RTX (200 µg/mL) and excipient were kindly provided by Dr. Alexis Nahama (Sorrento Therapeutics). Female BALB/c mice received either a single interscapular subcutaneous dose of 300 µg/kg of RTX (29), or an equivalent volume of the excipient 6 days before IR or sham IR (0 vs 27 Gy), and were injected (via tail vein) with 4T1-Luc2 cells as described above. Mice were randomly allocated to one of four treatment groups: 1) 0 Gy + RTX excipient (referred as “SHAM-EXCIPIENT”); 2) 27 Gy + RTX excipient (“IR- EXCIPIENT”); 3) 0 Gy + RTX (“SHAM-RTX”); or 4) 27 Gy + RTX (“IR-RTX”). To confirm successful ablation of TRPV1 neurons in the trigeminal pathway, mice were assessed weekly via topical administration of 0.01% capsaicin into the left eye (20 µL in approximately 26 °C 0.9% sterile saline). Responses were video recorded and later reviewed by a blinded observer who counted and recorded the number of facial wipes over 1 minute immediately following topical application of capsaicin. A 50% reduction from baseline in the number of wipes per minute constituted a successful ablation.

3.2.10 Statistical analysis

Pilot studies (n = 8 mice per group) were performed to calculate the expected effect and sample size (JMP 14.1; SAS Institute Inc., Cary, NC, USA), with $\alpha = 0.05$ and 80% power; calculated sample sizes for each experiment are listed in Table 3.1. All statistical tests were performed using commercial software (Prism version 6, GraphPad Software, Inc., La Jolla, CA). Normality was assessed using the Shapiro-Wilk normality test. An unpaired t-test (2-tailed), or 2-way repeated measures ANOVA analysis, was used for normally distributed data; p-values were adjusted for multiple comparisons using Tukey's or Sidak post hoc test. Nonparametric data were analyzed using Friedman and/or Mann-Whitney tests. The Kaplan-Meier method and the log-rank test were used for survival analysis. P-values less than 0.05 were considered significant.

Table 3.1: List of experiments and sample sizes used.

| List of experiment | n per experimental group | Total n/ experiment | Total n used |
|---|--------------------------|---------------------|--------------|
| Measurement of RAP in female BALB/c mice using a single irradiation fraction (Supplemental data) | 16 | 32 | 32 |
| Measurement of RAP in female C57BL/6 mice using a single irradiation fraction (Supplemental data) | 20 | 40 | 39 |
| Tumor-growth promoting effect of RAP in breast carcinoma tumor-bearing female BALB/c mice (4T1-Luc2 model) | 20 | 40 | 30 |
| Tumor-growth promoting effect of RAP in breast carcinoma tumor-bearing male BALB/c mice (4T1-Luc2 model) | 12 | 24 | 24 |
| Tumor-growth promoting effect of RAP in breast carcinoma tumor-bearing female BALB/c mice (4T1-Luc2 model); local vs total body vs sham irradiation | 12 | 36 | 36 |
| Tumor-growth promoting effect of RAP in breast carcinoma tumor-bearing female BALB/c mice (4T1-Luc2 model) after manipulating cage temperatures | 8 | 32 | 31 |

Table 3.1 (continued)

| | | | |
|--|----|----|----|
| Tumor-growth promoting effect of RAP in melanoma tumor-bearing female C57BL/6 mice (B16F10-Luc2 model) | 20 | 40 | 39 |
| Tumor-growth promoting effect of RAP in oral carcinoma tumor-bearing female C57BL/6 mice (MOC2-Luc2 model) | 16 | 32 | 30 |
| Tumor-growth promoting effect of RAP in oral carcinoma tumor-bearing female C57BL/6 mice (MOC2-Luc2 model); survival assessment | 16 | 32 | 29 |
| Effects of systemic ablation of TRPV1-expressing neurons on tumor growth in breast carcinoma tumor-bearing female BALB/c mice (4T1-Luc2 model) | 20 | 80 | 73 |

3.3 Results

3.3.1 Single fraction (27 Gy) irradiation of the rostral tongue is associated with mucositis and pain in BALB/c and C57BL/6 mice

We confirmed that single-fraction (27 Gy) irradiation of the rostral tongue of female and male BALB/c mice causes mild glossitis (score of 1) 8 to 9 days post-IR, with moderate-to-severe glossitis (score > 2) at days 10 to 12 post-IR (Figure 3.2A). As compared with sham-irradiated controls, severe glossitis was associated with significant reductions in body weight (> 15% from baseline) (Figure 3.2B) and with measures of severe acute RAP (Figure 3.2, C and D). Specifically, IR mice demonstrated decreased ability to shred nest material provided and decreased ability to build an adequate nest, and they lost the ability to properly groom. All of these alterations returned to baseline values by days 19-21 post-IR. We observed the same toxicities and associated behavioral impairments in female C57BL/6 mice that developed moderate-to-severe glossitis (Figure 3.2, E and F).

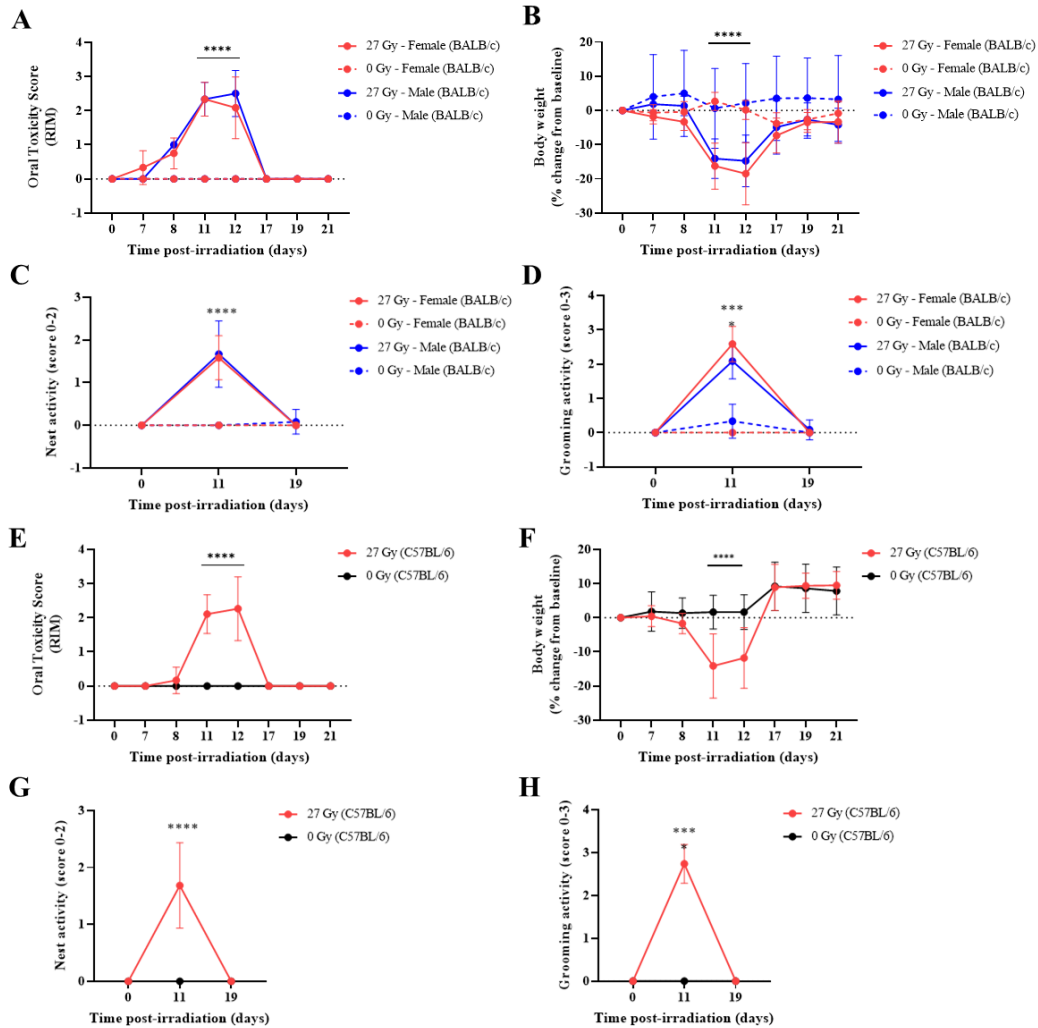


Figure 3.2: Tongue irradiation in BALB/c and C57BL/6 mice results in RAP. (A) All tongue-irradiated BALB/c mice (female and male) experienced severe glossitis ($p < 0.0001$), (B) with significant reductions ($>15\%$) in body weight from baseline ($p < 0.0001$), (C) as well as impaired nesting ($p < 0.0001$), and (D) grooming ($p < 0.0001$) activities at day 11 post-irradiation (27 Gy), as compared to sham-irradiated controls (0 Gy). (E) In female C57BL/6 mice, single-fraction (27 Gy) irradiation of the rostral tongue caused moderate-to-severe RIM (score > 2), (F) severe body weight loss ($> 15\%$), and impairment of (G) nesting and (H) grooming activities (IR vs SHAM, $p > 0.0001$ for both assays at day 11 post-IR). Data presented as mean \pm standard deviation (SD); * $p < 0.05$, ** $p < 0.01$; *** $p < 0.001$; **** $p < 0.0001$; ns., not significant.

3.3.2 Lung tumor burden in BALB/c mice is significantly increased when 4T1-Luc2 cells are intravenously injected at the time of severe mucositis and pain

In each experimental group, luciferase activity in the lungs was measured via transthoracic BLI at 17 days post-IR. The signal steadily increased until day 21, at which time tumor burden

was significantly greater in female IR mice versus SHAM controls (5.2-fold increase, $p < 0.0001$; Figure 3.3A). Similar results were observed in male BALB/c mice; by day 21, irradiated male mice had a 2.7-fold increase in transthoracic BLI compared with controls (IR vs SHAM, $p = 0.0079$; Figure 3.3C). Imaging results (tumor burden) were substantiated via post-mortem (*ex vivo*) evaluation (IR vs SHAM, female $p < 0.0001$, male $p < 0.0001$; Figure 3.3, B and D).

3.3.3 Off-target radiation does not increase the burden of 4T1 lung tumors

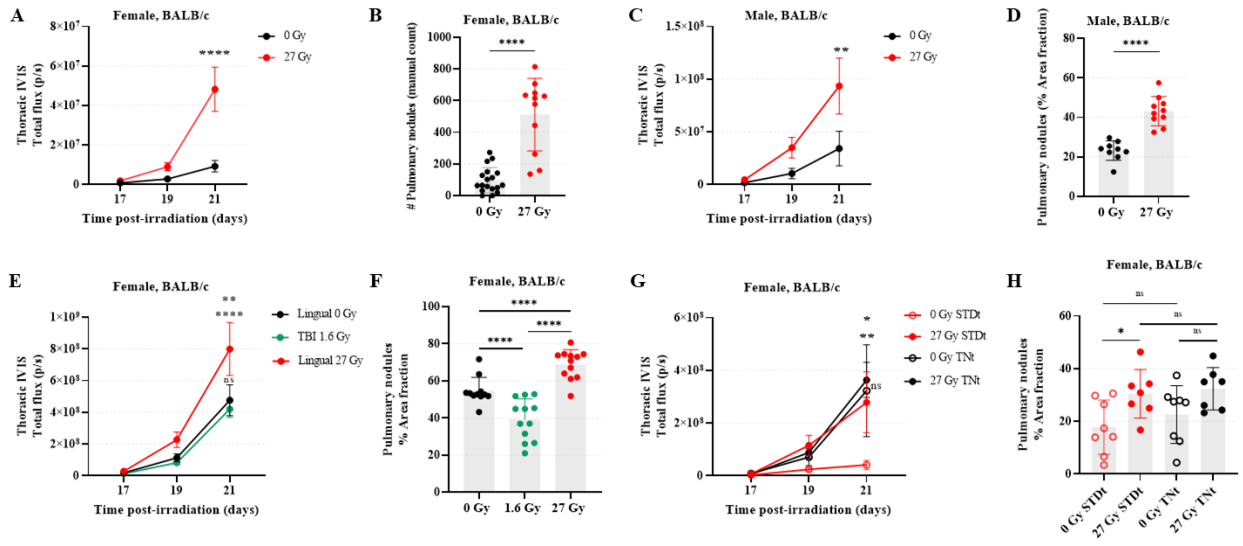
Transthoracic BLI results revealed that tumor burden was statistically significantly greater in IR mice than in SHAM (1.8-fold increase, $p = 0.0039$) and TBI (1.9-fold increase, $p = 0.0008$) mice at day 21 post-IR (Figure 3.3E). Furthermore, tumor burden was no different between SHAM and TBI groups at any time point ($p > 0.05$; Figure 3.3E). We confirmed these results post-mortem by calculating and comparing the percent area of lung covered by visible nodules. IR mice significantly presented a higher burden of 4T1-Luc2 tumor nodules as compared to SHAM mice (IR vs SHAM, $p = 0.0002$; IR vs TBI $p < 0.0001$). Interestingly, in this analysis, there was an apparent reduction in lung tumor burden in the mice having undergone TBI as opposed to sham irradiation ($p = 0.0009$; Figure 3.3F).

3.3.4 Standard (subthermoneutral) housing conditions do not appear to enhance 4T1 lung tumor burden

This experiment was designed to assess whether cage warming to create thermoneutral environmental temperatures would eliminate the apparent tumor burden promoting effects of high-dose tongue irradiation (e.g., by reducing environmental stress and thus potentially restoring an effective host response against tumor growth). Here, we were able to replicate our prior experimental finding that with standard mouse housing conditions, tongue irradiation is associated

with increased tumor burden in the 4T1-Luc2 model (6.7-fold increase; IR- STDt vs SHAM-STDt, $p = 0.0028$; Figure 3.3, G and H). Warming the cages enhanced tumor burden in sham-irradiated mice (7.8-fold increase; SHAM-STDt vs SHAM-TNt, $p = 0.0271$), but contrary to our expectation, tongue irradiation had no impact on the burden of 4T1-Luc2 tumors when mice were housed in thermoneutral temperature conditions (1.1-fold increase: IR-TNt vs SHAM-TNt, $p = 0.9800$; and 1.3-fold increase: IR-STDt vs IR-TNt, $p = 0.6599$). Tumor burden rapidly increased in all IR and SHAM mice housed under thermoneutral housing conditions, and their tumor growth rate was more similar to that of an irradiated mouse in the STDt environment than an unirradiated mouse in the STDt environment. We confirmed these results by calculating the percent area of lung covered by visible nodules (*ex vivo* lung assessment), however, here we did not observe a statistically significant difference between SHAM groups (STDt vs TNt, $p = 0.3841$).

Figure 3.3: Tumor burden promoting effect of RAP in breast carcinoma tumor-bearing female and male BALB/c mice (4T1-Luc2 model). (A) A two-way analysis of variance (ANOVA) followed by Sidak post hoc test showed a significant transthoracic BLI signal increase (expressed as total flux [p/s]) in IR BALB/c female mice experiencing RAP (n = 12) compared to SHAM controls (n = 18) 21 days after IR (p < 0.0001); data presented as mean ± SEM. (B) The number of pulmonary nodules was markedly higher in IR mice compared to SHAM mice (p < 0.0001, unpaired t-test); data presented as mean ± SD. (C) Similar to results in female mice, a two-way analysis of variance (ANOVA) followed Sidak post hoc test showed a significant transthoracic signal increase (expressed as total flux [p/s]) in IR male mice (n = 11) compared to SHAM mice (n = 11) 21 days after IR (p = 0.0079); data presented as mean ± SEM. (D) The presence of nodules on the lung's surface was significantly higher in IR (n = 10) compared to SHAM (n = 9) male mice (p < 0.0001, unpaired t-test); data presented as mean ± SD. (E) A two-way analysis of variance (ANOVA) followed Tukey's post hoc test showed a significant transthoracic signal increase (expressed as total flux [p/s]) in IR female mice (n = 12) compared to SHAM (n = 12; p = 0.0039) and TBI female mice (n = 12; p = 0.0008) 21 days after IR. No difference was found between the two control (SHAM and TBI) groups (p = 0.8441); data presented as mean ± SEM. (F) IR mice developed significantly more lung tumors compared to SHAM mice (p = 0.0002) and TBI mice (p < 0.0001), however, tumor burden was markedly decreased in the TBI group vs SHAM group (p = 0.0009, unpaired t-test); data presented as mean ± SD. (G) The effects of ambient temperature on the tumor burden promoting effect of RAP in breast carcinoma tumor-bearing female BALB/c mice (4T1-Luc2 model) was evaluated (n = 8/group). A two-way analysis of variance (ANOVA) followed Sidak's post hoc test showed a significant transthoracic signal increase (expressed as total flux [p/s]) in IR STDt mice versus their respective SHAM group (p = 0.0028). A marked difference was also found between both SHAM groups, with tumor growth significantly accelerated in SHAM mice housed at thermoneutral conditions (STDt vs. TNt, p = 0.0271). No difference was found between IR-TNt mice and their respective SHAM controls (p = 0.9800), nor between both IR groups (STDt vs. TNt, p = 0.6599); data presented as mean ± SEM. (H) The presence of pulmonary tumor nodules was significantly higher in IR-STDt mice versus the SHAM-STDt group (p = 0.0267). No difference between was found between the SHAM controls (STDt vs. TNt, p = 0.3841), nor between the IR groups (STDt vs. TNt, p = 0.6950), nor between the TNt cohorts (p = 0.0744, unpaired t-tests). Data presented as mean ± SD; *p < 0.05, ** p < 0.01; ***p < 0.001; ****p < 0.0001; ns., not significant.



3.3.5 Tongue irradiation does not increase the burden of B16F10-Luc2 lung tumors, but was associated with early (lung tumor attributable) death in MOC2-Luc2 bearing mice

In the B16F10-Luc2 melanoma model, mean transthoracic BLI signal appeared to increase at 27 and 29 days post-IR, but there was no difference in tumor burden between IR and SHAM mice at any time point (Figure 3.4A). Based upon postmortem evaluation, tongue irradiation caused a non-significant 1.5-fold increase in lung tumor burden versus sham irradiation (Figure 3.4B). In the MOC2-Luc2 model, transthoracic BLI signals were first detected at day 19 post-IR in all mice, but there was no further increase in signal intensity on day 28 post-IR, and by day 39 post-IR there was still no substantial change (Figure 3.4C). We did however observe increased respiratory effort and early death in some of the irradiated mice; we therefore repeated this experiment using a new cohort, and monitored respiratory status and survival. Irradiated mice started to display progressive respiratory effort 30 days post-IR, leading to death in all cases. By contrast, only a few sham-irradiated mice developed mild respiratory effort after day 30 post-IR, and almost all survived to day 52 (end of study) when all mice were euthanized. Pulmonary nodules (determined by visual inspection of lungs) were found in all mice at the time of death. The median overall survival time of IR mice was 39 days (95% CI: 30 to 47 days), and 48.5 days (95% CI: 36 to 52 days) for SHAM mice (Log-Rank p-value = 0.0002; Figure 3.4D).

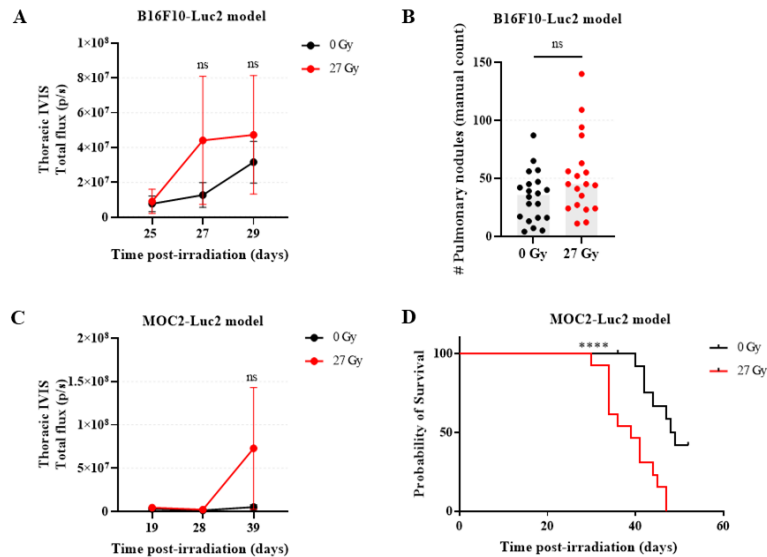


Figure 3.4: Tumor burden promoting effect of RAP in melanoma (B16F10-Luc2) and oral (MOC2-Luc2) tumor-bearing female C57BL/6 mice. (A) A two-way analysis of variance (ANOVA) followed Sidak's post hoc test showed no difference in transthoracic BLI signal (expressed as total flux [p/s]) between IR B16F10-bearing mice ($n = 20$) and SHAM mice ($n = 20$) at day 27 and 29 post-IR ($p = 0.4158$ and 0.93530 , respectively for each day); data presented as mean \pm SEM. (B) The presence of pulmonary nodules did not differ between groups ($p = 0.0592$, unpaired t-test); data presented as mean \pm SD. (C) A two-way analysis of variance (ANOVA) followed Sidak's post hoc test showed no difference in transthoracic BLI signal (expressed as total flux [p/s]) between IR MOC2-bearing mice ($n = 16$) and SHAM mice ($n = 16$) 39 days after IR ($p = 0.0897$); data presented as mean \pm SEM. (D) Kaplan–Meier analysis of survival showed a significant difference in survival between IR and SHAM MOC2-Luc2 bearing mice (Log-Rank p -value = 0.0002), with median survival times of 39 (95% CI: 30 to 47) vs. 48.5 (95% CI: 36 to 52) days, respectively. * $p < 0.05$, ** $p < 0.01$; *** $p < 0.001$; **** $p < 0.0001$; ns., not significant.

3.3.6 The growth-promoting effects that tongue irradiation had on 4T1 lung tumors was mitigated by systemic ablation of TRPV1 sensory nerves

Neither RTX nor excipient caused oral lesions (e.g., glossitis) or weight loss in SHAM animals. By 10 to 13 days after tongue irradiation, the vast majority of excipient-treated mice had developed moderate-to-severe RIM (score > 2) and profound weight loss ($> 15\%$). By contrast, varying degrees of RIM were found in resiniferatoxin-treated mice; by day 11 post-IR, approximately 44% presented RIM scores of 0, approximately 19% RIM of 1, and approximately

38% RIM of > 2 (mean 1.25, SD = 1.3). In these animals, weight loss was minimal ($< 5\%$) (Figure 3.5, A and B).

Overall, RTX treatment of IR mice reduced tumor burden to levels similar to those in the SHAM groups. As expected, and based upon aforementioned experimental results, excipient-treated irradiated mice had a 10-fold higher mean transthoracic BLI signal as compared with the excipient-treated sham-irradiated control mice at day 21 post-IR ($p < 0.0001$; Figure 3.5, C). There was minimal increase in the transthoracic BLI signal in IR-RTX mice compared to SHAM-RTX animals (2-fold increase: IR-RTX vs SHAM-RTX, $p = 0.9155$; Figure 3.5C), and furthermore, transthoracic BLI signal revealed that RTX markedly reduced tumor burden in irradiated mice (7.5-fold decrease: IR-RTX vs IR-EXCIPIENT, $p > 0.0001$; Figure 3.5C). Importantly, resiniferatoxin treatment itself had no measurable impact on tumor burden as measured by transthoracic BLI in sham-irradiated mice (SHAM-RTX vs SHAM-EXCIPIENT, $p = 0.9933$; Figure 3.5C).

We confirmed these results in post-mortem evaluations (Figure 3.5, D and E). A statistically significant difference was observed between excipient-treated irradiated and sham-irradiated mice ($p > 0.0001$), and between excipient and RTX-treated irradiated mice, with smaller tumor burden detected in the RTX group ($p = 0.0004$). There was a slight yet significant reduction in tumor burden in SHAM-RTX mice compared to SHAM-EXCIPIENT ($p = 0.0137$), and a significant increase in tumor burden in IR-RTX mice as compared with SHAM-RTX mice ($p = 0.0008$).

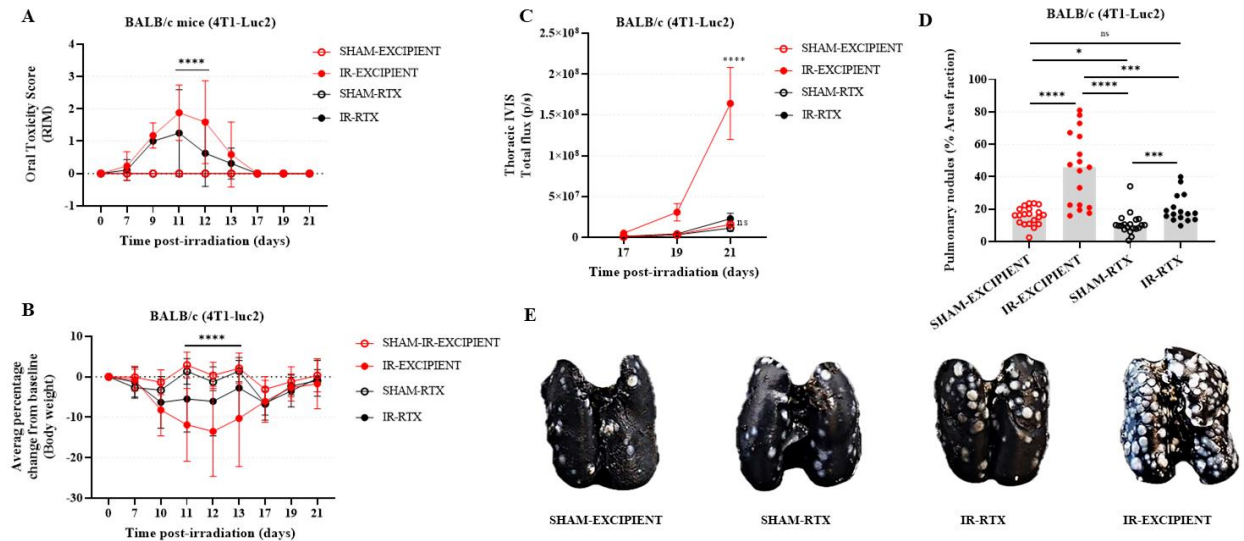


Figure 3.5: Effects of systemic ablation of TRPV1-expressing neurons on tumor burden in breast carcinoma tumor-bearing female BALB/c mice (4T1-Luc2 model). (A) All IR (RTX and EXCIPIENT) mice developed glossitis, (B) as well as reductions in body weight. However, moderate-to-severe glossitis scores (score ≥ 2) were only found in IR-EXCIPIENT mice, which also experienced significant decreases in body weight ($> 15\%$ loss). Treatment with RTX significantly reduced the severity of glossitis ($p > 0.0001$), and the degree of body weight loss ($p < 0.0001$) at days 11-12 post-IR. (C) A two-way analysis of variance (ANOVA) followed by a Tukey's post hoc test revealed a significant increase in the growth of 4T1-Luc2 cells (BLI imaging) in IR-EXCIPIENT mice versus the IR-RTX mice, and both SHAM (RTX or EXCIPIENT) groups ($p > 0.0001$ in all cases); data presented as mean \pm SEM. No difference was found between SHAM-EXCIPIENT and both RTX groups (IR and SHAM) ($p > 0.05$), nor between the IR-RTX and SHAM-RTX groups ($p = 0.9155$). (D) The presence of pulmonary nodules was markedly higher in IR-EXCIPIENT mice as compared with SHAM-EXCIPIENT mice ($p > 0.0001$), and with both IR and SHAM groups treated with RTX ($p < 0.0004$ and 0.0001 , respectively). Tumor burden was significantly lower in SHAM-RTX mice in comparison to their respective IR group ($p = 0.0008$, unpaired t-test). Within the SHAM groups, RTX slightly but still significantly reduced the burden of pulmonary nodules ($p = 0.0137$, unpaired t-test). Data presented as mean \pm SD; * $p < 0.05$, ** $p < 0.01$; *** $p < 0.001$; **** $p < 0.0001$; ns., not significant. (E) Representative images of each cohort's pulmonary tumor burden.

3.4 Discussion

Pain resulting from cancer, or cancer treatment, is known to be a clinical bellwether in humans for cancer prognosis. For example, severe pain is strongly associated with poor survival in pancreatic adenocarcinoma, and pain predicts disease progression in castration-resistant prostate cancer (Ceyhan et al., 2009; Koo et al., 2015). Experimental work has shown that pain at one site

can enhance tumor progression at distant sites (Page et al., 2001). For many cancers, tumor behavior is influenced by the nervous system, and direct communication between nerves and cancer cells can promote tumor growth and metastasis; glioma cells form synapses with neurons (Venkataramani et al., 2019; Venkatesh et al., 2019), and prostate cancer growth/metastasis can be stymied by ablation of neighboring nerves (Ayala et al., 2008; Magnon et al., 2013). Increasingly, it is recognized that molecules involved in pain signaling are also involved in cancer progression, and beyond interactions in the local tumor microenvironment, activation of certain neuronal signaling pathways by the same molecules can also facilitate metastatic cancer progression (Demir et al., 2012; Gasparini et al., 2019). Pain is a common complication of definitive radiotherapy, especially at certain anatomic sites, such as breast, head, and neck. In fact, 70% of patients undergoing curative-intent head and neck irradiation will struggle with treatment-associated pain (Astrup et al., 2015; Trotti et al., 2003) that is poorly responsive to available analgesics (Moslemi et al., 2016); unfortunately, 30-40% of treated patients (especially papillomavirus-negative tumors) will eventually fail local control or develop metastasis, but it is entirely unknown whether RAP might contribute to those oncologic failures (Argiris et al., 2008). Here, we report for the first time that in an experimental animal model of lung metastasis, severe acute orofacial RAP is associated with rapid tumor progression, and that effect can be mitigated via chemical ablation of sensory neurons which transmit noxious (painful) signals.

Our experimentation began with the 4T1-Luc2 model because it is an accessible cell line for which tumor growth is rapid (thus permitting efficient experimental design); additionally, because of stable and strong transfection of the luciferase reporter, and the ability to use a mouse strain with unpigmented skin (the syngeneic host is white BALB/c mice), the resultant lung tumors can reliably be visualized *in vivo* using BLI. The effect that prior tongue irradiation had on

promotion of lung tumor growth after tail vein injection was strong, especially in female mice, and for that reason we utilized this model system for many of the subsequent experiments. Interestingly, tongue irradiation and pain did not affect the growth of B16F10-Luc2 cells in C57BL/6 mice, which suggests that the phenomenon may be tumor type dependent. The apparent tumor-promoting effects of tongue irradiation (and pain) were recapitulated in the MOC2-Luc2 model, where C57BL/6 mice undergoing tail vein injection of tumor cells at the time of maximally severe RAP experienced early lung tumor-attributable deaths; this result is important because it helps to establish the translational relevance of this phenomenon by linking a complication of oral irradiation with altered growth of an oral cancer cell line (Chen et al., 2019; Judd et al., 2012). Nonetheless, it is worth considering that our experiments did not include the assessment of animals with spontaneously occurring tumors. Additionally, our system for studying the effects of local tissue irradiation on distant tumor growth is limited by the fact that the tail vein injection model fails to recapitulate all steps of the metastatic cascade, especially the early processes involving migration of cells away from the primary tumor and into the vasculature (Rashid et al., 2013).

In 1948, Kaplan and Murphy described an apparent increase in the risk of early metastasis amongst patients undergoing radiotherapy for epidermoid carcinomas (Kaplan, 1948). In 1978, Strong and colleagues also reported a correlation between primary tumor irradiation and a higher incidence of metastasis in head and neck cancer patients (Strong et al., 1978). Similar reports exist for cancers of the urinary bladder and uterine cervix (Anderson & Dische, 1981; Fagundes et al., 1992). This has been evaluated in experimental models, and that literature has been reviewed extensively (S. Y. Lee et al., 2017; Vilalta et al., 2016; Von Essen, 1991). However, the science remains unclear; if radiation does promote local or distant metastasis, based on the published reports, this phenomenon seems most likely in the setting of subtherapeutic radiation dosing.

However, firm conclusions cannot be made based upon the existing evidence. Our experiments were designed to address two methodologic concerns of prior research. First, Repasky and colleagues have shown that standard mouse housing temperatures (approximately 20°C) are about 10°C lower than the temperature at which mice expend no excess energy keeping themselves warm or cool (i.e., the thermoneutral temperature), and a consequence is a metabolic stress that directly limits the translational value of standard mouse tumor experiments (Kathleen M Kokolus et al., 2013; Povinelli et al., 2015; Repasky et al., 2013). The current thinking is that this metabolic stress, mediated by beta adrenergic signaling, allows tumor escape from immune surveillance, and thus comes with the risk of exaggerating tumor growth, and treatment effects. Based on this, we expected that repeating our experiments under thermoneutral conditions (approximately 30-31°C) would ameliorate some of the body weight loss that mice otherwise display when experiencing severe glossitis, and that we would also see slower tumor growth kinetics. By contrast, we observed more severe weight loss and behavioral impairments indicative of pain (data not shown), and tumor growth was actually accelerated. Additional experimentation is warranted to verify these unexpected results, and certainly, our work is limited by the fact that while cage temperature was monitored, core body temperature was not. Nonetheless, these results support the idea that our experimental results were not a “false positive” signal as a result of thermal stress caused by standard housing conditions. Second, there is approximately 1.6 Gy of radiation absorbed by the (shielded) body when using our single fraction 27 Gy tongue irradiation protocol. This total body exposure is insufficient to induce oral mucositis, pain behaviors, or significant changes in expression of the ion channels that regulate RAP (Lai et al., 2021). However, while the immune function was not assessed in this study, that amount of radiation dose may be sufficient to alter immune function. For that reason, out-of-field nontarget radiation dose should be considered

whenever studying biology that may be influenced by bystander effects (Mancuso et al., 2008). Our data demonstrate that a 1.6 Gy total body radiation dose exposure does not enhance lung tumor growth in 4T1-Luc2-bearing mice. Interestingly, our data actually show the opposite: mice having undergone 1.6 Gy total body irradiation actually had reduced lung tumor burdens in comparison to sham-irradiated mice. One possible explanation is that the prior exposure of the lungs to low dose radiation may have had anti-inflammatory effects (e.g., reduction of reactive oxygen species and decreased levels of the pro-inflammatory cytokines) that were protective against tumor growth (Rubner et al., 2012).

To establish direct evidence that accelerated lung tumor growth was attributable to pain, rather than some other feature of tongue-irradiation, we sought to demonstrate that this observed effect was reduced when pain was reduced. However, as in humans, orofacial RAP appears difficult to treat in mice; our unpublished data indicate minimal to no benefit from administration of non-steroidal anti-inflammatory drugs (meloxicam, and carprofen), opioids (liposomal formulations of buprenorphine, and hydromorphone), or a combination thereof. As an alternative, we used the ultra-potent TRPV1 agonist, RTX, which is a potent analgesic by virtue of its ability to cause ablation of TRPV1-expressing noci-receptive sensory neurons (Brown et al., 2015; Iadarola & Gonnella, 2013; Iadarola et al., 2018). Additional rationale is derived from the fact that a majority of sensory neurons innervating the tongue express TRPV1 (Wu et al., 2018), and TRPV1 appears to be an important regulator of RAP (Cun-Jin et al., 2019; Lai et al., 2021). Here, we found that a single high-dose of RTX (300 μ g/kg given subcutaneously) led to substantial and lasting ophthalmic desensitization to a TRPV1 agonist (capsaicin), and when given before radiation, led to reductions in both glossitis severity and behavioral measures of RAP (i.e., grooming and nesting). We also found that the provision of RTX abrogated the tumor-promoting

effects of tongue irradiation that we'd previously observed in the 4T1-Luc2 model. Whilst these results support our hypothesis, it is worth considering that RTX was administered systemically. TRPV1 receptors are widely expressed in afferents innervating airways and lungs (Bessac & Jordt, 2008; Rehman et al., 2013; Zhang et al., 2008), which points to the possibility that non-analgesic mechanisms may explain some or all of the effects we measured. While RTX has previously been shown to reduce tumor growth in certain non-painful models of cancer (Farfariello et al., 2014), in the syngeneic 4T1-Luc2 model, it actually appears that RTX accelerates early tumor growth via increased vascular leakage (Bencze et al., 2021). Finally, despite these concerns, here we robustly showed that RTX reduced the growth of pulmonary tumors in both irradiated and non-irradiated mice, demonstrating that reduced activity of TRPV1 neurons can decelerate the growth of tumors at sites distant from where RAP is generated.

In conclusions, this body of research provides experimental evidence suggesting that acute RAP may contribute to an early death by hastening pulmonary metastasis. We demonstrated that both male and female mice develop more lung tumors when 4T1-Luc2 murine breast carcinoma cells are intravenously injected into their syngeneic host at the time of maximally severe tongue RAP. Similarly, MOC2-Luc2 lung tumor-attributable death was hastened when tumor cells were injected at the time of maximally severe RAP. Our experimental data clearly indicate that this accelerated tumor growth was not a result of off-target radiation, nor was it an artifact of the environmental stress caused by standard animal housing temperatures. This points towards tongue tissue irradiation as the cause for accelerated growth of tumors in the lungs, and because lung tumor growth rates are normalized when RAP was reduced via RTX treatment, we conclude that the effect is related to radiation-induced neuronal activation and/or signaling (e.g., pain signaling). Future work should seek to understand whether these effects remain significant when using

clinically-relevant fractionated irradiation schemata, when effective local (site of irradiation) analgesic techniques are employed, and in animals with spontaneously-occurring tumors. It will also be necessary to study this phenomenon in the context of multimodal therapy, which may include systemic antineoplastic chemotherapeutics and/or immunotherapeutics. Finally, it will be important to understand whether in addition to promoting tumor growth at distant (unirradiated) sites, there are also radiation dose-modifying effects of RAP on primary tumor control.

3.5 References

- Adriaenssens, E., Vanhecke, E., Saule, P., Mougel, A., Page, A., Romon, R., Nurcombe, V., Le Bourhis, X., & Hondermarck, H. (2008). Nerve growth factor is a potential therapeutic target in breast cancer. *Cancer Research*, 68(2), 346-351.
- Anderson, P., & Dische, S. (1981). Local tumor control and the subsequent incidence of distant metastatic disease. *International Journal of Radiation Oncology* Biology* Physics*, 7(12), 1645-1648.
- Argiris, A., Karamouzis, M. V., Raben, D., & Ferris, R. L. (2008). Head and neck cancer. *The Lancet*, 371(9625), 1695-1709.
- Astrup, G. L., Rustøen, T., Miaskowski, C., Paul, S. M., & Bjordal, K. (2015). Changes in and predictors of pain characteristics in patients with head and neck cancer undergoing radiotherapy. *Pain*, 156(5), 967-979.
- Ayala, G. E., Dai, H., Powell, M., Li, R., Ding, Y., Wheeler, T. M., Shine, D., Kadmon, D., Thompson, T., & Miles, B. J. (2008). Cancer-related axonogenesis and neurogenesis in prostate cancer. *Clinical Cancer Research*, 14(23), 7593-7603.
- Barton, M., Keane, T., Gadalla, T., & Maki, E. (1992). The effect of treatment time and treatment interruption on tumour control following radical radiotherapy of laryngeal cancer. *Radiotherapy and oncology*, 23(3), 137-143.
- Bencze, N., Schvarcz, C., Kriszta, G., Danics, L., Szőke, É., Balogh, P., Szállási, Á., Hamar, P., Helyes, Z., & Botz, B. (2021). Desensitization of Capsaicin-Sensitive Afferents Accelerates Early Tumor Growth via Increased Vascular Leakage in a Murine Model of Triple Negative Breast Cancer. *Frontiers in Oncology*, 2597.

- Bessac, B. F., & Jordt, S.-E. (2008). Breathtaking TRP channels: TRPA1 and TRPV1 in airway chemosensation and reflex control. *Physiology*.
- Bonner, J. A., Harari, P. M., Giralt, J., Azarnia, N., Shin, D. M., Cohen, R. B., Jones, C. U., Sur, R., Raben, D., & Jassem, J. (2006). Radiotherapy plus cetuximab for squamous-cell carcinoma of the head and neck. *New England Journal of Medicine*, 354(6), 567-578.
- Bonner, J. A., Harari, P. M., Giralt, J., Cohen, R. B., Jones, C. U., Sur, R. K., Raben, D., Baselga, J., Spencer, S. A., & Zhu, J. (2010). Radiotherapy plus cetuximab for locoregionally advanced head and neck cancer: 5-year survival data from a phase 3 randomised trial, and relation between cetuximab-induced rash and survival. *The lancet oncology*, 11(1), 21-28.
- Brown, D. C., Agnello, K., & Iadarola, M. J. (2015). Intrathecal resiniferatoxin in a dog model: efficacy in bone cancer pain. *Pain*, 156(6), 1018-1024.
- Callahan, B. L., Gil, A. S., Levesque, A., & Mogil, J. S. (2008). Modulation of mechanical and thermal nociceptive sensitivity in the laboratory mouse by behavioral state. *The Journal of Pain*, 9(2), 174-184.
- Ceyhan, G. O., Bergmann, F., Kadihasanoglu, M., Altintas, B., Demir, I. E., Hinz, U., Müller, M. W., Giese, T., Büchler, M. W., & Giese, N. A. (2009). Pancreatic neuropathy and neuropathic pain—a comprehensive pathomorphological study of 546 cases. *Gastroenterology*, 136(1), 177-186. e171.
- Chen, M. M., Harris, J. P., Orosco, R. K., Sirjani, D., Hara, W., & Divi, V. (2018). Association of time between surgery and adjuvant therapy with survival in oral cavity cancer. *Otolaryngology–Head and Neck Surgery*, 158(6), 1051-1056.

- Chen, Y.-F., Liu, C.-J., Lin, L.-H., Chou, C.-H., Yeh, L.-Y., Lin, S.-C., & Chang, K.-W. (2019). Establishing of mouse oral carcinoma cell lines derived from transgenic mice and their use as syngeneic tumorigenesis models. *BMC cancer*, 19(1), 1-11.
- Choi, W.-J., Baek, S., Joo, E.-Y., Yoon, S.-H., Kim, E., Hong, B., Hwang, J.-H., & Kim, Y.-K. (2017). Comparison of the effect of spinal anesthesia and general anesthesia on 5-year tumor recurrence rates after transurethral resection of bladder tumors. *Oncotarget*, 8(50), 87667.
- Cun-Jin, S., Jian-Hao, X., Xu, L., Feng-Lun, Z., Jie, P., Ai-Ming, S., Duan-Min, H., Yun-Li, Y., Tong, L., & Yu-Song, Z. (2019). X-ray induces mechanical and heat allodynia in mouse via TRPA1 and TRPV1 activation. *Molecular pain*, 15, 1744806919849201.
- Demir, I. E., Friess, H., & Ceyhan, G. O. (2012). Nerve-cancer interactions in the stromal biology of pancreatic cancer. *Frontiers in physiology*, 3, 97.
- Descamps, S., Lebourhis, X., Delehedde, M., Boilly, B., & Hondermarck, H. (1998). Nerve growth factor is mitogenic for cancerous but not normal human breast epithelial cells. *Journal of Biological Chemistry*, 273(27), 16659-16662.
- Fagundes, H., Perez, C. A., Grigsby, P. W., & Lockett, M. A. (1992). Distant metastases after irradiation alone in carcinoma of the uterine cervix. *International Journal of Radiation Oncology* Biology* Physics*, 24(2), 197-204.
- Farfariello, V., Liberati, S., Morelli, M. B., Tomassoni, D., Santoni, M., Nabissi, M., Giannantoni, A., Santoni, G., & Amantini, C. (2014). Resiniferatoxin induces death of bladder cancer cells associated with mitochondrial dysfunction and reduces tumor growth in a xenograft mouse model. *Chemico-biological interactions*, 224, 128-135.

- Gaskill, B. N., Karas, A. Z., Garner, J. P., & Pritchett-Corning, K. R. (2013). Nest building as an indicator of health and welfare in laboratory mice. *JoVE (Journal of Visualized Experiments)* (82), e51012.
- Gasparini, G., Pellegatta, M., Crippa, S., Schiavo Lena, M., Belfiori, G., Doglioni, C., Taveggia, C., & Falconi, M. (2019). Nerves and pancreatic cancer: new insights into a dangerous relationship. *Cancers*, 11(7), 893.
- Grandis, J. R., & Tweardy, D. J. (1993). Elevated levels of transforming growth factor α and epidermal growth factor receptor messenger RNA are early markers of carcinogenesis in head and neck cancer. *Cancer Research*, 53(15), 3579-3584.
- Ho, A. S., Kim, S., Tighiouart, M., Mita, A., Scher, K. S., Epstein, J. B., Laury, A., Prasad, R., Ali, N., & Patio, C. (2018). Quantitative survival impact of composite treatment delays in head and neck cancer. *Cancer*, 124(15), 3154-3162.
- Hunter, J., Butterworth, J., Perkins, N., Bateson, M., & Richardson, C. (2014). Using body temperature, food and water consumption as biomarkers of disease progression in mice with E μ -myc lymphoma. *British journal of cancer*, 110(4), 928-934.
- Hylander, B. L., & Repasky, E. A. (2016). Thermoneutrality, mice, and cancer: a heated opinion. *Trends in cancer*, 2(4), 166-175.
- Iadarola, M. J., & Gonnella, G. L. (2013). Resiniferatoxin for Pain Treatment: An Interventional Approach to Personalized Pain Medicine. *The open pain journal*, 6, 95-107.
- Iadarola, M. J., Sapio, M. R., Raithel, S. J., Mannes, A. J., & Brown, D. C. (2018). Long-term pain relief in canine osteoarthritis by a single intra-articular injection of resiniferatoxin, a potent TRPV1 agonist. *Pain*, 159(10), 2105-2114.

- Jirkof, P., Fleischmann, T., Cesarovic, N., Rettich, A., Vogel, J., & Arras, M. (2013). Assessment of postsurgical distress and pain in laboratory mice by nest complexity scoring. *Laboratory animals*, 47(3), 153-161.
- Judd, N. P., Allen, C. T., Winkler, A. E., & Uppaluri, R. (2012). Comparative analysis of tumor-infiltrating lymphocytes in a syngeneic mouse model of oral cancer. *Otolaryngology--Head and Neck Surgery*, 147(3), 493-500.
- Kaplan, H. S. (1948). THE EFFECT OF LOCAL ROENTGEN IRRADIATION ON THE BIOLOGICAL BEHAVIOR. *Journal*, 9, 407.
- Kerr, B. J., & David, S. (2007). Pain behaviors after spinal cord contusion injury in two commonly used mouse strains. *Experimental neurology*, 206(2), 240-247.
- Kokolus, K. M., Capitano, M. L., Lee, C.-T., Eng, J. W.-L., Waight, J. D., Hylander, B. L., Sexton, S., Hong, C.-C., Gordon, C. J., & Abrams, S. I. (2013). Baseline tumor growth and immune control in laboratory mice are significantly influenced by subthermoneutral housing temperature. *Proceedings of the National Academy of Sciences*, 110(50), 20176-20181.
- Kokolus, K. M., Capitano, M. L., Lee, C.-T., Eng, J. W. L., Waight, J. D., Hylander, B. L., Sexton, S., Hong, C.-C., Gordon, C. J., Abrams, S. I., & Repasky, E. A. (2013). Baseline tumor growth and immune control in laboratory mice are significantly influenced by subthermoneutral housing temperature. *Proceedings of the National Academy of Sciences*, 110(50), 20176.
- Koo, K. C., Park, S. U., Kim, K. H., Rha, K. H., Hong, S. J., Yang, S. C., & Chung, B. H. (2015). Prognostic impacts of metastatic site and pain on progression to castrate resistance and mortality in patients with metastatic prostate cancer. *Yonsei medical journal*, 56(5), 1206-1212.

- Lai, Y., Bäumer, W., Meneses, C., Roback, D. M., Robertson, J. B., Mishra, S. K., Lascelles, B. D. X., & Nolan, M. W. (2021). Irradiation of the Normal Murine Tongue Causes Upregulation and Activation of Transient Receptor Potential (TRP) Ion Channels. *Radiation research*.
- Lee, E. K., Ahn, H. J., Zo, J. I., Kim, K., Jung, D. M., & Park, J. H. (2017). Paravertebral block does not reduce cancer recurrence, but is related to higher overall survival in lung cancer surgery: a retrospective cohort study. *Anesthesia & Analgesia*, 125(4), 1322-1328.
- Lee, H. S., Ha, A. W., & Kim, W. K. (2012). Effect of resveratrol on the metastasis of 4T1 mouse breast cancer cells in vitro and in vivo. *Nutrition research and practice*, 6(4), 294-300.
- Lee, S. Y., Jeong, E. K., Ju, M. K., Jeon, H. M., Kim, M. Y., Kim, C. H., Park, H. G., Han, S. I., & Kang, H. S. (2017). Induction of metastasis, cancer stem cell phenotype, and oncogenic metabolism in cancer cells by ionizing radiation. *Molecular cancer*, 16(1), 1-25.
- Magnon, C., Hall, S. J., Lin, J., Xue, X., Gerber, L., Freedland, S. J., & Frenette, P. S. (2013). Autonomic nerve development contributes to prostate cancer progression. *Science*, 341(6142).
- Mancuso, M., Pasquali, E., Leonardi, S., Tanori, M., Rebessi, S., Di Majo, V., Pazzaglia, S., Toni, M. P., Pimpinella, M., & Covelli, V. (2008). Oncogenic bystander radiation effects in Patched heterozygous mouse cerebellum. *Proceedings of the National Academy of Sciences*, 105(34), 12445-12450.
- Mazul, A. L., Stepan, K. O., Barrett, T. F., Thorstad, W. L., Massa, S., Adkins, D. R., Daly, M. D., Rich, J. T., Paniello, R. C., & Pipkorn, P. (2020). Duration of radiation therapy is associated with worse survival in head and neck cancer. *Oral Oncology*, 108, 104819.

- Mendoza, A., Gharpure, R., Dennis, J., Webster, J. D., Smedley, J., & Khanna, C. (2013). A novel noninvasive method for evaluating experimental lung metastasis in mice. *Journal of the American Association for Laboratory Animal Science*, 52(5), 584-589.
- Menéndez, L., Juárez, L., García, E., García-Suárez, O., Hidalgo, A., & Baamonde, A. (2006). Analgesic effects of capsazepine and resiniferatoxin on bone cancer pain in mice. *Neuroscience Letters*, 393(1), 70-73.
- Moslemi, D., Nokhandani, A. M., Otaghsaraei, M. T., Moghadamnia, Y., Kazemi, S., & Moghadamnia, A. A. (2016). Management of chemo/radiation-induced oral mucositis in patients with head and neck cancer: A review of the current literature. *Radiotherapy and oncology*, 120(1), 13-20.
- Nagaya, T., Nakamura, Y., Okuyama, S., Ogata, F., Maruoka, Y., Choyke, P. L., Allen, C., & Kobayashi, H. (2017). Syngeneic Mouse Models of Oral Cancer Are Effectively Targeted by Anti-CD44-Based NIR-PIT. *Molecular Cancer Research*, 15(12), 1667-1677.
- Naylor, W., & Mallett, J. (2001). Management of acute radiotherapy induced skin reactions: a literature review. *European Journal of Oncology Nursing*, 5(4), 221-233.
- Negus, S. S., Neddenriep, B., Altarifi, A. A., Carroll, F. I., Leitl, M. D., & Miller, L. L. (2015). Effects of ketoprofen, morphine, and kappa opioids on pain-related depression of nesting in mice. *Pain*, 156(6), 1153.
- Nobumoto, A., Nagahara, K., Oomizu, S., Katoh, S., Nishi, N., Takeshita, K., Niki, T., Tominaga, A., Yamauchi, A., & Hirashima, M. (2008). Galectin-9 suppresses tumor metastasis by blocking adhesion to endothelium and extracellular matrices. *Glycobiology*, 18(9), 735-744.

- Page, G. G., Ben-Eliyahu, S., Yirmiya, R., & Liebeskind, J. C. (1993). Morphine attenuates surgery-induced enhancement of metastatic colonization in rats. *Pain*, 54(1), 21-28.
- Page, G. G., Blakely, W. P., & Ben-Eliyahu, S. (2001). Evidence that postoperative pain is a mediator of the tumor-promoting effects of surgery in rats. *Pain*, 90(1-2), 191-199.
- Povinelli, B. J., Kokolus, K. M., Eng, J. W.-L., Dougher, C. W., Curtin, L., Capitano, M. L., Sailsbury-Ruf, C. T., Repasky, E. A., & Nemeth, M. J. (2015). Standard sub-thermoneutral caging temperature influences radiosensitivity of hematopoietic stem and progenitor cells. *PLoS One*, 10(3), e0120078.
- Rashid, O. M., Nagahashi, M., Ramachandran, S., Dumur, C. I., Schaum, J. C., Yamada, A., Aoyagi, T., Milstien, S., Spiegel, S., & Takabe, K. (2013). Is tail vein injection a relevant breast cancer lung metastasis model? *Journal of thoracic disease*, 5(4), 385.
- Rehman, R., Bhat, Y. A., Panda, L., & Mabalirajan, U. (2013). TRPV1 inhibition attenuates IL-13 mediated asthma features in mice by reducing airway epithelial injury. *International immunopharmacology*, 15(3), 597-605.
- Repasky, E. A., Evans, S. S., & Dewhirst, M. W. (2013). Temperature matters! And why it should matter to tumor immunologists. *Cancer immunology research*, 1(4), 210-216.
- Rubner, Y., Wunderlich, R., Rühle, P.-F., Kulzer, L., Werthmüller, N., Frey, B., Weiss, E.-M., Keilholz, L., Fietkau, R., & Gaipl, U. (2012). How Does Ionizing Irradiation Contribute to the Induction of Anti-Tumor Immunity? [Review]. *Frontiers in Oncology*, 2(75).
- Russo, G., Haddad, R., Posner, M., & Machtay, M. (2008). Radiation treatment breaks and ulcerative mucositis in head and neck cancer. *The Oncologist*, 13(8), 886-898.
- Schmidt-Ullrich, R., Mikkelsen, R., Dent, P. e., Todd, D., Valerie, K., Kavanagh, B., Contessa, J., Rorrer, W., & Chen, P. (1997). Radiation-induced proliferation of the human A431

- squamous carcinoma cells is dependent on EGFR tyrosine phosphorylation. *Oncogene*, 15(10), 1191-1197.
- Scully, C., Epstein, J., & Sonis, S. (2003). Oral mucositis: a challenging complication of radiotherapy, chemotherapy, and radiochemotherapy: part 1, pathogenesis and prophylaxis of mucositis. *Head & Neck: Journal for the Sciences and Specialties of the Head and Neck*, 25(12), 1057-1070.
- Strong, M. S., Vaughan, C. W., Kayne, H. L., Aral, I. M., Ucmakli, A., Feldman, M., & Healy, G. B. (1978). A randomized trial of preoperative radiotherapy in cancer of the oropharynx and hypopharynx. *The American Journal of Surgery*, 136(4), 494-500.
- Suwinski, R., Sowa, A., Rutkowski, T., Wydmanski, J., Tarnawski, R., & Maciejewski, B. (2003). Time factor in postoperative radiotherapy: a multivariate locoregional control analysis in 868 patients. *International Journal of Radiation Oncology* Biology* Physics*, 56(2), 399-412.
- Trotti, A., Bellm, L. A., Epstein, J. B., Frame, D., Fuchs, H. J., Gwede, C. K., Komaroff, E., Nalysnyk, L., & Zilberberg, M. D. (2003). Mucositis incidence, severity and associated outcomes in patients with head and neck cancer receiving radiotherapy with or without chemotherapy: a systematic literature review. *Radiotherapy and oncology*, 66(3), 253-262.
- Usoskin, D., Furlan, A., Islam, S., Abdo, H., Lönnerberg, P., Lou, D., Hjerling-Leffler, J., Haeggström, J., Kharchenko, O., & Kharchenko, P. V. (2015). Unbiased classification of sensory neuron types by large-scale single-cell RNA sequencing. *Nature neuroscience*, 18(1), 145-153.

- Venkataramani, V., Tanev, D. I., Strahle, C., Studier-Fischer, A., Fankhauser, L., Kessler, T., Körber, C., Kardorff, M., Ratliff, M., & Xie, R. (2019). Glutamatergic synaptic input to glioma cells drives brain tumour progression. *Nature*, *573*(7775), 532-538.
- Venkatesh, H. S., Morishita, W., Geraghty, A. C., Silverbush, D., Gillespie, S. M., Arzt, M., Tam, L. T., Espenel, C., Ponnuswami, A., & Ni, L. (2019). Electrical and synaptic integration of glioma into neural circuits. *Nature*, *573*(7775), 539-545.
- Vera-Llonch, M., Oster, G., Hagiwara, M., & Sonis, S. (2006). Oral mucositis in patients undergoing radiation treatment for head and neck carcinoma: risk factors and clinical consequences. *Cancer: Interdisciplinary International Journal of the American Cancer Society*, *106*(2), 329-336.
- Vilalta, M., Rafat, M., & Graves, E. E. (2016). Effects of radiation on metastasis and tumor cell migration. *Cellular and Molecular Life Sciences*, *73*(16), 2999-3007.
- Von Essen, C. (1991). Radiation enhancement of metastasis: a review. *Clinical & experimental metastasis*, *9*(2), 77-104.
- Wong, P. C., Dodd, M. J., Miaskowski, C., Paul, S. M., Bank, K. A., Shiba, G. H., & Facione, N. (2006). Mucositis pain induced by radiation therapy: prevalence, severity, and use of self-care behaviors. *Journal of pain and symptom management*, *32*(1), 27-37.
- Wu, P., Arris, D., Grayson, M., Hung, C.-N., & Ruparel, S. (2018). Characterization of sensory neuronal subtypes innervating mouse tongue. *PLoS One*, *13*(11), e0207069.
- Zhang, G., Lin, R. L., Wiggers, M., Snow, D. M., & Lee, L. Y. (2008). Altered expression of TRPV1 and sensitivity to capsaicin in pulmonary myelinated afferents following chronic airway inflammation in the rat. *The Journal of physiology*, *586*(23), 5771-5786.

3.6 Supplementary Material

3.6.1 Cell lines preparation and protocol optimization

Bright field microscopy (Micromaster II Microscope, Fisher Scientific) was performed to assess *in vitro* cell morphology, phenotype, and growth kinetics. 4T1 and MOC2 cell lines were engineered to constitutively express Firefly Luciferase-2 (Luc2) under a CMV promoter with zeocin resistance (500 ug/mL), whereas a dual labeled luciferase and GFP-expressing B16F10 Red F-Luc2 was used in our melanoma model. The ability to express luciferase genes and cell's tumorigenicity were characterized *in vitro* and *in vivo*, respectively, through bioluminescence imaging (IVIS Lumina II *in vivo* imaging system, PerkinElmer Ltd., Waltham, MA, USA). Sterility testing and pathogen screening (IMPACT™ IV polymerase chain reaction (PCR) evaluation) were performed to assess for contamination; PCR results were negative for all assessed pathogens (MHV, MPV, MVM, Mycoplasma pulmonis, Mycoplasma sp., PVM, Sendai, and TMEV).

In previous pilot studies, we established three murine lung tumor models by intravenously injecting 4T1-Luc2, B16F10-Luc2 or MOC2-Luc2 cell lines into either BALB/c or C57BL/6 mice, monitoring cancer progression *in vivo* and *ex vivo*. Mice either received a single high-dose of lingual irradiation (27 Gy) or sham irradiation (0 Gy). All tumor cell lines were inoculated 11 days after irradiation (peak of glossitis severity). Two pilot studies of 8 mice each determined optimal dosage of 4T1-Luc2 cells, as well as injection route, *in vivo* imaging protocol, *ex vivo* lung staining technique and quantification of lung's tumor burden. Dose was defined based on published information for that tumor model (H. S. Lee et al., 2012): 2×10^5 4T1-Luc2 cells/mouse suspended in 0.1 mL of sterile PBS were injected intravenously (sterile 26-gauge needle) into female BALB/c mice. Tumor growth was monitored *in vivo* using bioluminescence imaging (BLI) by taking

images at days 7, 14, 17, 19 and 21 post-injections. The first pilot evaluated a retro-orbital injection approach, showing a progressive growth of pulmonary tumors (expressed as transthoracic BLI total/flux signal) within the first week after injections, starting at day 17 post-IR. A comparable tumor-burden difference was found between both groups at day 21 post-IR. At this time point, mice started to develop signs of body weight loss and respiratory disease (pulmonary assessment of advanced metastasis (PAAM) technique) (Mendoza et al., 2013). Mice were euthanized on day 21 post-IR, and lungs were removed. An *ex vivo* tumor burden evaluation was performed by counting the number of nodules that were visible on the lung's surface. Here we established that 3 mL of 15% ink solution (diluted with PBS) and later fixation of lungs using a formalin-based solution (Fekete's solution) was sufficient to highlight these growths within all lung's lobes (white nodules on a black background). Exophthalmia, as a result of local tumor growth after injections, was a common challenge in this pilot. A second pilot assessed the tail vein injection (TVI) approach. Similarly, lung tumor growth initiated in all mice at day 17 post-IR (6 days post-injection), and differences between groups were significant at day 21 post-IR (*in vivo* BLI analysis). There were no major complications, and we therefore decided to select the TVI approach for subsequent experiments. For the B16F10-Luc2 and MOC2-Luc2 models, two consecutive pilots (n = 8/each) for each model were performed to determine optimal dosage, injection route, *in vivo* imaging protocol, *ex vivo* lung staining technique and quantification of lung tumor burden. Briefly, mice were inoculated 11 days after irradiation via tail vein injections with either B16F10-Luc2 (2×10^5 cells/mouse suspended in 0.1 mL of sterile PBS) or MOC2-Luc2 cells (1×10^6 cells/mouse suspended in 0.2 mL of sterile PBS). Inoculation doses were established from previous work (Nagaya et al., 2017; Nobumoto et al., 2008). We first observed lung bioluminescence in the B16F10-Luc2 and MOC2-Luc2 injected mice at day 25 and 19 post-IR, respectively. At

euthanasia, visible tumor nodules were found in the lungs of most mice. Only MOC2-Luc2 cells were stained with India ink (as above) and de-stained with Fekete's solution. B16F10-Luc2 cells did not require staining because their melanin pigmentation allowed easy visualization on unstained lungs; therefore, lungs were inflated using Fekete's solution, and later stored in the same solution.

3.6.2 Assessment of radiation associated mucositis and pain

Observations in previous experiments (unpublished) indicated that normal laboratory rodent behaviors, such as nesting and grooming, were perturbed in mice that had been irradiated and developed RIM/RAP. Both activities are highly dependent on mouth and tongue function (i.e., to shred the material or licking the forepaws, respectively), therefore, we decided to use assessments of how well these activities were performed as markers of pain. To our knowledge, no prior work has evaluated nesting and grooming behaviors in the context of oral pain in mice, therefore, we adapted published protocols (Callahan et al., 2008; Gaskill et al., 2013; Jirkof et al., 2013; Kerr & David, 2007; Negus et al., 2015). Briefly, mice were transferred to individual testing cages containing one commercially available cotton fiber nestlet (5 cm x 5 cm, 5 mm thick, approximately 2.5 g each), food and water. After 12 hours (dark cycle), nesting (i.e., building activity) and grooming (i.e., physical appearance evaluation) activities were evaluated by a trained, unblinded evaluators using a predefined scoring system. Briefly, nesting activity was measured using a 3-point scale: 0 (zero) – Most of the nestlet has been completely torn into small pieces; pieces arranged together into one area of the cage; 1 – Incomplete shredding of the nestlet; large pieces may remain and may remain scattered around the cage (not all arranged together); and 2 – nestlet was not noticeably touched. Self-grooming behavior was categorized using a 4-point scale: 0 (zero) – Clean, smooth haircoat; 1 – Fur on body begins to look messy, but face remains normal;

2 – Face and body look messy, with hair “standing on end”; and 3 – Disheveled; wet/greasy appearance, possible discoloration of coat, erythema (reddened skin), and areas of hair loss (alopecia).

Additional comments: The scoring system used here slightly differ from the one described in Chapter 2. The categorization used here was developed before the completion of Chapter 2.

3.6.3 Modulation of ambient temperature

A series of pilot experiments were performed to determine how to modify housing temperature conditions of adult mice to create cage floor temperatures of 30 to 31°C (previously associated with thermoneutrality in mice;(Repasky et al., 2013). First, we determined the temperatures of standard mouse cages without animals. We measured the floor temperature of 20 standard mouse cages using a 4-channel rapid read thermometer (General Tools DT4947SD thermocouple thermometer). All cages were kept inside our mouse colony at standard room temperature (21-22°C), placed on steel shelving units, and filled with a normal amount of bedding and no mouse behavioral enrichment material. Five cage floor “zones” were assessed: the center, and each of the four corners. Temperature was recorded three times a day (8:00 A.M., 2:00 P.M., and 6:00 P.M.), each day for a week. In general, all zones were a similar temperature, ranging from 21.5°C to 22.7°C, with an average of 22.1°C (SD = 0.27). No differences were found between the different times of the day, nor between days. Then we measured temperatures of all zones in a single cage with bedding containing adult CD-1 mice (n = 4/cage). After an hour with mice in the cage, temperatures ranged from 22.4°C to 24.5°C, with an average of 23.5°C (SD = 0.87). In a separate experiment, we measured temperatures of 4 cages (bedding only; no animals) placed atop a 10-inch x 20.5-inch heat mat (iPower Seed Starter Heat Mat) with the thermostat set at 25.6°C. After 90 minutes, zone temperatures ranged from 29°C to 32°C, with an average of 30.5°C (SD =

3.5). Ninety minutes after adding 4 CD-1 adult mice to each cage, we found that temperatures ranged from 29.5 °C to 32.5 °C, with an average of 31°C (SD = 2.3). Body temperature of the mice was not measured.

Afterword

As mentioned before, one of the main goals of this dissertation was to study the tumor-promoting effects of RAP using a mouse model of oral squamous cell carcinoma (i.e., MOC2-Luc2 model). During the conduction of the current study, we had difficulty assessing tumor burden in C57BL/6 mice using BLI imaging, thus, we used survival as a surrogate of tumor progression for the MOC2-Luc2 model. The obvious next step for this model was to mitigate RAP and reassess survival using the same methods mentioned above. Because we have historically obtained more consistent results using the 4T1-Luc2 model (BALB/c mice), we first assessed changes in tumor progression after RAP was alleviated using RTX in this strain. The encouraging results obtained from the 4T1-Luc2 motivated us to repeat this experiment in C57BL/6 mice, and assess survival in MOC2-Luc2 bearing mice injected with RTX using the same experimental approach as we used in BALB/c mice (i.e., 300 µg/kg). However, when the same dose of RTX was administered to C57BL/6 mice obtained from the same supplier (i.e., Charles River Laboratories), unacceptable toxicity was observed. Specifically, one mouse died very quickly after injection (within minutes) of apparent respiratory arrest while still under anesthesia, while others never fully recovered from anesthesia and died within the first 6 hours after injection (8 of 40 mice). Mice that didn't die within the first hours post-injection, displayed severe ataxia after recovering full conscienceless (post-anesthesia); in some of those animals, ataxia progressed to severe depression and coma, and eventually died (2 of 40) or were euthanized (3 of 40). In total, 13 mice died as a consequence of RTX (32.5% mortality). Mice that survived made a full recovery approximately 10 days after injection, and RTX produced in these mice a good degree of ablation (in comparison to control excipient mice, 9 versus 62 wipes/minute; no baseline measurements were conducted). Body weight loss ranged from 10 to 15% within the first 48-72 hours after injection, and improved

(baseline values) by 5 to 10 days post injection. Due to the presence of these unintended side effects after injecting 300 µg/kg of RTX in C57BL/6 mice, we cancelled the experiment that was designed to study how tumor growth (MOC2-Luc2 model) is impacted by RTX-induced neuronal ablation. On the next chapter (Chapter 4), we describe our process for RTX dose optimization, including both a description of the observed tolerability and ablative efficacy of various protocols tested in C57BL/6 mice.

**Chapter 4: “Systemic Administration of Resiniferatoxin in C57BL/6 Mice:
Troubleshooting Unexpected Morbidity and Mortality.”**

4.1 Introduction

The transient receptor potential vanilloid subtype 1 (TRPV1) is a well-characterized non-selective cation channel primarily found in the C and A δ sensory fibers arising from the dorsal root and trigeminal ganglia (Caterina & Julius, 2001; Ma, 2002; Tominaga et al., 1998). TRPV1-expressing neurons constitute approximately 30-50% of all somatosensory neurons within the rodent sensory ganglia, acting as important sensors for noxious stimuli such as heat, acidic pH, mechanical pressure, and irritant vanilloids (e.g., capsaicin) (Caterina & Park, 2006; Chung et al., 2008; Kobayashi et al., 2005; Tominaga et al., 1998). An increasing number of studies have shown that the polymodal transducer TRPV1 plays a pivotal role in the transmission and modulation of nociceptive information, making this channel a compelling molecular target candidate for the development of non-opioid-based therapeutic alternatives for the management of difficult-to-treat pain, such as orofacial pain in patients undergoing radiotherapy (Caterina & Park, 2006; Cui et al., 2016; Eriksson et al., 2005; Masumoto et al., 2013; Neubert et al., 2008; Nishino et al., 2016; Price et al., 2021). When TRPV1 ion channels are activated, a substantial influx of extracellular sodium and calcium ions into the nerve terminal is triggered, causing neuronal excitation and subsequent generation and propagation of action potentials along axons. These events will initiate the cycle of inter-neuronal, synaptic communication between the peripheral and central nervous systems, resulting in the perception of acute pain (Julius, 2013). Remarkably, this initial and acute neuronal excitation can be followed by the desensitization (reduction in channel activity) or ablation (degeneration of nerve fibers and eventual death) of sensory nerve fibers when an excessive calcium ions influx occurs as a result of prolonged or repetitive exposures to TRPV1 agonists, like capsaicin, which provides pain relief (Caterina & Park, 2006; Choi et al., 2016; Mitchell et al., 2010; Yang & Zheng, 2017).

Resiniferatoxin (RTX), a highly potent irritant and inflammatory compound found in some plants of the genus *Euphorbia*, is a naturally occurring capsaicin analog (Szallasi & Blumberg, 1989). Relative to capsaicin, RTX is a more selective and ultra-potent agonist of TRPV1 channels (Brederson et al., 2013; Brown et al., 2005; Kissin & Szallasi, 2011; Payne et al., 2005). In preclinical research, RTX has been widely used in *in vivo* studies as a tool to desensitize or ablate TRPV1-expressing neurons, attenuating inflammatory, neuropathic, postoperative incisional, articular, and bone cancer pain, without causing unacceptable systemic side effects (Kissin et al., 2005; Lee et al., 2012; Menéndez et al., 2006; Neubert et al., 2008; Raithel et al., 2018). In rodents, RTX can be administered by various doses and routes to produce long-lasting local ablation of TRPV1-expressing neurons (up to 10 weeks), and thereby, induce analgesia without affecting proprioception and motor function (Karai et al., 2004; Mitchell et al., 2010). In general, systemic RTX is used in mice at doses ranging from 10 to 300 $\mu\text{g}/\text{kg}$ (Menéndez et al., 2006). However, doses higher than 30 $\mu\text{g}/\text{kg}$ are commonly administered in escalating schemes, such as 30 $\mu\text{g}/\text{kg}$ given on day 1, 70 $\mu\text{g}/\text{kg}$ on day 2, and 100 $\mu\text{g}/\text{kg}$ on day 3 (Elekes et al., 2007; Wang et al., 2015). Some of the routes described in small laboratory animals are systemic (subcutaneous), intrathecal, intraarticular, epidural, perineural, and or direct application to peripheral nerve endings (Bishnoi et al., 2011; Caterina & Julius, 2001; Kissin et al., 2005; Lee et al., 2012; Neubert et al., 2008; Suzuki et al., 2009).

In our laboratory, we have used RTX as a tool to palliate the pain that accompanies oral mucositis as a result of lingual irradiation in 10-week-old female BALB/c mice (NCrl substrain) purchased from Charles River Laboratories (CRL). Using a single systemic administration of RTX at a dose of 300 $\mu\text{g}/\text{kg}$, effective ablation occurred (as evidenced by a loss of capsaicin-induced eye wiping responses). Furthermore, RTX was well-tolerated; specifically, we saw mild signs of

ataxia and depression which quickly resolved within the first 12 hours post-administration, and no mortality was associated with this dose. This approach appeared to significantly mitigate orofacial pain when mice were experiencing severe radiation-induced oral mucositis (see Chapter 2). However, when the same dose of RTX was administered to sex and age-matched C57BL/6 mice obtained from the same supplier (NCrI substrain), adequate ablation was produced but unacceptable toxicity was observed (i.e., mortality of 32.5%; see Chapter 3 (“Afterword” section)). This mortality was unexpected, especially when considering that there are no reports in the literature describing this effect. Given the value of RTX as a research tool and the extensive use of C57BL/6 mice in pain research, we wanted to determine whether there is an RTX dosing regimen that would be well-tolerated in this mouse strain, but also effective in ablating TRPV1-expressing neurons. The purpose of this chapter is to describe our process for RTX dose optimization, including a description of the observed tolerability and ablative efficacy of various protocols tested in different substrains of C57BL/6 mice.

4.2 Material and Methods

We performed work to understand the tolerability (i.e., side effects and mortality) and efficacy of RTX-mediated ablation of TRPV1-expressing neurons in adult C57BL/6 mice. Experimental conditions (i.e., age, sex, vendor/genetic background) and RTX dose varied across experiments in a prospective and stepwise fashion manner based on the severity of adverse events and ablation success. All experimental procedures were approved by the North Carolina State University (NCSU) Institutional Animal Care and Use Committee (protocol #: 19-810-B). Experiments conducted in this study represented collaborative work between the author and other members of our laboratory.

4.2.1 Overall experimental rationale and scheme

Given the adverse effects encountered in past work when 300 $\mu\text{g}/\text{kg}$ RTX was administered in C57BL/6 mice from CRL (NCrI substrain, herein referred as “B6/NCrI”), we decided to repeat this experiment in a new cohort and split the applied dose into three consecutive, increasing doses (i.e., 50 $\mu\text{g}/\text{kg}$ on day 1, then 100 $\mu\text{g}/\text{kg}$ on day 2, and 150 $\mu\text{g}/\text{kg}$ on day 3) in sex and age-matched B6/NCrI mice obtained from the same supplier. In this first experiment, unacceptable toxicity was associated with 50 $\mu\text{g}/\text{kg}$ RTX (given once) within the first 12 hours post-RTX administration (i.e., 70% mortality), therefore, we canceled the remaining dose administrations and ended the experiment. For the next experiment, we requested older mice based on the idea that younger mice might be more sensitive than adults to neurotoxins like RTX. Here we chose a vendor that could deliver mice as fast as possible (time limitations related to the COVID-19 pandemic); therefore, 14-week-old female C57BL/6J substrain mice were purchased from Jackson Laboratories (JAX), herein referred as “B6/J”. In this experiment, we decided to shift our approach and evaluate the tolerability and ablative effectivity of RTX using substantially lower and higher dosages. Mice here either received 2 $\mu\text{g}/\text{kg}$ RTX (dose that one would expect fewer associated systemic side effects) or 600 $\mu\text{g}/\text{kg}$ RTX (dose that one would expect to cause a profound sensory nerve desensitization/block). The total dose of 2 $\mu\text{g}/\text{kg}$ RTX was associated with high tolerability (0% mortality) but low ablative effectivity, while 600 $\mu\text{g}/\text{kg}$ RTX was associated with high ablative effectivity but low tolerability (62.5% mortality within the first 56 hours post-RTX administration). Thus, in a separate experiment, we tested the effects of an intermediated dose (i.e., 10 $\mu\text{g}/\text{kg}$), which was expected to avoid the potential side effects of RTX and to improve the success of ablation. To facilitate data comparison, here we used 16-weeks old B6/J mice. Sex and age-matched mice obtained from the same supplier (also same genetic background) were injected

with 300 µg/kg RTX for comparison purposes. In this experiment, none of the mice injected with either 10 or 300 µg/kg RTX died (0% mortality), and neuronal ablation was sufficient for both applied dosages. Because 10 µg/kg RTX demonstrated to be the most tolerable way to approach systemic ablation of TRPV1-expressing neurons in B6/J mice, we decided to repeat this experiment using a larger sample size in B6/NCrl mice at 11 weeks of age. We selected this substrain and age because we commonly use in our laboratory 10- to 14-weeks-old B6/NCrl mice to model radiation-associated mucositis pain. Unfortunately, and while adequate ablative efficacy was encountered, there was low tolerability (60.8% mortality within the first 48 hours post-RTX administration). In reviewing animal records and results, we noticed a trend wherein B6/J mice seemed to tolerate RTX better than B6/NCrl mice. To determine whether the excess morbidity/mortality found in B6/NCrl was related to the vendor (and potentially related to differences in genetic backgrounds), a final experiment was performed. Here, we decided to evaluate the tolerability and ablation efficacy of 10 µg/kg RTX in female and male B6/J mice (13-week-old). Details about experimental conditions and applied RTX dose of each cohort is presented in Table 4.1.

Table 4.1: Details about experimental conditions, applied RTX dose, and mortality rate of each experiment and cohort.

| Experiment number | Strain | Sex | Age at injection (weeks) | Mouse vendor | Cohort(s)/ experiment | RTX dose ($\mu\text{g}/\text{kg}$) | Total sample size | Total sample size per cohort | Dose scheme | Follow-up duration (days) | Mortality (%) |
|-------------------|--------------|--------------------------|--------------------------|--------------|-----------------------|--------------------------------------|-------------------|------------------------------|--|---------------------------|---------------------|
| 1 | C57BL/6 NCrI | Female | 10 | CHL | 1 | 50 | 10 | N/A | Single dose | 10 | 70 |
| 2 | C57BL/6J | Female | 14 | JAX | 2 | 2.a) 2 2.b) 600 | 12 | 2.a) 4 mice 2.b) 8 mice | 2.a) 1 $\mu\text{g}/\text{kg}$ every 24 hrs. 2.b) Single dose | 3 | 2.a) 0 2.b) 62.5 |
| 3 | C57BL/6J | Female | 16 | JAX | 2 | 3.a) 10 3.b) 300 | 12 | 3.a) 8 mice 3.b) 4 mice | Single dose | 42 | 0 (both cohorts) |
| 4 | C57BL/6 NCrI | Female | 11 | CHL | 1 | 10 | 46 | N/A | Single dose | 3 | 60.8 |
| 5 | C57BL/6J | 5.a) Female 5.b) Male | 13 | JAX | 2 | 10 | 16 | 5.a) 8 mice 5.b) 8 mice | Single dose | 126 | 5.a) 0 5.b) 12.5 |

4.2.2 Animals

A total of 96 adult C57BL/6 mice were purchased from either CRL (B6/NCrl substrain) or JAX (B6/J substrain). Upon arrival, animals were quarantined for 72 hours and then acclimated to the colony room for at least

4.2.3 RTX administration

We used a pharmaceutical-grade formulation of RTX (200 µg/mL) that was kindly provided by Dr. Alexis Nahama from Sorrento Therapeutics. RTX doses were drawn up into a syringe in a fume hood and kept on ice until administration. Briefly, mice were anesthetized with isoflurane (2%, flow rate of 3-4 L/minute) using an induction box (anesthesia induction) and mask with a custom-built non-rebreathing circuit (anesthesia maintenance). Shortly after mice exhibited unconsciousness, the skin of the interscapular region was gently grasped and lifted using silicone coated soft forceps, and RTX was subcutaneously injected using a 30-gauge needle on a low dead space insulin syringe (volumes ranging from 5 to 30 µL). After systemic administration, mice were kept under anesthesia for 1 minute and then recovered in prewarmed standard (non-ventilated) mouse cages containing disposable multi-layered pads and bedding. Warming of the cages was done using a 10" x 20.5" heat mat (iPower Seed Starter Heat Mat, iPower Products, purchased from Amazon) that was placed underneath the mouse cages (thermostat was set to 80°F).

4.2.4 Animal monitoring

Mice were first examined hourly and then daily after RTX administration for signs of pain or distress (i.e., abnormal posture, twitching or trembling), nervous system dysfunction (i.e., depression/lethargy, ataxia, seizures, or coma), respiratory system dysfunction (i.e., changes in respiration patterns), weight loss, and/or spontaneous death. Measurement of body weight

(expressed as percentage change from baseline) acted as a surrogate marker of overall health; based on our experience working with this mouse strain, body weight reduction was considered either mild (<5%), moderate (6 to 15%), or severe (>15%) in this study. Complications were documented, and mice received routine medical management appropriate for the presenting symptoms (e.g., warming pads for hypothermia, eye lubricants to prevent corneal ulcers associated with prolonged anesthesia recoveries, warm physiologic saline for dehydration). Criteria for euthanasia included: weight loss exceeding 30%, long-lasting inability to ambulate well enough to reach food and/or water (longer than 72 hours post-RTX administration), or severe dyspnea (i.e., struggling to breath). Euthanasia was performed using asphyxiation (3.5 L/minute CO₂ chamber), followed by cervical dislocation. The follow-up period differed between experiments (based on mortality) but ranged from 3 to 126 days after RTX administration.

4.2.5 Assessment of RTX-mediated ablation of TRPV1-expressing neurons

To confirm successful systemic ablation of TRPV1-expressing neurons, we topically applied capsaicin (Sigma-Aldrich, MO, USA) into the left eye as described elsewhere (Takahashi et al., 2016); for this technique, capsaicin was diluted using 0.9% sterile saline (concentration: 0.01%; volume: 15 μ L; solution temperature: 68-72°F). Responses were video recorded and later reviewed by a blinded observer who counted and recorded the number of facial wipes over 1 minute immediately following ocular application of capsaicin. A reduction in the number of wipes per minute from baseline measures higher than 50% constituted a sufficient ablation; the rationale behind this criterion was determined based on the reduction observed in BALB/c mice when RTX was provided (reduction in wipes above 50% highly correlated with a significant reduction in pain-like behaviors). Baseline measures were obtained before RTX administration in all experiments for comparison purposes.

4.2.6 Post-mortem assessment

Post-mortem assessment (either gross or microscopic necropsy examination) was carried out in select animals (see later). Post-mortem evaluation was predominately focused on the following structures: lungs, heart, thymus, trigeminal ganglions (TG), spinal cord, and brain. The aforementioned tissues were harvested after gross necropsy examination. Collected tissues were fixed in 10% neutral buffered formalin for 24 hours, and then processed by routine methods and embedded in paraffin at the NCSU Veterinary Histopathology Laboratory. Horizontally-oriented sections (~5 μm) were stained with hematoxylin and eosin (H&E) and evaluated by a veterinary anatomic pathologist, board-certified by the American College of Veterinary Pathologists (Dr. Debra Tokarz).

4.2.7 Calcium imaging

TG neurons samples were collected from select animals (see later) immediately after euthanasia and digested in collagenase and dispase (Sigma-Aldrich, MO, USA) in Hanks' Balanced Salt Solution (HBSS, NY, USA) at ~30°F. Isolated cells were resuspended in 25 μL Dulbecco's Modified Eagle Medium (DMEM, Gibco, Paisley, UK), placed onto an 18 mm coverslip coated with poly-L-lysine and laminin. Neurons were then incubated in 1 mL complete media that contained DMEM medium with 10% fetal bovine serum (FBS, heat-inactivated) and 2% Pen Strep (Gibco BRL Products, NY, USA) at room temperature with 5% CO₂. All calcium imaging procedures were performed 12 hours after plating the neurons. Briefly, neurons were incubated with Fura-2AM (Biotium, CA, USA) in complete media for 30 minutes before imaging. The coverslip was held by a Quick Release Magnetic Imaging Chamber (Warner Instruments, CT, USA) and cells were visualized using an inverted microscope (Nikon Eclipse TE200 microscope, Nikon Instruments Inc., NY, USA). Locke solution (kept at room temperature) flowed through the

chamber continuously and perfused the coverslip during imaging. Fura-2AM was used as an indicator of changes in intracellular calcium concentrations using ratiometric measurement of fluorescent intensity at 340 and 380 nm wavelength (340/380 nm). TG neurons were manually circled (identification was based on morphology and size; diameter of ~50 μm) using NIS-Elements AR software (version 5.02.01, Nikon Instruments Inc, NY, USA). Neurons were stimulated using capsaicin (1 $\mu\text{mol/L}$, Sigma-Aldrich, MO, USA) and potassium chloride (KCl, 150 mmol/L, Fisher Scientific, NH, USA), with at least 1-minute interval between stimulations. A positive response was defined as a neuron that had a maximum 340/380 nm ratio greater than 110% of the baseline (pre-stimulation) 340/380 nm ratio; responses lower than 110% were defined as unresponsive (negative). Only cells that positively responded to KCl were included in the analysis. Results were expressed as the proportion (in percentage) of neurons that had a positive response to capsaicin stimulation.

4.2.8 Cellular immunofluorescence staining

After calcium imaging, TG neurons on the coverslips were immediately fixed using 4% neutral buffered formalin (for 10 minutes), then washed with phosphate-buffered saline (PBS). The coverslips were incubated in blocking solution (5% goat serum and 0.05% Triton-X 100 in PBS) for 1 hour at room temperature. TRPV1 expression was detected by applying a primary antibody at 39.2°F overnight (mouse anti-mouse, 1:1000; Abcam, MA, USA). The coverslips were washed with PBS 3 times followed by incubation with secondary antibody (Alexaflour 594 conjugated goat anti-mouse, 1:1000, for TRPV1) for 1 hour at room temperature. The coverslips were then washed with PBS 3 times, mounted using ProLong Gold antifade reagent with DAPI (Invitrogen, OR, USA), and then incubated overnight at room temperature. Images were acquired by inverted microscopy (Nikon TE200, Nikon Instruments Inc, NY, USA), and neurons were

manually contoured using ImageJ software (US National Institutes of Health, USA). Positively TRPV1-stained neurons in TG samples were quantified as a percent of all DAPI-stained cells.

4.2.9 Statistical analysis

Descriptive statistics were computed using mean, standard deviation (SD), range, and proportion (i.e., number or percentage of either animals/total or neurons/total). All statistical tests were performed using commercial software (Prism version 6, GraphPad Software, Inc., La Jolla, CA).

4.3 Results

4.3.1 Experiment 1

Initially, we planned to evaluate the tolerability and ablative efficacy of 300 µg/kg RTX using 3 consecutive (once daily) increasing doses (50, 100, and 150 µg/kg) in 10-week-old female B6/NCrl mice. However, unexpected increased mortality (as compared to past work) was found after applying 50 µg/kg RTX. Specifically, all mice (n = 10) showed severe ataxic gait followed by depression within the first hour after 50 µg/kg RTX was administered. However, 7 mice (7/10) developed lethargy (lateral recumbency), increased respiratory rate, and unresponsiveness to touch (loss of pinch reflex) within the next 6 hours. Among these 7 mice, all died within the first 12 hours post-RTX. Only 3 mice (3/10) survived the first 24 hours post-RTX. Therefore, a mortality of 70% was found in this experiment; no further RTX doses were administered in these mice. In the surviving mice (3/10), signs of ataxic gait and depression persisted for the first 6 days post-RTX. In these mice, overall weight loss was severe within the first 3 days post-RTX (overall mean reduction + SD: -16.2 + 4.0%, range: -24 to -11%), and persisted until day 6 post-RTX (Figure

4.1A). On this day (day 6), mice started to present signs of improvement in their activity levels, appetite, and ataxic gait, returning to normal mouse behavior at day 8 post-RTX. On day 6 post-RTX, we assessed the ablative efficacy of 50 $\mu\text{g}/\text{kg}$ RTX. As shown in Figure 4.1B, an insufficient neuronal ablation was found in all 3 mice (i.e., overall reduction less than 40% from baseline). Therefore, mice were euthanized the next day. A gross necropsy was performed 12 to 24 hours after death in all mice, however, no gross lesions were seen in the lungs, heart, thymus, trigeminal ganglions, spinal cord, or brain.

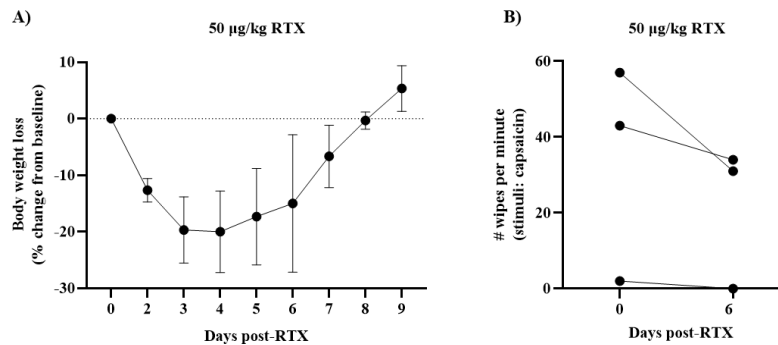


Figure 4.1: Systemic administration of RTX at a dose of 50 $\mu\text{g}/\text{kg}$ (given once) in 10-week-old female C57BL/6NCrl mice (n = 10). (A) Overall body weight loss was severe within the first 3 days post-RTX (n = 3); mice returned to baseline values by day 8 post-RTX. (B) Neuronal ablation was considered insufficient (i.e., overall reduction less than 40% from baseline) in the surviving mice (n = 3). Data expressed as mean + SD.

4.3.2 Experiment 2

Since 50 $\mu\text{g}/\text{kg}$ caused an even higher mortality rate than 300 $\mu\text{g}/\text{kg}$, we used in this next experiment either a substantially lower or higher RTX dose in B6/J mice (16-weeks old, female). RTX at a dose of 2 $\mu\text{g}/\text{kg}$ (n = 4) induced mild depression within the first hour post-RTX, and none of the mice died (mortality rate: 0%). As shown in Figure 4.2A, overall weight loss within

the first 3 days post-RTX was mild (overall mean reduction + SD: $-1.9 + 4.0\%$, range: -6 to 4%), and normal mouse behaviors were observed in this cohort 12 hours post-RTX. Conversely, $600 \mu\text{g}/\text{kg}$ RTX induced early signs of nervous system damage and increased death. Specifically, all mice ($n = 8$) developed within the first few hours post-RTX ataxic gait and depression, muscle rigidity in the neck, forelimbs, and hindlimbs, increased respiratory rate, unresponsiveness to touch (loss of pinch reflex), and/or lethargy. Death associated with RTX administration occurred 2 hours ($2/8$), 36 hours ($3/8$), and 56 hours ($1/8$) post-RTX. Therefore, a mortality of 62.5% was found in this cohort. Overall weight loss in those mice that survived the first 48 hours post-RTX ($5/8$) was moderate (overall mean reduction + SD: $-9.2 + 4.7\%$, range: -16 to -3%). All surviving mice in this cohort ($n = 2$) were purposely euthanized by day 3 post-RTX. As shown in Figure 4.2B, neuronal ablation (examined until day 3 post-RTX) was insufficient in the $2 \mu\text{g}/\text{kg}$ cohort (i.e., overall reduction less than 15% from baseline) and exceptional in the $600 \mu\text{g}/\text{kg}$ cohort (i.e., overall reduction higher than 90% reduction from baseline).

A full necropsy (i.e., microscopic assessment) was performed in all those mice that received $600 \mu\text{g}/\text{kg}$ RTX ($8/8$). During the histological evaluation, we did not find pathological abnormalities in those mice that died 2 hours post-RTX ($2/8$), however, relevant histopathologic changes were found in mice that survived the first 24 hours post-RTX ($6/8$), which were: Alzheimer type II astrocyte changes in the brain (2 mice; Figure 4.2C), scattered acute neuronal necrosis in TGs (4 mice; Figure 4.2D), widespread lymphocyte necrosis in thymus (4 mice; Figure 4.2E), and minimal focal acute necrosis in the bilateral ventricular myocardium (2 mice; Figure 4.2F). Pathological evidence of spinal cord or respiratory tract (upper or lower) disease were not found in this cohort.

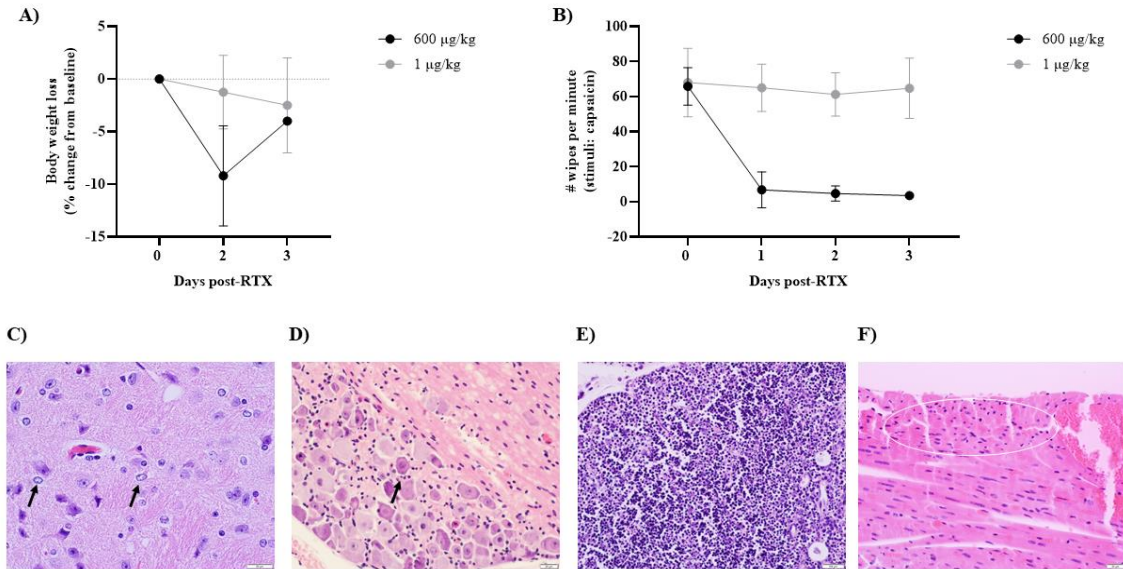


Figure 4.2: Systemic administration of RTX at a dose of either 2 µg/kg (n = 4) or 600 µg/kg (n = 8) in 14-week-old female C57BL/6J mice. (A) Overall body weight loss was mild in the 2 µg/kg cohort and moderate in the 600 µg/kg cohort. (B) Neuronal ablation was considered insufficient (i.e., overall reduction less than 15% from baseline) in the 2 µg/kg cohort (n = 4), and sufficient (i.e., overall reduction higher than 90% reduction from baseline) in the 600 µg/kg cohort (n = 2 to 6). Data expressed as mean + SD. Histopathological examination conducted in 600 µg/kg cohort revealed the next lesions: (C) Alzheimer type II astrocyte changes (black arrow, 20 µm, 60X magnification), (D) scattered acute neuronal necrosis of varying severity in TG samples (black arrow, 20 µm, 40X magnification), (E) extensive areas of lymphocyte necrosis in thymus (100 µm, 10X magnification), and (F) minimal focal acute necrosis in the bilateral ventricular myocardium (area marked with white circle, 20 µm, 40X magnification).

4.3.3 Experiment 3

After determining that none of the previously tested RTX doses were able to produce both high tolerability and ablative efficacy in C57BL/6 mice (i.e., 2, 50, and 600 µg/kg), we decided to test a relatively intermediate-dose of RTX (i.e., 10 µg/kg, given once) in 16-week-old female B6/J

mice ($n = 8$), and compare tolerability and ablative efficacy against sex and age-matched B6/J mice obtained from the same vendor which received a relative high-dose of RTX (i.e., 300 $\mu\text{g}/\text{kg}$, given once; $n = 4$). We used those same mice that previously received 2 $\mu\text{g}/\text{kg}$ of RTX (“Experiment 2”) to evaluate the tolerability and ablative efficacy associated with 300 $\mu\text{g}/\text{kg}$ RTX; mice received a 2-week break between administrations.

In general, the vast majority of mice (no distinction between cohorts) showed early signs of depression and/or ataxic gait within the first hours post-RTX. However, these signs only lasted for the first 24 hours post-RTX; all mice returned to normal behavior on the next day (i.e., 48 hours post-RTX). Moreover, no death was associated with either 10 or 300 $\mu\text{g}/\text{kg}$ RTX in this experiment (0% mortality). As shown in Figure 4.3A, overall weight loss in the 10 $\mu\text{g}/\text{kg}$ cohort was moderate within the first 3 days post-RTX (overall mean reduction + SD: $-9.0 + 3.7\%$, range: -16 to 0%). Likewise, overall weight loss in the 300 $\mu\text{g}/\text{kg}$ cohort was moderate during the same period (overall mean reduction + SD: $-11.0 + 4.1\%$, range: -21 to -4%). Body weight gain and normal mouse behaviors were observed by day 4 post-RTX in all mice (from both cohorts). Neuronal ablation (examined until day 8 post-RTX for both cohorts) was sufficient for both applied dosages (i.e., overall reduction higher than 70% from baseline; Figure 4.3B).

Because no difference in tolerability and ablation efficacy were found between cohorts, and because we know from past work that adult female B6/NCrl mice do not tolerate 300 $\mu\text{g}/\text{kg}$ RTX, we decided to euthanize mice that received 300 $\mu\text{g}/\text{kg}$ RTX on day 8 post-RTX (no gross lesions were seen in lungs, heart, thymus, TGs, spinal cord, or brain in this cohort), and continue assessing the ablative efficacy of 10 $\mu\text{g}/\text{kg}$ RTX to determine if ablation was sustained. Neuronal ablation was assessed once weekly in those 8 mice that received 10 $\mu\text{g}/\text{kg}$ RTX. As shown in Figure 4.3B, the degree of neuronal ablation found at 24 hours post-RTX (i.e., overall reduction

higher than 70% from baseline) was sustained for at least 42 days. Therefore, 10 $\mu\text{g}/\text{kg}$ RTX given subcutaneously to 16-week-old female B6/J mice was tolerable, and resulted in long-lasting ablation.

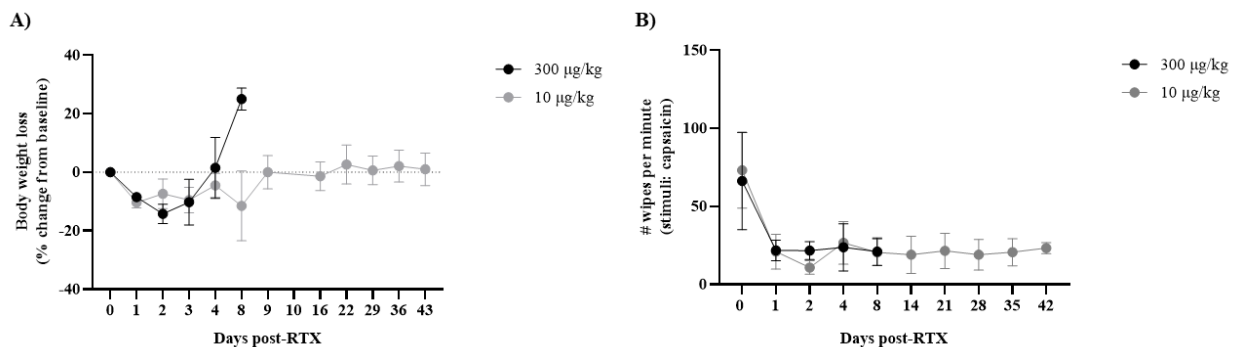


Figure 4.3: Systemic administration of RTX at a dose of either 10 $\mu\text{g}/\text{kg}$ ($n = 8$) or 300 $\mu\text{g}/\text{kg}$ ($n = 4$) in 16-week-old female C57BL/6J mice. (A) Overall body weight loss was moderate in both cohorts within the first 3 days post-RTX; body weight in both cohorts returned to baseline values approximately by day 4 post-RTX. (B) Neuronal ablation was considered sufficient (i.e., overall reduction higher than 70% reduction from baseline) in both 10 $\mu\text{g}/\text{kg}$ ($n = 8$) and 600 $\mu\text{g}/\text{kg}$ cohorts ($n = 4$). Data expressed as mean + SD.

4.3.4 Experiment 4

After determining that 10 $\mu\text{g}/\text{kg}$ RTX was well tolerated and effective at ablating TRPV1-expressing neurons in adult female B6/J mice, we repeated this experiment in sex-matched B6/NCrl mice ($n = 46$); here, RTX was administered when animals were 11 weeks of age. Unexpectedly, yet in line with previous results obtained from this substrain, early signs of nervous system damage and death were found. Specifically, several mice (20/46) died within the first 24 hours post-RTX; some either never recovered from anesthesia ($n = 3$), while others quickly showed tremor, ataxia, and lethargy after administration, and were later found dead inside the cage ($n =$

17). From those surviving mice (26/46), 8 died approximately 48 hours post-RTX. Therefore, a mortality of 60.8% was found in this experiment. Overall weight loss in this cohort was moderate within the first 2 days post-RTX (overall mean reduction + SD: -9.8.0 + 10.4%, range: -33 to 7%; Figure 4.4A), but in general, mice quickly recovered baseline values by day 3 post-RTX. As shown in Figure 4.4B, overall neuronal ablation (examined until day 3 post-RTX) in these mice was sufficient (i.e., overall reduction of 60% from baseline).

4.3.5 Experiment 5

Because TRPV1 ablation using 10 µg/kg RTX was well tolerated in B6/J mice, we decided to attempt replication of our results by repeating “Experiment 3” in a larger group that both contained female (n = 8) and male (n = 8) B6/J mice. In this experiment, RTX was administered at a dose of 10 µg/kg (given once) when animals were 13 weeks of age, and we evaluated the tolerability and ablative efficacy over a period of 126 days post-administration.

In this experiment, the vast majority of mice showed early signs of depression and ataxic gait within the first hours post-RTX. However, these signs only lasted for 6-12 hours after administration, returning to their normal state 24 hours after. In total, only 1 mouse died 24 hours post-RTX (male cohort), therefore, 10 µg/kg RTX resulted in 6.25% mortality (0% in female, and 12.5% in male). As shown in Figure 4.4C, overall weight loss within the first 48 hours post-RTX was moderate in female mice (overall mean reduction + SD: -7.6 + 6.3%, range: -18 to 4%), and values returned to baseline measures by day 5 post-RTX. In male mice, overall weight loss was also moderate (overall mean reduction + SD: -9.1 + 1.6%, range: -14 to -6%), and values returned to baseline measures by day 9 post-RTX. As shown in Figure 4.4D, both female and male mice displayed high levels of neuronal ablation (i.e., higher than 80% reduction from baseline for both

cohorts) after RTX administration; this effect lasted for at least 126 days (end of the study) in both female and male mice.

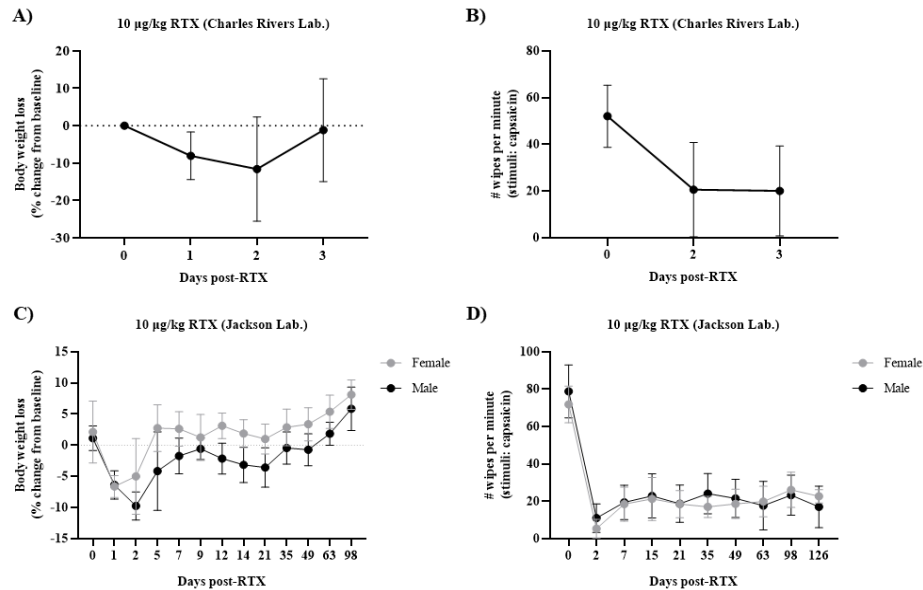


Figure 4.4: Systemic administration of RTX at a dose of 10 µg/kg in female B6/NCr1 (n = 46) or female and male B6/J mice (n = 16). (A) Overall body weight loss was moderate within the first 2 days post-RTX in 11-week-old female B6/NCr1 mice; body weight returned to baseline values approximately by day 3 post-RTX. (B) Neuronal ablation was considered sufficient in B6/NCr1 mice (i.e., overall reduction higher than 60% reduction from baseline; n = 13). (C) Overall body weight loss was moderate within the first 2 days post-RTX in 13-week-old female and male B6/J mice; body weight returned to baseline values in female and male mice by days 5 and 9 post-RTX, respectively. (D) Neuronal ablation was considered sufficient (i.e., overall reduction higher than 80% reduction from baseline) in both female (n = 8) and male (n = 8) B6/J mice. Data expressed as mean + SD.

Calcium imaging and immunofluorescent studies were done after all B6/J mice were euthanized (i.e., day 126 post-RTX). For this procedure, we only used TG samples from 4 mice per sex. From the calcium imaging analysis (Figure 4.5A) we found that the total proportion of TG neurons that responded to capsaicin was 12.8%; specifically, 11.5% in female and 15.1% in male mice. Immunofluorescent analysis (Figure 4.5B) revealed that the total proportion of TRPV1-positive TG neurons corresponded to 22.1%; specifically, 17.6% in female and 26.0% in male mice (representative images in Figure 4.5C).

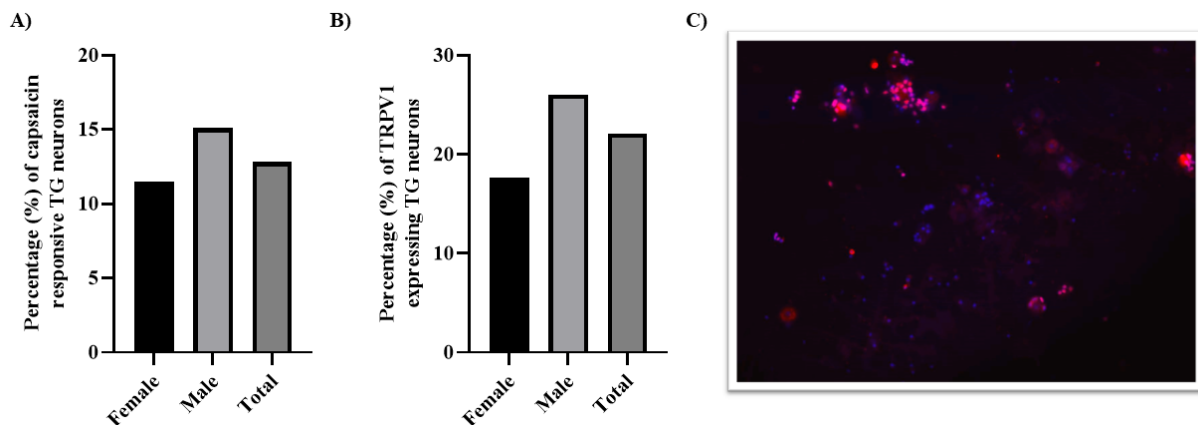


Figure 4.5: Calcium imaging and immunofluorescences studies in 13-week-old female and male B6/J mice (n = 16; 10 μ g/kg RTX). (A) The overall total proportion of TG neurons that positively responded to capsaicin during calcium imaging was 12.8% (female: 11.5%, male: 15.1%). (B) The overall total proportion of TRPV1-positive TG neurons (immunofluorescence analysis) corresponded to 22.1% (female: 17.6%, male: 26.0%). Data expressed as mean + SD. (C) Representative immunofluorescence images of the TG neurons in female B6/J mice injected with 10 μ g/kg RTX; the red fluorescence is the stained TRPV1-protein, and the blue fluorescence is the DAPI stained cell nuclei (20X magnification, scale bar = 50 μ m).

4.4 Discussion

The ablation of TRPV1-expressing neuron populations via RTX has been broadly used in preclinical research as a tool to prevent or alleviate pain hypersensitivity in a safe and effective manner. However, and as mentioned before, we noticed during the conduct of past experiments a remarkable difference in tolerability (in terms of mortality) between two commonly used laboratory mouse strains when a single high-dose of RTX (300 µg/kg) was administered subcutaneously (0% versus 32.5% mortality in BALB/c and C57BL/6 mice, respectively). The high mortality in C57BL/6 mice was quite unexpected since there is no evidence from studies in experimental animals indicating that systemic RTX (at used route and dose) may cause significant death in these mouse strains. To our knowledge, there is only one study that has suggested the possibility that RTX may increase mouse mortality when higher doses are used (Lee et al., 2018); in this preliminary study, the authors gave a single dose of RTX solution (dose: 10, 50, or 200 µg/kg, respectively) intraperitoneally into 8-week-old adult male ICR mice, and a significantly increased mortality was associated to high-dose RTX (0% mortality in the 10 µg/kg group, 25% mortality in the 50 µg/kg group, and 100% mortality in the 200 µg/kg group). Since RTX injections were done in the same experimental conditions in our studies (e.g., same sex, age, environment, mouse vendor, anesthesia, and recovery procedures), and moreover, because it has been demonstrated that TRPV1 expression (and increase capsaicin-related sensitivity thereof) is significantly higher in C57BL/6 mice in comparison to BALB/c mice (Ono et al., 2015), we first assumed that this increased RTX-related mortality may be a result of a strain difference.

In this study, we originally planned to test the tolerability and ablative efficacy of 300 µg/kg RTX spitted into three consecutives, increasing doses in C57BL/6 mice (B6/NCrl substrain). The idea here was to avoid any potential side effect associated to higher doses, such as death

related to respiratory stress (i.e., bronchoconstriction) as postulated by others in the past (Lee et al., 2018). However, we unfortunately encountered an excessive mortality and low ablative efficacy when a single RTX dose of 50 $\mu\text{g}/\text{kg}$ was administered on day 1. In this experiment, the signs that we observed in the past (Chapter 3) in B6/NCrl mice injected with a single dose of 300 $\mu\text{g}/\text{kg}$ RTX (i.e., severe depression and ataxic gait) were substantially more pronounced and were followed by sudden death within the first hours post-RTX in 70% of the animals. Intriguingly, RTX mortality in these mice did not greatly differ from the tolerability observed in B6/J substrain mice injected with a single high-dose of 600 $\mu\text{g}/\text{kg}$ RTX in subsequent experimentation. While sudden death was less commonly seen in the 600 $\mu\text{g}/\text{kg}$ cohort in comparison to the 50 $\mu\text{g}/\text{kg}$ cohort, we did see a wider variety of signs in these mice (B6/J) that were indicative of severe respiratory and/or nervous damage. However, and opposite to what we were expecting, no histopathological alterations were found in lungs or spinal cord samples of any mouse. In this experiment, only two B6/J mice presented signs of Alzheimer type II astrocyte changes in brain samples, which is a change that is classically described in hepatic encephalopathy/hyperammonemia (Norenberg et al., 1997) and other systemic metabolic disturbances (Butterworth et al., 1987); nevertheless, brain tissues appeared to be histologically unremarkable in most mice (even in those mice that showed respiratory stress, motor abnormalities, and unresponsiveness). Remarkably, we found in some mice indications of minimal focal acute myocardium necrosis, acute neuronal necrosis, and marked widespread lymphocyte necrosis in heart, trigeminal ganglions, and thymus samples, respectively. These last findings were particularly interesting because capsaicin-induced apoptotic cell death in these tissues has been previously described in rats (Santoni et al., 2004; Szöke et al., 2002; Zhang et al., 2012). Therefore,

RTX-induced death could potentially be related (or at least partially related) to a failure in these structures.

Because none of the tested RTX doses (i.e., 2, 50, and 600 $\mu\text{g}/\text{kg}$) resulted in a tolerable and effective TRPV1-ablation in the used C57BL/6 substrains, we decided to examine and compare RTX-tolerability and ablative efficacy between B6/J mice that either received 10 $\mu\text{g}/\text{kg}$ or 300 $\mu\text{g}/\text{kg}$ RTX, which are two of the most commonly used doses in adult mice (Menéndez et al., 2006). According to our results, both dose regimens seemed to be tolerable in mice, and moreover, they showed to have a similar effectivity ablating TRPV1 populations. While only 4 mice received the 300 $\mu\text{g}/\text{kg}$ dose, it was interesting to find that RTX at this dose seemed to be safer in B6/J mice in comparison to B6/NCrl mice (as stated in Chapter 3), thus, results here were suggestive of a distinct intolerance of RTX between C57BL/6 substrains. However, it was impossible to make any definitive conclusion at this stage. Taking into consideration all experiments, we can preliminarily conclude at this stage that RTX at a dose of 10, 300 or 600 $\mu\text{g}/\text{kg}$ induce good levels of ablation in B6/J mice, with varying tolerability responses (i.e., higher doses, such as 600 $\mu\text{g}/\text{kg}$, increase the risk to develop side effects). Moreover, we can also preliminarily conclude that RTX at a dose of 50 or 300 $\mu\text{g}/\text{kg}$ produce inconsistent results regarding tolerability and ablation efficacy in B6/NCrl mice (i.e., both 50 and 300 $\mu\text{g}/\text{kg}$ induce serious toxicity, but higher doses (300 $\mu\text{g}/\text{kg}$) produce adequate ablation). To our knowledge, there are no preclinical studies comparing tolerability and/or ablation degree using varying doses of RTX in mice. Therefore, we cannot know with certainty why two very different dosages, such as 10 and 300 $\mu\text{g}/\text{kg}$, yield to the same ablative degree in some C57BL/6 substrains, as well as we cannot know why two very different dosages, such as 50 and 300 $\mu\text{g}/\text{kg}$, may produce different degrees of ablation in other C57BL/6 substrains. However, we can assume from basic

pharmacokinetic principles that there is a potential ablative threshold dose-effect. In particular, it appears that doses higher than 10 µg/kg do not increase the degree of ablation (e.g., 300 and 600 µg/kg), but conversely, they increase the risk to develop serious toxicities (at least in B6/J substrains). Yet, this should be tested in other mouse strains to be sure, especially when considering the results obtained from B6/NCrl strains. Concerning to the duration of ablation, here we showed that the degree of ablation was sustained for at least 6 weeks in those B6/J mice that received 10 µg/kg RTX. The prolonged effect of RTX is particularly relevant since it provides additional support for the long-term ablative effects of RTX in animals (Bates et al., 2010; Mitchell et al., 2010; Okun et al., 2011), and moreover, it also highlights how drugs targeting the “capsaicin receptor”, TRPV1, could be important clinically for long-term treatment of chronic pain problems (Brown, 2016; Palazzo et al., 2010; Premkumar, 2010).

After determining that RTX at a dose of 10 µg/kg was the most tolerable way to approach long-lasting ablation of TRPV1-expressing neurons in C57BL/6 mice (at least in B6/J substrains), we decided to repeat this experiment using B6/NCrl mice from CRL. In this experiment, we found that RTX-associated mortality did not greatly differ from the one documented in “Experiment 1”, when 50 µg/kg was administered to mice from the same vendor and genetic background. In particular, almost half of the mice suddenly died few hours after 10 µg/kg RTX was administered. While the ablative efficacy of RTX was adequate in those surviving mice, this reduction (60%) was not superior to the one observed in “Experiment 3” when the same dose was used in B6/J mice obtained from JAX (70%). These results finally led us to realize that the low tolerability found in this particular strain (C57BL/6) was potentially related to the genetic background (vendor-dependent) of certain substrains, such as B6/NCrl. While we were not expecting this radical difference in tolerability between substrains, there is evidence in the literature indicating that the

inconsistency of research findings across studies can be attributable to the genotypic and phenotypic differences between inbred C57BL/6 substrains, as well as the differing environmental variables occurring at different vendors (Åhlgren & Voikar, 2019; Lariviere et al., 2001; Mogil & Wilson, 1997). Indeed, several genetic or genomic structural variations affecting phenotypes among C57BL/6 substrains have been described in the past by others; for example, differing susceptibility to intermittent hypoxia between C57BL/6N and C57BL/6J (Ge et al., 2019), or differences in response to high-fat diet intervention between C57BL/6J and C57BL/6NJ mice (Fisher-Wellman et al., 2016). In the realm of pain research, some authors have described that acute thermal nociception (measured using reflexive-based methods like the tail withdrawal and hot plate assays) appears to be enhanced in C57BL/6J in comparison to C57BL/6NCrl substrains (Bryant et al., 2008; Matsuo et al., 2010). Therefore, the generalization of results from a single mouse substrain can exacerbate the current “reproducibility crisis” in basic research, compromising the reproducibility and reliability of results.

To further confirm that external factors, such as genetic background associated to the commercial mouse supplier, might contribute to disparate results between inbred C57BL/6 substrain mice, we re-evaluated the tolerability and ablative efficacy of 10 µg/kg RTX in B6/J mice. To obtain a better idea of the effects of RTX, we also assessed here whether RTX tolerability and/or the degree of ablation varied across sexes, and whether the degree of ablation can be sustained on time. Results here confirmed that 10 µg/kg RTX is well-tolerable in B6/J mice (mild and short-lived side effects, such as depression, weight loss or ataxic gait). While the frequency and severity of RTX-related adverse side effects did not differ across sexes, we did notice that weight gain was relatively quicker in female mice in comparison to male mice (5 versus 9 days to return to baseline values, respectively). Moreover, the mortality associated with this RTX dose –

while low – was only present in the male cohort (1 of 8 mice). Although RTX-associated toxicity was mildly higher in males, we cannot conclude from the present data that the variation in outcomes is sex-dependent given the small sample size used. Moreover, there is no evidence in the literature indicating that the toxicity of RTX varies between females and males in any species; to our knowledge, there is only one study in the literature that has revealed that the toxic side effects associated with TRPV1 agonists, such as capsaicin, varies across sexes from the same mouse strain (Treat et al., 2022). However, in this study they showed that capsaicin-related toxicity (i.e., death) was increased in female in comparison to male mice. In terms of neuronal ablation, and line with previous results, 10 µg/kg RTX showed to be effective in reducing capsaicin-related eye wiping responses, an outcome measure that is vastly used to test TRPV1 ablation in preclinical settings (Bates et al., 2010; Mishra & Hoon, 2010; Pecze et al., 2009; Pogorzala et al., 2013). The degree of this reduction was equally high for both cohorts (> 80% from baseline in female and male mice), as well as the duration of ablation. Indeed, the ablation efficacy of this RTX dose was maintained for long periods (i.e., for at least 18 weeks) in both cohorts, with no obvious alterations in behavior or physical health. This finding further validates the use of RTX as a research tool to produce long-lasting desensitization in B6/J substrains, without affecting proprioception and motor functions. Finally, we performed calcium imaging and immunofluorescent studies at the end of this study to further corroborate ablation of TRPV1-expressive neuron populations at the peripheral nervous system level. On one hand, calcium imaging studies demonstrated that ~11 to 15% of trigeminal ganglion neurons responded to capsaicin, which differs from the responsiveness that we normally observe in our laboratory when using non-RTX mice from the same substrain (i.e., ~30 to 40%; unpublished) or from a different mouse strain (i.e., ~40 to 45% in CD-1 mice; Nolan et al., 2017). Therefore, it appears that 10 µg/kg RTX was effective in decreasing the

activity of TRPV1 in TG neurons. On the other hand, the immunofluorescent analysis revealed that approximately 22% of the DAPI-positive neurons were immunostained for TRPV1, which does not differ from the proportion described in other studies that have used non-RTX mice from the same strain (i.e., ~30%, Huang et al., 2012). This finding was indicative that 10 $\mu\text{g}/\text{kg}$ RTX did not reduce TRPV1 protein levels at the TG level, however, Huang and colleagues did not specify in their work which substrain was used. In addition, we noticed that the *ex vivo* response to capsaicin in female TG neurons, as well as the percent of neurons expressing TRPV1, were lower than the ones observed in the male cohort. While these results are just preliminary, they are in accordance with previous studies conducted in rats, where it was evidenced that the expression of TRPV1 channels in TG was higher in male in comparison to female (Bai et al., 2018). Taking all these pieces of evidence together, we could theorize that the difference in toxicity between sexes that was found in this study might be explained by a difference in TRPV1 expression, and therefore, supporting the idea that the ablative effects of RTX might be potentially sex-dependent.

Limitations of this study should be mentioned. First, we did not use the same number of animals across experiments, and moreover, sample sizes were in general small. Therefore, some of our findings may not be extendable to other research facilities. For example, the ablative efficacy of 2, 50, and 300 $\mu\text{g}/\text{kg}$ RTX was only tested in 3-4 mice per cohort, so definitive conclusions regarding to this aspect cannot be made. Moreover, we did not compare tolerability and ablative efficacy across sexes in most studies (except for “Experiment 5”). The rationale behind that lay on the fact that we were unsure about the potential toxicity associated with each dose, therefore, we limited our experimentation to females to avoid additional mouse death (at least until we found a well-tolerable dose). Regarding mortality, we need to clarify that we did not measure corporal body temperature in our mice after injections. This is important because both

RTX and anesthesia can produce significant drops in rectal temperature in this species (Horii et al., 2019; Tóth et al., 2011), thus, we cannot discard the idea that the mortality observed in our experiments might be a result of hypothermia (even if the cages were properly warmed). Another important limitation in our study was related to the fact that ablation of TRPV1-expressing neurons was only confirmed behaviorally. Certainly, the lack of control (non-RTX) mice and small sample sizes limited the interpretations of calcium imaging and immunofluorescent analyses. This was unfortunate, however, the confirmation of RTX-related ablation by means of capsaicin sensitivity using the eye-wiping test has been widely applied in research, and it appears to be an adequate indicator of the level of ablation (Bates et al., 2010; Pecze et al., 2009). Yet, further molecular/cellular analyses (as the ones described here) should be done to confirm ablation at the peripheral and central nervous system levels. In addition, we should also assess in future investigations the effect of systemic RTX in other biological systems. Indeed, we were unable to determine the cause of death in most of our studies, and the lack of appropriate control slides limited the interpretations of the lesions found in the 600 µg/kg cohort. Therefore, it will be important to add additional knowledge regarding the systemic effect of RTX before validating its use in our model of pain and cancer. Finally, the observed differences between substrains validate the idea that further investigations are required before making absolute conclusions. For example, none of the experiments conducted in this work appropriately compared the effects of RTX in the different C57BL/6 substrains within the same experiment; therefore, we cannot exclude the idea that other environmental factors within our research facilities may contribute to the observed difference in response. Moreover, we cannot confirm that all C57BL/6 substrains from either JAX or CRL will have the same tolerability or ablative effectivity in response to RTX observed in this study. Indeed, both vendors have developed several C57BL/6 substrains and phenotypical,

genetical, and behavioral variations between them have been demonstrated in the past (as mentioned above). This emphasizes the concept that published research findings should always include details about the substrains included to improve the replicability of results.

In summary, we conclude from this body of work that the tolerability and ablative efficacy of systemic RTX greatly differs between mouse substrains, and potentially, between mouse strains. Results here validate the use of systemic RTX at a dose of 10 µg/kg to produce effective and long-lasting ablation of TRPV1-expressing neurons in a safe manner in female and male C57BL/6J mice from JAX. However, appropriate support care (e.g., measure of corporal temperature, fluids, DietGel, cage warming) are imperative to reduce the risk to develop RTX-associated side effects. Moreover, and considering the results from past and current investigations in our research group, we can also state that 300 µg/kg RTX represents a good strategy to ablate TRPV1-populations (at least in a short-term fashion) in C57BL/6J mice from JAX and BALB/cNCrl mice from CRL; however, it will be interesting to test the 10 µg/kg protocol in BALB/cNCrl mice to determine whether lower doses can be used. On the contrary, C57BL/6NCrl mice from CRL seem to be particularly prone to develop serious toxicities as consequence of systemic RTX using doses ranging from 10 to 300 µg/kg. Therefore, we cannot recommend the use of these RTX protocols in this substrain. While results in this substrain may be seen as a potential difficulty in research, we consider that data here actually represents a valuable opportunity to study the mechanisms by which RTX produce varying grades of tolerability and ablation across C57BL/6 strains, thus, improving reproducibility across multiple laboratories. Finally, these findings constitute a very significant step forward in our research group to continue investigating the effects of radiation-associated mucositis pain in the progression of murine oral cancer (MOC2-Luc2 model) using RTX (at dose of 10 µg/kg) as a valuable tool for the relief pain in C57BL/6J mice.

4.5 References

- Åhlgren, J., & Voikar, V. (2019). Experiments done in Black-6 mice: what does it mean? *Lab animal*, 48(6), 171-180.
- Bai, X., Zhang, X., & Zhou, Q. (2018). Effect of Testosterone on TRPV1 Expression in a Model of Orofacial Myositis Pain in the Rat. *Journal of Molecular Neuroscience*, 64(1), 93-101.
- Bates, B. D., Mitchell, K., Keller, J. M., Chan, C.-C., Swaim, W. D., Yaskovich, R., Mannes, A. J., & Iadarola, M. J. (2010). Prolonged analgesic response of cornea to topical resiniferatoxin, a potent TRPV1 agonist. *Pain*, 149(3), 522-528.
- Bishnoi, M., Bosgraaf, C. A., & Premkumar, L. S. (2011). Preservation of acute pain and efferent functions following intrathecal resiniferatoxin-induced analgesia in rats. *The Journal of Pain*, 12(9), 991-1003.
- Brederson, J.-D., Kym, P. R., & Szallasi, A. (2013). Targeting TRP channels for pain relief. *European journal of pharmacology*, 716(1-3), 61-76.
- Brown, D. C. (2016). Resiniferatoxin: the evolution of the “molecular scalpel” for chronic pain relief. *Pharmaceuticals*, 9(3), 47.
- Brown, D. C., Iadarola, M. J., Perkowski, S. Z., Erin, H., Shofer, F., Laszlo, K. J., Olah, Z., & Mannes, A. J. (2005). Physiologic and antinociceptive effects of intrathecal resiniferatoxin in a canine bone cancer model. *The Journal of the American Society of Anesthesiologists*, 103(5), 1052-1059.
- Bryant, C. D., Zhang, N. N., Sokoloff, G., Fanselow, M. S., Ennes, H. S., Palmer, A. A., & McRoberts, J. A. (2008). Behavioral differences among C57BL/6 substrains: implications for transgenic and knockout studies. *Journal of neurogenetics*, 22(4), 315-331.

- Butterworth, R. F., Giguère, J.-F., Michaud, J., Lavoie, J., & Layrargues, G. P. (1987). Ammonia: key factor in the pathogenesis of hepatic encephalopathy. *Neurochemical pathology*, 6(1), 1-12.
- Caterina, M. J., & Julius, D. (2001). The vanilloid receptor: a molecular gateway to the pain pathway. *Annual review of neuroscience*, 24(1), 487-517.
- Caterina, M. J., & Park, U. (2006). TRPV1: a polymodal sensor in the nociceptor terminal. *Current topics in membranes*, 57, 113-150.
- Choi, E. J., Choi, Y. M., Jang, E. J., Kim, J. Y., Kim, T. K., & Kim, K. H. (2016). Neural Ablation and Regeneration in Pain Practice. *The Korean journal of pain*, 29(1), 3-11.
- Chung, M.-K., Güler, A. D., & Caterina, M. J. (2008). TRPV1 shows dynamic ionic selectivity during agonist stimulation. *Nature neuroscience*, 11(5), 555-564.
- Cui, M., Gosu, V., Basith, S., Hong, S., & Choi, S. (2016). Polymodal transient receptor potential vanilloid type 1 nociceptor: structure, modulators, and therapeutic applications. *Advances in protein chemistry and structural biology*, 104, 81-125.
- Elekes, K., Helyes, Z., Németh, J., Sándor, K., Pozsgai, G., Kereskai, L., Börzsei, R., Pintér, E., Szabó, Á., & Szolcsányi, J. (2007). Role of capsaicin-sensitive afferents and sensory neuropeptides in endotoxin-induced airway inflammation and consequent bronchial hyperreactivity in the mouse. *Regulatory peptides*, 141(1-3), 44-54.
- Eriksson, J., Jablonski, A., Persson, A.-K., Hao, J.-X., Kouya, P. F., Wiesenfeld-Hallin, Z., Xu, X.-J., & Fried, K. (2005). Behavioral changes and trigeminal ganglion sodium channel regulation in an orofacial neuropathic pain model. *Pain*, 119(1-3), 82-94.

- Fisher-Wellman, K. H., Ryan, T. E., Smith, C. D., Gilliam, L. A., Lin, C.-T., Reese, L. R., Torres, M. J., & Neuffer, P. D. (2016). A direct comparison of metabolic responses to high-fat diet in C57BL/6J and C57BL/6NJ mice. *Diabetes*, 65(11), 3249-3261.
- Ge, M. Q., Yeung, S. C., Mak, J. C. W., & Ip, M. S. M. (2019). Differential metabolic and inflammatory responses to intermittent hypoxia in substrains of lean and obese C57BL/6 mice. *Life Sciences*, 238, 116959.
- Horii, Y., Shiina, T., Uehara, S., Nomura, K., Shimaoka, H., Horii, K., & Shimizu, Y. (2019). Hypothermia induces changes in the alternative splicing pattern of cold-inducible RNA-binding protein transcripts in a non-hibernator, the mouse. *Biomedical Research*, 40(4), 153-161.
- Huang, D., Li, S., Dhaka, A., Story, G. M., & Cao, Y.-Q. (2012). Expression of the transient receptor potential channels TRPV1, TRPA1 and TRPM8 in mouse trigeminal primary afferent neurons innervating the dura. *Molecular pain*, 8, 1744-8069-1748-1766.
- Julius, D. (2013). TRP channels and pain. *Annual review of cell and developmental biology*, 29, 355-384.
- Karai, L., Brown, D. C., Mannes, A. J., Connelly, S. T., Brown, J., Gandal, M., Wellisch, O. M., Neubert, J. K., Olah, Z., & Iadarola, M. J. (2004). Deletion of vanilloid receptor 1-expressing primary afferent neurons for pain control. *The Journal of clinical investigation*, 113(9), 1344-1352.
- Kissin, E. Y., Freitas, C. F., & Kissin, I. (2005). Effects of intraarticular resiniferatoxin in experimental knee-joint arthritis. *Anesthesia and analgesia*, 101(5), 1433.

- Kissin, I., & Szallasi, A. (2011). Therapeutic targeting of TRPV1 by resiniferatoxin, from preclinical studies to clinical trials. *Current topics in medicinal chemistry*, 11(17), 2159-2170.
- Kobayashi, K., Fukuoka, T., Obata, K., Yamanaka, H., Dai, Y., Tokunaga, A., & Noguchi, K. (2005). Distinct expression of TRPM8, TRPA1, and TRPV1 mRNAs in rat primary afferent neurons with a δ /c-fibers and colocalization with trk receptors. *Journal of Comparative Neurology*, 493(4), 596-606.
- Lariviere, W. R., Chesler, E. J., & Mogil, J. S. (2001). Transgenic studies of pain and analgesia: mutation or background genotype? *Journal of Pharmacology and Experimental Therapeutics*, 297(2), 467-473.
- Lee, M. G., Huh, B. K., Choi, S. S., Lee, D. K., Lim, B. G., & Lee, M. (2012). The effect of epidural resiniferatoxin in the neuropathic pain rat model. *Pain Physician*, 15(4), 287-296.
- Lee, Y.-C., Lu, S.-C., & Hsieh, Y.-L. (2018). Establishing a mouse model of a pure small fiber neuropathy with the ultrapotent agonist of transient receptor potential vanilloid Type 1. *JoVE (Journal of Visualized Experiments)* (132), e56651.
- Ma, Q.-P. (2002). Expression of capsaicin receptor (VR1) by myelinated primary afferent neurons in rats. *Neuroscience Letters*, 319(2), 87-90.
- Masumoto, K., Tsukimoto, M., & Kojima, S. (2013). Role of TRPM2 and TRPV1 cation channels in cellular responses to radiation-induced DNA damage. *Biochimica et Biophysica Acta (BBA)-General Subjects*, 1830(6), 3382-3390.
- Matsuo, N., Takao, K., Nakanishi, K., Yamasaki, N., Tanda, K., & Miyakawa, T. (2010). Behavioral profiles of three C57BL/6 substrains. *Frontiers in Behavioral Neuroscience*, 4, 29.

- Menéndez, L., Juárez, L., García, E., García-Suárez, O., Hidalgo, A., & Baamonde, A. (2006). Analgesic effects of capsazepine and resiniferatoxin on bone cancer pain in mice. *Neuroscience Letters*, 393(1), 70-73.
- Mishra, S. K., & Hoon, M. A. (2010). Ablation of TrpV1 neurons reveals their selective role in thermal pain sensation. *Molecular and Cellular Neuroscience*, 43(1), 157-163.
- Mitchell, K., Bates, B. D., Keller, J. M., Lopez, M., Scholl, L., Navarro, J., Madian, N., Haspel, G., Nemenov, M. I., & Iadarola, M. J. (2010). Ablation of rat TRPV1-expressing Adelta/C-fibers with resiniferatoxin: analysis of withdrawal behaviors, recovery of function and molecular correlates. *Molecular pain*, 6(1), 1-13.
- Mogil, J., & Wilson, S. (1997). Nociceptive and morphine antinociceptive sensitivity of 129 and C57BL/6 inbred mouse strains: implications for transgenic knock-out studies. *European Journal of Pain*, 1(4), 293-297.
- Neubert, J. K., Mannes, A. J., Karai, L. J., Jenkins, A. C., Zawatski, L., Abu-Asab, M., & Iadarola, M. J. (2008). Perineural resiniferatoxin selectively inhibits inflammatory hyperalgesia. *Molecular pain*, 4, 1744-8069-1744-1743.
- Nishino, K., Tanamachi, K., Nakanishi, Y., Ide, S., Kojima, S., Tanuma, S., & Tsukimoto, M. (2016). Radiosensitizing Effect of TRPV1 Channel Inhibitors in Cancer Cells. *Biol Pharm Bull*, 39(7), 1224-1230.
- Nolan, M. W., Long, C. T., Marcus, K. L., Sarmadi, S., Roback, D. M., Fukuyama, T., Baeumer, W., & Lascelles, B. D. X. (2017). Nocifensive behaviors in mice with radiation-induced oral mucositis. *Radiation research*, 187(3), 397-403.

- Norenberg, M. D., Huo, Z., Neary, J. T., & Roig-Cantesano, A. (1997). The glial glutamate transporter in hyperammonemia and hepatic encephalopathy: relation to energy metabolism and glutamatergic neurotransmission. *Glia*, 21(1), 124-133.
- Okun, A., DeFelice, M., Eyde, N., Ren, J., Mercado, R., King, T., & Porreca, F. (2011). Transient inflammation-induced ongoing pain is driven by TRPV1 sensitive afferents. *Molecular pain*, 7, 1744-8069-1747-1744.
- Ono, K., Ye, Y., Viet, C. T., Dang, D., & Schmidt, B. L. (2015). TRPV1 expression level in isolectin B4-positive neurons contributes to mouse strain difference in cutaneous thermal nociceptive sensitivity. *Journal of neurophysiology*, 113(9), 3345-3355.
- Palazzo, E., Luongo, L., de Novellis, V., Berrino, L., Rossi, F., & Maione, S. (2010). Moving towards supraspinal TRPV1 receptors for chronic pain relief. *Molecular Pain*, 6(1), 1-11.
- Payne, C. K., Mosbaugh, P. G., Forrest, J. B., Evans, R. J., Whitmore, K. E., Antoci, J. P., Perez-Marrero, R., Jacoby, K., Diokno, A. C., & O'REILLY, K. J. (2005). Intravesical resiniferatoxin for the treatment of interstitial cystitis: a randomized, double-blind, placebo controlled trial. *The Journal of urology*, 173(5), 1590-1594.
- Pecze, L., Pelsőczy, P., Kecskés, M., Winter, Z., Papp, A., Kaszás, K., Letoha, T., Vizler, C., & Oláh, Z. (2009). Resiniferatoxin mediated ablation of TRPV1+ neurons removes TRPA1 as well. *Canadian journal of neurological sciences*, 36(2), 234-241.
- Pogorzala, L., Mishra, S., & Hoon, M. (2013). The Cellular Code for Mammalian Thermosensation. *The Journal of neuroscience: the official journal of the Society for Neuroscience*, 33, 5533-5541.
- Premkumar, L. S. (2010). Targeting TRPV1 as an alternative approach to narcotic analgesics to treat chronic pain conditions. *The AAPS journal*, 12(3), 361-370.

- Price, M. L., Lai, Y. H., Marcus, K. L., Robertson, J. B., Lascelles, B. D. X., & Nolan, M. W. (2021). Early radiation-induced oral pain signaling responses are reduced with pentoxifylline treatment. *Veterinary Radiology & Ultrasound*, 62(2), 255-263.
- Raithel, S. J., Sapio, M. R., LaPaglia, D. M., Iadarola, M. J., & Mannes, A. J. (2018). Transcriptional changes in dorsal spinal cord persist after surgical incision despite preemptive analgesia with peripheral resiniferatoxin. *Anesthesiology*, 128(3), 620-635.
- Santoni, G., Amantini, C., Lucciarini, R., Perfumi, M., Pompei, P., & Piccoli, M. (2004). Neonatal capsaicin treatment affects rat thymocyte proliferation and cell death by modulating substance P and neurokinin-1 receptor expression. *Neuroimmunomodulation*, 11(3), 160-172.
- Suzuki, S., Gerner, P., Colvin, A. C., & Binshtok, A. M. (2009). C-fiber-selective peripheral nerve blockade. *The open pain journal*, 2, 24-29.
- Szallasi, A., & Blumberg, P. (1989). Resiniferatoxin, a phorbol-related diterpene, acts as an ultrapotent analog of capsaicin, the irritant constituent in red pepper. *Neuroscience*, 30(2), 515-520.
- Szöke, E., Seress, L., & Szolcsányi, J. (2002). Neonatal capsaicin treatment results in prolonged mitochondrial damage and delayed cell death of B cells in the rat trigeminal ganglia. *Neuroscience*, 113(4), 925-937.
- Takahashi, N., Matsuda, Y., Sato, K., de Jong, P. R., Bertin, S., Tabeta, K., & Yamazaki, K. (2016). Neuronal TRPV1 activation regulates alveolar bone resorption by suppressing osteoclastogenesis via CGRP. *Scientific reports*, 6(1), 1-11.

- Tominaga, M., Caterina, M. J., Malmberg, A. B., Rosen, T. A., Gilbert, H., Skinner, K., Raumann, B. E., Basbaum, A. I., & Julius, D. (1998). The cloned capsaicin receptor integrates multiple pain-producing stimuli. *Neuron*, 21(3), 531-543.
- Tóth, D. M., Szőke, É., Bölcskei, K., Kvell, K., Bender, B., Bősze, Z., Szolcsányi, J., & Sándor, Z. (2011). Nociception, neurogenic inflammation and thermoregulation in TRPV1 knockdown transgenic mice. *Cellular and Molecular Life Sciences*, 68(15), 2589-2601.
- Treat, A., Henri, V., Liu, J., Shen, J., Gil-Silva, M., Morales, A., Rade, A., Tidgewell, K. J., Kolber, B., & Shen, Y. (2022). Novel TRPV1 Modulators with Reduced Pungency Induce Analgesic Effects in Mice. *ACS Omega*, 7(3), 2929-2946.
- Wang, X.-L., Tian, B., Huang, Y., Peng, X.-Y., Chen, L.-H., Li, J.-C., & Liu, T. (2015). Hydrogen sulfide-induced itch requires activation of Cav3. 2 T-type calcium channel in mice. *Scientific reports*, 5(1), 1-15.
- Yang, F., & Zheng, J. (2017). Understand spiciness: mechanism of TRPV1 channel activation by capsaicin. *Protein & cell*, 8(3), 169-177.
- Zhang, R.-L., Guo, Z., Wang, L.-L., & Wu, J. (2012). Degeneration of capsaicin sensitive sensory nerves enhances myocardial injury in acute myocardial infarction in rats. *International journal of cardiology*, 160(1), 41-47.

Chapter 5: “Characterization of Radiation-induced Oral Mucositis and Validity Testing of a Subjective Oral Pain Scale in Pet Dogs Undergoing Definitive Radiation Therapy for the Treatment of Oral, Nasal and Cranial Cavity Tumors.”

5.1 Introduction

Radiation therapy (RT) plays an important role in the treatment of head and neck cancer (HNC). However, curative-intent RT modalities can adversely affect exposed tissues, which, in turn, can lead to the development of painful toxicities, such as radiation-induced oral mucositis (RIM) (Borbasi et al., 2002; Lalla et al., 2019; Scully et al., 2003). While various pharmacological and non-pharmacological methods are currently available to manage the pain that arise along with RIM, usually termed as radiation-associated pain (RAP) (see Chapter 1 for details), most HNC patients demonstrate a poor response to these analgesic strategies (Barber et al., 2007; Christoforou et al., 2019; Cook et al., 2022). The impact of untreated or poorly treated RAP can be overwhelming as it affects the patient's quality of life, oral cavity functioning, and the continuity of RT, and thus, limiting the efficacy of RT to control tumor progression (Bese et al., 2007; Brzozowska & Gołębiowski, 2019; Carlotto et al., 2013; Elting et al., 2007). Based on this evidence, researchers in the field are racing to find novel and better strategies to improve RAP management (Astrup et al., 2015; Chen et al., 2011; Muzumder et al., 2018).

Rodent models have been, and continue to be, important in generating new information to understand the biological mechanistic processes underlying many conditions, such as pain, as well as relevant in the discovery of new candidate therapeutic targets (Brown, 2021; Kersten et al., 2017; Tappe-Theodor & Kuner, 2014). However, small animal models cannot perfectly mimic the complex processes involved in the initiation and progression of pain, neither can translate the human response to new therapeutic alternatives (Mogil, 2009, 2019; Piel et al., 2014). Certainly, the leap from rodent models to the clinic is a large one and has been partly blamed for the poor translation of basic research (De Jong & Maina, 2010; Mak et al., 2014). To meet the increasing demand for novel, safe and effective pain therapies, the biomedical research community working

on translational pain research has proposed to incorporate into drug development programs higher order preclinical species to bridge the gap between basic and clinical research (Cho et al., 2021; Klinck et al., 2017; Kol et al., 2015; Lascelles et al., 2018). For example, the use of companion animals may provide clinically relevant models of human diseases (Kol et al., 2015). In the last years, some canine comparative models have been developed to improve our understanding of the natural progression of certain diseases (e.g., osteosarcoma, osteoarthritis), and to examine interventions that could potentially improve clinical outcomes in humans (Brown et al., 2005; Iadarola et al., 2018; Menéndez et al., 2006; Minnema et al., 2020; Miyagi et al., 2017; Ranieri et al., 2013). Despite apparent phenotypic differences, domesticated dogs share a genetic, physiological, and environmental basis with their human counterpart, increasing the chances of better modeling the multifactorial variabilities found in human studies (Paoloni & Khanna, 2008).

Companion dogs, like people, suffer from the spontaneous development of HNC in the same anatomical locations, use similar RT treatment regimens, and develop painful RIM, impacting their quality of life, oral function, and treatment outcomes (Boss et al., 2022; Denneberg & Egenvall, 2009; Farcas et al., 2014; Hunley et al., 2010). In this scenario, pet-owned dogs represent an exceptional alternative to test novel analgesic alternatives for managing RAP. However, if the dog model of HNC and RAP is planned to be used in translational research, then the model needs to be fully characterized, and relevant and valid outcome measures need to be developed. Because RAP has been majorly linked to RIM in humans, we will describe in this chapter the characteristics of RIM in pet dogs undergoing definitive-intent RT for the treatment of oral, nasal, and cranial cavity tumors. To date, various owner-reported questionnaire instruments have been developed to quantify different types of pain and the impact of pain on the dog's quality of life (Brown et al., 2008; Holton et al., 2001; Wiseman-Orr et al., 2004). However, none of the

so far developed outcomes measures have been designed specifically for the assessment of RAP within the oral cavity. Therefore, in this study, we will also assess aspects of reliability and validity of a novel client metrology instrument designed to measure oral RAP in this species.

5.2 Material and Methods

All procedures performed in this study were conducted in accordance with the Institutional Animal Care and Use Committee (IACUC) of the University of Pennsylvania (protocol number: A3079-01). Protocols were additionally reviewed and approved by The Veterinary Internal Review Board – comprised of clinicians, veterinarians actively practicing within the University of Pennsylvania Veterinary Hospital (VHUP) – to ensure that the animals were adequately protected. The Veterinary Clinical Investigations Center (VCIC) at VHUP oversaw recruitment, patient care, and data collection.

5.2.1 Subjects

Client-owned dogs of any age, breed, and of either sex (neutered or intact) for which the owners had chosen to pursue standard of care definitive-intent RT (DRT) for cancer treatment were recruited to this single-arm prospective observational, non-interventional clinical study between 2009 and 2011. Inclusion criteria were: (1) dogs with a histopathologically-confirmed solid malignancy of the oral or nasal cavity, or an imaging diagnosis of a tumor within the cranial cavity, (2) dog owner(s) provided informed consent for routine clinical care including a standard course of DRT at the VHUP, and (3) dog owner(s) agreed to fill out questionnaires throughout treatment and for 3 weeks following the last treatment. Dogs were excluded from data analysis if they received any concomitant cancer treatment (i.e., surgery or chemotherapy) during the course of DRT and follow-up.

5.2.2 Recruitment and patient care

Recruitment within the VHUP was done by the VCIC staff and supported by specialized veterinarians and research scientists in the field of veterinary radiation oncology. Cases from outside VHUP were recruited by direct mailings to general practices and referring veterinarians. Information about the study and recruitment was also distributed using print advertisements in local newspapers, radio spots on local stations, and digital flyers provided by the VCIC website. Animal care and handling were performed by licensed veterinarians and veterinary technicians.

5.2.3 Data collection

Data collection was performed from initiation to the completion of DRT and during the 3 weeks of follow-up examination. Specifically, data were obtained from 9 total visits: enrollment (i.e., immediately before the first DRT fraction delivery; considered as baseline); five visits during DRT (after dogs received approximately 25, 50, 70, 90, and 100% of the total DRT planned course); and three weekly follow-up visits.

5.2.4 Definitive-intent radiation therapy (DRT)

Three-dimensional conformal DRT was planned using a commercial software (Prowess 3D-RTP); DRT was delivered using a Siemens 6 MV linear accelerator. In an overall treatment time of 5 weeks, RT regimens of approximately 45-54 Gy were planned to be delivered in 15-18 single daily fractions using 3 Gy/fraction (Monday through Friday schedule). A certified veterinary anesthesia technician was always on-site to monitor and provide care to dogs during anesthesia and recovery.

5.2.5 Patient's characteristics

Information regarding age, sex, neuter status, breed, body weight and condition, tumor type, and location, date of cancer diagnosis, scheduled DRT regimen (number of fractions, Gy/fraction, and fraction interval planned), and medication history was collected at enrollment (i.e., prior first DRT fraction delivery). Other relevant information gathered at enrollment included appetite and diet acceptance levels, current diet, presence of oral mucositis (prior DRT), and use of prophylactic dental cleaning strategies performed immediately before DRT initiation.

5.2.6 Assessment of oral radiation-induced mucositis

Clinical features of radiation-induced oral mucositis (herein termed as "RIM") were evaluated separately in: (1) dogs that received irradiation for oral tumors (herein referred to as "oral DRT"), (2) dogs that received irradiation for nasal tumors (herein referred to as "nasal DRT"), and (3) dogs that received irradiation for intracranial tumors (herein referred to as "cranial DRT").

5.2.6.1 Time course and severity: At each visit, the severity of RIM was graded according to the Veterinary Radiation Therapy Oncology Group (VROG) radiation therapy acute morbidity scoring system. VROG scores (herein referred to as "VROGs") were rated from 0 to 3 according to the condition of the oral mucosa as follow: (0) no change over baseline; (1) erythema, dry desquamation, alopecia/epilation; (2) patchy moist desquamation; and (3) confluent moist desquamation with edema and/or ulceration, necrosis, hemorrhage (Appendix 5.1).

5.2.6.2 Adverse side-effects: Occurrence and severity of side-effects potentially associated with RIM were assessed by means of body weight and body condition score, level of appetite and diet acceptance, the necessity of feeding tube, unscheduled breaks in DRT, and failure to complete the prescribed course. Additionally, signs consistent with nasal mucositis (i.e., sneezing, nasal

discharge) and radiation dermatitis (i.e., crusting, redness, alopecia) were used for estimation of adverse side effects.

5.2.7 Measures of pain and function interference

In this section, measures of pain and interference of function by pain were assessed and compared across oral, nasal, and cranial DRT groups. For each visit, pain and pain's interference with dogs' function over the last 7 days were assessed using the Canine Brief Pain Inventory (CBPI; Appendix 5.2), which is an owner-completed clinical metrology instrument (CMI) (Brown et al., 2008). The CBPI contains three subscales designed to assess pain severity (i.e., "Pain Severity Scale", PSS), the degree to which pain interferes with function or the ability to perform activities (i.e., "Pain Interference Scale", PIS), and overall quality of life ("Overall Impression Scale", OIS). In addition, owners were asked to complete a new questionnaire, the "Oral Pain Scale" (OPS) at the same time that they completed the CBPI (OPS developed by Dorothy Brown at VHUP; Appendix 5.3). The OPS is a questionnaire designed to assess the impact of oral pain; the 7 questions included in this scale asked about owners' perceptions of how pain was interfering with certain oral functions (such as eating, drinking, barking, chewing, etc.) in the last 7 days.

5.2.8 Statistical analysis

All the collected data was kindly provided in March 2020 by Dr. Dorothy Brown at VHUP to the authors at the North Carolina State University College of Veterinary Medicine (NCSU-CVM). The principal author reviewed, organized, and analyzed the data. All statistical analyses were done using two commercial statistical software packages: GraphPad Prism (version 7.0) and IBM SPSS Statistics (version 28.0).

5.2.8.1 Data characterization and grading: Change (i.e., reduction or increase) in body weight after DRT initiation was characterized as the percentage change from baseline (i.e., enrollment). Body condition was assessed using the Purina Body Condition Scoring (Appendix 5.4); body condition score (BCS) of 4 or 5 on a 9-point scale was considered ideal, whereas BCSs < 4/9 were considered underweight and those >5/9 were considered overweight (Ineson et al., 2019). The level of appetite and acceptance of the usual diet by dogs, as well as the type of diet, were characterized by asking owners to complete a questionnaire developed by the VHUP staff (Appendix 5.5). Appetite and acceptance of regular diet were rated on a 0-10 numerical rating scale (NRS) ranging from 0 (“no appetite” or “completely unacceptable”, respectively) to 10 (“excellent appetite” or “very acceptable”, respectively). Data regarding the type of current diet were coded as “hard”, “soft” or “mixed”. Nasal mucositis and radiation dermatitis were graded on a 0-10 NRS that ranged from 0 (“none”) to 10 (“severe”); both of these questions were included in the VRTOGs assessment form (Appendix 5.1). The 4 questions of the PSS were scored on a 0-10 NRS ranging from 0 (“no pain”) to 10 (“extreme pain”), while the 6 and 7 questions of the PIS and OPS, respectively, were scored on a 0-10 NRS ranging from 0 (“does not interfere”) to 10 (“completely interferes”). The single question of the OIS was rated on a 5-item Likert scale that categorized quality of life as either poor (score of 0), fair (score of 1), good (score of 2), very good (score of 3), or excellent (score of 4). Scores of the PSS, PIS, and OPS were averaged across questions to create a single score for each of these subsections. OPS item questions were coded during this analysis as follow: (1) “Ability to eat its normal diet” coded as “OPS_Eat”; (2) “Ability to drink liquids” coded as “OPS_Drink”; (3) “Ability to vocalize (bark, whine, growl) normally” coded as “OPS_Vocalize”; (4) “Ability to swallow saliva (which leads to excessive drooling)” coded as “OPS_Swallow”; (5) “Willingness to be pet or stroked on the head” coded as “OPS_Pet”;

(6) “Willingness to move the head and neck” coded as “OPS_Move”; and (7) “Willingness to play with toys (tug, chew on balls, fetch)” coded as “OPS_Play”.

5.2.8.2 General data handling: Normal distribution of the numeric data was evaluated by the Shapiro-Wilk normality test, and appropriate parametric or non-parametric statistical tests were applied. Statistical significance was assessed by using Student's t-test (parametric, 2-tailed unpaired) or Mann-Whitney test (non-parametric, 2-tailed unpaired) for comparisons between two groups. For comparison of three or more groups, a 1-way ANOVA (analysis of variance) with Dunn's multiple comparison test (parametric data) or Kruskal-Wallis's test with Dunn's test for correction for multiple comparisons (non-parametric data) were used. For comparison of two or more groups with two independent variables, a 2-way repeated-measures ANOVA analysis was used; p-values were adjusted for multiple comparisons using Tukey's or Dunnett's post hoc test. Numerical data were plotted as mean + standard deviation (SD). Descriptive statistics were computed using mean, SD, median, range, and/or variance and proportion of cases (i.e., number or percentage of cases/total). Correlations were measured by means of Spearman or Pearson coefficients for non-parametric and parametric data, respectively. Significant p-values for all analyses were set at < 0.05 .

5.2.8.3 Risk factor assessment: To determine risk factors for RIM, regression studies were conducted.

5.2.8.3.a Ordinal regression: Simple regression analysis was used to determine if any of the variables collected at baseline (independent variables) were associated with the VRTOG scores (dependent variable) documented after completing DRT (i.e., at visit 5). Independent variables were treated as discrete categorical variables (described in 5.2.8.3.c), while the dependent variable (VRTOG) was treated as a 3-level ordinal variable (0 = VRTOG scores of 0, 1 = VRTOG scores

of 1, and 2 = VRTOG scores > 2). The relationship between dependent and independent variables was estimated using R², slope (95% confidence intervals (CI)), and p-values. For each of those independent variables that showed a statistically significant association, we examined the occurrence of VRTOG scores > 0 in the total population using Chi-square analysis (results expressed in percentage).

5.2.8.3.b) Logistic regression: Logistic regression was used to assess the ability of variables collected at baseline (independent variables) to predict severe grades of RIM after DRT completion (i.e., VRTOG scores of 3; dependent variable). Independent variables were treated as discrete categorical variables (described in 5.2.8.3.c), while the dependent variable (VRTOG) was treated as a 2-level ordinal variable (0 = VRTOG scores below 3, and 1 = VRTOG scores equal to 3). For this analysis, Spearman or Pearson coefficients for non-parametric and parametric data, respectively, were calculated (significant p-values set at < 0.05). For those independent variables that demonstrated predictive significance, we examined the occurrence of VRTOG scores of 3 in the total population using Chi-square analysis (results expressed in percentage).

5.2.8.3.c) Data categorization for regression analyses: Data were coded for both regression analyses as: (1) Sex: 0 = male, 1 = female; (2) Life stage: 0 = young/mature adult, 1 = senior/end of life (calculated using the AAHA Canine Life Stage Guidelines;(Bartges et al., 2012); (3) Breed: 0 = mixed, 1 = purebred; (4) Neuter Status: 0 = intact, 1 = neutered; (5) Tumor location: 0 = oral, 1 = nasal, 2 = cranial; (6) Body weight: 0 = small (< 10 kg), 1 = medium (10 to 25 kg), 2 = large (> 25 kg); (7) BCS: 0 = scores < 4, 1 = scores ranging from 4 to 5, 2 = scores > 6; (8) Signs of oral mucositis (OM) prior DRT initiation: 0 = no, 1 = yes; (9), Prophylactic dental cleaning prior DRT initiation: 0 = no, 1 = yes; (10) Appetite: 0 = scores < 4, 1 = scores ranging from 4 to 6, 2 = scores > 7; (11) Diet Acceptance: 0 = scores < 4, 1 = scores ranging from 4 to 6, 2 = scores > 7;

(12) Current diet: 0 = hard, 1 = soft, 2 = mixed; (13) Use of systemic anti-inflammatory drugs (NSAID or corticosteroid): 0 = no, 1 = yes; (14) Use of systemic narcotics: 0 = no, 1 = yes; (15) Use of antiemetics/gastroprotectants: 0 = no, 1 = yes; and (16) Use of antibiotics: 0 = no, 1 = yes.

5.2.8.4 Assessment of aspects of reliability and validity of the “Oral Pain Scale” (OPS):

Reliability and validity assessments were done to determine whether the newly developed OPS appeared to be an appropriate CMI tool to measure the underlying theoretical construct (i.e., orofacial pain associated to RIM). We evaluated reliability/validity by means of internal consistency, construct and concurrent validity, extreme group validation, and responsiveness. The temporal choice for internal consistency, construct and concurrent validity evaluations corresponded to the first visit where VRTOG grades > 2 were found (i.e., visit 2), while the temporal choice for extreme group validation evaluations corresponded to the time that DRT was completed (i.e., visit 5). The temporal choices for responsiveness examination corresponded to the time of enrollment (i.e., visit 0), time that DRT was completed (i.e., visit 5), and time that the last follow-up occurred (i.e., visit 8).

5.2.8.4.a) Reliability assessment: Internal consistency was examined by means of Cronbach’s alpha, inter-item correlation matrix, and item-total statistics; Reliability was considered satisfactory (based on the rule of thumb) if: (1) Cronbach’s alpha coefficient > 0.7, (2) individual inter-item correlation means > 0.3, (3) no significant change (i.e., $p > 0.05$) in mean and variance occurred when certain item-question was removed, and if (4) item-total correlation and Cronbach’s alpha coefficient values decreased when certain item question was removed.

5.2.8.4.b) Validation assessment: Construct validity was examined using Principal Component Analysis (PCA). PCA was used as a factor extraction method; we accepted factors with eigenvalues greater than 1. As a rule of thumb, items with a factor loading of at least 0.4 were

considered relevant. Before the extraction of the constructs, we examined the adequacy of the sample and the suitability of data (i.e., to determine how many factors to retain) using the following methods: (1) Kaiser-Meyer-Olkin (KMO) and Bartlett's Test of Sphericity (BTS), (2) communality, and (3) cumulative percent of variance extracted. Data was considered suitable for PCA if KMO index > 0.50 , and BTS resulted significant (i.e., $p < 0.05$). As a rule of thumb, item communalities were considered less than appropriate if values were < 0.30 . A cumulative percent of variance higher than 50% was considered adequate. Concurrent validity was assessed by determining the correlation between the OPS and VRTOG scores. Specifically, each OPS item question was multiplied by the associated factor derived from the PCA, and the resulting values were then summed to obtain a total factor (TF) score per animal. Extreme group validation was evaluated by comparing OPS scores between dogs experiencing the lowest (i.e., scores of 0) and highest (i.e., scores of 3) VRTOGs at the same assessment time point. Responsiveness was assessed by comparing OPS scores documented at enrollment against those documented after dogs received their full DRT course and at the end of the study (during follow-up).

5.3 Results

5.3.1 Patient's characteristics

5.3.1.1 Demographic profile: Between 2009 and 2011, 61 dogs were enrolled, but 3 dogs were later excluded (2 dogs died within the first week after enrollment, and 1 dog underwent concurrent chemotherapy). A total of 58 dogs were included in this analysis. At enrollment ($n = 58$), there were 34 male and 24 female dogs. The median age at admission was 9.0 years, and the median body weight and condition score were 28.2 kgs and 5.0 BCS, respectively. In total, 16 dogs were identified as mixed breed dogs, and 42 as purebred dogs. See Table 5.1 for details.

Table 5.1: Demographics of dogs at enrollment (n = 58).

| Demographics at admission | |
|----------------------------------|--|
| Sex (number of cases) | |
| Female | 34 (6 sexually intact, 28 neutered) |
| Male | 24 (all neutered) |
| Age (years) | |
| Mean \pm SD (range) | 8.8 \pm 2.8 (2 - 14) |
| Body weight (kgs) | |
| Mean \pm SD (range) | 26.2 \pm 12.2 (5.6 - 48.3) |
| Body condition (BCS) | |
| Mean \pm SD (range) | 5.4 \pm 1.0 (3 - 9) |
| Breed (number of cases) | |
| Mixed breed | 16 |
| Purebred | 42 |
| Labrador Retriever | 8 |
| Golden Retriever | 5 |
| Boxer | 4 |
| English Springer Spaniel | 2 |
| German Shepherd | 2 |
| Jack Russell Terrier | 2 |
| West Highland White Terrier | 2 |
| Other purebred (one dog/breed): | Welsh Springer Spaniel, Standard Poodle, Pekingese, Toy Manchester Terrier, Cocker Spaniel, Greyhound, Dachshund, Brussels Griffon, Siberian Husky, Australian Cattle Dog, Boston Terrier, Bassett Hound, Cairn Terrier, American Pit Bull Terrier, Beagle, Basenji, and Malamute. |

5.3.1.2 Tumor location and type: Tumors were localized in one of 3 cavities: oral (23 dogs), nasal (18 dogs), and cranial (17 dogs). The most common specific locations reported for oral tumors were the maxilla (8 dogs, 34.7%), for nasal tumors the nose (17 dogs, 94.4%), and for cranial tumors the brain (14 dogs, 82.4%). Tumor types are enumerated in Table 5.2.

Table 5.2: Tumor types diagnosed at enrollment (n = 58).

| Tumor type | Number of cases |
|-------------------------------|-----------------|
| Adenocarcinoma | 2 |
| Ameloblastoma | 5 |
| Carcinoma | 6 |
| Squamous cell carcinoma | 4 |
| Osteosarcoma | 1 |
| Chondrosarcoma | 3 |
| Chondrosarcoma + osteosarcoma | 2 |
| Fibrosarcoma | 4 |
| Glioma | 4 |
| Lymphoma | 1 |
| Macroadenoma | 1 |
| Mast cell tumor | 4 |
| Meningioma | 8 |
| Oligodendroglioma | 1 |
| Polyps | 1 |
| Unknown | 11 |

5.3.1.3 DRT scheme: The mean number of days between cancer diagnosis and enrollment was of 59.6 days (SD: 94.0 days, median: 30.5 days, range: 1 to 442 days). Dogs were treated with 3 Gy daily per RT fraction, however, the total number of fractions and, thus the total DRT dose delivered, differed from the original treatment plan. In particular, dogs from the oral DRT group received 15 to 18 fractions, with total DRT doses ranging from 45 to 54 Gy; dogs from the nasal DRT group received 9 to 18 fractions, with total DRT doses ranging from 27 to 54 Gy; and dogs from the cranial DRT group received 11 to 15 fractions, with total DRT doses ranging from 33 to 45 Gy.

5.3.1.4 Concomitant medication: During the study, 27% of the dogs received a systemic anti-inflammatory drug (NSAIDs: 6 dogs; corticosteroids: 15 dogs). Other concomitant medications

included opioids (11 dogs), antiemetics and gastroprotectants (11 dogs), antibiotics (13 dogs), and experimental herbal therapeutic and/or nutritional supplements (5 dogs).

5.3.1.5 Other relevant information gathered at enrollment: From the total enrolled dogs, only 1 dog presented with oral mucositis before enrollment (i.e., dog with primary nasal cavity tumor). Dental prophylaxis prior to DRT was done in a total of 16 dogs (10 oral DRT dogs, 5 nasal DRT dogs, and 1 cranial DRT dog). In general, dogs had no appetite and diet acceptance impairments prior to DRT initiation. Mean + SD scores for appetite and diet acceptance were 9.1 + 1.8 (median: 10, range: 3 to 10), and 8.8 + 2.3 (median: 10, range: 1 to 10), respectively. The current diet at enrollment consisted of either hard (6 dogs) or soft (18 dogs) pellet-based diet, however, most dogs received a diet regimen that mixed both modalities (34 dogs). The number of cases for each variable is detailed in Table 5.3.

Table 5.3: Information about oral mucositis, dental prophylaxis, appetite, diet acceptance, and type of diet documented at enrollment.

| Variable | Number of cases |
|---------------------------------|-----------------|
| Oral mucositis prior DRT | 1 |
| Dental prophylaxis | 16 |
| Appetite (score) | |
| 0 - 3 | 3 |
| 4 - 6 | 2 |
| 7 - 10 | 53 |
| Diet acceptance (score) | |
| 0 - 3 | 4 |
| 4 - 6 | 1 |
| 7 - 10 | 53 |
| Type of diet | |
| Hard | 6 |
| Soft | 18 |
| Mixed | 34 |

5.3.2 Clinical features of oral radiation-induced oral mucositis in pet dogs

Clinical features of RIM were evaluated in dogs undergoing oral DRT (n = 23), nasal DRT (n = 18) and cranial DRT (n = 17). Details about visits (i.e., mean + SD days elapsed between each visit) and DRT dose administered by each assessment time point (mean + SD) are listed in Tables 5.4 and 5.5, respectively.

Table 5.4. Summary statistics of elapsed days from DRT initiation (enrollment) to the end of this study (i.e., 3 weeks after DRT finalization).

| Visit # | Day(s) post-DRT initiation | | | |
|----------|----------------------------|-----------|---------------|--------------|
| | <i>Mean</i> | <i>SD</i> | <i>Median</i> | <i>Range</i> |
| 0 | 0.0 | 0.0 | 0.0 | 0 |
| 1 | 5.3 | 1.9 | 6.0 | 3 - 12 |
| 2 | 11.8 | 2.9 | 11.0 | 7 - 21 |
| 3 | 17.6 | 2.9 | 17.0 | 10 - 27 |
| 4 | 22.9 | 3.0 | 22.0 | 15 - 31 |
| 5 | 29.6 | 3.0 | 29.0 | 22 - 38 |
| 6 | 36.5 | 2.9 | 36.0 | 29 - 44 |
| 7 | 43.6 | 3.1 | 43.0 | 36 - 54 |
| 8 | 50.8 | 3.1 | 50.0 | 43 - 61 |

Table 5.5. Total DRT dose administered by each assessment time point (i.e., from DRT initiation to completion).

| Visit # | Total DRT dose administered (expressed in percentage) | | | |
|----------|---|-----------|---------------|--------------|
| | <i>Mean</i> | <i>SD</i> | <i>Median</i> | <i>Range</i> |
| 0 | 0.0 | 0.0 | 0.0 | 0 - 0 |
| 1 | 23.9 | 6.3 | 22.0 | 13 - 44 |
| 2 | 49.8 | 9.4 | 47.0 | 35 - 89 |
| 3 | 73.2 | 7.9 | 72.0 | 60 - 100 |
| 4 | 93.5 | 1.7 | 94.0 | 87 - 100 |
| 5 | 100.0 | 0.0 | 100.0 | 100 - 100 |

5.3.2.1 Time course and severity: We first characterized the time course of RIM using VRTOGs for each group at each assessment time point, and compared differences in VRTOGs between visit 0 and the following visits (details in Table 5.6). Then, VRTOGs documented on each visit were compared across all groups (Figure 5.1).

5.3.2.1.a) Oral DRT group: The first signs of RIM (i.e., VRTOGs > 0 in 4/23 dogs) were seen at visit 1 when dogs had received ~ 25% of the prescribed DRT course; overall mean score at this visit was 0.2 (SD: 0.4; range: 0 to 1; difference from baseline non-significant). At the following visit (visit 2), higher grade RIM (i.e., VRTOGs > 2 in 14/23 dogs) was seen when dogs had received ~ 50% of the prescribed DRT course; the overall mean score at this visit was 1.6 (SD: 0.7; range: 0 to 3; difference from baseline significant). At visit 3, RIM increased in severity (i.e., VRTOGs > 2 in 21/23 dogs) when dogs had received ~ 75% of the prescribed DRT course; the overall mean score at this visit was 2.2 (SD: 0.7; range: 0 to 3; difference from baseline significant). Maximal RIM severity (i.e., VRTOGs > 2 in 22/23 dogs) was seen at visit 4 when dogs had received ~ 90% of the prescribed DRT course; the overall mean score at this visit was 2.4 (SD: 0.7; range: 0 to 3; difference from baseline significant). Signs of RIM resolution (i.e., score reduction) started to be evident at subsequent visits; overall mean (SD) VRTOGs at visits 5, 6, and 7 were 1.8 (SD: 1.1), 1.3 (SD: 0.9), and 1.0 (SD: 0.7), respectively (difference from baseline significant for all visits). By the last follow-up visit (visit 8), the overall mean VRTOGs was 0.6 (SD: 0.7; range: 0 to 2; difference from baseline non-significant). Complete RIM resolution by the end of the study was seen in a total of 56.5% of dogs (13 of 23).

5.3.2.1.b) Nasal DRT group: The first signs of RIM (i.e., VRTOGs > 0 in 2/18 dogs) were seen at visit 1 when dogs had received ~ 25% of the prescribed DRT course; overall mean score at this visit was 0.2 (SD: 0.5; range: 0 to 2; difference from baseline non-significant). At the following

visit (visit 2), higher grade RIM (i.e., VRTOGs > 2 in 12/18 dogs) was seen when dogs had received ~ 50% of the prescribed DRT course; the overall mean score at this visit was 1.6 (SD: 0.9; range: 0 to 3; difference from baseline significant). Maximal RIM severity (i.e., VRTOGs > 2 in 15/17 dogs; 1 died) was seen when dogs had received ~ 75% of the prescribed DRT course (visit 3); the overall mean score at this visit was 2.2 (SD: 0.5; range: 1 to 3; difference from baseline significant). Maximal RIM severity (i.e., VRTOGs > 2 in 14/16 dogs; 1 died) was also seen at visit 4 when dogs had received ~ 90% of the prescribed DRT course; the overall mean score at this visit was 2.2 (SD: 0.8; range: 0 to 3; difference from baseline significant). RIM severity (i.e., VRTOGs > 2 in 13/15 dogs; 1 died) continued to be maximal at visit 5 when dogs had received ~ 100% of the prescribed DRT course; the overall mean score at this visit was 2.2 (SD: 0.7; range: 1 to 3; difference from baseline significant). Signs of RIM resolution (i.e., score reduction) started to be evident at subsequent visits (follow-up visits); overall mean (SD) VRTOGs at visits 6 and 7 were 1.1 (SD: 0.8), and 0.6 (SD: 0.7), respectively (difference from baseline significant only for visit 6). By the last follow-up visit (visit 8), the overall mean VRTOGs was 0.6 (SD: 0.7; range: 0 to 2; difference from baseline non-significant). Complete RIM resolution by the end of the study was seen in a total of 50% of dogs (6 of 12; no follow-up in 3 dogs).

5.3.2.1.c) Cranial DRT group: The first signs of RIM (i.e., VRTOGs > 0 in 5/17 dogs) were seen at visit 1 when dogs had received ~ 25% of the prescribed DRT course; overall mean score at this visit was 0.4 (SD: 0.7; range: 0 to 2; difference from baseline non-significant). At the following visit (visit 2), higher grade RIM (i.e., VRTOGs > 2 in 5/17 dogs) was seen when dogs had received ~ 50% of the prescribed DRT course; the overall mean score at this visit was 0.7 (SD: 0.9; range: 0 to 2; difference from baseline significant). RIM decreased in severity (i.e., VRTOGs > 2 in 3/17 dogs) when dogs had received ~ 75% of the prescribed DRT course (visit 3); the overall mean

score at this visit was 0.5 (SD: 0.8; range: 0 to 2; difference from baseline non-significant). At the following visit (visit 4), higher grade RIM (i.e., VRTOGs > 2 in 6/17 dogs) was seen when dogs had received ~ 90% of the prescribed DRT course; the overall mean score at this visit was 0.9 (SD: 0.9; range: 0 to 2; difference from baseline significant). Maximal RIM severity (i.e., VRTOGs > 2 in 8/17 dogs) was seen at visit 5 when dogs had received ~ 100% of the prescribed DRT course; the overall mean score at this visit was 1.0 (SD: 1.0; range: 0 to 2; difference from baseline significant). Signs of RIM resolution (i.e., score reduction) started to be evident at subsequent visits; overall mean (SD) VRTOGs at visits 6 and 7 were 0.5 (SD: 0.6), and 0.4 (SD: 0.7), respectively (difference from baseline non-significant). By the last follow-up visit (visit 8), the overall mean VRTOGs was 0.1 (SD: 0.4; range: 0 to 1; difference from baseline non-significant). Complete RIM resolution by the end of the study was seen in a total of 86.7% of dogs (2 of 15; no follow-up in 2 dogs).

Table 5.6: RIM time course and severity (using VRTOGs, scale: 0 - 3) across groups at each assessment time point.

| VRTOGs | | | | | | | | | | | | | | | |
|---------|----------|-----|--------|--------|----------|-----------|-----|--------|--------|----------|-------------|-----|--------|--------|---------|
| Visit # | Oral DRT | | | | | Nasal DRT | | | | | Cranial DRT | | | | |
| | Mean | SD | Median | Range | p-value | Mean | SD | Median | Range | p-value | Mean | SD | Median | Range | p-value |
| 0 | 0.0 | 0.0 | 0.0 | 0 to 0 | - | 0.0 | 0.0 | 0 | 0 to 0 | - | 0.0 | 0.0 | 0.0 | 0 to 0 | - |
| 1 | 0.2 | 0.4 | 0.0 | 0 to 1 | 0.9579 | 0.2 | 0.5 | 0 | 0 to 2 | 0.9818 | 0.4 | 0.7 | 0.0 | 0 to 2 | 0.4209 |
| 2 | 1.6 | 0.7 | 2.0 | 0 to 3 | <0.0001* | 1.6 | 0.9 | 2 | 0 to 3 | <0.0001* | 0.7 | 0.9 | 0.0 | 0 to 2 | 0.0277* |
| 3 | 2.2 | 0.7 | 2.0 | 0 to 3 | <0.0001* | 2.2 | 0.5 | 2 | 1 to 3 | 0.0002* | 0.5 | 0.8 | 0.0 | 0 to 2 | 0.1917 |
| 4 | 2.4 | 0.7 | 3.0 | 0 to 3 | <0.0001* | 2.2 | 0.8 | 2 | 0 to 3 | 0.0003* | 0.9 | 0.9 | 1.0 | 0 to 2 | 0.0007* |
| 5 | 1.8 | 1.1 | 2.0 | 0 to 3 | <0.0001* | 2.2 | 0.7 | 2 | 1 to 3 | 0.0004* | 1.0 | 1.0 | 1.0 | 0 to 2 | 0.0002* |
| 6 | 1.3 | 0.9 | 1.0 | 0 to 3 | <0.0001* | 1.1 | 0.8 | 1 | 0 to 2 | 0.0003* | 0.5 | 0.6 | 0.0 | 0 to 2 | 0.2339 |
| 7 | 1.0 | 0.7 | 1.0 | 0 to 2 | <0.0001* | 0.6 | 0.7 | 0.5 | 0 to 2 | 0.0759 | 0.4 | 0.7 | 0.0 | 0 to 2 | 0.3706 |
| 8 | 0.6 | 0.7 | 0.0 | 0 to 2 | 0.0520 | 0.6 | 0.7 | 0.5 | 0 to 2 | 0.1666 | 0.1 | 0.4 | 0.0 | 0 to 1 | 0.9968 |

Comments: Difference from baseline analyzed using Dunnett's multiple comparisons test (ordinary 2-way ANOVA); statistically significant p-values set at * $p < 0.05$.

5.3.2.1.d) *VRTOGs comparison across groups at each assessment time point*: VRTOGs were significantly higher in oral versus cranial DRT groups at visits 2, 3, 4, 5 and 6 (visit 2, $p = 0.0006$; visit 3-4, $p < 0.0001$; visit 5, $p = 0.0032$; visit 6, $p = 0.0031$), and in nasal versus cranial DRT groups at visits 2, 3, 4, and 5 (visit 2, $p = 0.0010$; visit 3-5, $p < 0.0001$). No statistically significant differences were not found between nasal and oral DRT groups at any time point (Figure 5.1).

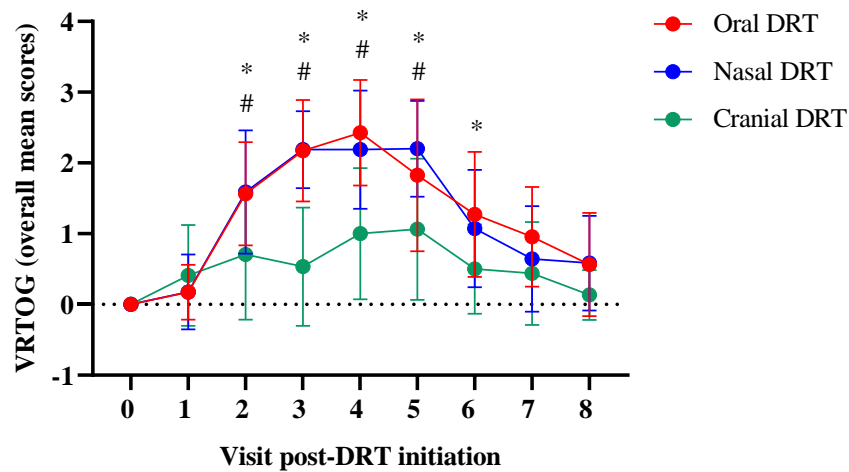


Figure 5.1: RIM progression over time for oral, nasal, and cranial DRT groups. Plots of overall VRTOGs for each group over time. Comparisons between groups were done using 2-way ANOVA analysis (with Tukey's multiple comparisons test); data were expressed as mean + SD. The symbol represents a significant difference between oral and cranial DRT groups ($*p < 0.05$), and between nasal and cranial DRT groups ($\#p < 0.05$).

5.3.2.2 Adverse side-effects

5.3.2.2.a) *Oral DRT group*: Weight progressively decreased at each visit after DRT initiation (Table 5.7), reaching maximal decrease when dogs had received ~ 90% of the prescribed DRT course (visit 4); overall mean reduction at this visit was -5.0% (SD: 3.3%, range: -13.3 to 0.8%); a significant decrease in weight from baseline was seen at visits 3, 4, 5 and 6, and signs of weight

recovery started to be evident from visit 5. Overall BCS was 5.7 (considered an ideal body condition), and scores did not significantly change from baseline at any assessment time point (Table 5.8). Signs of impairment in appetite (Table 5.9) or diet acceptance (Table 5.10) were not seen at any time point, and none of the dogs required feeding tube placement (not shown). Nasal mucositis (Table 5.11) and radiodermatitis (Table 5.12) progressively increased in severity following DRT initiation. Maximal nasal mucositis severity was seen when dogs had received ~ 90% of the prescribed DRT course (visit 4); overall mean score of 1.1 (SD: 2.0; range: 0 to 7); a significant increase in scores from baseline was seen at visits 4 and 5, and signs of score decrease started to be evident from visit 5. Maximal radiodermatitis severity was seen when dogs had received ~ 100% of the prescribed DRT course (visit 5); overall mean score of 4.1 (SD: 2.2; range: 1 to 8), a significant increase in scores from baseline was seen from visit 4 to 8, and signs of score decrease started to be evident from visit 6. In this group, a total of 13% of dogs (3 of 23) had DRT interruption related to RIM, and 39.1% of dogs (9 of 23) failed to complete the prescribed DRT course.

5.3.2.2.b) Nasal DRT group: Weight progressively decreased at each visit after DRT initiation (Table 5.7), reaching maximal decrease when dogs had received ~ 100% of the prescribed DRT course (visit 5); overall mean reduction at this visit was -4.5% (SD: 5.3%, range: -16.5 to 6.4%); a significant decrease in weight from baseline was only seen at visit 5, and signs of weight recovery started to be evident from visit 6. Overall BCS was 5.0 (considered an ideal body condition), and scores did not significantly change from baseline at any assessment time point (Table 5.8). Signs of impairment in appetite (Table 5.9) or diet acceptance (Table 5.10) were not seen at any time point, and none of the dogs required feeding tube placement (not shown). Nasal mucositis (Table 5.11) and radiodermatitis (Table 5.12) progressively increased in severity following DRT

initiation. Maximal nasal mucositis severity was seen at the first follow-up visit (visit 6); overall mean score of 2.0 (SD: 2.7; range: 0 to 8); a significant increase in scores from baseline was seen at visits 5 and 6, and signs of score decrease started to be evident from visit 7. Maximal radiodermatitis severity was seen when dogs had received ~ 100% of the prescribed DRT course (visit 5); overall mean score of 6.3 (SD: 1.9; range: 3 to 10), a significant increase in scores from baseline was seen from visit 4 to 8, and signs of score decrease started to be evident from visit 6. In this group, a total of 5.6% of dogs (1 of 18) had DRT interruption related to RIM, and 38.9% of dogs (7 of 18) failed to complete the prescribed DRT course.

5.3.2.2.c) Cranial DRT group: Weight progressively decreased at each visit after DRT initiation (Table 5.7), reaching maximal decrease when dogs had received ~ 50% of the prescribed DRT course (visit 2); overall mean reduction at this visit was -1.8% (SD: 3.8%, range: -12.9 to 4%); a significant decrease in weight from baseline was not seen in this group, and signs of weight recovery started to be evident from visit 3. Overall BCS was 5.1 (considered an ideal body condition), and scores did not significantly change from baseline at any assessment time point (Table 5.8). Signs of impairment in appetite (Table 5.9) or diet acceptance (Table 10) were not seen at any time point, and none of the dogs required feeding tube placement (not shown). Signs of nasal mucositis (Table 5.10) and radiodermatitis (Table 5.11) appeared to be absent in this group. Maximal nasal mucositis severity was seen at visit 1 (overall mean score of 0.1 (SD: 0.2; range: 0 to 1)), and maximal radiodermatitis severity was seen at visit 6 (overall mean score of 0.3 (SD: 0.8; range: 0 to 3)); a significant increase in nasal mucositis and radiodermatitis scores from baseline were not seen. In this group, none of the dogs (0 of 17) had DRT interruption related to RIM, and 17.6% of dogs (3 of 17) failed to complete the prescribed DRT course.

Table 5.7: Body weight change from baseline (%) for each group, at each assessment time point.

| Body weight (percentage change from baseline) | | | | | | | | | | | | | | | |
|---|----------|-------|--------|--------------|----------|-----------|-------|--------|--------------|----------|-------------|------|--------|--------------|---------|
| Visit # | Oral DRT | | | | | Nasal DRT | | | | | Cranial DRT | | | | |
| | Mean | SD | Median | Range | p-value | Mean | SD | Median | Range | p-value | Mean | SD | Median | Range | p-value |
| 0 | 0.0% | 0.0 % | 0.0% | 0 to 0 | - | 0.0% | 2.1 % | 0.0% | 0 to 0 | - | 0.0% | 0.0% | 0.0% | 0 to 0 | - |
| 1 | -2.4% | 4.0 % | -1.7% | -16.4 to 3.1 | 0.3406 | -0.1% | 3.0 % | -0.2% | -4.2 to 5.3 | 0.9999 | -0.1% | 2.8% | 0.0% | -5.6 to 4.2 | 0.9994 |
| 2 | -3.3% | 3.0 % | -3.2% | -9.5 to 2.1 | 0.0853 | -0.8% | 3.1 % | -1.5% | -7.1 to 5.3 | 0.9971 | -1.8% | 3.8% | -0.3% | -12.9 to 4 | 0.6565 |
| 3 | -4.1% | 3.3 % | -4.8% | -9.5 to 2.5 | 0.0167 * | -1.9% | 3.5 % | -2.6% | -7.8 to 2.7 | 0.6406 | -1.1% | 3.6% | -1.2% | -8.6 to 6.6 | 0.9277 |
| 4 | -5.0% | 3.3 % | -4.2% | -13.3 to 0.8 | 0.0025 * | -2.2% | 5.2 % | -0.5% | -10.1 to 1.3 | 0.5920 | -0.7% | 3.5% | -1.0% | -7 to 8 | 0.9936 |
| 5 | -4.8% | 3.8 % | -5.2% | -10.5 to 2.5 | 0.0018 * | -4.5% | 5.3 % | -4.4% | -16.5 to 6.4 | 0.0185 * | 0.0% | 4.9% | -1.5% | -4.7 to 11.4 | >0.9999 |
| 6 | -3.7% | 5.4 % | -3.3% | -12.3 to 6 | 0.0426 * | -1.9% | 4.2 % | -2.4% | -9.4 to 3.9 | 0.7668 | 0.9% | 5.8% | -2.0% | -4.4 to 17.5 | 0.9931 |
| 7 | -3.3% | 4.9 % | -3.4% | -11.9 to 5.9 | 0.0853 | -2.9% | 4.6 % | -3.4% | -8.3 to 8.4 | 0.3567 | 2.7% | 7.2% | -0.6% | -4.5 to 23.3 | 0.3228 |
| 8 | -1.3% | 5.2 % | -1.7% | -10.9 to 7.9 | 0.8673 | -2.9% | 4.8 % | -4.1% | -9.3 to 8.8 | 0.3892 | 3.6% | 9.2% | 0.3% | -4.1 to 25 | 0.0764 |

Comments: Difference from baseline analyzed using Dunnett's multiple comparisons test (ordinary 2-way ANOVA); statistically significant p-values set at * $p < 0.05$.

Table 5.8: Body conditions scores (0-9) in each group, at each assessment time point.

| Body condition (score) | | | | | | | | | | | | | | | |
|------------------------|----------|-----|--------|--------|---------|-----------|-----|--------|----------|---------|-------------|-----|--------|--------|---------|
| Visit # | Oral DRT | | | | | Nasal DRT | | | | | Cranial DRT | | | | |
| | Mean | SD | Median | Range | p-value | Mean | SD | Median | Range | p-value | Mean | SD | Median | Range | p-value |
| 0 | 5.8 | 1.3 | 5.5 | 4 to 9 | - | 5.0 | 0.8 | 5.0 | 4 to 6 | - | 5.3 | 0.8 | 5.0 | 3 to 6 | - |
| 1 | 5.8 | 1.2 | 6.0 | 4 to 9 | 0.9999 | 5.3 | 0.8 | 5.0 | 4 to 6 | 0.9721 | 5.2 | 0.9 | 5.0 | 3 to 7 | 0.9998 |
| 2 | 5.7 | 1.3 | 5.0 | 4 to 9 | 0.9978 | 4.9 | 0.8 | 5.0 | 4 to 6 | 0.9996 | 5.1 | 0.7 | 5.0 | 4 to 7 | 0.9976 |
| 3 | 5.8 | 1.4 | 5.0 | 4 to 9 | 0.9997 | 4.9 | 0.9 | 5.0 | 4 to 6 | 0.9996 | 5.2 | 0.8 | 5.0 | 4 to 7 | 0.9997 |
| 4 | 5.7 | 1.5 | 5.0 | 4 to 9 | 0.9994 | 4.8 | 0.9 | 5.0 | 3.5 to 6 | 0.9994 | 5.1 | 0.6 | 5.0 | 4 to 6 | 0.9979 |
| 5 | 5.7 | 1.5 | 5.5 | 4 to 9 | 0.9995 | 5.0 | 0.8 | 5.0 | 3.5 to 6 | 0.9999 | 5.0 | 0.8 | 5.0 | 3 to 6 | 0.9736 |
| 6 | 5.7 | 1.5 | 5.0 | 4 to 9 | 0.9969 | 5.1 | 0.9 | 5.0 | 3.5 to 6 | 0.9996 | 5.2 | 1.0 | 5.0 | 3 to 7 | 0.9996 |
| 7 | 5.6 | 1.6 | 5.0 | 4 to 9 | 0.9747 | 5.0 | 0.9 | 5.0 | 4 to 6 | >0.9999 | 5.3 | 0.9 | 5.0 | 3 to 7 | >0.9999 |
| 8 | 5.6 | 1.5 | 5.0 | 4 to 9 | 0.9747 | 4.9 | 0.8 | 5.0 | 4 to 6 | 0.9997 | 5.1 | 0.9 | 5.0 | 3 to 7 | 0.9994 |

Comments: Difference from baseline analyzed using Dunnett's multiple comparisons test (ordinary 2-way ANOVA); statistically significant p-values set at * $p < 0.05$.

Table 5.9: Appetite scores (0-10) for each group, at each assessment time point.

| Appetite (score) | | | | | | | | | | | | | | | |
|------------------|----------|-----|--------|---------|---------|-----------|-----|--------|---------|---------|-------------|-----|--------|---------|---------|
| Visit # | Oral DRT | | | | | Nasal DRT | | | | | Cranial DRT | | | | |
| | Mean | SD | Median | Range | p-value | Mean | SD | Median | Range | p-value | Mean | SD | Median | Range | p-value |
| 0 | 8.9 | 2.0 | 10.0 | 3 to 10 | - | 9.6 | 0.7 | 10.0 | 8 to 10 | - | 8.9 | 2.3 | 10.0 | 3 to 10 | - |
| 1 | 7.8 | 2.7 | 9.0 | 1 to 10 | 0.2808 | 8.8 | 1.5 | 9.0 | 5 to 10 | 0.8336 | 8.8 | 2.2 | 10.0 | 3 to 10 | 0.9996 |
| 2 | 7.9 | 2.5 | 9.0 | 2 to 10 | 0.4174 | 9.0 | 1.5 | 10.0 | 5 to 10 | 0.9515 | 9.2 | 1.8 | 10.0 | 3 to 10 | 0.9995 |
| 3 | 8.4 | 1.9 | 9.0 | 4 to 10 | 0.9640 | 8.7 | 2.4 | 10.0 | 2 to 10 | 0.7056 | 9.3 | 2.3 | 10.0 | 1 to 10 | 0.9974 |
| 4 | 8.3 | 2.3 | 9.0 | 3 to 10 | 0.8881 | 8.4 | 2.4 | 9.5 | 2 to 10 | 0.3665 | 9.3 | 2.3 | 10.0 | 1 to 10 | 0.9976 |
| 5 | 8.2 | 2.4 | 9.0 | 1 to 10 | 0.7521 | 8.9 | 1.6 | 9.0 | 5 to 10 | 0.8890 | 8.9 | 2.3 | 10.0 | 2 to 10 | >0.9999 |
| 6 | 9.0 | 2.1 | 10.0 | 3 to 10 | 0.9997 | 9.1 | 1.3 | 10.0 | 6 to 10 | 0.9823 | 9.5 | 1.3 | 10.0 | 5 to 10 | 0.9569 |
| 7 | 9.7 | 0.7 | 10.0 | 7 to 10 | 0.5815 | 9.8 | 0.6 | 10.0 | 8 to 10 | 0.9996 | 9.8 | 0.5 | 10.0 | 8 to 10 | 0.7028 |
| 8 | 9.5 | 1.4 | 10.0 | 4 to 10 | 0.8192 | 9.3 | 1.9 | 10.0 | 3 to 10 | 0.9995 | 9.4 | 1.6 | 10.0 | 4 to 10 | 0.9881 |

Comments: Difference from baseline analyzed using Dunnett's multiple comparisons test (ordinary 2-way ANOVA); statistically significant p-values set at *p < 0.05.

Table 5.10: Diet acceptance scores (0-10) for each group, at each assessment time point.

| Diet acceptance (score) | | | | | | | | | | | | | | | |
|-------------------------|----------|-----|--------|---------|---------|-----------|-----|--------|---------|---------|-------------|-----|--------|---------|---------|
| Visit # | Oral DRT | | | | | Nasal DRT | | | | | Cranial DRT | | | | |
| | Mean | SD | Median | Range | p-value | Mean | SD | Median | Range | p-value | Mean | SD | Median | Range | p-value |
| 0 | 8.4 | 2.7 | 10.0 | 1 to 10 | - | 9.4 | 0.9 | 10.0 | 7 to 10 | - | 8.5 | 3.0 | 10.0 | 1 to 10 | - |
| 1 | 7.2 | 3.4 | 9.0 | 0 to 10 | 0.4983 | 9.2 | 1.2 | 10.0 | 6 to 10 | 0.9996 | 8.6 | 2.7 | 10.0 | 2 to 10 | 0.9999 |
| 2 | 7.0 | 3.3 | 8.0 | 0 to 10 | 0.3543 | 8.7 | 2.1 | 10.0 | 3 to 10 | 0.9461 | 9.2 | 1.9 | 10.0 | 3 to 10 | 0.9494 |
| 3 | 7.4 | 2.9 | 8.0 | 0 to 10 | 0.6523 | 8.9 | 2.0 | 10.0 | 4 to 10 | 0.9891 | 8.9 | 2.5 | 10.0 | 1 to 10 | 0.9972 |
| 4 | 7.0 | 3.6 | 9.0 | 0 to 10 | 0.3086 | 7.5 | 3.8 | 9.5 | 0 to 10 | 0.129 | 8.8 | 2.4 | 10.0 | 1 to 10 | 0.9995 |
| 5 | 7.2 | 3.1 | 8.0 | 1 to 10 | 0.4629 | 7.9 | 3.2 | 9.0 | 0 to 10 | 0.3808 | 8.6 | 2.4 | 10.0 | 2 to 10 | 0.9998 |
| 6 | 8.3 | 2.4 | 9.0 | 1 to 10 | >0.9999 | 8.7 | 1.8 | 10.0 | 5 to 10 | 0.9616 | 8.9 | 1.9 | 10.0 | 4 to 10 | 0.9993 |
| 7 | 9.0 | 1.7 | 10.0 | 4 to 10 | 0.9569 | 9.8 | 0.4 | 10.0 | 9 to 10 | 0.9995 | 9.5 | 1.2 | 10.0 | 6 to 10 | 0.8088 |
| 8 | 9.3 | 1.6 | 10.0 | 3 to 10 | 0.7844 | 9.7 | 0.6 | 10.0 | 8 to 10 | 0.9996 | 9.1 | 1.7 | 10.0 | 4 to 10 | 0.9813 |

Comments: Difference from baseline analyzed using Dunnett's multiple comparisons test (ordinary 2-way ANOVA); statistically significant p-values set at *p < 0.05.

Table 5.11: Nasal mucositis scores (0-10) for each group, at each assessment time point.

| Nasal mucositis (score) | | | | | | | | | | | | | | | |
|-------------------------|----------|-----|--------|--------|---------|-----------|-----|--------|--------|---------|-------------|-----|--------|--------|---------|
| Visit # | Oral DRT | | | | | Nasal DRT | | | | | Cranial DRT | | | | |
| | Mean | SD | Median | Range | p-value | Mean | SD | Median | Range | p-value | Mean | SD | Median | Range | p-value |
| 0 | 0.0 | 0.0 | 0.0 | 0 to 0 | - | 0.6 | 1.3 | 0.0 | 0 to 4 | - | 0.0 | 0.0 | 0.0 | 0 to 0 | - |
| 1 | 0.0 | 0.0 | 0.0 | 0 to 0 | >0.9999 | 0.7 | 1.4 | 0.0 | 0 to 4 | 0.9997 | 0.1 | 0.2 | 0.0 | 0 to 1 | 0.9998 |
| 2 | 0.1 | 0.6 | 0.0 | 0 to 3 | 0.9994 | 0.9 | 1.2 | 0.0 | 0 to 3 | 0.9452 | 0.1 | 0.5 | 0.0 | 0 to 2 | 0.9996 |
| 3 | 0.6 | 1.3 | 0.0 | 0 to 5 | 0.3931 | 1.3 | 1.6 | 0.0 | 0 to 5 | 0.4273 | 0.0 | 0.0 | 0.0 | 0 to 0 | >0.9999 |
| 4 | 1.1 | 2.0 | 0.0 | 0 to 7 | 0.0142* | 1.7 | 2.0 | 2.0 | 0 to 6 | 0.0500 | 0.0 | 0.0 | 0.0 | 0 to 0 | >0.9999 |
| 5 | 0.8 | 1.5 | 0.0 | 0 to 4 | 0.0947* | 1.7 | 1.7 | 1.5 | 0 to 5 | 0.0417* | 0.0 | 0.0 | 0.0 | 0 to 0 | >0.9999 |
| 6 | 0.5 | 1.3 | 0.0 | 0 to 5 | 0.5777 | 2.0 | 2.7 | 1.0 | 0 to 8 | 0.0038* | 0.0 | 0.0 | 0.0 | 0 to 0 | >0.9999 |
| 7 | 0.3 | 0.7 | 0.0 | 0 to 2 | 0.9331 | 1.4 | 1.7 | 1.0 | 0 to 6 | 0.2215 | 0.0 | 0.0 | 0.0 | 0 to 0 | >0.9999 |
| 8 | 0.1 | 0.3 | 0.0 | 0 to 1 | 0.9996 | 1.6 | 1.3 | 1.5 | 0 to 4 | 0.1224 | 0.0 | 0.0 | 0.0 | 0 to 0 | >0.9999 |

Comments: Difference from baseline analyzed using Dunnett's multiple comparisons test (ordinary 2-way ANOVA); statistically significant p-values set at * $p < 0.05$.

Table 5.12: Radiodermatitis scores (0-10) for each group, at each assessment time point.

| Radiodermatitis (score) | | | | | | | | | | | | | | | |
|-------------------------|----------|-----|--------|--------|----------|-----------|-----|--------|---------|----------|-------------|-----|--------|--------|---------|
| Visit # | Oral DRT | | | | | Nasal DRT | | | | | Cranial DRT | | | | |
| | Mean | SD | Median | Range | p-value | Mean | SD | Median | Range | p-value | Mean | SD | Median | Range | p-value |
| 0 | 0.3 | 1.3 | 0.0 | 0 to 0 | - | 0.0 | 0.0 | 0.0 | 0 to 0 | - | 0.0 | 0.0 | 0.0 | 0 to 0 | - |
| 1 | 0.0 | 0.0 | 0.0 | 0 to 0 | 0.9922 | 0.0 | 0.0 | 0.0 | 0 to 0 | >0.9999 | 0.2 | 0.5 | 0.0 | 0 to 2 | 0.9994 |
| 2 | 0.4 | 1.1 | 0.0 | 0 to 4 | 0.9994 | 0.5 | 1.2 | 0.0 | 0 to 4 | 0.8353 | 0.2 | 1.0 | 0.0 | 0 to 4 | 0.9970 |
| 3 | 1.1 | 1.4 | 1.0 | 0 to 4 | 0.2166 | 1.0 | 1.4 | 1.0 | 0 to 5 | 0.2110 | 0.1 | 0.3 | 0.0 | 0 to 1 | 0.9998 |
| 4 | 2.9 | 2.8 | 2.5 | 0 to 8 | <0.0001* | 2.7 | 2.3 | 3.0 | 0 to 6 | <0.0001* | 0.1 | 0.5 | 0.0 | 0 to 2 | 0.9996 |
| 5 | 4.1 | 2.2 | 4.0 | 1 to 8 | <0.0001* | 6.3 | 1.9 | 6.0 | 3 to 10 | <0.0001* | 0.2 | 0.5 | 0.0 | 0 to 2 | 0.9994 |
| 6 | 3.4 | 2.0 | 3.0 | 1 to 7 | <0.0001* | 3.9 | 1.8 | 3.0 | 2 to 8 | <0.0001* | 0.3 | 0.8 | 0.0 | 0 to 3 | 0.9968 |
| 7 | 2.0 | 1.2 | 2.0 | 0 to 4 | 0.0002* | 3.2 | 1.3 | 3.0 | 1 to 5 | <0.0001* | 0.3 | 0.8 | 0.0 | 0 to 3 | 0.9884 |
| 8 | 1.7 | 1.3 | 2.0 | 0 to 4 | 0.0029* | 2.4 | 1.4 | 2.0 | 1 to 5 | <0.0001* | 0.3 | 0.8 | 0.0 | 0 to 3 | 0.9968 |

*Comments: Difference from baseline analyzed using Dunnett's multiple comparisons test (ordinary 2-way ANOVA); statistically significant p-values set at *p < 0.05.*

5.3.2.3 Risk factors: Ordinal regression analysis revealed that tumor location ($R^2 = 0.0403$; 95% CI, -0.6707 to 0.0156; $p = 0.0403$), appetite ($R^2 = 0.1843$; 95% CI, -0.0376 to 0.1439; $p = 0.0012$), and diet acceptance ($R^2 = 0.1535$; 95% CI, -0.2006 to 1.200; $p = 0.0071$) significantly correlated with the occurrence of RIM at the end of DRT (Table 5.13). The likelihood (calculated by means of Chi-squared analysis) to develop VRTOGs > 0 in the total population was greater for those patients exhibiting tumors in the oral (35.2%) and nasal cavity (27.8%) in comparison to patients exhibiting tumors in the cranial cavity (16.7%). Also, the likelihood of developing VRTOGs > 0 was greater for those patients exhibiting high scores (i.e., scores above 6) of appetite and diet acceptance (77.8% for both variables) in comparison to the patients exhibiting lower scores (1.2% for both variables), however, only 1 dog presented scores below 6 at enrollment. Sex, life stage, breed, neuter status, body weight, BCS, oral mucositis and dental prophylaxis before DRT, current diet, systemic-anti-inflammatory drugs, narcotics, antiemetics/gastroprotectants, antibiotics, and novel therapeutics or herbal/nutritional supplements were not significantly associated with the occurrence of RIM.

In line with the ordinal regression analysis, the logistic regression analysis (Table 5.13) revealed that tumor location ($p = 0.0419$) was a significant predictor of severe RIM (i.e., VRTOGs of 3). The likelihood (calculated by means of Chi-squared analysis) of developing severe RIM in the total population was greater for those patients exhibiting tumors in the oral (13.0%) and nasal cavity (9.3%) in comparison to those patients exhibiting tumors in the cranial cavity (0%). Dog breed appeared to be a significant predictor of severe RIM (i.e., VRTOGs of 3) according to our regression analysis ($p = 0.0067$). In particular, the likelihood of developing severe RIM was greater for mixed-breed dogs (13.0%) in comparison to purebred dogs (9.3%). Sex, life stage, neuter status, body weight, BCS, oral mucositis and dental prophylaxis before DRT, appetite, diet

acceptance, current diet, systemic-anti-inflammatory drugs, narcotics, antiemetics or gastroprotectants, antibiotics, and novel therapeutics or herbal/nutritional supplements did not predict severe RIM.

Table 5.13: Oral RIM risk factors (ordinal and logistic regression).

| Variables | Ordinal regression | | Logistic regression | |
|----------------------------------|-----------------------------|----------------|---------------------|----------------|
| | <i>R² square</i> | <i>p-value</i> | <i>Slope</i> | <i>p-value</i> |
| Sex | 0.0165 | 0.3534 | -0.308 to 0.848 | 0.9424 |
| Life stage | 0.0355 | 0.1721 | -0.176 to 0.961 | 0.4715 |
| Breed | 0.0477 | 0.1123 | -1.165 to 0.066 | 0.0067* |
| Neuter status | 0.0224 | 0.2592 | -0.421 to 1.532 | 0.9025 |
| Tumor location | 0.0783 | 0.0403* | -0.670 to -0.0156 | 0.0419* |
| Body weight | 0.0426 | 0.1339 | -0.087 to 0.634 | 0.1271 |
| BCS | 0.0648 | 0.0686 | -0.039 to 1.040 | 0.2498 |
| Oral mucositis (pre-DRT) | 0.0299 | 0.2112 | -0.772 to 3.414 | 0.0607 |
| Dental prophylaxis | 0.0096 | 0.4802 | -0.411 to 0.862 | 0.2310 |
| Appetite | 0.1843 | 0.0012* | 0.376 to 1.43 | 0.2176 |
| Diet acceptance | 0.1535 | 0.0071* | -0.200 to 1.200 | 0.2529 |
| Current diet | 0.0282 | 0.2248 | -0.159 to 0.663 | 0.2016 |
| Systemic anti-inflammatory drugs | 0.0037 | 0.6593 | -0.466 to 0.731 | 0.1326 |
| Narcotics | 0.0045 | 0.6288 | -0.138 to 1.232 | 0.7977 |
| Antiemetics/ gastroprotectants | 0.0111 | 0.4467 | -0.947 to 0.423 | 0.6078 |

Table 5.13 (continued)

| | | | | |
|---|---------|--------|--------------------|--------|
| Antibiotics | 0.00414 | 0.6439 | -0.945 to 0.589 | 0.3893 |
| Novel Therapeutics, herbal/nutritional Supplements | 0.00020 | 0.9192 | -1.049 to 1.161 | 0.9089 |

*Comments: Slope is represented here as 95% confidence intervals; correlation was assessed using the Spearman coefficient. Significant *p-values set at < 0.05.*

5.3.3 Assessment of aspects of reliability and validity of the “Oral Pain Scale” in dogs with RIM

5.3.3.1 Change in individual OPS question scores overtime during and following RT: Before addressing the reliability assessment, we examined the evolution of OPS scores for each item question for each group. In general, overall mean scores for each of the item question were low at all time points for all groups (Figure 5.2). In the oral DRT group, we saw a similar pattern across all questions; scores gradually increased above baseline level after ~ 50% of the prescribed DRT course was delivered (visit 2), and tended to reach their peak earlier than the other groups. Specifically, maximal OPS scores were found when dogs had received ~ 90% of the prescribed DRT course (at the time of maximal RIM severity), and scores at this time point were higher than the ones documented for nasal and cranial DRT groups for the following questions: “OPS_Eat”, “OPS_Drink”, “OPS_Vocalize” “OPS_Swallow”, and “OPS_Play”. After DRT completion, scores gradually decreased reaching baseline values by visit 8. In the nasal DRT group, the change in scores over time was similar to the one displayed by oral DRT dogs, but the curve was shifted slightly to the right (delay in increased scores). Specifically, scores from all OPS questions were increased over their baseline level after ~ 75% of the prescribed DRT course was delivered (visit 3), and tended to reach their peak one week later than the oral DRT group when dogs had received ~ 100% of the prescribed DRT course (at the time of maximal RIM severity). At this visit, OPS

scores were higher than those displayed by the oral DRT group for the “OPS_Pet” question, and higher than scores displayed by the cranial DRT group for the following questions: “OPS_Eat”, “OPS_Pet”, and “OPS_Play”. After reaching the peak, scores from the nasal DRT group gradually decreased reaching baseline values at the end of the study (visit 8). In the cranial DRT group, we did not notice a substantial change from baseline in scores for most OPS questions throughout the study.

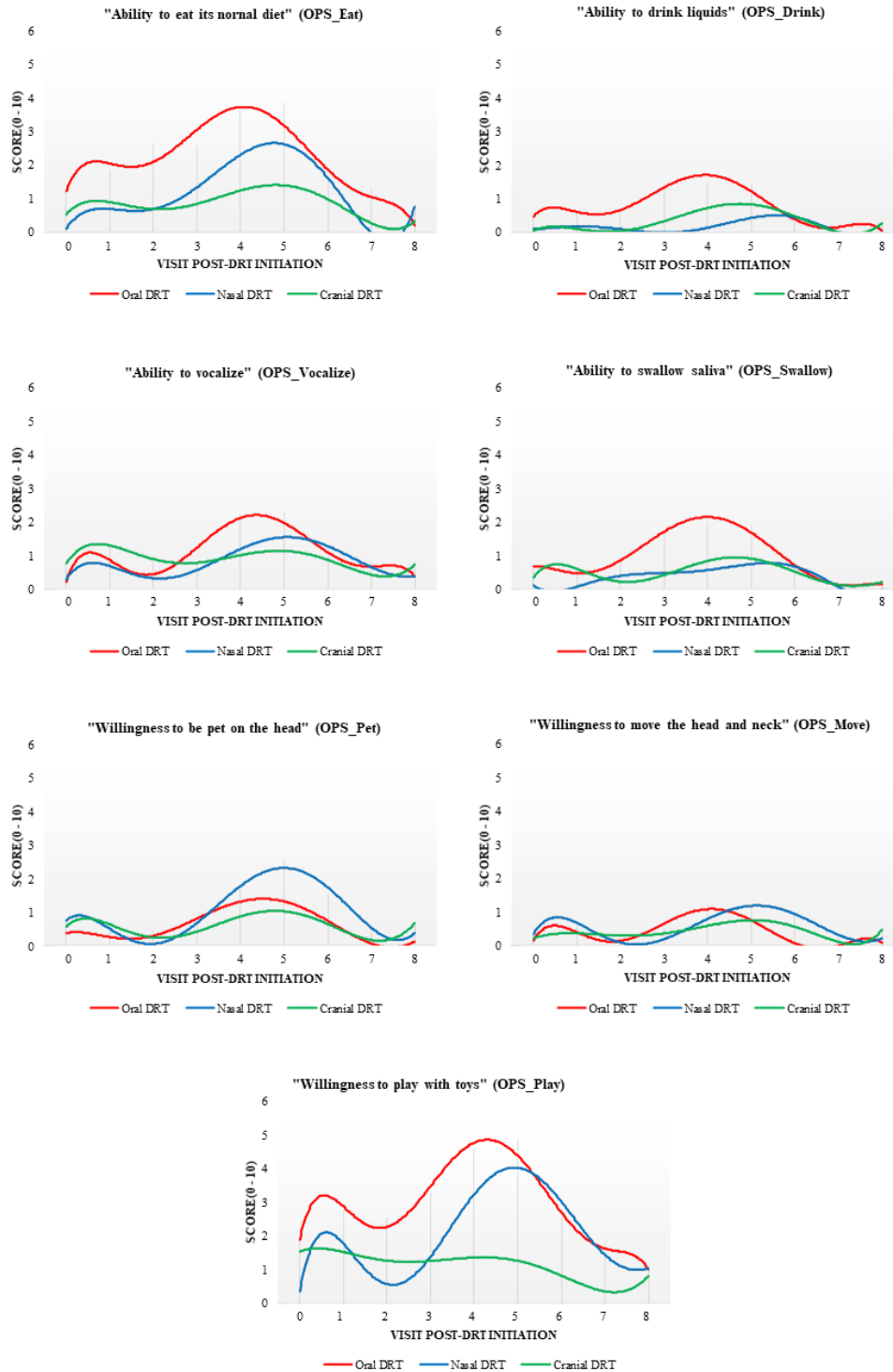


Figure 5.2: Change in individual OPS question scores overtime during and following RT.

Plots of change in OPS scores for each question over the study period for each group (polynomial trendlines, fluctuation's order: 6).

5.3.3.2 Reliability assessment: According to the obtained Cronbach’s alpha coefficient, the OPS had a high internal consistency (α of 0.867). As shown in Table 5.14, individual inter-item correlation means for all questions ranged from 0.409 to 0.575 indicating no item redundancy.

Table 5.14: Inter-correlation matrix (assessment time point: visit 2).

| Item question | Inter-item correlation matrix | | | | | | | Inter-item correlation means |
|---------------------|-------------------------------|-----------|--------------|-------------|---------|----------|----------|------------------------------|
| | OPS_Eat | OPS_Drink | OPS_Vocalize | OPS_Swallow | OPS_Pet | OPS_Move | OPS_Play | |
| OPS_Eat | - | 0.505 | 0.483 | 0.543 | 0.428 | 0.316 | 0.494 | 0.462 |
| OPS_Drink | 0.505 | - | 0.586 | 0.641 | 0.574 | 0.478 | 0.664 | 0.575 |
| OPS_Vocalize | 0.483 | 0.586 | - | 0.419 | 0.463 | 0.576 | 0.77 | 0.550 |
| OPS_Swallow | 0.543 | 0.641 | 0.419 | - | 0.574 | 0.33 | 0.427 | 0.489 |
| OPS_Pet | 0.428 | 0.574 | 0.463 | 0.574 | - | 0.293 | 0.515 | 0.475 |
| OPS_Move | 0.316 | 0.478 | 0.576 | 0.33 | 0.293 | - | 0.458 | 0.409 |
| OPS_Play | 0.494 | 0.664 | 0.77 | 0.427 | 0.515 | 0.458 | - | 0.555 |

Overall mean, variance, and inter-item correlation at visit 2 were 0.778, 2.947, and 0.502, respectively. According to the item-total statistics analysis (Table 5.15), the resulting overall mean score of this scale decreased from 0.778 to 0.655, 0.773, and 0.624 if the item questions “OPS_Eat”, “OPS_Vocalize”, or “OPS_Play” were removed, respectively. Conversely, the resulting overall mean score of this scale increased from 0.778 to 0.851, 0.819, 0.853, and 0.874 if the item questions “OPS_Drink”, “OPS_Swallow”, “OPS_Pet” or “OPS_Move” were removed, respectively. Regarding variance, the overall variance of this scale increased from 2.947 to 2.974, 3.314, 3.221, and 3.327 if the item questions “OPS_Drink”, “OPS_Vocalize”, “OPS_Swallow”,

or “OPS_Pet” were removed, respectively, and decreased from 2.947 to 2.373 and 2.039 if the item questions “OPS_Eat” or “OPS_Play” were removed, respectively. Additionally, the resulting overall item-total correlation did not improve if any of the item questions were removed, however, the item-total correlation was lower if the questions “OPS_Drink”, “OPS_Vocalize”, or “OPS_Play” were removed. Cronbach’s α did not increase when any item questions were deleted. In summary, based on these data, we concluded that the OPS has adequate reliability and that all originally included item questions (i.e., “OPS_Eat”, “OPS_Drink”, “OPS_Vocalize”, “OPS_Swallow”, “OPS_Move”, “OPS_Pet”, and “OPS_Play”) contribute to the resulting OPS scores. Therefore, all item questions were included in the validation assessment.

Table 5.15: Item-total statistics (assessment time point: visit 2).

| Item question | Item-Total Statistics | | | |
|---------------|----------------------------|--------------------------------|----------------------------------|----------------------------------|
| | Scale Mean if Item Deleted | Scale Variance if Item Deleted | Corrected Item-Total Correlation | Cronbach's Alpha if Item Deleted |
| OPS_Eat | 0.655 | 2.373 | 0.508 | 0.792 |
| OPS_Drink | 0.851 | 2.974 | 0.490 | 0.782 |
| OPS_Vocalize | 0.773 | 3.314 | 0.494 | 0.750 |
| OPS_Swallow | 0.819 | 3.221 | 0.504 | 0.786 |
| OPS_Pet | 0.853 | 3.327 | 0.506 | 0.796 |
| OPS_Move | 0.874 | 3.382 | 0.517 | 0.810 |
| OPS_Play | 0.624 | 2.039 | 0.493 | 0.773 |

5.3.3.3 Validity assessment

5.3.3.3.a) *Factor analysis:* Before performing factor analysis, sampling adequacy was verified using KMO, BTS, and communalities. Here, we found a KMO value of 0.841, and BTS was significant ($p < 0.001$). Moreover, the calculated communalities for each question were above 0.4 (Table 5.16), and the cumulative percent of variance was higher than 50% (i.e., 57.9%). Therefore,

factor analysis was determined to be appropriate. Only one factor component was extracted from PCA (Table 5.17). Therefore, the OPS appeared to be a uni-dimension scale (i.e., item questions fit into a single theoretical construct).

Table 5.16: Communalities (assessment time point: visit 2).

| Item question | Communality extracted |
|----------------------|------------------------------|
| OPS_Eat | 0.499 |
| OPS_Drink | 0.718 |
| OPS_Vocalize | 0.669 |
| OPS_Swallow | 0.545 |
| OPS_Pet | 0.526 |
| OPS_Move | 0.405 |
| OPS_Play | 0.687 |

Table 5.17: Factor loadings extracted from the PCA (assessment time point: visit 2).

| Item question | Factor loading |
|----------------------|-----------------------|
| OPS_Eat | 0.707 |
| OPS_Drink | 0.848 |
| OPS_Vocalize | 0.818 |
| OPS_Swallow | 0.738 |
| OPS_Pet | 0.725 |
| OPS_Move | 0.637 |
| OPS_Play | 0.829 |

5.3.3.3.b) *Concurrent validity:* Concurrent validity was assessed using those scores documented at the time that most dogs (no group distinction) developed VRTOG scores > 2 (i.e., visit 2). According to this analysis, there was a low correlation (i.e., Spearman $r = 0.077$; $p = 0.5672$; 95%

confidence interval: -0.1928 to 0.3354) between the OPS (by means of TF scores) and VRTOG scores documented at this specific visit.

5.3.3.3.c) Extreme group comparison: Extreme group comparison was assessed using those scores documented at the time that dogs (no group distinction) completed their prescribed DRT course (i.e., visit 5). According to this analysis, the OPS was able to discriminate dogs with VRTOG scores of 0 (zero) from those with VRTOG scores > 2 ($p = 0.0466$).

5.3.3.3.d) Responsiveness: The responsiveness of this CMI tool (OPS) was assessed by comparing those scores documented at the time that dogs (no group distinction) were enrolled in this study (visit 0) with those documented when dogs completed their prescribed DRT course (visit 5), and at the end of the study (visit 8). According to this analysis, the OPS was effective in discriminating baseline scores (before DRT) from those scores documented at the end of DRT when RIM was most severe ($p < 0.0001$). When baseline OPS scores were compared to those documented at the end of follow-up (i.e., RIM resolution), no statistically significant difference was found ($p = 0.5743$).

5.3.4 Pain assessment using PSS, PIS, OIS, and OPS in pet dogs with RIM

We compared the scores from the PSS, PIS, OIS, and OPS between all groups (i.e., oral versus nasal versus cranial DRT) at all visits (visit 0 versus visit 2 to 8).

5.3.4.1 Pain severity scale (PSS): As shown in Figure 5.3, low scores (i.e., overall PSS scores < 1.5) were found in all dogs at enrollment (baseline measure), and they did not significantly change from baseline during the first 3 weeks after DRT initiation (overall p -values > 0.1). These scores were maintained until the end of the study for the cranial DRT group (overall mean scores < 1.2 , and overall difference from baseline non-significant). However, higher grade PSS scores were seen in oral and nasal DRT groups after completing $\sim 90\%$ of the prescribed DRT course (visit 4).

Scores at this visit were significantly higher in oral and nasal DRT groups as compared to the cranial DRT group (oral versus cranial DRT, $p < 0.0001$; nasal versus cranial DRT, $p < 0.0001$), and scores in both oral and nasal DRT groups were significantly higher at this visit than those documented at baseline ($p < 0.0001$ for both comparisons). Maximal scores were found in oral and nasal DRT groups after they completed their prescribed DRT course (visit 5). In these dogs, PSS scores at visit 5 were significantly higher than those reported for the cranial DRT group ($p < 0.0001$ for both comparisons), and significantly higher than baseline ($p < 0.0001$ for both comparisons). Scores were decreased in both oral and nasal DRT groups in the next visit (first follow-up assessment; visit 6). Yet, scores here remained significantly higher than those documented for the cranial DRT group (oral versus cranial DRT, $p = 0.0229$; nasal versus cranial DRT, $p = 0.0024$), and significantly higher than those documented at baseline (oral DRT, $p = 0.0440$; nasal DRT, $p = 0.0299$). Scores returned to baseline levels for oral and nasal DRT groups after visit 7 (oral DRT, $p = 0.9358$; nasal DRT, $p = 0.9997$), and continued to be low until the end of the study (visit 8; oral DRT, $p = 0.9632$; nasal DRT, $p = 0.9926$). No statistically significant differences were found between groups at visits 7 and 8.

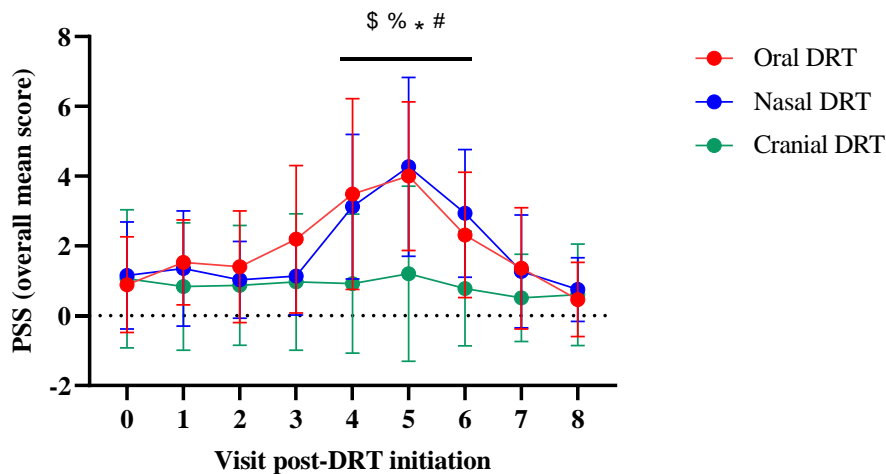


Figure 5.3: Pain severity scale (PSS). Plots of overall PSS score for each group over time.

Comparisons between visit 0 (baseline) and visits 2 to 8 were done using a 2-way ANOVA analysis (with Dunnett's multiple comparisons test); symbols represent the difference from baseline in oral ($^{\$}p < 0.05$) and nasal ($^{\%}p < 0.05$) DRT groups. Comparisons between groups were done using 2-way ANOVA analysis (with Tukey's multiple comparisons test); symbols represent the difference between oral and cranial DRT groups ($^*p < 0.05$) and between nasal and cranial DRT groups ($^{\#}p < 0.05$). Data expressed as mean + SD.

5.3.4.2 Pain interference scale (PIS): As shown in Figure 5.4, low-grade scores (i.e., overall PIS scores < 2) were found in all dogs at enrollment (baseline measure), and they did not significantly change from baseline (overall p-values > 0.1). This behavior pattern was maintained until the end of the study for all groups (overall difference from baseline $p > 0.4$). In general, no statistically significant differences in scores were found across groups at any time point, except for visit 6. At this visit, the nasal DRT group had PIS scores significantly higher than the oral DRT group ($p = 0.0107$).

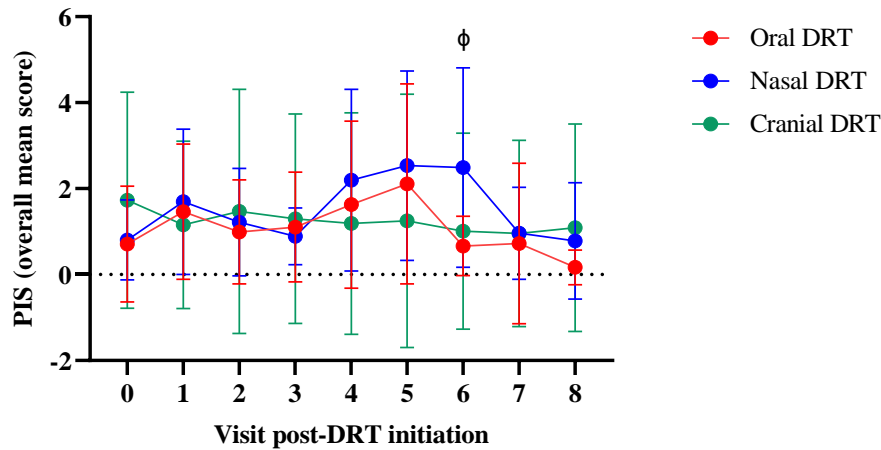


Figure 5.4: Pain interference scale (PIS). Plots of overall PIS score for each group over time. Comparisons between visit 0 (baseline) and visits 2 to 8 were done using a 2-way ANOVA analysis (with Dunnett's multiple comparisons test). Comparisons between groups were done using 2-way ANOVA analysis (with Tukey's multiple comparisons test); symbols represent the difference between oral and nasal DRT groups ($\phi < 0.05$). Data expressed as mean + SD.

5.3.4.3 Overall impression scale (OIS): In general, high-grade scores (i.e., OIS scores ranging from 3.5 to 4, scale 0-5) were found in most dogs at enrollment and maintained until the last visit (Figure 5.5). However, a significant decrease in scores (as compared to baseline measures) was found in the oral DRT group after completing ~ 90% of the prescribed DRT course (visit 4; $p = 0.0253$). However, no statistically significant differences were found between groups at this time point. A maximal decrease in scores was found in oral and nasal DRT groups at visit 5 (DRT completion). Here, scores from both groups were significantly lower than baseline (oral DRT, $p = 0.0005$; nasal DRT, $p = 0.0120$), and were also significantly lower than those documented for the cranial DRT group (oral versus cranial DRT, $p = 0.0163$; nasal versus cranial DRT, $p = 0.0030$). In these groups (oral and nasal DRT), scores started to increase in the following visit (visit 6),

returning to baseline values by visit 7. No statistically significant differences from baseline were found at any time point for the cranial DRT group.

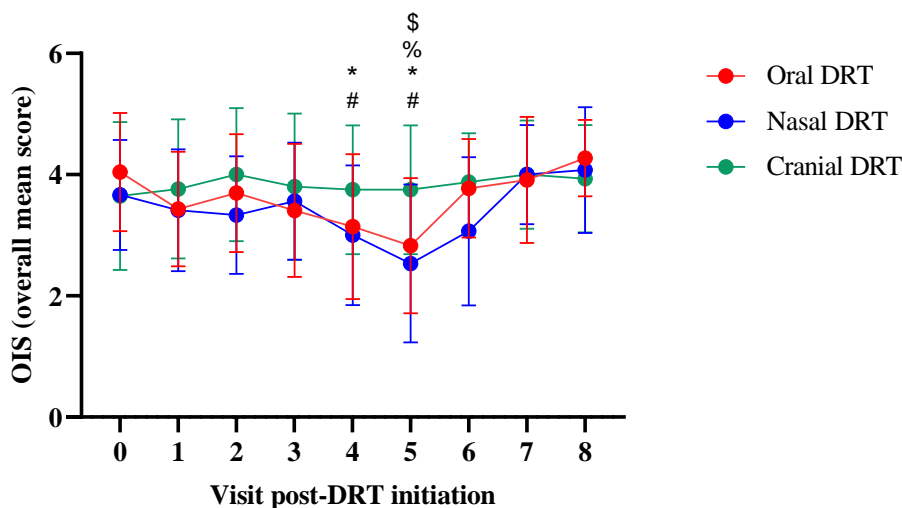


Figure 5.5: Overall impression scale (OIS). Plots of overall OIS score for each group over time. Comparisons between visit 0 (baseline) and visits 2 to 8 were done using a 2-way ANOVA analysis (with Dunnett's multiple comparisons test); symbols represent the difference from baseline in oral ($\$p < 0.05$) and nasal ($\%p < 0.05$) DRT groups. Comparisons between groups were done using 2-way ANOVA analysis (with Tukey's multiple comparisons test); symbols represent the difference between oral and cranial DRT groups ($*p < 0.05$) and between nasal and cranial DRT groups ($\#p < 0.05$). Data expressed as mean + SD.

5.3.4.4 Oral pain scale (OPS): As shown in Figure 5.6, low-grade scores (i.e., overall OPS scores < 0.6) were found in all dogs at enrollment (baseline measure), and they did not significantly change from baseline during the first 2 weeks after DRT initiation (overall p-values > 0.1). However, higher grade scores were seen in the oral DRT group after completing ~ 75% of the prescribed DRT course (visit 3). At this visit, scores from the oral DRT group were significantly

higher than baseline measures ($p = 0.0298$) and significantly higher in comparison to nasal and cranial DRT groups (oral versus nasal DRT, $p = 0.0083$; oral versus cranial DRT, $p = 0.0214$). In the next visit (visit 4), maximal scores were found the oral DRT group after completing ~ 90% of the prescribed DRT course; scores from the oral DRT groups remained significantly higher than baseline measures ($p = 0.0002$) and were significantly higher in comparison to cranial DRT group ($p < 0.0103$). In this visit (visit 4), an increase in scores was also found in nasal and cranial DRT groups, however, no differences from baseline were found for both groups. After DRT completion, maximal scores were found in nasal and cranial DRT groups; scores here were only significantly higher than baseline measures in the nasal DRT group ($p = 0.0062$). In this visit, scores from the oral DRT group were significantly higher than the cranial DRT group ($p = 0.0388$), and they were also significantly higher than baseline ($p = 0.0004$). No relevant differences were found between oral and nasal DRT groups, nor between nasal nor cranial DRT groups at this time point. A rapid decrease in OPS scores was seen in all dogs in the next visit (first follow-up assessment; visit 6), and continued decreasing until the end of the study. In these visits (visit 6 to 8), no statistically significant differences were found between groups, nor between assessment time points for any group.

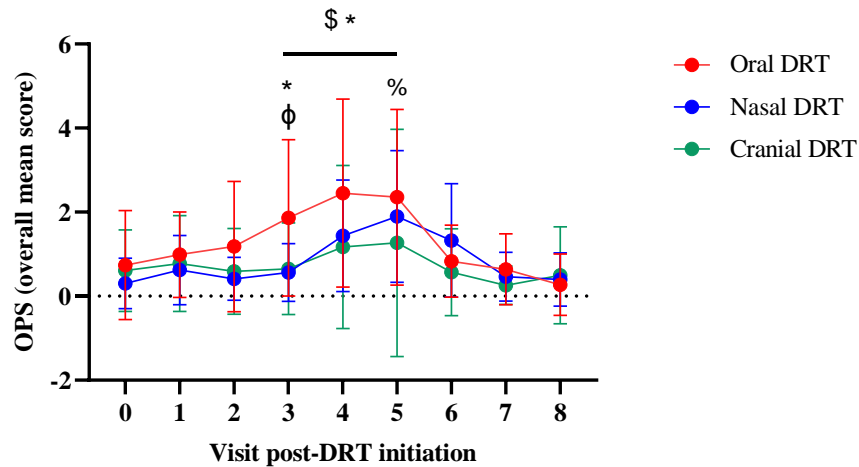


Figure 5.6: Oral pain scale (OPS). Plots of overall OPS score for each group over time. Comparisons between visit 0 (baseline) and visits 2 to 8 were done using a 2-way ANOVA analysis (with Dunnett's multiple comparisons test); symbols represent the difference from baseline in oral ($^{\$}p < 0.05$) and nasal ($^{\%}p < 0.05$) DRT groups. Comparisons between groups were done using 2-way ANOVA analysis (with Tukey's multiple comparisons test); symbols represent the difference between oral and cranial DRT groups ($^*p < 0.05$), nasal and cranial DRT groups ($^{\#}p < 0.05$), and between oral and nasal DRT groups ($^{\phi}p < 0.05$). Data expressed as mean + SD.

5.3.5 Exploration of individual question responsiveness and discriminatory ability

While the OPS was able to discriminate oral DRT from nasal and cranial DRT groups at certain times during the course of this study, the results here suggested that oral irradiation resulted in low levels of oral pain/interference (low overall mean OPS scores). This observation differs from those made by pain and radiation oncology specialists in clinical practice who suggest that most dogs submitted to oral irradiation (as in humans) display a great level of oral pain/interference by the end of DRT. Therefore, we decided to explore the behavior patterns of each question included in the PSS, PIS, and OPS to understand whether there were individual questions that detected oral

pain or dysfunction better than other questions. For each scale, we compared scores of each individual item question documented at visit 4 (when RIM was most severe for oral/nasal DRT groups) between groups and between baseline measures.

5.3.5.1 Group comparison: As shown in Figure 5.7, the 4 item questions of the PSS and the item question “Enjoyment of life” of the PIS were able to discriminate between oral and cranial DRT groups. Meanwhile, the OPS item questions “Ability to eat its normal diet” and “Willingness to play with toys” were able to discriminate between oral and cranial DRT dogs (Figure 5.8). No difference in scores was found between oral and nasal DRT dogs when the PSS, PIS, or OPS was applied.

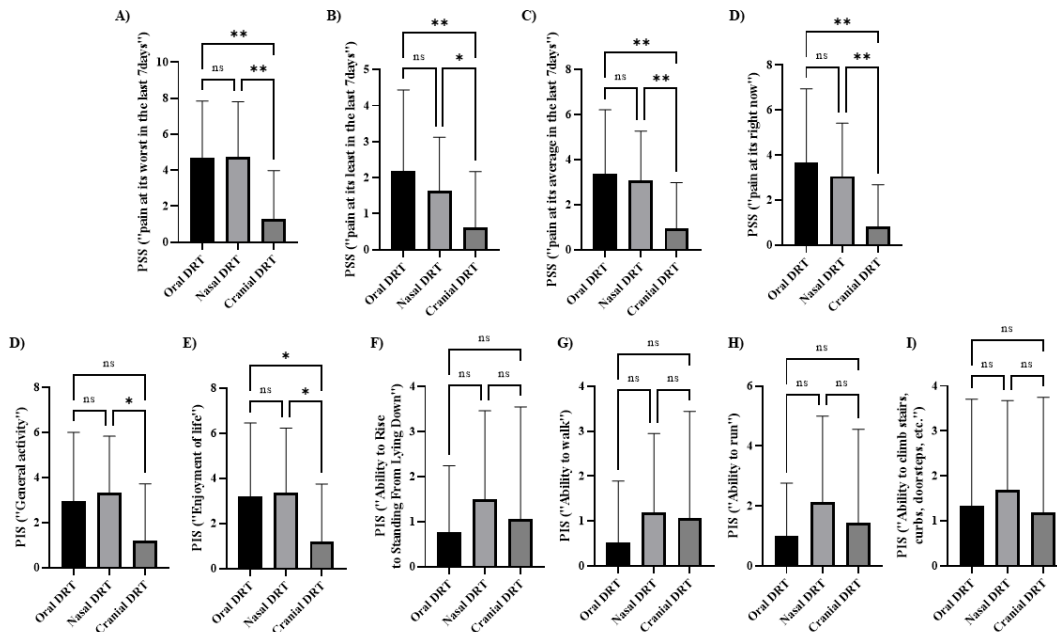


Figure 5.7. Individual item question’ scores for the PSS (A to D) and PIS (D to I) questionnaires. Data analyzed using Kruskal-Wallis’s test, followed by Dunn’s multiple comparisons test; statistically significant p-values set at *p < 0.05; **p < 0.01; ***p < 0.001; ****p < 0.0001; ns., not significant.

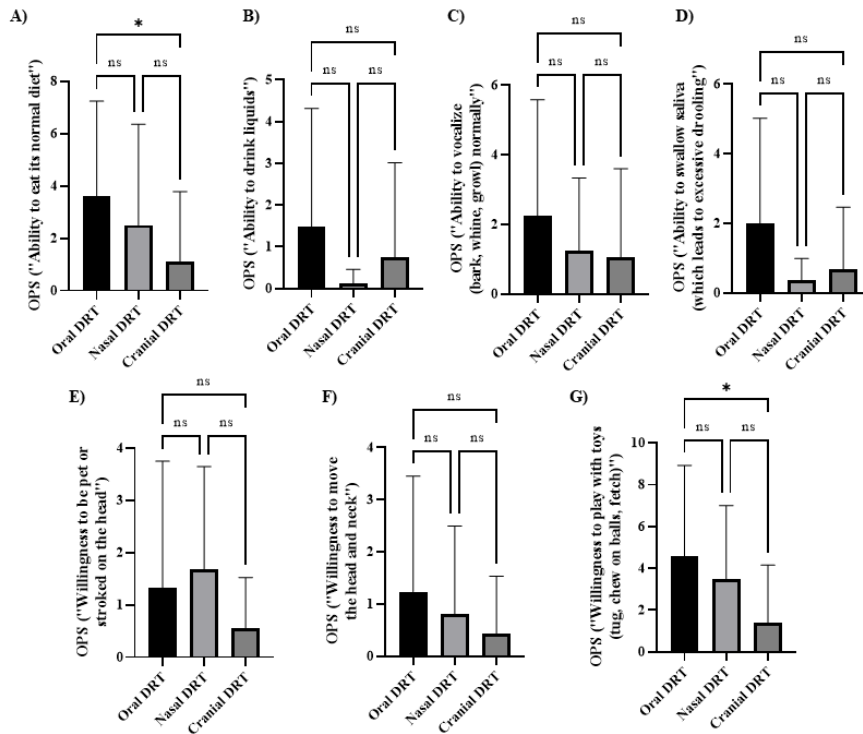


Figure 5.8. Individual item question’ scores for the OPS (A to G) questionnaires. Data analyzed using Kruskal-Wallis’s test, followed by Dunn's multiple comparisons test; statistically significant p-values set at * $p < 0.05$; ** $p < 0.01$; *** $p < 0.001$; **** $p < 0.0001$; ns., not significant.

5.3.5.2 Baseline comparison for each group: As shown in Table 5.18, the following item questions were able to discriminate baseline measures from visit 4: “Pain at its worst in the last 7 days”, “Pain at its least in the last 7 days”, “Pain at its average in the last 7 days”, “Pain at its right now”, “General activity”, “Enjoyment of life”, “Overall quality of life”, “Ability to eat its normal diet”, “Ability to vocalize”, “Ability to swallow”, and “Willingness to play with toys”.

Table 5.18: Comparison of individual item question scores documented at baseline against those documented at visit 4 (comparison using p-values).

| Scale | Item question | Oral DRT | Nasal DRT | Cranial DRT |
|------------|--------------------------------------|----------|-----------|-------------|
| PSS | Pain worst | <0.0001* | 0.0008* | 0.9831 |
| | Pain least | <0.0001* | 0.0004 | 0.6702 |
| | Pain average | <0.0001* | 0.0002* | 0.8375 |
| | Pain now | 0.0003* | <0.0001* | 0.9198 |
| PIS | General activity | 0.0002* | 0.0113* | 0.8385 |
| | Enjoyment of life | <0.0001* | 0.0004* | 0.7281 |
| | Ability to rise | 0.6273 | 0.4271 | 0.707 |
| | Ability to walk | 0.8589 | 0.4682 | 0.2283 |
| | Ability to run | 0.3219 | 0.2704 | 0.1303 |
| | Ability to climb | 0.2812 | 0.1992 | 0.1344 |
| OIS | Quality of life | 0.0005* | 0.012* | 0.9996 |
| OPS | Ability to eat | 0.0071* | 0.0025* | 0.3261 |
| | Ability to drink | 0.0959 | 0.3145 | 0.3519 |
| | Ability to vocalize | 0.0004* | 0.0537 | 0.8039 |
| | Ability to swallow | 0.0374* | 0.1055 | 0.3135 |
| | Willingness to be pet | 0.1243 | 0.02* | 0.2779 |
| | Willingness to move head/neck | 0.0845 | 0.2246 | 0.7249 |
| | Willingness to play with toys | 0.0053* | 0.0014* | 0.7082 |

Comments: Data analyzed using Mann Whitney test; statistically significant p-values set at *p < 0.05.

5.3.5.3 New scale development: Based on these results, and taking into consideration the results from sections 5.3.3 and 5.3.4, we concluded that the following item questions seemed to be best in tracking the changes in VRTOG scores: (1) “Pain at its worst in the last 7 days”, (2) “Pain at its least in the last 7 days”, (3) “Pain at its average in the last 7 days”, (4) “Pain at its right now”, (5) “Enjoyment of life”, (6) “Ability to eat its normal diet”, and (7) “Willingness to play with toys”. Therefore, we combined these questions and used them to compare groups (oral versus nasal versus cranial DRT) and changes from baseline. Scores here were averaged across questions to create a single overall score.

5.3.5.3.a) Reliability assessment: Before conducting any multiple comparison analysis, we tested the reliability of this scale by means of internal consistency using Cronbach’s alpha coefficient; the temporal choice for evaluation corresponded to visit 4 (all dogs’ scores included). The internal consistency of this scale was very high, with a Cronbach’s α of 0.957.

5.3.5.3.b) Score evolution assessment: The evolution of scores over time was very similar to the evolution of PSS scores (Figure 5.9). Regarding the group comparison, no difference was found between oral and nasal DRT groups at any time point. Significantly higher scores – as compared to cranial DRT dogs – were found in the oral DRT group at visits 3, 4, and 5, and in the nasal DRT group at visits 4, 5, and 6 (1-week delay as compared to the oral DRT group). Regarding baseline comparisons, significant differences from baseline were found in the oral DRT dogs at visits 4 and 5, and in nasal DRT dogs at visits 4, 5, and 6. No statistically significant differences were found at any time point for the cranial DRT group.

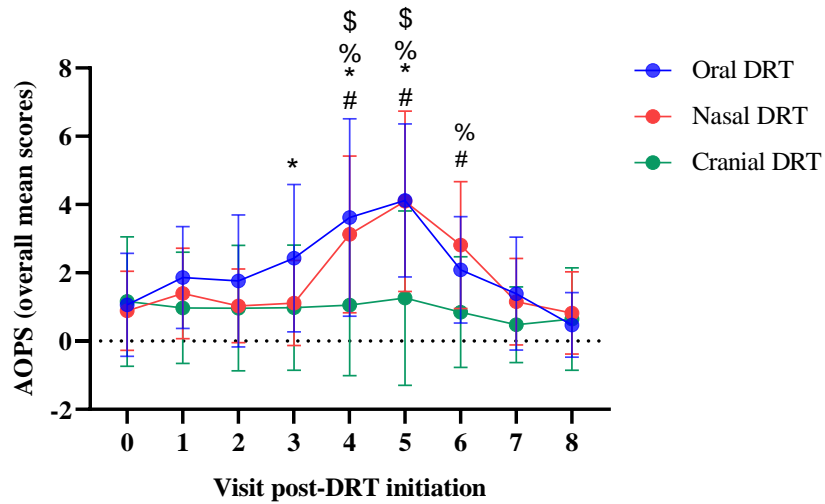


Figure 5.9: Adapted OPS (AOPS). Plots of overall AOPS score for each group over time. Comparisons between visit 0 (baseline) and visits 2 to 8 were done using a 2-way ANOVA analysis (with Dunnett's multiple comparisons test); symbols represent difference from baseline in oral ($^{\$}p < 0.05$) and nasal ($^{\%}p < 0.05$) DRT groups. Comparisons between groups were done using 2-way ANOVA analysis (with Tukey's multiple comparisons test); symbols represent the difference between oral and cranial DRT groups ($^*p < 0.05$) and between nasal and cranial DRT groups ($^{\#}p < 0.05$). Data expressed as mean + SD.

5.4 Discussion

In this body of work, we demonstrated that the clinical features of RIM as a result of oral, nasal, or cranial irradiation in pet dogs share similarities (in terms of progression, severity, and secondary side effects) with its human counterpart. In general, we found that oral, nasal, and cranial irradiations are associated with the establishment of RIM; however, the progression and severity of RIM varies depending on tumor location. In particular, our results indicated that oral/nasal DRT dogs – in comparison to cranial DRT dogs – are significantly more likely to

develop rapid RIM after the DRT initiation, as well as to develop high-grade RIM (VRTOGs >2) when increasing DRT doses are being delivered. Moreover, the risk to develop secondary side effects related to RIM (e.g., reduction in body weight, loss of appetite, decreased diet acceptance, nasal mucositis, radiodermatitis, and RT interruptions) is also higher in oral/nasal DRT dogs in comparison to cranial DRT dogs. Finally, and opposite to the “Pain Interference Scale” and “Overall Impression Scale” from the CBPI, we showed that the “Pain Severity Scale” (also from the CBPI) and the newly developed “Oral Pain Scale” are effective in detecting changes in RIM progression, as well as in discriminating dogs with higher grades of RIM (i.e., oral/nasal DRT dogs) against dogs with lower RIM grades (i.e., cranial DRT dogs). Yet, the suitability of these CMI to measure oral pain/interference in this particular scenario still need further examination.

In the first part of this study, we described the epidemiology and clinical features of RIM in pet dogs for which the owners had chosen to pursue DRT for cancer treatment. Results from this single-arm prospective observational, non-interventional clinical study indicated that, like in humans, RIM usually arises in the second week of DRT in most dogs that received either oral, nasal, or intracranial irradiation (Sroussi et al., 2017; Ying et al., 2020). While clinically relevant levels of RIM (i.e., VRTOGs > 1) were found in some dogs with cranial tumors when increased doses of irradiation were delivered, high-grade RIM (i.e., VRTOGs > 2) was only encountered in dogs with oral and nasal tumors (incidence up to 50-60%). According to our results, high-grade RIM in oral/nasal DRT dogs was typically seen in the fourth or fifth week of DRT (when dogs received more than 90% of the prescribed course). This finding certainly agrees with most studies done in human HNC, which have indicated that most HNC patients develop high-grade RIM when most of the prescribed DRT course is delivered, which usually occur 4 to 5 weeks following DRT initiation (Franco et al., 2017; Sonis et al., 1999; Sroussi et al., 2017). While there is little evidence

showing that RIM is developed in patients receiving only DRT for the treatment of intracranial malignancies, results here are in agreement with the study conducted by other authors (Yergolkar et al., 2020), who indicated that the frequency of RIM development is higher in HNC patients (50%) in comparison to patients with intracranial (brain) masses (11.5%) receiving cancer therapy (chemotherapy or radiation therapy, or combination of both). Although the severity of RIM decreased after completing the prescribed course of radiotherapy in this study, RIM seemed to persist for at least three weeks after DRT completion in dogs undergoing oral and nasal irradiation. Indeed, incomplete RIM resolution by the end of this study was seen in up to 50% of dogs with oral/nasal masses, similar to what it has been described in human HNC (Redding, 2005; Sonis, 2011).

In this work, we also described the occurrence and severity of adverse effects potentially associated to the development of RIM. According to our results, the incidence of critical weight loss (i.e., defined by most studies as a reduction $> 5\%$ from baseline during DRT) in oral and nasal DRT dogs – which was 69.6% and 55.5%, respectively – does not greatly differ from to the one reported previously in their human counterparts, with is up to 52.2% in patients receiving irradiation for oral cavity/oropharynx tumors, and up to 46% in patients receiving irradiation for nasopharynx tumors (Langius et al., 2013; Nazari et al., 2021). Remarkably, we also found – but to a lesser extent – critical weight loss in the cranial DRT group (29.4% incidence). While this finding was not entirely surprising for us since few cranial DRT dogs (5 of 17) developed some degree of RIM during DRT, it was interestingly to see this side effect in this cohort since neither RIM nor RIM-related weight loss has been reported in their human counterpart. Regarding BCS, here we also found interesting, yet conflict results. Although body mass index (BMI), which is the pet version of BCS, does not commonly change from pre-treatment measures during DRT in

human HNC, low BMI are commonly documented before DRT initiation, which has been highly associated with critical weight loss during DRT and to poorer prognosis (Lee et al., 2019; Lønbro et al., 2016; Nazari et al., 2021; Pai et al., 2012). In this work, most dogs (from all cohorts) presented adequate BCS at baseline, and as in humans, there was little-to-absent fluctuation in scores throughout the study. Therefore, we can preliminarily conclude from this work that RIM does not affect BCS in dogs during oral, nasal, or cranial DRT, yet remarkably, and unlike humans, HNC canine patients do not present pre-treatment low BCS. To our knowledge, a poor predictive association between low BCS and critical weight loss during DRT or poorer prognosis has not been reported in this species. Thus, this evidence could potentially be the rationale to promote further investigations in that area in order to determine whether the dog is a clinically predictable animal model of RIM and RAP. Another interestingly discrepancy between dogs and humans that was found in this study is related to the use of feeding tubes. Here, we only found that one dog from the oral DRT required feeding tube placement during DRT, with a total incidence of 4.3%. While this dog presented high-grade RIM (score of 3) and RIM-related DRT interruption when the feeding tube was implemented, the incidence of this side effect was significantly lower than the one reported in human HNC, which can range from 15% to 50% (Beaver et al., 2001; Trotti et al., 2003). Moreover, this incidence did not differ from the one documented in the cranial DRT group (1 dog with grade RIM of 0; 5.9% incidence). Therefore, these results could potentially reveal the possibility that the scale used here to grade the severity of RIM in dogs (i.e., VRTOG) might not perfectly match the scales used in humans. As detailed in Chapter 1, most RIM scales used in humans include the parameter “requires parenteral or enteral support” or “unable to ingest solid/liquid diet” to indicate maximal RIM severity, however, maximal RIM scores here were not associated to parenteral/enteral support. In this context, it seems pertinent to further investigate the

translational value of these assessment scoring systems in order to improve clinical translation. In that same line, results from the vast majority of clinical studies done in the human HNC population agree on the fact that both appetite and/or diet acceptance are significantly reduced once RIM is established following DRT initiation (despite the fact that incidences for appetite loss or reduced diet acceptance have been poorly detailed) (Bansal et al., 2004; Chencharick & Mossman, 1983; Ogama et al., 2010; Ravasco et al., 2005; Yucel et al., 2014). Here however, and while we found a greater incidence in oral/nasal dogs in comparison to cranial dogs, the frequency and severity of these side effects was relatively low (lower than 30%). This evidence suggests, in the author's opinion, that the reduction in food/water intake (either as a result of appetite lost or oral dysfunction), and thus body weight loss, might be exacerbated in HNC patients with high grade RIM by the emotional components (e.g., psychological and social factors) that arise as a result of RAP, which are components that may not be present or may not be as relevant in dogs as in humans. Since it has been extensively proven that cancer pain (which includes RAP) is a complex and multidimensional experience that affects and is affected by psychological and social factors (Porter & Keefe, 2011), these results points to the importance of determining the role of the emotional components of RAP in order to improve the development of mechanism-based therapies in HNC. Other side effects found in this study include nasal mucositis and radiodermatitis. Like RIM, the progress of these two toxicities depends on the field size, the interval between fractions, dose-per-fraction, previous exposure to chemotherapy, concurrent chemotherapy or presence of co-morbid medical conditions, and they usually arise along with RIM in advances human HNC cases submitted to aggressive courses of DRT (Kawamura et al., 2019; Narayan et al., 2008; Riva et al., 2019); in human patients with intracranial masses, however, these RT-related side effects have not been reported. Similarly, here we found that both nasal mucositis and radiodermatitis

were present in oral and nasal DRT dogs, and its severity was associated to an increase in RIM severity; these side effects, as in humans, were not frequent nor severe in cranial DRT dogs. Concerning to the treatment course modifications associated to RIM, we demonstrated that the incidence of DRT interruption was higher in orally irradiated dogs (13%) in comparison to nasally (5.6%) and intracranially (0%) irradiated dogs, which seems to be an effect possibly linked to the radiotherapy field or to the extension of mucosal damage. This is relevant when examining the translation value of companion dogs for the study of RIM in human HNC because poorly managed oral complications has been highly associated with treatment course interruptions or delays, which further impacts the outcome in these patients (Russo et al., 2008). According to five clinical studies reporting this outcome in human HNC, the aggregate incidence of radiation therapy breaks or modifications resulting from ulcerative oral mucositis is 11% (Adelstein et al., 1997; Bensadoun et al., 1999; Brizel et al., 1998; Dische et al., 1997; Lefebvre et al., 1996), which is comparable to the incidence reported here in dogs submitted to oral DRT. Finally, here we also reported that up to 39% of oral/nasal DRT dogs failed to complete the prescribed course of DRT, while a lower incidence was seen in cranial DRT dogs (17.6%). Although is not clear whether this outcome was related to RIM in our study (lack of specification in our database), the decision to stop ongoing DRT in humans does not always relate to RIM, and other causes may lead this outcome (such as personal reasons, associated costs, presence of other serious medical problems, among others), and its incidence greatly differs across studies, ranging from 6 to 23% in HNC patients subjected to DRT (Rosenthal, 2007; Wong et al., 2006).

In this study, we also examined the risk factors for RIM in dog patients receiving oral, nasal, and cranial DRT (no group distinction). While the current understanding of risk factors in human HNC is limited, and the literature is often conflicting, some studies have reported that

relevant factors for the prediction of RIM include total radiation dose, fractionated DRT modalities, volume of mucosa irradiated, use of concurrent chemotherapy, low body mass, prolonged neutrophil recruitment, female sex, young or old age (Barasch & Peterson, 2003; Raber-Durlacher et al., 2000; Rapoport et al., 1999; Sonis et al., 2004). As expected (and based on the aforementioned clinical features of RIM), tumor location (i.e., oral/nasal cavity tumors) revealed to be a valuable predictive indicator of RIM progression and severity in pet dogs. However, results here – while revealing – are hard to be interpreted because outcomes in this type of analysis greatly depend on how the data is managed. Specifically, no other study has gathered patients with oral, nasal, and cranial cavity tumors in the same risk factor assessment study. This is important because most analyses have examined risk factors within the same disease (i.e., HNC). However, and while we were expecting this outcome, it was important to confirm in this study that RIM is not an event that randomly occurs in canine HNC, but instead, its highly correlated to the radiation target. In this analysis we also found that dogs with excellent appetite and diet acceptance at the time of DRT initiation had more chances to develop some grade of RIM over the course of DRT. This outcome was particularly interesting because while this has not been described in human, and moreover, HNC patients commonly report nutritional impairments due to the location of masses in sensitive areas such as the oropharynxes (Wong et al., 2006), it appeared that these factors could potentially influence the development of canine RIM. Based on Priya and colleagues' work (Priya et al., 2020), we hypothesize that alterations of the oral microbial flora as a consequence of diet and/or lack of appropriate dental care could potentially explain why variables such as appetite and diet acceptance were considered as risk factors for the progression of RIM, however, but we cannot assure this with certainty without performing further investigations. Finally, we also noticed that mixed-breed dogs had a higher risk to develop severe RIM in comparison to purebred dogs (13%

versus 9.5%). However, it is important to highlight that we did not divide the purebred category into more specific categories (42 breeds in total), and furthermore, because there was not a breed that was being overrepresented in this study (Labrador Retriever being the most common breed (n = 8)), it is impossible to determine whether dog breed is a true predictive factor. Thus, further investigation is needed to understand the effects of breed in the progression of canine RIM.

After having a better understanding about the clinical features and progression of RIM in pet dogs, we assessed the reliability and validity of the newly developed OPS. Given the lack of appropriate tools to measure oral RAP in canine HNC, this owner-completed questionnaire was designed especially for this work. First, we examined the evolution of OPS scores for each item question in each group (i.e., oral, nasal and cranial DRT). In general, we saw in this assessment that the pattern behavior across all questions included in the OPS was similar the pattern of RIM progression for each group. Specifically, we found that the increase in RIM severity correlated with an increase in OPS scores, and moreover, the magnitude of this increase varied depending on tumor location. Indeed, higher scores were seen in those dogs that had higher grades of RIM (i.e., oral/nasal DRT), and conversely, lower scores were seen in dogs that developed lower grades of RIM (i.e., cranial DRT). However, when assessing each individual question contained in this scale, we saw that some questions were better in tracking the changes in VRTOGs, such as the questions related to the dog's ability to eat appropriately ("OPS_Eat") and to play (chew) with their toys ("OPS_Play"). Nevertheless, the OPS had a high internal consistency and all questions seemed to be highly related to each other according to our reliability assessment, therefore, all questions were included in our factor analysis. According to factor analysis, it appeared that the OPS is a uni-dimension scale, and that all questions included in this scale fitted into the same theoretical construct (i.e., pain/interference with oropharyngeal functions). Therefore, this finding was a good

first step to confirm that the OPS could potentially be a useful CMI to assess oral RAP. In our validity assessment, we first noticed that there was a low correlation between OPS scores and VRTOGs > 2 when dogs received $\sim 50\%$ of the total prescribed DRT course (concurrent validity). This was not surprising because, as mentioned before, OPS scores were in general low and we did not separate during this analysis the different experimental groups (i.e., oral versus nasal versus cranial). Therefore, we cannot conclude that there is a lack of correlation between these outcomes by only using concurrent validity as an assessment modality. Indeed, the OPS showed to be effective in discriminating dogs with severe RIM (VRTOGs > 2) against those that never developed RIM (VRTOGs of 0) according to our extreme group validation evaluation. In addition, it was also effective in tracking the changes in VRTOGs over time according to our responsiveness evaluation. Therefore, we can conclude at this stage that while the OPS do not seem to be the best strategy to accurately measure the magnitude of oral RAP, it could be potentially good in differentiating dogs with and without RAP in the oral cavity, and potentially, also good in detecting the effects of therapeutic interventions for managing RIM in this species.

After testing the reliability and validity of the OPS, we measured pain (potentially associated with RIM) using all the available CMIs. First, we assessed pain (PSS), pain interference (PIS), and quality of life (OIS) using the CBPI, a CMI that has been extensively used in veterinary research and medicine to assess non-oral pain (Brown et al., 2008). Here we saw that the PSS appeared to be good at tracking the changes in VRTOGs. According to this scale, and similar to HNC humans (Huang et al., 2003), pain was marginal during the first weeks following DRT initiation, yet it rapidly increased in severity (as indicated by a marked increase in scores) when $\sim 90\%$ of the prescribed DRT was delivered (i.e., 4 weeks after DRT initiation), reaching maximal pain severity at the time that oral and nasal irradiated dogs displayed maximal RIM severity. After

DRT completion, PSS scores gradually decreased until the end of the study, and thus, potentially mirroring the resolution of RIM. Moreover, and according to this scoring system, pain was minimal for the cranial DRT group (at least significantly lower than oral/nasal DRT scores), and scores did not fluctuate over time suggesting that relevant levels of pain were not experienced in this group throughout this study. Scores from the PIS were in general minimal according to this scale system for all the assessed time points in all dogs, and curve fluctuations were not in agreement with the severity of RIM. This was not a surprise since this scale was originally designed to assess the interference of pain in actions that are not dependent on the oral function, but instead, it was designed to assess the impairment of other type of activities (e.g., walking, running, or climbing) that are commonly impaired in dogs with osteoarthritis or osteosarcoma pain in legs or upper arms (Brown et al., 2009; Brown et al., 2005). Results from the OIS, however, were unexcepted. According to this scale, dogs in general had a good quality of life at baseline, over the course of treatment, and 3 weeks after, and it was only temporally affected at the end of DRT in oral/nasal dogs. These results certainly differ from numerous studies that have revealed that quality of life in HNC patients is severely affected from the start of DRT, which can last for months or year after DRT completion (Epstein et al., 2001; Kemmler et al., 1999; Peterman et al., 2001; Wiseman-Orr et al., 2004). However, the author of this work believes that a scale with a stand-alone final question to score the animal's quality of life might not be as reliable as the other scales due to the ambiguity nature of the “quality of life” concept in dogs.

Lastly, and confirming what is was previously stated, the behavior pattern of the OPS was remarkably similar to the progression pattern of RIM for each group. However, we had the impression that the pain/interference levels indicated by this scale were, in general, low (as indicated by overall scores at the lower range of the scale). While we cannot assure here whether

these low scores are a true reflection of the level of pain/interference experienced by dogs since scores are determined by the owner (not the dog), we had the impression that the OPS might not be adequately measuring the magnitude of oral RAP; this an assumption solely based on empirical evidence (veterinary clinicians commonly report that severe pain/interference is associated to canine RIM). Therefore, we decided to combine the questions that seemed to reflect greater levels of pain/interference into one single scale. The idea here was to design a scale that could potentially be more accurate at tracking the changes in RIM, as well as its severity. Unfortunately, this adapted scale was not superior to the other scales. Specifically, the duration and severity of pain did not greatly differ from the one obtained from the PSS alone, and moreover, its responsiveness was not superior to the OPS.

Limitations of this study should be mentioned. First, and in general, conclusions of most outcomes were hard to be obtained because there were several pieces of information missing in this analysis that could be greatly impacting the results, like tumor stage or medical history. Therefore, we cannot know with certainty that the clinical course of RIM in these dogs was not influenced by tumor staging, as well as we cannot know whether pain killers (opioids) or anti-inflammatory agents were influencing (i.e., palliating signs of pain or reducing the severity of RIM, respectively) in the pain outcomes measures. Moreover, several of the scales applied in this study, such as the appetite and diet acceptance questionnaires, PSS, PIS, and OIS questionnaires, have not been previously validated to be used in this specific scenario. Therefore, results from these scales could not necessarily be reflecting the functional impact of RIM. Also, as mentioned before, the results obtained from the risk factor assessment were highly dependent on how the data were handled, and additional or more refined categorizations should be used to further understand the predictive value of the variables used in this study. Finally, and one important limitation in this

study was related to the treatment modality applied. Because data collection was done a decade ago, dogs were treated here with three-dimensional conformal radiotherapy, which is no longer used in most veterinary hospitals. Currently, cancer treatment by means of radiation therapy is mainly accomplished using more modern technology, such as intensity-modulated radiation therapy. This modality can dramatically decrease the toxicities related to DRT (Chao, 2002; De Sanctis et al., 2019). Therefore, our results might not be correctly capturing the studied outcomes (i.e., epidemiology and clinical course of RIM, as well as the risk factors and secondary side effects associated to RIM). In this context, it will be important to reassess these parameters using DRT modalities that are currently being implemented in veterinary to confirm, or complement, our results. Although the reliability and validity assessment of the OPS should not be affected by this limitation, the progression and severity of oral RAP described here (as indicated by the applied CMI) might also not be accurately reflecting the individuals' level of pain as a result of oral, nasal, or cranial DRT when more modern techniques are being applied, limiting the translation of our results into the clinical practice (both in human and veterinary medicine).

In conclusion, the results obtained from this collective work provides the first body of evidence suggesting that the clinical features of RIM (i.e., progression, severity, and secondary side effects) as a result of oral, nasal, or cranial DRT in pet dogs share similarities with its human counterpart. Nevertheless, future investigations should include more rigorous preclinical settings (e.g., modern DRT techniques, deeper understanding about patient's clinical history, appropriate samples sizes) in order to, on one hand, confirm the translatability of pet dogs as preclinical models of RIM in the context of HNC, and on the other hand, provide a clinically relevant comparative model for evaluating novel therapeutic intervention strategies for managing RIM in human clinical trials. In regard to the pain assessment, we can preliminarily conclude that canine HNC, as in

human HNC, is associated to pain and pain-related interference with normal dog's activities once RIM is established. Certainly, both the PSS and OPS provide encouraging findings that further support the idea that the progression and severity of oral RAP echoes the progression and severity of RIM in this species. However, it would be important that future studies reevaluate the reliability and validity of these CMIs in this specific scenario before testing novel drug candidate interventions for RAP treatment, especially when considering the important limitations found in this study. Moreover, the use of complementary pain assessment techniques (e.g., quantitative sensory testing, canine grimace scales, or automated facial analysis), appropriate analgesic strategies, and relevant control groups (e.g., dogs with pain in areas distant to the head and neck area) are imperative in order to confirm the sensitivity and specificity of these pain screening tools. Taking all together, we cannot confirm from our results that pet dogs offer a higher degree of translational success than other species (e.g., mice, rats), however, this work represent an important first step to start validating canine oral RAP (in the context of RIM and HNC) as suitable preclinical model for improved translation of preclinical finding into the clinic, and furthermore, to increase the probability of the successful development of new and safe analgesic therapeutics.

5.5 References

- Adelstein, D. J., Saxton, J. P., Lavertu, P., Tuason, L., Wood, B. G., Wanamaker, J. R., Eliachar, I., Strome, M., & Van Kirk, M. A. (1997). A phase III randomized trial comparing concurrent chemotherapy and radiotherapy with radiotherapy alone in resectable stage III and IV squamous cell head and neck cancer: preliminary results. *Head & Neck: Journal for the Sciences and Specialties of the Head and Neck*, 19(7), 567-575.
- Astrup, G. L., Rustøen, T., Miaskowski, C., Paul, S. M., & Bjordal, K. (2015). Changes in and predictors of pain characteristics in patients with head and neck cancer undergoing radiotherapy. *Pain*, 156(5), 967-979.
- Bansal, M., Mohanti, B., Shah, N., Chaudhry, R., Bahadur, S., & Shukla, N. (2004). Radiation related morbidities and their impact on quality of life in head and neck cancer patients receiving radical radiotherapy. *Quality of Life Research*, 13(2), 481-488.
- Barasch, A., & Peterson, D. E. (2003). Risk factors for ulcerative oral mucositis in cancer patients: unanswered questions. *Oral Oncology*, 39(2), 91-100.
- Barber, C., Powell, R., Ellis, A., & Hewett, J. (2007). Comparing pain control and ability to eat and drink with standard therapy vs Gelclair: a preliminary, double centre, randomised controlled trial on patients with radiotherapy-induced oral mucositis. *Supportive Care in Cancer*, 15(4), 427-440.
- Bartges, J., Boynton, B., Vogt, A. H., Krauter, E., Lambrecht, K., Svec, R., & Thompson, S. (2012). AAHA canine life stage guidelines. *Journal of the American Animal Hospital Association*, 48(1), 1-11.
- Beaver, M. E., Matheny, K. E., Roberts, D. B., & Myers, J. N. (2001). Predictors of weight loss during radiation therapy. *Otolaryngology—Head and Neck Surgery*, 125(6), 645-648.

- Bensadoun, R., Franquin, J., Ciais, G., Darcourt, V., Schubert, M., Viot, M., Dejou, J., Tardieu, C., Benezery, K., & Nguyen, T. (1999). Low-energy He/Ne laser in the prevention of radiation-induced mucositis. *Supportive Care in Cancer*, 7(4), 244-252.
- Bese, N. S., Hendry, J., & Jeremic, B. (2007). Effects of prolongation of overall treatment time due to unplanned interruptions during radiotherapy of different tumor sites and practical methods for compensation. *International Journal of Radiation Oncology* Biology* Physics*, 68(3), 654-661.
- Borbasi, S., Cameron, K., Quedsted, B., Olver, I., To, B., & Evans, D. (2002). More Than a Sore Mouth: Patients' Experience of Oral Mucositis [Article]. *Oncology nursing forum*, 29(7), 1051. <https://doi.org/10.1188/02.ONF.1051-1057>
- Boss, M.-K., Ke, Y., Bian, L., Harrison, L. G., Lee, B.-I., Prebble, A., Martin, T., Trageser, E., Hall, S., & Wang, D. D. (2022). Therapeutic intervention using a Smad7-based Tat protein to treat radiation-induced oral mucositis. *International Journal of Radiation Oncology* Biology* Physics*, 112(3), 759-770.
- Brizel, D. M., Albers, M. E., Fisher, S. R., Scher, R. L., Richtsmeier, W. J., Hars, V., George, S. L., Huang, A. T., & Prosnitz, L. R. (1998). Hyperfractionated irradiation with or without concurrent chemotherapy for locally advanced head and neck cancer. *New England Journal of Medicine*, 338(25), 1798-1804.
- Brown, D. C., Boston, R., Coyne, J. C., & Farrar, J. T. (2009). A novel approach to the use of animals in studies of pain: validation of the canine brief pain inventory in canine bone cancer. *Pain medicine*, 10(1), 133-142.

- Brown, D. C., Boston, R. C., Coyne, J. C., & Farrar, J. T. (2008). Ability of the canine brief pain inventory to detect response to treatment in dogs with osteoarthritis. *Journal of the American Veterinary Medical Association*, 233(8), 1278-1283.
- Brown, D. C., Iadarola, M. J., Perkowski, S. Z., Erin, H., Shofer, F., Laszlo, K. J., Olah, Z., & Mannes, A. J. (2005). Physiologic and antinociceptive effects of intrathecal resiniferatoxin in a canine bone cancer model. *The Journal of the American Society of Anesthesiologists*, 103(5), 1052-1059.
- Brown, S. D. M. (2021). Advances in mouse genetics for the study of human disease. *Human Molecular Genetics*, 30(R2), R274-R284.
- Brzozowska, A., & Gołębiowski, P. (2019). Acute radiation-induced oral mucositis in patients subjected to radiotherapy due to head and neck cancer. *Polish Journal of Public Health*, 129(1).
- Carlotto, A., Hogsett, V. L., Maiorini, E. M., Razulis, J. G., & Sonis, S. T. (2013). The Economic Burden of Toxicities Associated with Cancer Treatment: Review of the Literature and Analysis of Nausea and Vomiting, Diarrhoea, Oral Mucositis and Fatigue. *Pharmacoeconomics*, 31(9), 753-766.
- Chao, K. C. (2002). Protection of salivary function by intensity-modulated radiation therapy in patients with head and neck cancer. *Seminars in radiation oncology* (Vol. 12, No. 1, pp. 20-25). WB Saunders.
- Chen, S.-C., Liao, C.-T., & Chang, J. T.-C. (2011). Orofacial pain and predictors in oral squamous cell carcinoma patients receiving treatment. *Oral Oncology*, 47(2), 131-135.
- Chencharick, J. D., & Mossman, K. L. (1983). Nutritional consequences of the radiotherapy of head and neck cancer. *Cancer*, 51(5), 811-815.

- Cho, C., Deol, H. K., & Martin, L. J. (2021). Bridging the Translational Divide in Pain Research: Biological, Psychological and Social Considerations. *Frontiers in pharmacology*, 12, 603186-603186.
- Christoforou, J., Karasneh, J., Manfredi, M., Dave, B., Walker, J. S., Dios, P. D., Epstein, J., Kumar, N., Glick, M., & Lockhart, P. B. (2019). World Workshop on Oral Medicine VII: Non-opioid pain management of head and neck chemo/radiation-induced mucositis: A systematic review. *Oral diseases*, 25, 182-192.
- Cook, A., Modh, A., Ali, H., Sheqwara, J., Chang, S., Ghanem, T., Momin, S., Wu, V., Tam, S., & Money, S. (2022). Randomized Phase 3, Double-Blind, Placebo-Controlled Study of Prophylactic Gabapentin for the Reduction of Oral Mucositis Pain During the Treatment of Oropharyngeal Squamous Cell Carcinoma. *International Journal of Radiation Oncology* Biology* Physics*, 112(4), 926-937.
- De Jong, M., & Maina, T. (2010). Of mice and humans: are they the same?—Implications in cancer translational research. *Journal of Nuclear Medicine*, 51(4), 501-504.
- De Sanctis, V., Merlotti, A., De Felice, F., Trignani, M., Dell'Oca, I., Lastrucci, L., Molteni, M., Frakulli, R., Bunkheila, F., & Bacigalupo, A. (2019). Intensity modulated radiation therapy and oral mucosa sparing in head and neck cancer patients: a systematic review on behalf of Italian Association of Radiation Oncology—head and neck working group. *Critical reviews in oncology/hematology*, 139, 24-30.
- Denneberg, N. Å., & Egenvall, A. (2009). Evaluation of dog owners' perceptions concerning radiation therapy. *Acta Veterinaria Scandinavica*, 51(1), 1-10.

- Dische, S., Saunders, M., Barrett, A., Harvey, A., Gibson, D., & Parmar, M. (1997). A randomised multicentre trial of CHART versus conventional radiotherapy in head and neck cancer. *Radiotherapy and Oncology*, 44(2), 123-136.
- Elting, L. S., Cooksley, C. D., Chambers, M. S., & Garden, A. S. (2007). Risk, outcomes, and costs of radiation-induced oral mucositis among patients with head-and-neck malignancies. *Int J Radiat Oncol Biol Phys*, 68(4), 1110-1120.
- Epstein, J. B., Robertson, M., Emerton, S., Phillips, N., & Stevenson-Moore, P. (2001). Quality of life and oral function in patients treated with radiation therapy for head and neck cancer. *Head & Neck*, 23(5), 389-398.
- Farcas, N., Arzi, B., & Verstraete, F. (2014). Oral and maxillofacial osteosarcoma in dogs: a review. *Veterinary and Comparative Oncology*, 12(3), 169-180.
- Franco, P., Martini, S., Di Muzio, J., Cavallin, C., Arcadipane, F., Rampino, M., Ostellino, O., Pecorari, G., Demo, P. G., & Fasolis, M. (2017). Prospective assessment of oral mucositis and its impact on quality of life and patient-reported outcomes during radiotherapy for head and neck cancer. *Medical Oncology*, 34(5), 81.
- Holton, L., Pawson, P., Nolan, A., Reid, J., & Scott, E. (2001). Development of a behaviour-based scale to measure acute pain in dogs. *Veterinary Record*, 148(17), 525-531.
- Huang, H.-Y., Wilkie, D. J., Chapman, C. R., & Ting, L.-L. (2003). Pain Trajectory of Taiwanese with Nasopharyngeal Carcinoma Over the Course of Radiation Therapy. *Journal of pain and symptom management*, 25(3), 247-255.
- Hunley, D. W., Mauldin, G. N., Shiomitsu, K., & Mauldin, G. E. (2010). Clinical outcome in dogs with nasal tumors treated with intensity-modulated radiation therapy. *The Canadian Veterinary Journal*, 51(3), 293.

- Iadarola, M. J., Sapio, M. R., Raithel, S. J., Mannes, A. J., & Brown, D. C. (2018). Long-term pain relief in canine osteoarthritis by a single intra-articular injection of resiniferatoxin, a potent TRPV1 agonist. *Pain*, 159(10), 2105-2114.
- Ineson, D. L., Freeman, L. M., & Rush, J. E. (2019). Clinical and laboratory findings and survival time associated with cardiac cachexia in dogs with congestive heart failure. *Journal of Veterinary Internal Medicine*, 33(5), 1902-1908.
- Kawamura, M., Yoshimura, M., Asada, H., Nakamura, M., Matsuo, Y., & Mizowaki, T. (2019). A scoring system predicting acute radiation dermatitis in patients with head and neck cancer treated with intensity-modulated radiotherapy. *Radiation Oncology*, 14(1), 1-9.
- Kemmler, G., Holzner, B., Kopp, M., Dünser, M., Margreiter, R., Greil, R., & Sperner-Unterweger, B. (1999). Comparison of Two Quality-of-Life Instruments for Cancer Patients: The Functional Assessment of Cancer Therapy-General and the European Organization for Research and Treatment of Cancer Quality of Life Questionnaire-C30. *Journal of Clinical Oncology*, 17(9), 2932-2932.
- Kersten, K., de Visser, K. E., van Miltenburg, M. H., & Jonkers, J. (2017). Genetically engineered mouse models in oncology research and cancer medicine. *EMBO molecular medicine*, 9(2), 137-153.
- Klinck, M. P., Mogil, J. S., Moreau, M., Lascelles, B. D. X., Flecknell, P. A., Poitte, T., & Troncy, E. (2017). Translational pain assessment: could natural animal models be the missing link? *Pain*, 158(9), 1633-1646.
- Kol, A., Arzi, B., Athanasiou, K. A., Farmer, D. L., Nolta, J. A., Rebhun, R. B., Chen, X., Griffiths, L. G., Verstraete, F. J. M., Murphy, C. J., & Borjesson, D. L. (2015). Companion animals:

- Translational scientist's new best friends. *Science translational medicine*, 7(308), 308ps21-308ps21.
- Lalla, R. V., Brennan, M. T., Gordon, S. M., Sonis, S. T., Rosenthal, D. I., & Keefe, D. M. (2019). Oral mucositis due to high-dose chemotherapy and/or head and neck radiation therapy. *JNCI Monographs*, 2019(53), 1gz011.
- Langius, J. A. E., Bakker, S., Rietveld, D. H. F., Kruizenga, H. M., Langendijk, J. A., Weijs, P. J. M., & Leemans, C. R. (2013). Critical weight loss is a major prognostic indicator for disease-specific survival in patients with head and neck cancer receiving radiotherapy. *British Journal of Cancer*, 109(5), 1093-1099.
- Lascelles, B., Brown, D., Maixner, W., & Mogil, J. (2018). Spontaneous painful disease in companion animals can facilitate the development of chronic pain therapies for humans. *Osteoarthritis and cartilage*, 26(2), 175-183.
- Lee, S.-C., Wang, T.-J., & Chu, P.-Y. (2019). Predictors of weight loss during and after radiotherapy in patients with head and neck cancer: a longitudinal study. *European Journal of Oncology Nursing*, 39, 98-104.
- Lefebvre, J.-L., Chevalier, D., Luboinski, B., Kirkpatrick, A., Collette, L., & Sahnoud, T. (1996). Larynx preservation in pyriform sinus cancer: preliminary results of a European Organization for Research and Treatment of Cancer phase III trial. *JNCI: Journal of the National Cancer Institute*, 88(13), 890-899.
- Lønbro, S., Petersen, G. B., Andersen, J. R., & Johansen, J. (2016). Prediction of critical weight loss during radiation treatment in head and neck cancer patients is dependent on BMI. *Supportive Care in Cancer*, 24(5), 2101-2109.

- Mak, I. W., Evaniew, N., & Ghert, M. (2014). Lost in translation: animal models and clinical trials in cancer treatment. *American journal of translational research*, 6(2), 114-118.
- Menéndez, L., Juárez, L., García, E., García-Suárez, O., Hidalgo, A., & Baamonde, A. (2006). Analgesic effects of capsazepine and resiniferatoxin on bone cancer pain in mice. *Neuroscience Letters*, 393(1), 70-73.
- Minnema, L., Wheeler, J., Enomoto, M., Pitake, S., Mishra, S. K., & Lascelles, B. D. X. (2020). Correlation of artemin and GFR α 3 with osteoarthritis pain: Early evidence from naturally occurring osteoarthritis-associated chronic pain in dogs. *Frontiers in Neuroscience*, 14, 77.
- Miyagi, M., Ishikawa, T., Kamoda, H., Suzuki, M., Inoue, G., Sakuma, Y., Oikawa, Y., Orita, S., Uchida, K., & Takahashi, K. (2017). Efficacy of nerve growth factor antibody in a knee osteoarthritis pain model in mice. *BMC Musculoskeletal Disorders*, 18(1), 1-8.
- Mogil, J. S. (2009). Animal models of pain: progress and challenges. *Nature Reviews Neuroscience*, 10(4), 283-294.
- Mogil, J. S. (2019). The translatability of pain across species. *Philosophical Transactions of the Royal Society B*, 374(1785), 20190286.
- Muzumder, S., Nirmala, S., Avinash, H., Sebastian, M. J., & Kainthaje, P. B. (2018). Analgesic and opioid use in pain associated with head-and-neck radiation therapy. *Indian journal of palliative care*, 24(2), 176.
- Narayan, S., Lehmann, J., Coleman, M. A., Vaughan, A., Yang, C. C., Enepekides, D., Farwell, G., Purdy, J. A., Laredo, G., & Nolan, K. (2008). Prospective evaluation to establish a dose response for clinical oral mucositis in patients undergoing head-and-neck conformal radiotherapy. *International Journal of Radiation Oncology* Biology* Physics*, 72(3), 756-762. e754.

- Nazari, V., Pashaki, A. S., & Hasanzadeh, E. (2021). The reliable predictors of severe weight loss during the radiotherapy of Head and Neck Cancer. *Cancer Treatment and Research Communications*, 26, 100281.
- Ogama, N., Suzuki, S., Umeshita, K., Kobayashi, T., Kaneko, S., Kato, S., & Shimizu, Y. (2010). Appetite and adverse effects associated with radiation therapy in patients with head and neck cancer. *European Journal of Oncology Nursing*, 14(1), 3-10.
- Pai, P.-C., Chuang, C.-C., Tseng, C.-K., Tsang, N.-M., Chang, K.-P., Yen, T.-C., Liao, C.-T., Hong, J.-H., & Chang, J. T.-C. (2012). Impact of pretreatment body mass index on patients with head-and-neck cancer treated with radiation. *International Journal of Radiation Oncology* Biology* Physics*, 83(1), e93-e100.
- Paoloni, M., & Khanna, C. (2008). Translation of new cancer treatments from pet dogs to humans. *Nature reviews Cancer*, 8(2), 147-156.
- Peterman, A., Cella, D., Glandon, G., Dobrez, D., & Yount, S. (2001). Mucositis in Head and Neck Cancer: Economic and Quality-of-Life Outcomes. *JNCI Monographs*, 2001(29), 45-51.
- Piel, M. J., Kroin, J. S., Van Wijnen, A. J., Kc, R., & Im, H.-J. (2014). Pain assessment in animal models of osteoarthritis. *Gene*, 537(2), 184-188.
- Porter, L. S., & Keefe, F. J. (2011). Psychosocial Issues in Cancer Pain. *Current Pain and Headache Reports*, 15(4), 263-270.
- Priya, A. H. H., Rajmohan, H. P. A. K., Raj, S. A., Archana, S., & Venkatanarasu, B. (2020). Evaluation of alteration in oral microbial flora pre-and postradiation therapy in patients with head and neck cancer. *Journal of Pharmacy & Bioallied Sciences*, 12(Suppl 1), S109.

- Raber-Durlacher, J., Weijl, N., Abu Saris, M., De Koning, B., Zwinderman, A., & Osanto, S. (2000). Oral mucositis in patients treated with chemotherapy for solid tumors: a retrospective analysis of 150 cases. *Supportive care in cancer*, 8(5), 366-371.
- Ranieri, G., Gadaleta, C., Patruno, R., Zizzo, N., Daidone, M., Hansson, M. G., Paradiso, A., & Ribatti, D. (2013). A model of study for human cancer: Spontaneous occurring tumors in dogs. Biological features and translation for new anticancer therapies. *Critical reviews in oncology/hematology*, 88(1), 187-197.
- Rapoport, A. P., Miller Watelet, L. F., Linder, T., Eberly, S., Raubertas, R. F., Lipp, J., Duerst, R., Abboud, C. N., Constine, L., & Andrews, J. (1999). Analysis of factors that correlate with mucositis in recipients of autologous and allogeneic stem-cell transplants. *Journal of Clinical Oncology*, 17(8), 2446-2446.
- Ravasco, P., Monteiro-Grillo, I., Marques Vidal, P., & Camilo, M. E. (2005). Impact of nutrition on outcome: a prospective randomized controlled trial in patients with head and neck cancer undergoing radiotherapy. *Head & Neck: Journal for the Sciences and Specialties of the Head and Neck*, 27(8), 659-668.
- Redding, S. W. (2005). Cancer therapy-related oral mucositis. *Journal of dental education*, 69(8), 919-929.
- Riva, G., Franco, P., Provenzano, E., Arcadipane, F., Bartoli, C., Lava, P., Ricardi, U., & Pecorari, G. (2019). Radiation-induced rhinitis: cytological and olfactory changes. *American Journal of Rhinology & Allergy*, 33(2), 153-161.
- Rosenthal, D. (2007). Consequences of mucositis-induced treatment breaks and dose reductions on head and neck cancer treatment outcomes. *The journal of supportive oncology*, 5, 23-31.

- Russo, G., Haddad, R., Posner, M., & Machtay, M. (2008). Radiation treatment breaks and ulcerative mucositis in head and neck cancer. *The Oncologist*, 13(8), 886-898.
- Scully, C., Epstein, J., & Sonis, S. (2003). Oral mucositis: a challenging complication of radiotherapy, chemotherapy, and radiochemotherapy: part 1, pathogenesis and prophylaxis of mucositis. *Head & Neck: Journal for the Sciences and Specialties of the Head and Neck*, 25(12), 1057-1070.
- Sonis, S. T. (2011). Oral mucositis. *Anticancer Drugs*, 22(7), 607-612.
- Sonis, S. T., Eilers, J. P., Epstein, J. B., LeVeque, F. G., Liggett Jr, W. H., Mulagha, M. T., Peterson, D. E., Rose, A. H., Schubert, M. M., & Spijkervet, F. K. (1999). Validation of a new scoring system for the assessment of clinical trial research of oral mucositis induced by radiation or chemotherapy. *Cancer*, 85(10), 2103-2113.
- Sonis, S. T., Elting, L. S., Keefe, D., Peterson, D. E., Schubert, M., Hauer-Jensen, M., Bekele, B. N., Raber-Durlacher, J., Donnelly, J. P., & Rubenstein, E. B. (2004). Perspectives on cancer therapy-induced mucosal injury: pathogenesis, measurement, epidemiology, and consequences for patients. *Cancer: Interdisciplinary International Journal of the American Cancer Society*, 100(S9), 1995-2025.
- Sroussi, H. Y., Epstein, J. B., Bensadoun, R. J., Saunders, D. P., Lalla, R. V., Migliorati, C. A., Heavilin, N., & Zumsteg, Z. S. (2017). Common oral complications of head and neck cancer radiation therapy: mucositis, infections, saliva change, fibrosis, sensory dysfunctions, dental caries, periodontal disease, and osteoradionecrosis. *Cancer medicine*, 6(12), 2918-2931.
- Tappe-Theodor, A., & Kuner, R. (2014). Studying ongoing and spontaneous pain in rodents—challenges and opportunities. *European Journal of Neuroscience*, 39(11), 1881-1890.

- Trotti, A., Bellm, L. A., Epstein, J. B., Frame, D., Fuchs, H. J., Gwede, C. K., Komaroff, E., Nalysnyk, L., & Zilberberg, M. D. (2003). Mucositis incidence, severity and associated outcomes in patients with head and neck cancer receiving radiotherapy with or without chemotherapy: a systematic literature review. *Radiotherapy and oncology*, 66(3), 253-262.
- Wiseman-Orr, M. L., Nolan, A. M., Reid, J., & Scott, E. M. (2004). Development of a questionnaire to measure the effects of chronic pain on health-related quality of life in dogs. *American Journal of Veterinary Research*, 65(8), 1077-1084.
- Wong, P. C., Dodd, M. J., Miaskowski, C., Paul, S. M., Bank, K. A., Shiba, G. H., & Facione, N. (2006). Mucositis pain induced by radiation therapy: prevalence, severity, and use of self-care behaviors. *Journal of pain and symptom management*, 32(1), 27-37.
- Yergolkar, A. V., Gundala, P., Murthy, M. K., & Vinayak, V. (2020). PCN64 Frequency of ORAL Mucositis in Male Patients Receiving Cancer Therapy. *Value in Health Regional Issues*, 22, S17.
- Ying, X., Liu, H., Wang, M., Peng, M., Ruan, P., Verma, V., & Han, G. (2020). Clinical response to apatinib combined with brain radiotherapy in EGFR wild-type and ALK-negative lung adenocarcinoma with multiple brain metastases. *Frontiers in Oncology*, 10, 517.
- Yucel, B., Akkaş, E. A., Okur, Y., Eren, A. A., Eren, M. F., Karapınar, H., Babacan, N. A., & Kılıçkap, S. (2014). The impact of radiotherapy on quality of life for cancer patients: a longitudinal study. *Supportive Care in Cancer*, 22(9), 2479-2487.

Chapter 6: Conclusions and Future Directions

The potential negative effect of radiation-associated pain (RAP) on cancer progression is a critically important, yet hitherto relatively ignored, area of research. While treatment failure in head and neck cancer (HNC) patients undergoing radiation therapy (RT) may be causally linked to the unplanned breaks in treatment related to acute, orofacial RAP (aoRAP) associated to RT-induced mucosal damage (Bese et al., 2007; Chen et al., 2011), little information exists regarding the direct effect of aoRAP in tumor biology, as well as its role in cancer development and progression. The purpose of this work was to fill some of the considerable gaps in knowledge regarding the tumor-promoting effects of aoRAP using sophisticated animal models of radiation therapy-related oral mucositis.

As a way to begin exploring the idea that aoRAP may have a relevant biological role in tumor development, we designed a set of experiments that largely recapitulate the work of Page and collaborators (Page et al., 1993; Page et al., 2001) to determine if animals with experimentally induced radiation-induced mucositis (RIM) and associated pain have evidence of enhanced tumor growth at distant (unirradiated) sites. However, standardized measures needed to be developed to confirm that mice were indeed experiencing aoRAP. While our laboratory has a strong set of behavioral assays to characterize aoRAP in our RIM model using withdrawal reflex-based and well-being-based indicators (e.g., eye wiping and burrowing assays, respectively), none of these tools provides a metric of spontaneous, non-evoked (voluntary) pain in the orofacial region. This is relevant since most episodes of pain in HNC following RT are located in the orofacial region, and moreover, they are often associated with increased reports of spontaneous pain and with low quality of life scores (Epstein B et al., 2007; Epstein et al., 2009; Franco et al., 2017; Lalla et al., 2014; Scully et al., 2003). Thus, it has been largely accepted that the use of health-related quality of life indices may be better at capturing the global experience of aoRAP in human HNC, and

currently, they represent one of the most valid strategies to assess the response to analgesic treatment interventions during RT (Epstein et al., 2001; Franco et al., 2017; Heutte et al., 2014; Meyer et al., 2009). In this context, it seems pertinent to theorize that, like in humans, aoRAP in mice might also have affective/motivational components, hence – and keeping in mind that our ultimately goal is to produce powerful tools for translational research – the addition of pain outcomes that include the assessment of voluntary, spontaneous mouse behaviors definitely represent an important requirement towards validation of our murine model of aoRAP.

In Chapter 2, we sought to robust the characterization of aoRAP in our model of RIM using voluntary, spontaneous home-cage activities (nesting and grooming) as proxy indicators. Although cageside measures – such as nesting and grooming activities – have shown to be useful and valid proxy indicators of welfare in small laboratory animal species, and they have been employed for estimating acute and spontaneous states of pain in mice (Gaskill et al., 2013; Negus et al., 2015), these activities have not been used as behavioral metrics to assess orofacial pain in mice. Therefore, here we introduced for the first time a novel set of behavioral-based instruments specifically designed in our laboratory to assess the impairment in nesting and grooming activities as a result of experimentally-induced RIM (glossitis), and thus aoRAP, in mice (BALB/c and C57BL/6 strains). As a theoretically interesting sidenote, it is important to highlight the fact that while we are interested in studying the direct effects of aoRAP in tumor progression, we cannot exclude the important role that RIM plays in the onset and progression of aoRAP (Fall-Dickson et al., 2007; Lalla et al., 2014; Sonis et al., 2000; Sonis, 2004). Hence, here we need to clarify that while both side effects are two independent events, their signalling pathways most likely converge at some level to give rise to the painful experience (aoRAP) related to RIM. Therefore, and when appropriate, the author here will be referring aoRAP related to RIM as “aoRIM/RAP”. According

to the results obtained from our newly developed assays, here we provided the first direct evidence that demonstrate that nesting and grooming activities are markedly impaired when mice experience high-grade lingual RIM (score > 2). Interestingly enough, these impairments can be significantly reduced after RIM resolution and after applying two analgesic strategies, anti-NGF mAb and resiniferatoxin (RTX), whose therapeutic targets (NGF and TRPV1, respectively) are known to play a relevant role in cancer pain processing (Bujak et al., 2019; Dudás et al., 2018; Ghilardi et al., 2005; Hirose et al., 2016; Kissin & Szallasi, 2011; Menéndez et al., 2006; Sevcik et al., 2005; Shinoda et al., 2008; Ye et al., 2011). These results open exciting possibilities to begin validating the idea that both activities are highly dependent on the mouth, and moreover, that they represent valid parameters for measuring the affective/motivational aspects of aoRIM/RAP in our model. However, we further need to investigate whether the responsiveness of our assays was either determined by the analgesic or the anti-inflammatory effects of anti-NGF mAb and RTX before confirming with certainty the presence of aoRAP in our RIM model. One proof-of-concept approach to confirm the presence of aoRAP (and thus potentially separating aoRAP from RIM) would be to assess the changes in nesting and grooming scores after applying local pain-relief strategies, such as topical applications of lidocaine into the mouse tongue. However, this approach has both pragmatic and mechanistic limitations. For example, injecting a solution into an edematous and ulcerative mucosa is not easy, and can potentially enhance mucosal damage and, thus, altering the progression and severity of aoRIM/RAP. Moreover, it has been proven that anesthetic solutions, such as the ones commonly used in research facilities (e.g., lidocaine) possess anti-inflammatory properties (Kelbel & Weiss, 2001). Therefore, we could potentially end up having the same uncertainties that were raised after using anti-NGF mAb and RTX. Regarding our assessment methodologies, the results of this study suggested that our proposed standardized

scoring systems provide reliable and valid tools to screen the progression and severity of aoRIM/RAP in mice. However, and even though our assays were comparable under different experimental conditions (across sexes, mouse strains, and irradiation modalities), it might be necessary to further assess the specificity and sensitivity of our behavioral assessment tools by adding adequate comparative animal groups, like the addition of other oral pain models (e.g., temporomandibular joint pain, tongue pain induced by formalin or Complete Freund's adjuvant (CFA)) and models of pain that arise in areas distant to the orofacial region (e.g., abdominal pain, limb pain). Another important limitation towards the translation of results includes the fact that aoRIM/RAP was not influenced in our model by other sources of pain/inflammation that are in general present in human HNC, such as the nociceptive/inflammatory events associated to tumor progression (e.g., enhanced release of cytokines or growth factors) or the pain that arise from complementary cancer therapies (e.g., surgery and chemotherapy) (Astrup et al., 2015; Benoliel et al., 2007; Cramer et al., 2018; Edwards et al., 2019; Schmidt, 2015). The addition of these variables is obviously relevant to improve preclinical to clinical translation; therefore, future work should be focused on developing adequate strategies to include these features into our murine model of aoRIM/RAP.

After determining, at least preliminarily, that RIM is associated to aoRAP in our mouse model, we assessed the influence of aoRIM/RAP on tumor progression (Chapter 3). In this study, we revealed for the first time that the presence of lingual RIM, and thus potentially aoRAP, appears to be associated to enhanced tumor progression in preclinical settings. In particular, we showed that the combination of high-grade RIM (scores > 2) and aoRAP-like behaviors (as indicated by our battery of assays) was significantly associated with an accelerated growth of 4T1-Luc2 tumors and an increased mortality associated to the progression of MOC2-Luc2 tumors. Moreover, we

robustly showed that the palliation of aoRIM/RAP achieved by RTX was associated to a reduction in the burden of 4T1-Luc2 tumors. Despite these exciting and novel findings, it remains to be determined whether the provision of RTX abrogated the tumor-promoting effects of aoRIM/RAP through inhibiting nociceptive or inflammatory pathways, or both. In addition, it will be also important to discard a possible influence of TRPV1-expressing afferents innervating airways and lungs abrogating the tumor-promoting effects of aoRIM/RAP. Therefore, further *ex vivo* and *in vitro* investigations, such as calcium imaging and immunofluorescence, respectively, should be performed in order to determine more accurately the targeted location of RTX, as well as the extension of its ablative effect, in this model. Notwithstanding, we can firmly state here that our work provided the first insights into the potential mechanism (i.e., TRPV1 activation) by which aoRIM/RAP accelerated the growth of tumors at sites distant and promoted cancer-related death. Certainly, these findings offer valuable insights towards the understanding the clinical significance of the crosstalk between oral mucositis pain and cancer, and will hopefully contribute to the development of effective strategies for managing aoRIM/RAP in HNC patients, and thus, improve outcomes. Unfortunately, we were unable to confirm whether aoRIM/RAP mitigation also improved the survival of MOC2-Luc2-bearing mice due to unexpected toxicity associated with the use of RTX. In C57BL/6 mice, high mortality was associated with RTX. Therefore, we decided to cancel subsequent planned experiments, and explore in a series of pilot studies the tolerability and ablative efficacy of different doses of RTX to find the most tolerable way to approach systemic ablation of TRPV1-expressing neurons in C57BL/6 mice (Chapter 4). Two surprising, yet interesting conclusions were obtained from these studies. First, we were able to determine that the risk to develop serious toxicities, such as death, from systemic RTX (300 µg/kg) is higher in C57BL/6 mice in comparison to BALB/c mice purchased from the same vendor. This new

information was quite revealing since this type of evidence has never been reported in the literature. Secondly, and even more unexpected, we discovered that the low tolerability found in C57BL/6 mice was related to the genetic background (vendor-dependent) of certain substrains. C57BL/6NCrl mice (a commonly used C57BL/6 substrain) were particularly prone to develop serious toxicities as a consequence of systemic RTX using doses ranging from 10 to 300 $\mu\text{g}/\text{kg}$. Conversely, RTX at same doses produced both effective and long-lasting ablation of TRPV1-expressing neurons in a safe manner in C57BL/6J mice (another commonly used C57BL/6 substrain). Based on this evidence, it seems pertinent to determine in future work how the genetic background of these substrains can lead to varying responses following RTX to help make preclinical data more reproducible and to successfully achieve clinical translation. Nevertheless, the results here provided initial validation to use RTX (at a dose of 10 $\mu\text{g}/\text{kg}$) in C57BL/6J mice as a tool to mitigate aoRIM/RAP and to investigate in future studies the effects of aoRIM/RAP in the progression of murine oral cancer (MOC2-Luc2 model).

Lastly, we were interested on adding a higher order pre-clinical species into our studies to complement and further support in future work the results obtained from rodent studies, and moreover, to potentially fill some of the knowledge gaps in this area that cannot be answered by only using mice. In Chapter 5, we provide the first body of evidence suggesting that the clinical features of RIM in pet dogs (i.e., progression, severity, and secondary side effects) as a result of HNC irradiation share similarities with its human counterpart. While there are many limitations that could potentially invalidate our results (e.g., sample size, RT modality, poor knowledge about the patient's medical history), the findings of this study represent an important first step to begin validating pet dogs as valuable translational animal models for the study of RIM and RIM-related therapeutic interventions in the context of HNC. Another important finding of this study relates to

the progression and severity of aoRAP (as indicated by the available clinical metrical instruments used in this work). According to the “Pain Severity Scale” from the Canine Brief Pain Inventory and the newly developed “Oral Pain Scale” (both designed by Dr. Dorothy Brown), the progression and severity of aoRAP, as in humans, echoes the progression and severity of RIM in this species. While we cannot confirm this statement since several issues need to be addressed to confirm the reliability and validity of these tools in this specific context, these findings provide enough rationale for supporting the conduct of future investigation regarding aoRIM/RAP in dogs, and hopefully, contributing to increase the probability of the successful development of new and safe analgesic therapeutics in both veterinary and human HNC. Next steps towards validation involves the use more appropriate RT modalities (such as intensity modulated RT) to match the progression and severity of RIM that pet dogs experience when more modern techniques are being applied, to increase our understanding about each patient’s clinical history to potentially detect risk factors of RIM and aoRAP in this species, to add relevant comparative control animals since intracranially irradiated dogs might not represent the best control group, and to increase the number of recruited animal to robust our results. Moreover, and since we are currently in an era where modern assessment techniques, such as automated pain assessment via machine learning, are available in the pain research field (Feighelstein et al., 2022; Feighelstein, 2021; Susam et al., 2018; Susam et al., 2021), we could substantially improve aoRAP screening in this canine model by the use of these complementary tools.

Taking all results together, we can conclude that our murine model of RIM and pain assessment tools provided in this work compelling evidence for a potential effect of aoRIM/RAP on cancer progression, and laid a foundation for future work to better understand the mechanisms underlying its tumor promoting effects. Moreover, we significantly contributed to the field of

translation pain research by initiating explorations in pet dogs aimed to validate the use of this preclinical model to understand the affective and neurobiological components associated with aoRIM/RAP, and its influence on cancer treatment failure in clinical settings.

6.1 References

- Astrup, G. L., Rustøen, T., Miaskowski, C., Paul, S. M., & Bjordal, K. (2015). Changes in and predictors of pain characteristics in patients with head and neck cancer undergoing radiotherapy. *Pain*, 156(5), 967-979.
- Benoliel, R., Epstein, J., Eliav, E., Jurevic, R., & Elad, S. (2007). Orofacial pain in cancer: part I—mechanisms. *Journal of dental research*, 86(6), 491-505.
- Bese, N. S., Hendry, J., & Jeremic, B. (2007). Effects of prolongation of overall treatment time due to unplanned interruptions during radiotherapy of different tumor sites and practical methods for compensation. *International Journal of Radiation Oncology* Biology* Physics*, 68(3), 654-661.
- Bujak, J. K., Kosmala, D., Szopa, I. M., Majchrzak, K., & Bednarczyk, P. (2019). Inflammation, cancer and immunity—implication of TRPV1 channel. *Frontiers in oncology*, 9, 1087.
- Chen, S.-C., Liao, C.-T., & Chang, J. T.-C. (2011). Orofacial pain and predictors in oral squamous cell carcinoma patients receiving treatment. *Oral Oncology*, 47(2), 131-135.
- Cramer, J. D., Johnson, J. T., & Nilsen, M. L. (2018). Pain in head and neck cancer survivors: prevalence, predictors, and quality-of-life impact. *Otolaryngology–Head and Neck Surgery*, 159(5), 853-858.
- Dudás, J., Dietl, W., Romani, A., Reinold, S., Glueckert, R., Schrott-Fischer, A., Dejaco, D., Johnson Chacko, L., Tuertscher, R., & Schartinger, V. H. (2018). Nerve Growth Factor (NGF)—Receptor Survival Axis in Head and Neck Squamous Cell Carcinoma. *International journal of molecular sciences*, 19(6), 1771.
- Edwards, H. L., Mulvey, M. R., & Bennett, M. I. (2019). Cancer-related neuropathic pain. *Cancers*, 11(3), 373.

- Epstein B, J. L., Gwede, C. K., Murphy, B., Garden, A. S., Meredith, R., Le, Q. T., Brizel, D., Isitt, J., & Cella, D. (2007). Longitudinal evaluation of the oral mucositis weekly questionnaire-head and neck cancer, a patient-reported outcomes questionnaire. *Cancer*, 109(9), 1914-1922.
- Epstein, J. B., Robertson, M., Emerton, S., Phillips, N., & Stevenson-Moore, P. (2001). Quality of life and oral function in patients treated with radiation therapy for head and neck cancer. *Head & Neck*, 23(5), 389-398.
- Epstein, J. B., Wilkie, D. J., Fischer, D. J., Kim, Y.-O., & Villines, D. (2009). Neuropathic and nociceptive pain in head and neck cancer patients receiving radiation therapy. *Head & neck oncology*, 1(1), 1-12.
- Fall-Dickson, J. M., Ramsay, E. S., Castro, K., Woltz, P., & Sportés, C. (2007). Oral mucositis-related oropharyngeal pain and correlative tumor necrosis factor- α expression in adult oncology patients undergoing hematopoietic stem cell transplantation. *Clinical therapeutics*, 29(11), 2547-2561.
- Feighelstein, M., Shimshoni, I., Finka, L. R., Luna, S. P., Mills, D. S., & Zamansky, A. (2022). Automated recognition of pain in cats. *Scientific Reports*, 12(1), 1-10.
- Feighelstein, M. G. (2021). Towards Automatic Recognition of Emotional States of Animals. In *Eight International Conference on Animal-Computer Interaction* (pp. 1-4).
- Franco, P., Martini, S., Di Muzio, J., Cavallin, C., Arcadipane, F., Rampino, M., Ostellino, O., Pecorari, G., Demo, P. G., & Fasolis, M. (2017). Prospective assessment of oral mucositis and its impact on quality of life and patient-reported outcomes during radiotherapy for head and neck cancer. *Medical Oncology*, 34(5), 81.

- Gaskill, B. N., Karas, A. Z., Garner, J. P., & Pritchett-Corning, K. R. (2013). Nest building as an indicator of health and welfare in laboratory mice. *JoVE (Journal of Visualized Experiments)* (82), e51012.
- Ghilardi, J. R., Röhrich, H., Lindsay, T. H., Sevcik, M. A., Schwei, M. J., Kubota, K., Halvorson, K. G., Poblete, J., Chaplan, S. R., Dubin, A. E., Carruthers, N. I., Swanson, D., Kuskowski, M., Flores, C. M., Julius, D., & Mantyh, P. W. (2005). Selective blockade of the capsaicin receptor TRPV1 attenuates bone cancer pain. *The Journal of neuroscience: the official journal of the Society for Neuroscience*, 25(12), 3126-3131.
- Heutte, N., Plisson, L., Lange, M., Prevost, V., & Babin, E. (2014). Quality of life tools in head and neck oncology. *European Annals of Otorhinolaryngology, Head and Neck Diseases*, 131(1), 33-47.
- Hirose, M., Kuroda, Y., & Murata, E. (2016). NGF/TrkA signaling as a therapeutic target for pain. *Pain Practice*, 16(2), 175-182.
- Kelbel, I., & Weiss, M. (2001). Anaesthetics and immune function. *Current Opinion in Anesthesiology*, 14(6), 685-691.
- Kissin, I., & Szallasi, A. (2011). Therapeutic targeting of TRPV1 by resiniferatoxin, from preclinical studies to clinical trials. *Current topics in medicinal chemistry*, 11(17), 2159-2170.
- Lalla, R. V., Bowen, J., Barasch, A., Elting, L., Epstein, J., Keefe, D. M., McGuire, D. B., Migliorati, C., Nicolatou-Galitis, O., Peterson, D. E., Raber-Durlacher, J. E., Sonis, S. T., & Elad, S. (2014). MASCC/ISOO clinical practice guidelines for the management of mucositis secondary to cancer therapy. *Cancer*, 120(10), 1453-1461.

- Menéndez, L., Juárez, L., García, E., García-Suárez, O., Hidalgo, A., & Baamonde, A. (2006). Analgesic effects of capsazepine and resiniferatoxin on bone cancer pain in mice. *Neuroscience Letters*, 393(1), 70-73.
- Meyer, F., Fortin, A., Gélinas, M., Nabid, A., Brochet, F., Têtu, B., & Bairati, I. (2009). Health-Related Quality of Life As a Survival Predictor for Patients With Localized Head and Neck Cancer Treated With Radiation Therapy. *Journal of Clinical Oncology*, 27(18), 2970-2976.
- Negus, S. S., Neddenriep, B., Altarifi, A. A., Carroll, F. I., Leidl, M. D., & Miller, L. L. (2015). Effects of ketoprofen, morphine, and kappa opioids on pain-related depression of nesting in mice. *Pain*, 156(6), 1153.
- Page, G. G., Ben-Eliyahu, S., Yirmiya, R., & Liebeskind, J. C. (1993). Morphine attenuates surgery-induced enhancement of metastatic colonization in rats. *Pain*, 54(1), 21-28.
- Page, G. G., Blakely, W. P., & Ben-Eliyahu, S. (2001). Evidence that postoperative pain is a mediator of the tumor-promoting effects of surgery in rats. *Pain*, 90(1-2), 191-199.
- Schmidt, B. L. (2015). The neurobiology of cancer pain. *Journal of oral and maxillofacial surgery*, 73(12), S132-S135.
- Scully, C., Epstein, J., & Sonis, S. (2003). Oral mucositis: a challenging complication of radiotherapy, chemotherapy, and radiochemotherapy: part 1, pathogenesis and prophylaxis of mucositis. *Head & Neck: Journal for the Sciences and Specialties of the Head and Neck*, 25(12), 1057-1070.
- Sevcik, M. A., Ghilardi, J. R., Peters, C. M., Lindsay, T. H., Halvorson, K. G., Jonas, B. M., Kubota, K., Kuskowski, M. A., Boustany, L., & Shelton, D. L. (2005). Anti-NGF therapy profoundly reduces bone cancer pain and the accompanying increase in markers of peripheral and central sensitization. *Pain*, 115(1-2), 128-141.

- Shinoda, M., Ogino, A., Ozaki, N., Urano, H., Hironaka, K., Yasui, M., & Sugiura, Y. (2008). Involvement of TRPV1 in nociceptive behavior in a rat model of cancer pain. *The journal of pain*, 9(8), 687-699.
- Sonis, S., Peterson, R., Edwards, L., Lucey, C., Wang, L., Mason, L., Login, G., Ymamkawa, M., Moses, G., & Bouchard, P. (2000). Defining mechanisms of action of interleukin-11 on the progression of radiation-induced oral mucositis in hamsters. *Oral Oncology*, 36(4), 373-381.
- Sonis, S. T. (2004). A biological approach to mucositis. *J Support Oncol*, 2(1), 21-32.
- Susam, B. T., Akcakaya, M., Nezamfar, H., Diaz, D., Xu, X., de Sa, V. R., Craig, K. D., Huang, J. S., & Goodwin, M. S. (2018). Automated pain assessment using electrodermal activity data and machine learning. 2018 40th Annual International Conference of the IEEE Engineering in Medicine and Biology Society (EMBC), (pp. 372-375). IEEE.
- Susam, B. T., Riek, N. T., Akcakaya, M., Xu, X., de Sa, V. R., Nezamfar, H., Diaz, D., Craig, K. D., Goodwin, M. S., & Huang, J. S. (2021). Automated Pain Assessment in Children Using Electrodermal Activity and Video Data Fusion via Machine Learning. *IEEE Transactions on Biomedical Engineering*, 69(1), 422-431.
- Ye, Y., Dang, D., Zhang, J., Viet, C. T., Lam, D. K., Dolan, J. C., Gibbs, J. L., & Schmidt, B. L. (2011). Nerve Growth Factor Links Oral Cancer Progression, Pain, and Cachexia, Anti-NGF as a Therapy in Head and Neck Cancer. *Molecular cancer therapeutics*, 10(9), 1667-1676.

APPENDICES

Appendix 5.1: Veterinary Radiation Therapy Oncology Group (VROG) acute morbidity scoring scheme.

Study ID

MRN

Radiation Therapy

Treatment # _____ of _____

Scheduled _____ Delivered _____

Oral Mucositis Study

VROG

Acute Radiation Morbidity Scoring Scheme

Date

Initials

Post Radiation Therapy

Day# _____ Post end of Radiation Therapy Treatment

Instructions: Fill in the oval below the description which best describes the condition of the patient's oral cavity/mucous membranes at this time.

| | | | |
|-------------------------|-----------------------------|---|---|
| No change over baseline | Injection without mucositis | Patchy mucositis with patient seemingly pain free | Confluent fibrinous mucositis necessitating analgesia; ulceration, hemorrhage, necrosis |
| <input type="radio"/> | <input type="radio"/> | <input type="radio"/> | <input type="radio"/> |

Signs consistent with nasal mucositis, (sneezing, nasal discharge)

| | | | | | | | | | | |
|-------------------------|-------------------------|-------------------------|-------------------------|-------------------------|-------------------------|-------------------------|-------------------------|-------------------------|-------------------------|--------------------------|
| <input type="radio"/> 0 | <input type="radio"/> 1 | <input type="radio"/> 2 | <input type="radio"/> 3 | <input type="radio"/> 4 | <input type="radio"/> 5 | <input type="radio"/> 6 | <input type="radio"/> 7 | <input type="radio"/> 8 | <input type="radio"/> 9 | <input type="radio"/> 10 |
| None | | | | | | | | | | Severe |

Signs consistent with radiation dermatitis (crusting, redness, alopecia)

| | | | | | | | | | | |
|-------------------------|-------------------------|-------------------------|-------------------------|-------------------------|-------------------------|-------------------------|-------------------------|-------------------------|-------------------------|--------------------------|
| <input type="radio"/> 0 | <input type="radio"/> 1 | <input type="radio"/> 2 | <input type="radio"/> 3 | <input type="radio"/> 4 | <input type="radio"/> 5 | <input type="radio"/> 6 | <input type="radio"/> 7 | <input type="radio"/> 8 | <input type="radio"/> 9 | <input type="radio"/> 10 |
| None | | | | | | | | | | Severe |

Appendix 5.2: The Canine Brief Pain Inventory (CBPI).

Description of pain:

Rate your dog's pain:

1. Fill in the oval next to the one number that best describes the pain at its **worst** in the last 7 days.

0 1 2 3 4 5 6 7 8 9 10

No pain Extreme pain

2. Fill in the oval next to the one number that best describes the pain at its **least** in the last 7 days

0 1 2 3 4 5 6 7 8 9 10

No pain Extreme pain

3. Fill in the oval next to the one number that best describes the pain at its **average** in the last 7 days.

0 1 2 3 4 5 6 7 8 9 10

No pain Extreme pain

4. Fill in the oval next to the one number that best describes the pain as it is **right now**.

0 1 2 3 4 5 6 7 8 9 10

No pain Extreme pain

Description of function:

Fill in the oval next to the one number that best describes how during the last 7 days **pain has interfered** with your dog's:

5. **General Activity**

0 1 2 3 4 5 6 7 8 9 10

Does not interfere Completely interferes

6. **Enjoyment of Life**

0 1 2 3 4 5 6 7 8 9 10

Does not interfere Completely interferes

7. **Ability to Rise to Standing From Lying Down**

0 1 2 3 4 5 6 7 8 9 10

Does not interfere Completely interferes

8. **Ability to Walk**

0 1 2 3 4 5 6 7 8 9 10

Does not interfere Completely interferes

9. **Ability to Run**

0 1 2 3 4 5 6 7 8 9 10

Does not interfere Completely interferes

10. **Ability to Climb Stairs, Curbs, Doorsteps, etc.**

0 1 2 3 4 5 6 7 8 9 10

Does not interfere Completely interferes

Overall impression:

11. Fill in the oval next to the one number that best describes your dog's overall quality of life over the last 7 days.

Poor Fair Good Very Good Excellent

Appendix 5.4: Body Condition Score (BCS).

Body Condition Scoring

Instructions: Fill in the oval next to the one number that best describes the patient's body condition today.

- 1 Ribs, lumbar vertebrae, pelvic bones and other bony prominences evident from a distance. No discernable body fat. Obvious loss of muscle mass.
- 2 Ribs, lumbar vertebrae and pelvic bones easily visible. No palpable fat. Some evidence of other bony prominence. Minimal loss of muscle mass.
- 3 Ribs easily palpated and may be visible with no palpable fat. Tops of lumbar vertebrae visible. Pelvic bones becoming prominent. Obvious waist and abdominal tuck.
- 4 Ribs easily palpable, with minimal fat covering. Waist easily noted, viewed from above. Abdominal tuck evident.
- 5 Ribs palpable without excess fat covering. Waist observed behind ribs when viewed from above. Abdomen tucked up when viewed from side.
- 6 Ribs palpable with slight excess fat covering. Waist is discernable viewed from above but is not prominent. Abdominal tuck apparent.
- 7 Ribs palpable with difficulty; heavy fat cover. Noticeable fat deposits over lumbar area and base of tail. Waist absent or barely visible. Abdominal tuck may be present.
- 8 Ribs not palpable under very heavy fat cover, or palpable only with significant pressure. Heavy fat deposits over lumbar area and base of tail. Waist absent. No abdominal tuck. Obvious abdominal distention may be present.
- 9 Massive fat deposits over thorax, spine and base of tail. Waist and abdominal tuck absent. Fat deposits on neck and limbs. Obvious abdominal distention.

Appendix 5.5: Appetite, diet acceptance and current diet form.

Appetite Assessment

Instructions: Fill in the oval next to the **ONE** number that describes your dog's appetite over the past 7 days.

- 0 1 2 3 4 5 6 7 8 9 10

No
Appetite

Excellent
Appetite

Acceptance of Regular Diet

Instructions: Fill in the oval next to the **ONE** number that describes how acceptable your dog's regular food has been to him over the past 7 days.

- 0 1 2 3 4 5 6 7 8 9 10

Completely
Unacceptable

Very
Acceptable

What diet is your dog currently eating?

Is this hard or soft food?

- Hard Soft Mixed

Text Field